

**“Technical Standards and Commentaries for Port
and Harbour Facilities in Japan”
- Supplemental Explanation Note -
(draft)**

National Institute for Land and Infrastructure Management

Port Facilities Division

Authors

ABE Tomohisa: Head, Port Planning Division, Port and Harbor Department, National Institute for Land and Infrastructure Management (NILIM), Ministry of Land, Infrastructure, Transport and Tourism (MLIT).

FUKUNAGA Yusuke: Former Senior Researcher, Port and Harbor Department, National Institute for Land and Infrastructure Management (NILIM), Ministry of Land, Infrastructure, Transport and Tourism (MLIT).

HIRAYAMA Katsuya: Head, Wave group, Coastal Hydraulic Engineering Department, **Port and Airport Research Institute (PARI).**

KAWAI Hiroyasu: Senior Director for Research (In charge of Coastal and Ocean Research), **Port and Airport Research Institute (PARI).**

KOHAMA Eiji: Head, Earthquake and Structural Dynamics Group, Earthquake Disaster Prevention Engineering Department, **Port and Airport Research Institute (PARI).**

MIYATA Masafumi: Former Head, Port Facilities Division, Port and Harbor Department, National Institute for Land and Infrastructure Management (NILIM), Ministry of Land, Infrastructure, Transport and Tourism (MLIT).

MORIKAWA Yoshiyuki: Director, Geotechnical Engineering Department, **Port and Airport Research Institute (PARI).**

NOZU Atsushi: Director, Geotechnical Engineering Department, **Port and Airport Research Institute (PARI).**

OHYA Yousuke: Principal Researcher, Earthquake Disaster Prevention Engineering Department, **Port and Airport Institute (PARI).**

OKADA Tomonari: Head, Marine Environment and Emergency Management Division, Coastal, Marine and Disaster Prevention Department, National Institute for Land and Infrastructure Management (NILIM), Ministry of Land, Infrastructure, Transport and Tourism (MLIT).

SASSA Shinji: Head, Soil Dynamics Group, Geotechnical Engineering Department, **Port and Airport Research Institute (PARI).**

SUZUKI Kojiro: Director, Coastal Hydraulic Engineering Department, **Port and Airport Research Institute (PARI).**

TAKAHASHI Hidenori: Head, Soil Stabilization Group, Geotechnical Engineering Department, **Port and Airport Research Institute (PARI).**

YAMAJI Toru: Director, Structural Engineering Department, **Port and Airport Research Institute (PARI).**

YONEYAMA Haruo: Director, Coastal and Ocean Development Department, **Port and Airport Research Institute (PARI).**

(March 2022)

CONTENTS

Chapter 1 General	1
1. Purpose of the Note	2
2. Composition of the Note	3
Chapter 2 Positioning and Record of Application of “Technical Standards and Commentaries for Port and Harbour Facilities in Japan”	4
1. Positioning and Record of Application of Technical Standards and Commentaries for Port and Harbour Facilities in Japan (TSCPHF Japanese Version)	5
2 Positioning and Record of Application of Technical Standards and Commentaries for Port and Harbour Facilities in Japan (TSCPHF English Version)	8
Chapter 3 Features of Technical Standards in Japan	10
1. General	11
1.1 Performance-Based Design System	11
1.2 Maintenance Oriented Design	18
2. Hydraulic Engineering Field	22
2.1 Techniques for Calculating Wave Transformation	22
2.1.1 Calculating wave transformation by the Boussinesq equation	22
2.1.2 Setting of swell-like waves.....	24
2.2 Determination of Wave Forces	27
2.2.1 Wave force formulas used in performance verification and their changes	27
2.2.2 Determination of wave force based on numerical analysis	28
2.3 Setting of Actions Related to Tsunamis and Storm Surges	30
2.3.1 Verification for tsunamis	30
2.3.2 Verification for storm surges	31
2.4 Characteristics of Verifying Reinforcing Embankment of Breakwater	33
2.5 Characteristics of Class 2 Channel Design Method	35
3. Geotechnical Field	37
3.1 Strong Ground Motion Observation Network and Setting Input Seismic Motion	37
3.2 Changes in Performance Verification Methods Based on the Seismic Coefficient Method.....	40
3.3 Seismic Design Based on Numerical Analysis.....	46
3.3.1 Verification of deformation by numerical analysis.....	46
3.3.2 Seismic design considering inelastic behavior of steel pipe piles	49
3.4 Liquefaction Prediction and Assessment.....	52
3.5 Ground Survey	54
3.6 Changes in Ground Improvement Techniques	57
4. Structural Aspect	60
4.1 Examination of change in performance over time.....	60

4.1.1 Verification of corrosion of reinforcing bar in concrete structures.....	60
Figure.3.4.1.2 Change over time in the distribution of the chloride ion concentration in concrete ..	61
(schematic illustration).....	61
4.1.2 Corrosion protection design of steel members	62
4.2 Methodology for Setting Fender Material Standards	64
5. Environmental Aspect.....	67
5.1 Design Technique for Green Port Structures	67
Chapter 4 Examples of Breakwater Design	70
1. Typical Structural Types in Japan	71
2. Caisson-type Composite Breakwater.....	76
3. Sloping Breakwater.....	94
Chapter 5 Examples of Mooring Facility Design.....	104
1. Typical Structural Types in Japan	105
2. Gravity Type Quaywall.....	107
3. Anchored Sheet-pile Quaywall	134
4. Open-type wharf on vertical piles	179
5. Steel Plate Cellular-Bulkhead Quaywall	216
Chapter 6 Reference Information Required Overseas.....	250
1. Setting of design tide levels, quay wall water depth and crown height.....	252
2. Setting of design seismic coefficient	255
3. Verification of circular slip failure by the modified Fellenius method	257
4. Verification of bearing capacity for eccentric and inclined loads by the simplified Bishop method	259
5. Standards for mooring posts and bollards.....	261
6. Design of fender systems.....	263
7. Earth pressure from filling soil acting on caisson outer wall.....	265
8. Design of piled piers	267
9. Scouring of front side of quay wall	269
10. Bearing capacity of pile foundations	273
11. Methods for assessment of liquefaction	275
12. Design wave.....	277
13. Cathodic protection.....	278
14. Selection of wave-dissipating concrete blocks.....	280
15. Friction enhancement mats (asphalt mats).....	282

Chapter 1 General

1. Purpose of the Note

This document is a concise summary of “Technical Standards and Commentaries for Port and Harbour Facilities in Japan” (referred to as TSCPHF (Japanese version), ¹⁾ which was issued in 2018 as the design standards for ports and harbors in Japan, and its English version (issued in 2020) (TSCPHF (English version) ²⁾, covering the transition of design standards, the editorial policy of the English edition, technical features, examples of the design of breakwaters and mooring facilities in line with design standards, and responses to frequently asked questions (FAQ) when these design standards are applied overseas.

The purpose of this document is to enable engineers involved in work related to ports and harbors in Japan and overseas to understand, in a short time, the overview and features of design standards for ports and harbors in Japan and the applicable measures in situations where the methods of setting design conditions and the applied design methods are different in Japan and overseas, and to facilitate more effective use of the Japanese design standards than in the past when carrying out port and harbor projects overseas.

1) Technical Standards and Commentaries for Port and Harbour Facilities in Japan: The Ports and Harbours Association of Japan. 2018.

“Technical Standards and Commentaries for Port and Harbour Facilities in Japan” is a book summarizing design techniques for ports and harbor facilities in the Japanese language. This book was written and edited mainly by experts on port and harbor design under the editorial supervision of the Ministry of Land, Infrastructure, Transport and Tourism of Japan (MLIT). The most recent edition was issued in 2018 by The Ports and Harbours Association of Japan.

2) Technical Standards and Commentaries for Port and Harbour Facilities in Japan (English version): The Overseas Coastal Development Institute of Japan. 2020. (<https://ocdi.or.jp/en/download-pdf>)

This is the English version of the above-mentioned Technical Standards in 1). The English translation was prepared by the Overseas Coastal Area Development Institute of Japan (OCDI). The most recent edition was published in 2020. This book can be downloaded free-of-charge via the above-mentioned website.

2. Composition of the Note

This document is comprised of the following 6 chapters. A brief summary of each chapter is presented below.

(1) Chapter 1 General

Chapter 1 explains the purpose and composition of this document.

(2) Chapter 2 Positioning and Record of Application of “Technical Standards and Commentaries for Port and Harbour Facilities in Japan”

Chapter 2 introduces the positioning and record of application of TSCPHF (Japanese and English versions).

(3) Chapter 3 Features of Technical Standards in Japan

Chapter 3 describes the background, history and reasons for the adoption of various design techniques in Japan as features of Japanese design techniques.

(4) Chapter 4 Examples of Breakwater Design

Chapter 4 presents examples of the design of caisson-type composite breakwaters and sloping breakwaters as representative structural types of breakwaters in Japan.

(5) Chapter 5 Examples of Mooring Facility Design

Chapter 5 presents examples of the design of gravity-type quaywalls, anchored sheet-pile quaywalls, open-type wharfs on vertical piles and steel plate cellular-bulkhead quaywalls as representative structural types of mooring facilities in Japan.

(6) Chapter 6 Reference Information Required Overseas

Chapter 6 introduces frequently asked questions (FAQ) from overseas port and harbor engineers concerning design techniques in Japan, together with examples of responses to those FAQ.

**Chapter 2 Positioning and Record of Application of “Technical Standards and
Commentaries for Port and Harbour Facilities in Japan”**

1. Positioning and Record of Application of Technical Standards and Commentaries for Port and Harbour Facilities in Japan (TSCPHF Japanese Version)

(1) Positioning

In Japan, construction, improvement and maintenance of port and harbor facilities must comply with the “Technical Standards for Port and Harbour Facilities” (hereinafter, “Technical Standards”). TSCPHF (Japanese version) is a commentary for the purpose of assisting domestic users in Japan in properly understanding the “Technical Standards” and supporting the smooth implementation of the “Technical Standards.”

(2) Points to note in the use of TSCPHF

TSCPHF (Japanese version) is comprised of the following three sections 1) to 3), which are arranged hierarchically according to their compulsory force.

1) Technical Standards

This section presents the original text of the article concerned, that is, the text of the Technical Standards (Ministerial Ordinance and Public Notice, issued by Ministry of Land, Infrastructure, Transport and Tourism of Japan). Deviations from these Technical Standards are not permitted.

2) Interpretation

The concrete concepts considered appropriate and minimum items to be confirmed when implementing the above Technical Standards are presented as “Interpretation.” This Interpretation must be observed by agencies of the national government.

3) Explanation

The Explanation section presents technical information which can be used as reference in the construction, improvement or maintenance of port and harbor facilities and examples of study items and study methods considered standard. Principal design methods and specific safety factors are presented in the Explanation. The application of a technique which is introduced in this section is left to the judgment of the facility developer and designer.

This section cites reference materials which are classified as follows. This reference literature must be used as required for the structural type, materials and design items subject to the design.

a) JIS (Japanese Industrial Standards) and standards of academic societies and associations

- The standards for principal materials refer to the content of JIS.
- The principal design methods for members (steel reinforced concrete, steel members, etc.) refer to the Concrete Standard Specifications issued by the Japan Society of Civil Engineers (JSCE).
- Soil investigation and testing methods refer to the standards issued by the Japanese Geotechnical Society.

b) Standards and guidelines issued by related organizations

- In cases where detailed guidelines in connection with the design and maintenance and management of port and harbor facilities have been issued by related organizations, those guidelines are referenced. The following are examples of the target structures and construction

methods in representative guidelines.

Breakwaters: “Breakwater sitting on soft ground”

Mooring facilities: “L-shaped block type quaywall”, “Jacket-type pier”, “Strutted frame type pier”, “Fenders”

Soil improvement: “Deep mixing method”, “Premixing type stabilization method”, “Lightweight treated soil method”, “Pneumatic flow mixing method”, “Reclaimed land liquefaction countermeasures method”

Maintenance and management: “General maintenance and management”, “Inspection and diagnosis”, “Corrosion protection and repair”, “Fender systems”

Bridges: “Highway Bridge”

c) Papers, books, research institute materials, etc.

- In addition to the above a) and b), papers, books, research institute materials, etc. that provide the grounds for standards and related technical information are also referenced.
- As research institute materials, materials published regularly by the following two domestic research institutes in Japan are referenced.
 - 1) National Research and Development Agency, National Institute of Maritime, Port and Aviation Technology, Port and Airport Research Institute (PARI)
 - 2) Ministry of Land, Infrastructure, Transport and Tourism (MLIT), National Institute for Land and Infrastructure Management (NILIM)

(3) History of Record and Application

The publication history of TSCPHF (Japanese version) is shown in **Table. 2.1.1**. This table presents the titles of the design standards since 1950 and summarizes the principal technical items.

**Table 2.1.1 History Chart of Technical Standards and Commentaries for
Port and Harbor Facilities in Japan**

Year of issue	Titles*	Introduced technical items	English version**
1950	Port and Harbour Construction Design Specification Handbook	<ul style="list-style-type: none"> Wave pressure formulae: Sainflou's formula (standing waves), Hiroi's formula (breaking waves) Standard dimensions for berths Introduction of earth pressure during earthquakes Seismic coefficient method (design seismic coefficient 0.05 to 0.3), etc. 	Not issued
1959	Port and Harbour Construction Design Handbook	<ul style="list-style-type: none"> Wave prediction by SMB method Introduction of Hudson's formula (weight of rubble) Countermeasures for soft ground Slope stability analysis (circular slip analysis) Design methods for sheet pile quaywalls and cell type quaywalls, etc. 	Not issued
1967	Design Standards for Port and Harbour Structures	<ul style="list-style-type: none"> Change in composition of table of contents (followed thereafter) Flowcharting of design procedures Graphical solution and diffraction diagrams for wave prediction Irregular-shaped wave-dissipating concrete blocks Dimensions of channel and basins: Function of ship length L Design seismic coefficient = Regional seismic coefficient \times Soil type coefficient \times Importance factor, etc. 	Not issued
1979	Technical Standards and Commentaries for Port and Harbour Facilities in Japan	<ul style="list-style-type: none"> Design system based on wave spectrum Introduction of Goda's wave pressure formulae Provisions for harbor calmness Auxiliary equipment of mooring facilities (lighting, etc.) Container wharfs, car ferry wharfs, etc. 	1980
1989	Technical Standards and Commentaries for Port and Harbour Facilities in Japan	<ul style="list-style-type: none"> Design methods for new types of breakwaters Bearing capacity design method for eccentric and inclined loads (Simplified Bishop method) Liquefaction prediction/determination method for sandy ground Various ground improvement methods (deep mixing method, SCP method, etc.) Maintenance and management methods for port and harbor facilities, etc. 	1991
1999	Technical Standards and Commentaries for Port and Harbour Facilities in Japan	<ul style="list-style-type: none"> Transition to SI unit system Seismic resistance design for Level 1 and Level 2 ground motion (high earthquake-resistance quaywalls) Limit state design method (concrete members), etc. 	2002
2007	Technical Standards and Commentaries for Port and Harbour Facilities in Japan	<ul style="list-style-type: none"> Transition to performance-based design system Introduction of partial factor method (reliability-based design method) Time-series seismic ground motion considering site effects of each port Seismic coefficient method considering deformation of structures, etc. 	2009
2018	Technical Standards and Commentaries for Port and Harbour Facilities in Japan	<ul style="list-style-type: none"> Addition of provisions for improvement design of existing structures Addition of comprehensive commentary on research techniques Introduction of swell type waves "Design tsunami" and "Excess design tsunami" Tsunami-resistant design of breakwaters (resilience of structures) Partial factors by load and resistance factor design (LRFD) approach, etc. 	2020

* The Ports and Harbours Association of Japan

** The Overseas Coastal Development Institute of Japan

Since the 1950s, a large number of port and harbor structures such as breakwaters, mooring facilities, etc. constructed in Japan have been designed based on the design standards shown in the above table. These facilities have also suffered damage due to typhoons, earthquakes and tsunamis many times, and on each

occasion, the design methods were improved and the results were incorporated in the design standards. Therefore, TSCPHF (Japanese version) and the design standards that were its predecessors are backed by the actual results of numerous projects under the severe natural conditions of Japan.

2 Positioning and Record of Application of Technical Standards and Commentaries for Port and Harbor Facilities in Japan (TSCPHF English Version)

(1) Positioning and history

Although TSCPHF (Japanese version) was established for domestic use in Japan, there was also a high need for use in port and harbor development projects in developing countries supported by Japan's ODA (Official Development Assistance). Therefore, the year after the publication of the 1979 edition of TSCPHF (Japanese version), TSCPHF (English version) was also issued (see **Table 2.1.1**). Following this, a new English version was issued each time the TSCPHF (Japanese version) was updated.

(2) Record of application

The content, forms and target regions of Japan's international cooperation in the field of ports and harbors have evolved together with the needs of the times. For example, in the 1970s and 1980s, Japan provided cooperation for port development supporting industrial growth in China, Indonesia, Thailand and other Southeast Asian countries, and Central and South American countries such as Brazil, etc. From 1980, when the response to container transportation became an increasingly large part of these efforts, Japan contributed to the development of a large number of ports, such as the Port of Columbo in Sri Lanka. In the 2000s, technical cooperation was provided with the aim of constructing port management systems and administration systems, improving terminal operation, etc. at a large number of ports in many countries including Vietnam, Cambodia and Mozambique, among others, and in the 2010s, port and harbor development was promoted from the viewpoint of public-private partnerships, for example, at the Port of Lach Huyen in Vietnam and Yangon Port (Myanmar International Terminals Thilawa: MITT) in Myanmar. The number of projects in Africa also increased rapidly in the 2010s..

Accordingly, TSCPHE has been adopted in several port construction projects.

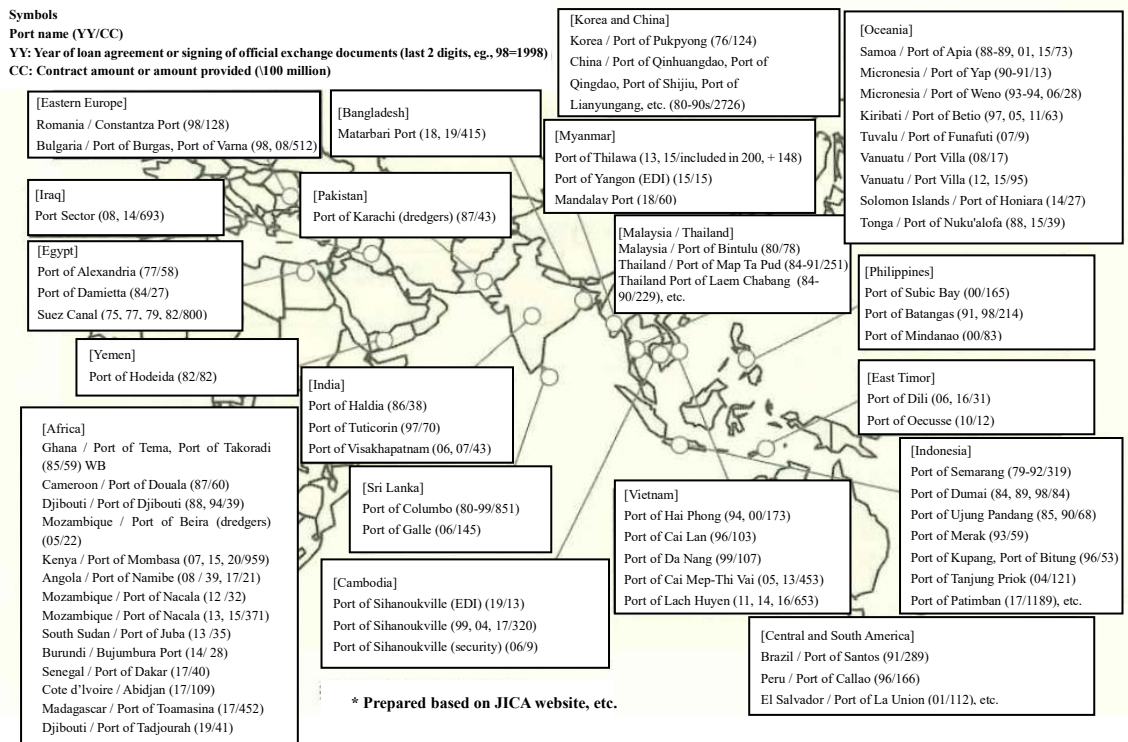


Figure. 2.2.1 Projects conducted by JICA's yen loans and grant-aid by country

Chapter 3 Features of Technical Standards in Japan

1. General

1.1 Performance-Based Design System

(1) Aims of introducing performance-based design system

Performance-based design has been adopted in “Technical Standards and Commentaries for Port and Harbour Facilities in Japan” (TSCPHF). The performance-based design system differs from the conventional specification-based design system, under which, in principle, the materials, design methods, etc. prescribed in the standard are applied. By contrast, under the performance-based design system, the mandatory items specified in laws and regulations are clearly differentiated from other arbitrary items in order to enhance the creativity of designers and provide them with the freedom to introduce new technologies so as to achieve more rational design outcomes.

Figure 3.1.1.1 shows a concrete image of this performance-based design system. As shown in the Figure, the “Items to be conformed to” (mandatory items) are the “Objective” and the contents of the “Performance requirements” and “Performance criteria.” The objective is defined as the “Reason why the facility is needed,” and the performance requirements are “Items expressing the performance that the facility must possess to achieve the objective in plain terms from the viewpoint of accountability.” The performance criteria are “Items expressing the criteria for verifications necessary to satisfy the performance requirements from the technical viewpoint.” “Performance verification,” which is the lowest level in this hierarchy, means the “Action of verifying that the performance criteria are satisfied.” In selecting a performance verification method under this performance-based design system, any method may be adopted if it can show that the performance requirements and performance criteria are satisfied. The Commentary portion of the TSCPHF presents the standard methods of performance verification techniques, but also permits adoption of other methods.

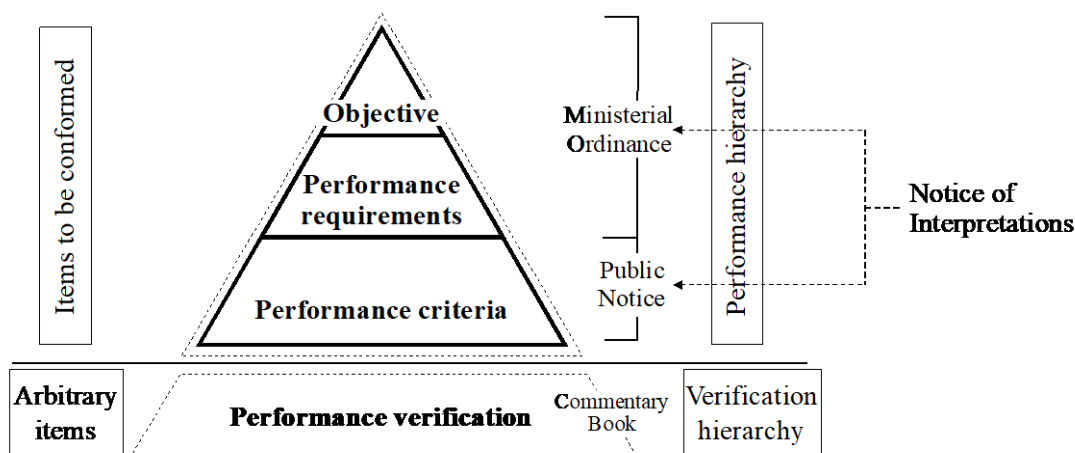


Figure. 3.1.1.1 Performance based design system
(Positioning of Performance Hierarchy and Performance Verification)

(2) Performance requirements, performance criteria and performance verification

The framework of the performance requirements, performance criteria and performance verification has been constructed with ISO 2394 (General principles on reliability for structures) and the technical documents which were drawn up in Japan based on ISO 2394 as the upper-level standard. The following presents a simple explanation of the important component items of this framework.

1) Classification of actions

Actions are classified as a) Permanent actions, b) Variable actions and c) Accidental actions, as defined below. The classification of actions corresponds mainly to their variation of magnitude over time and the risk that must be managed by society. **Table 3.1.1.1** shows examples of the concrete actions under each of these general classifications.

a) Permanent actions

Permanent actions are actions that are assumed to act on a structure continuously through its design service life. These are actions that have small variations over time in comparison with the average, and actions that tend to increase or decrease monotonically and constantly during the design service life until the variation of magnitude reaches a certain limit value.

b) Variable actions

Variable actions are actions in which the variation of magnitude from the average during the design service life of the structure is non-negligible and does not change unidirectionally. Their characteristic values are given probabilistically.

c) Accidental actions

Accidental actions are actions that are difficult to predict by probabilistic statistical techniques, or that cannot be ignored socially due to their extremely large characteristic values, even though the annual exceedance probability is small in comparison with variable actions.

Table 3.1.1.1 Classification of Dominating Actions

	Action
Permanent actions	Self-weight, earth pressure, environmental actions such as thermal stress, corrosion, environmental actions such as freezing and thawing, etc.
Variable actions	Waves, wind, water level (tide level), loads of cargo or vehicles, action due to ship berthing/traction, level 1 earthquake ground motion, etc.
Accidental actions	Unintended collision of a ship or other objects, fire, tsunami, level 2 earthquake ground motion, accidental waves, etc.

2) Definitions of performance requirements

Among the various performance requirements for facilities, the performance requirements for structural response are classified as a) Serviceability, b) Recoverability and c) Safety, as defined below, according to the allowable degree of damage. Arranged by the allowable degree of damage, the relationship is Serviceability < Restorability < Safety.

a) Serviceability

Serviceability means performance that enables use without inconvenience in use. The structural response against assumed actions is limited to a range where damage will not occur or can be restored in short term with minimal repairs to perform the required functions.

b) Recoverability

Recoverability is performance that enables continuous use with repairs in a range that is technically feasible and economically reasonable. The structural response against assumed actions is limited in a range where the specified functions can be recovered in a short time with minor repairs.

c) Safety

Safety is performance that secures the safety of human life, etc. Although a certain amount of damage occurs, the structural response against the assumed actions is to be such that the extent of damage is not fatal to the facility, and does not have a serious effect on ensuring the safety of human life, etc.

3) Basic concept of performance requirements

The basic concept of the performance requirements for port and harbor facilities in Japan is presented in the following a) and b), and is shown graphically in **Figure. 3.1.1.2**. The threshold value of 0.01 for the annual exceedance probability, which is the borderline between permanent/variable actions and accidental actions, was set for convenience and is a guideline for cases where the design service life is in the standard range of approximately 50 years.

a) Performance requirements for permanent actions and variable actions (actions having an annual exceedance probability of roughly 0.01 or more)

Serviceability is required in all facilities. If serviceability is secured, recoverability and safety against permanent actions and variable actions can also be regarded as secured.

b) Performance requirements for accidental actions (actions having an annual exceedance probability of approximately not more than 0.01)

Performance requirements for accidental actions (Level 2 earthquake ground motion: earthquake of the largest class) is required in high earthquake-resistant quaywalls and other critical facilities. As performance requirements, any of the requirements of serviceability, restorability or safety can be selected, according to the importance and functions of the facility.

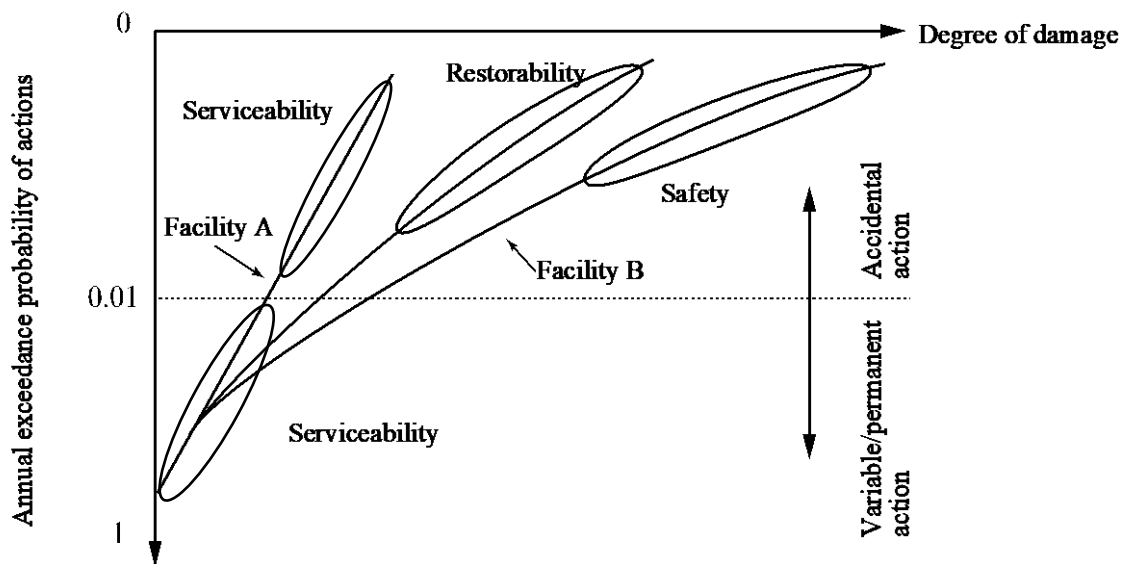


Figure. 3.1.1.2 Conceptual Diagram of the Relationship Between Classification of Actions and Performance Requirements

4) Response to tsunami exceeding design conditions (securing resilience)

In addition to the performance requirements of serviceability, restorability and safety mentioned in 2) and 3) above, TSCPHF also provides the basic concept of design for tsunamis of a scale exceeding the design tsunami for facilities (breakwaters, seawalls, water gates and landlocks) which may have a serious impact on

human life, property or economic activity if the facility is damaged by a tsunami. (here, “design tsunami” means the tsunami considered as an accidental action when setting the design conditions.)

Concretely, TSCPHF specifies that “Even in case of a tsunami having a strength of a scale that exceeds the design tsunami, it shall be possible to delay the critical effects of damage, etc. due to the action of that tsunami on the structural stability of the facility as long as possible.” Therefore, notwithstanding the content of the performance requirements (serviceability, recoverability, safety) against accidental actions set in the design, it is also necessary to secure the “resilience” of the above-mentioned facilities.

For example, in the case of a breakwater, “resilience” is necessary so that calm conditions can be restored in the harbor from immediately after the disaster and the area protected by the breakwater can demonstrate its disaster-mitigation function. “Resilience” is secured by implementing the maximum possible structural measures within the limits of the construction budget, so as to extend the time until the breakwater collapses as much as possible in case a strong tsunami exceeding the scale of the design tsunami overflows the breakwater.

5) Concrete examples of performance criteria

As explained in (1), performance criteria are defined as “Items expressing the criteria for verifications necessary to satisfy performance requirements from the technical viewpoint.” The standard performance criteria for each structural type of each facility are presented in the Commentary section of TSCPHF (see Chapter 2 1(2)).

As typical examples of performance criteria, **Table 3.1.1.2** shows the performance criteria (verification items) for permanent actions and variable actions for gravity type quaywalls. This table shows that a gravity type quaywall must satisfy serviceability for a design condition in which permanent actions are the dominating action. For this, verification of a minimum of three performance criteria is necessary, namely, “Circular slip failure of the ground,” “Sliding/overturning of the wall body” and “Failure of the bearing capacity of the foundation ground.” It is also necessary to satisfy serviceability for a design condition in which the dominating variable action is Level 1 earthquake ground motion (75-year return period). For this, the table shows that verification of a minimum of three performance criteria is required, that is, “Sliding and overturning of the wall body” and “Failure of the bearing capacity of the foundation ground.”

Table 3.1.1.2 Performance criteria (verification items) for permanent actions and variable actions for gravity type quaywalls

Ministerial Ordinance			Public Notice			Performance requirements	Design state		Verification item	Standard index to determine the limit value	
Article	Paragraph	Item	Article	Paragraph	Item		State	Dominating action			Non-dominating action
26	1	2	49	-	1	Serviceability	Permanent	Self-weight	Water pressure, surcharges	Circular slip failure of the ground	Action–resistance ratio with respect to circular slip failure
					2			Earth pressure	Self-weight, water pressure, surcharges	Sliding, overturning of the quay wall, bearing capacity of the foundation ground	Action–resistance ratios with respect to sliding, overturning, and bearing capacity
					Variable		Level 1 earthquake ground motion	Self-weight, earth pressure, water pressure, surcharges	Sliding, overturning of the quay wall, bearing capacity of the foundation ground	Action–resistance ratios with respect to sliding, overturning, and bearing capacity	

6) Performance verification methods

The performance verification methods in TSCPHF are comprised of the following two types.

a) Methods capable of taking account actions and the uncertainty of the performance of the facilities concerned

This method is a reliability-based design method. If the reliability-based design method is used, it must properly evaluate the actions and the uncertainty of various design parameters related to the performance of the facilities concerned, and properly set the target failure probabilities or reliability indices. Performance verification by a reliability-based design method based on the partial factor method must properly evaluate the uncertainty of the design parameters and set partial factors reflecting the target failure probabilities or reliability indices. TSCPHF describes calibrated partial factors for a limited number of structural types and verification items.

b) Other reliable methods

Other reliable methods are in principle performance verification methods for a specific and quantitative evaluation of the performance of the facilities concerned, and generally include numerical analysis methods, model test methods and *in-situ* test methods. However, if use of these methods is inappropriate, methods for indirect evaluation of the facilities concerned based on past experience (safety factor method or allowable stress design method), taking account of various conditions such as natural conditions, may be interpreted as one of the “other reliable methods.”

7) Performance verification equation in partial factor method

The performance verification equation in the partial factor method used in TSCPHF is shown below. This performance verification equation is based on the partial factor method by the load and resistance factor design (LRFD) approach. For details of the partial factor analysis method based on the LRFD approach, see TSCPHF [Reference (Common)] Chapter 2 “Fundamentals of the Reliability-based Design Method” and

References 1) and 2).

$$m \times \left(\gamma_i \frac{S_d}{R_d} \right) \leq 1.0$$

$$S_d = f(\gamma_{S_1} S_{1k}, \dots, \gamma_{S_n} S_{nk}) = f(\gamma_{S_1} S_{1k}(x_{1k} \dots x_{pk}), \dots, \gamma_{S_n} S_{nk}(x_{1k} \dots x_{pk}))$$

$$R_d = g(\gamma_{R_1} R_{1k}, \dots, \gamma_{R_m} R_{mk}) = g(\gamma_{R_1} R_{1k}(x_{1k} \dots x_{pk}), \dots, \gamma_{R_m} R_{mk}(x_{1k} \dots x_{pk}))$$

Where,

S_d : design value of response (action)

R : design value of limit value (resistance)

γ_i : factor for considering the importance of the structure and the social effects, etc. when it reaches the limit state (structure factor)

m : adjustment factor (see explanation in the following)

S_{jk} : characteristic value of action effect j ($j=1 \dots n$)

γ_{Sj} : partial factor to be multiplied with the characteristic value S_{jk} of action effect j

S_j () : equation for calculating the characteristic value S_{jk} of action effect j

R_{jk} : characteristic value of resistance (strength) ($j=1..m$)

γ_{Rj} : partial factor to be multiplied with the characteristic value of resistance (strength) j

R_j () : equation for calculating the characteristic value R_{jk} of resistance (strength) j

x_{ji} : characteristic value of design element x_j ($j=1..p$)

As shown in the above equation, in a performance verification by the partial factor method, the performance of a structure is verified by confirming that the value obtained by multiplying the action-strength ratio by the structure factor and adjustment factor is not more than 1.0. Here, the “action-strength ratio” is the ratio of the design values of the response values (stress, section force, action total value total action effect, displacement, etc.) caused by actions acting on the structure, and the design values of the limit values (yield strength, section strength, total resistance, allowable displacement, etc.) based on the resistance (strength) of the structure. Partial factors are values which are calculated by a statistical analysis or a reliable method as factors to be multiplied with the characteristic values of action effect or resistance (including the characteristic values of design parameters) in order to secure the target performance of a structure. “Partial factors by statistical analysis” means factors which are calculated by way of calibration using a reliability analysis.

As “Other reliable methods” in 6) b), a “method based on past experience” is used in some cases. (These methods are the safety factor method and the allowable stress design method, which have been used historically and have ample actual results based on numerous cases of application in the past.) In such cases, the verification is conducted using an adjustment factor, after setting all partial factors at 1.0 for convenience, in order to clarify the fact that this approach is different from a verification using partial factors calculated by statistical analysis. The “adjustment factor” is a factor for adjusting the result so as to obtain a structure profile with the same level of safety as that assumed by the “method based on past experience,” and corresponds to the allowable safety factor in the conventional safety factor method and allowable stress design method.

Partial factors presented in the TSCPHF are established with consideration of their applicability to the performance verification methods in this document. Therefore, in principle, partial application of the partial factors in other standards to the performance verification formulas in this document should be avoided.

-
- 1) Takenobu, M., Nishioka, S., Sato, T., & Miyata, M. (2015). A Basic Study of the Level 1 Reliability Design Method Based on Load and Resistance Factor Approach - Performance verifications of sliding failure and overturning failure for caisson type quay walls in permanent situation -. *Technical Note of the National Institute of Land and Infrastructure Management (NILIM)*, No. 880.
 - 2) Takenobu, M., Miyata, M., Otake, Y., & Sato, T. (2019). A basic study on the application of LRFD in “the technical standard for port and harbour facilities in Japan”: a case of gravity type quay wall in a persistent design situation. *Georisk: Assessment and Management of Risk for Engineered System and Geohazards*, 13(3), 195-204.

1.2 Maintenance Oriented Design

(1) Overview

When a port facility is designed according to TSCPHF, measures necessary to ensure appropriate maintenance of the facility must be taken. The measures recommended by TSCPHF for this purpose are shown below:

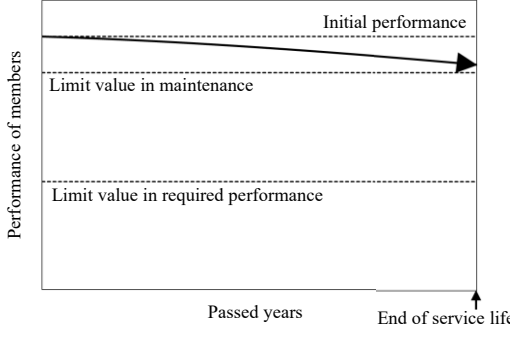
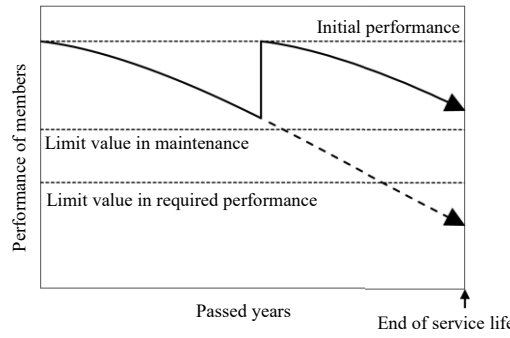
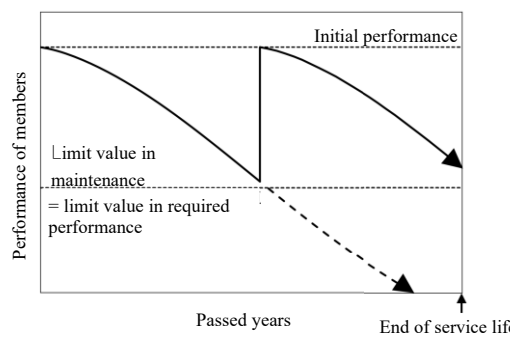
- (i) Establish an appropriate basic policy for maintenance (maintenance level) for each constituent member of the port facility. Specifically, the policy should cover assumptions concerning the types and degree of damage or deterioration that will occur during the design service life of the facility and the methods for conducting inspections and repairs in order to maintain the performance and functions of the facility at or above the required level.
- (ii) Develop a design so that the predetermined maintenance level can be reasonably achieved.
- (iii) Develop a design that allows smooth implementation of inspections, diagnosis, maintenance work, etc. appropriate for ensuring the predetermined maintenance level.
- (iv) Ensure accurate communication of maintenance-related information among all stakeholders and engineers involved in the maintenance stage to ensure appropriate and sound maintenance (formulation of the maintenance plan proposal).

Among the above, (i) contains especially important concepts. Therefore, the basic concept of maintenance levels and actual case examples of such maintenance are explained below.

(2) Maintenance level categories and concepts

The maintenance level of a port facility, that is, the target facility to be maintained, should be determined by predicting changes in the performance of the facility over time based on various conditions that affect the facility, such as environmental conditions and use, the structural type of the facility, the structural and material characteristics of the constituent members of the facility and other factors in light of the purpose of establishing the facility, its service life and its required performance. Maintenance levels are generally divided into the three categories shown in **Table 3.1.2.1**.

Table 3.1.2.1 Classification and basic concept of maintenance levels for members of port and harbor facilities

Category	Basic concept of damage or deterioration
<p>■ Maintenance Level I (Preventive countermeasures)</p>  <p align="center">Schematic diagram showing prediction of performance degradation at Maintenance Level I</p>	<p>○ Level at which a high level countermeasures for damage or deterioration are taken to keep damage or deterioration to a level at which the performance requirements can be satisfied during the service life of the facility</p>
<p>■ Maintenance Level II (Preventive maintenance)</p>  <p align="center">Schematic diagram showing prediction of performance degradation at Maintenance Level II</p>	<p>○ Level at which relatively small-scale countermeasures are taken repeatedly at the stage where damage or deterioration is kept relatively minor to prevent performance degradation, so as to avoid conditions where the performance requirements cannot be satisfied during the service life of the facility</p>
<p>■ Maintenance Level III (Breakdown maintenance)</p>  <p align="center">Schematic diagram showing prediction of performance degradation at Maintenance Level III</p>	<p>○ Level at which a certain degree of damage or deterioration is tolerated as long as performance requirements are satisfied, and major action is taken once or twice during the service life of the facility to repair damage or deterioration once it has occurred</p>

(3) Example of setting maintenance levels

As an example of setting maintenance levels, **Figure 3.1.2.1** shows the case of a jacket-type wharf, and **Table 3.1.2.2** shows the basic concept of setting the maintenance level for the members of the jacket-type wharf.

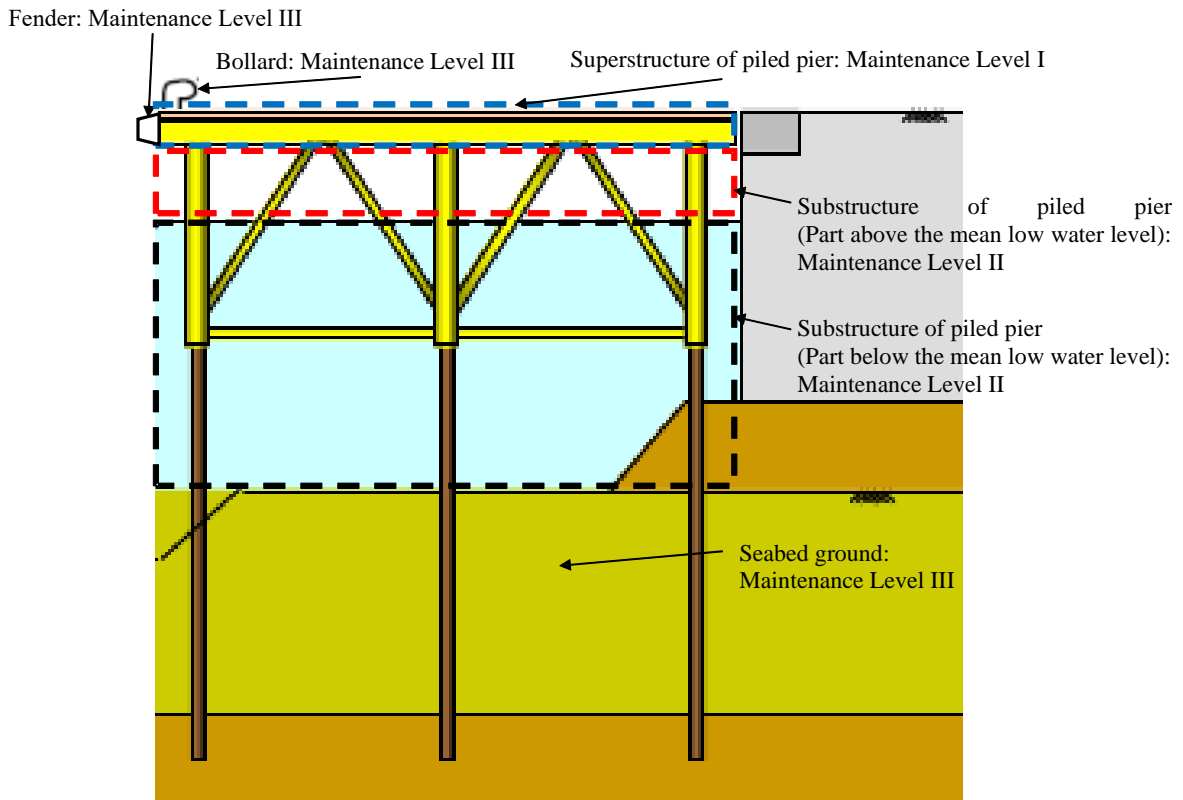


Figure. 3.1.2.2 Maintenance levels of jacket-type wharf

Table 3.1.2.2 Basic concept of setting the maintenance levels of members of the jacket-type wharf

Member		Maintenance level	Basic concept of setting maintenance levels
Superstructure of piled pier		I	In the superstructure of a piled pier, epoxy coated reinforcing bar is adopted for both precast and in-situ deck concrete as a prevention measure against a chloride ion-induced corrosion. According to the verification at the design stage for corrosion of reinforcing steel by entry of chloride ions, the corrosion life of the reinforcing bars is estimated to exceed the 50-year design service life of the facility. Therefore, the superstructure is classified as Maintenance Level I, i.e., advanced countermeasures are planned at the design stage to prevent anomalies during the design service life of the facility.
Substructure of piled pier (Part above the mean low water level)		II	The design life of a super high build coating, which is selected as an alternative corrosion protection measure to a traditional corrosion allowance method, is about 30 years, and some repair work will be necessary within the design service life. Therefore, this part of the substructure is classified as Maintenance Level II, which involves planning of preceding measures to prevent anomalies during the design service life from the design stage.
Substructure of piled pier (Part below the mean low water level)		II	The design life of anodes for cathodic protection, which is chosen as an alternative corrosion protection measure to a traditional corrosion allowance method, is about 50 years, which is equivalent to the design service life of the facility. However, since the lifespan of anodes varies depending on environmental conditions, it is necessary to check the mass of the anodes and measure the effect of cathodic protection with a potentiometer, and take appropriate countermeasures based on those checks and measurement results to ensure that the anodes function properly during the design service life. Therefore, this part is classified as Maintenance Level II, which involves preventing anomalies by planning to implement preventive maintenance measures at the design stage.
Seabed ground		III	Although the seabed ground is an important member, it is difficult to set deterioration prediction items or predict deterioration. Therefore, the seabed ground is classified as Maintenance Level III, which assumes that maintenance countermeasures will be implemented before a member becomes unable to satisfy its performance requirements.
Fenders Bollards		III	These components are classified as Maintenance Level III, which assumes that breakdown maintenance countermeasures will be implemented before a member becomes unable to satisfy its performance requirements.

2. Hydraulic Engineering Field

2.1 Techniques for Calculating Wave Transformation

2.1.1 Calculating wave transformation by the Boussinesq equation

(1) Overview

When designing port facilities, it is generally necessary to assume most unfavorable waves to the structural stability or use of the facilities considering wave transformations such as refraction, diffraction, wave shoaling and wave breaking associated with the propagation of deepwater waves. The model using the energy balance equation for refraction and wave shoaling outside a port as well as the one using the Helmholtz equation for diffraction and reflection inside a harbor are well known as numerical calculation models for such wave transformations in shallow water.^{1,2} On the other hand, the Boussinesq equation, which is categorized as a time-dependent wave equation and has all the characteristics of the above mentioned such equations, can also consider the nonlinearity or dispersibility that characterizes wave transformations to some extent. Therefore, since the development of numerical calculation models using the Boussinesq equation was actively promoted in Japan in the 1990s, the equation is now widely used to calculate waves in the design of port facilities. One of those models is the Boussinesq model NOWT-PARI, which was developed by the Port and Airport Research Institute, National Institute of Maritime, Port and Aviation Technology (a National Research and Development Agency)³. A schematic illustration of wave transformation calculation using the NOWT-PARI model is shown in **Figure. 3.2.1.1**.

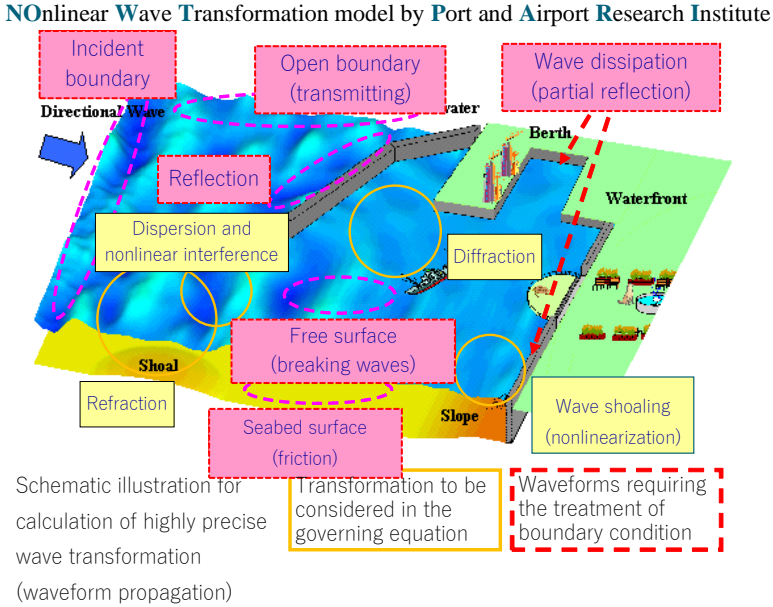


Figure. 3.2.1.1 Schematic illustration of wave transformation calculation using the Boussinesq model (NOWT-PARI)

(2) Need for boundary treatment

At the wave-generating boundary, waves should enter the calculation area obtained by demarcating a certain part of the sea area. At this time, it is necessary to give offshore waves with appropriate directional wave spectrum shapes, which are regarded as multi-directional random waves, by applying the wave-generating theory⁴ used in serpent-type wave generators installed in plane wave tanks. An open boundary is

set to prevent re-reflection of waves transmitted from the calculation area to offshore at the area boundary. A method that dissipates transmitted waves by placing a sufficiently wide sponge layer around the calculation area is often used in the Boussinesq model.

In the calculation area, a reflecting boundary is set at the boundary between the land and water. A common practice is to place an appropriately wide sponge layer⁵⁾ to approximate the characteristics of wave reflection by wave-dissipating structures at the land-water boundary, excluding vertical walls for which the reflectance is assumed to be 1. For wave absorbing work using wave-dissipating blocks, when parameters such as the block dimension, the porosity and the slope shape are set, a porous layer that can reproduce appropriate reflectance depending on the incident waves may be placed. Wave height attenuation and reduction of reflected waves by slopes or the beach topography is reproduced by using the wave breaking and run-up boundary and treating the bottom friction boundary.

The wave breaking boundary is generally modeled so that wave attenuation occurs once waves are judged to be breaking. In this case, the calculation methods are largely divided into a method that assumes the shape of a breaker and specifies the area affected by the dispersion of momentum or energy^{7),8),9)}, and a method in which a turbulence equation is solved to determine the dispersion range of energy^{10),11)}. A recent trend in research in other countries has centered on application of a method that reflects sudden wave field changes when waves break in difference calculations in order to express the attenuation of breaking waves.

Calculation methods for the wave run-up boundary are largely divided into those^{9),13)} that set a slot or a porous layer in the slope to ensure a significant water depth with a calculation grid near the shoreline, and others¹¹⁾ that switch between the water grid and the land grid depending on the presence of a significant water depth. The former can be substituted by giving a sufficiently small value to the porosity of the porous layer used at the reflection boundary,¹⁴⁾ and the latter is also applied to calculations of overtopping waves for revetments and coastal levees^{15),16)}.

For the bottom friction boundary, the flow is generally assumed to be turbulent with large Reynolds number, and the frictional resistance at the wall surface is often modeled as being proportional to the square of the flow velocity⁷⁾.

(3) Calculation methods and scope of application

When waves used in the design of a port facility are calculated using the Boussinesq model, it is necessary to set the range of the calculation area so as to ensure appropriate reproduction of the wave transformation to be considered and to determine the appropriate boundary conditions. It is necessary to set a sufficiently fine differential grid interval and differential time interval to reduce errors or destabilization of the finite differential calculation with consideration of the load on the computer (computation time or memory capacity) required for the finite differential calculation of wave propagation. If the calculation area is too large or appropriate boundary conditions cannot be set, it is necessary to consider reducing the calculation load or compensating for wave transformation reproducibility by combining the Boussinesq model with some other wave transformation calculation method^{17),18)}.

It is advisable to set the computational region which has the wave-generating boundary where the directional wave spectrum obtained from wave observations or wave prediction is input and includes the port facility as calculation target in the effective wave-generating area of multi-directional random waves. It is also advisable to assign an open boundary at least in the offshore side and lateral side of the calculation area.

When preparing the mesh data of water depth and bathymetry for the calculation area, a seabed topographic chart with a spatial resolution appropriate for the differential grid interval should be used. In cases where the water depth is comparatively shallow relative to the height or length of the target waves, appropriate treatment of the wave breaking boundary, wave run-up boundary and bottom friction boundary is required.

When calculating waves related to factors that affect the use of port facilities, such as harbor calmness, it is necessary to set a reflection boundary along barriers such as breakwaters and revetments and to properly reproduce wave transformations such as diffraction, reflection, propagation and transmission. On the other hand, when calculating waves related to the structural stability of port facilities, it is recommended to set a non-reflective boundary behind the target port facility, rather than as a reflective boundary, so that the wave parameters can be obtained as progressive waves considering the influence of the seabed and the surrounding bathymetry. However, when the inundation due to wave overtopping and drainage processes in the area behind a revetment or other structure are directly calculated using the Boussinesq model in conjunction with a wave transformation calculation, a new wave overtopping and drainage boundary that can appropriately represent the inflow and outflow of the overtopping water masses may be introduced and set.

2.1.2 Setting of swell-like waves

(1) Overview

In verifying the performance of a port facility, wave conditions such as the wave height, period and direction must be set appropriately. These wave conditions should be set by using a statistical analysis based on long-term wave observation data. When sufficient wave observation data are not available, the common practice is to supplement the data with a wave hindcasting. Here, it is recommended that the wave return period also be set for swells in order to properly take account of swells with a longer period than the waves typically considered in conventional designs. More specifically, the recommended procedure is to extract the peak wave height of the swell by focusing on the period and wave steepness, consider the probabilistic wave height obtained by statistical processing of extreme waves as design deepwater waves of the swell when deemed necessary, perform model experiments or wave transformation calculations for the design tide level in order to conduct a performance verification.

(2) Deepwater wave parameters of swells

NOWPHAS (Nationwide Ocean Wave information network for Ports and HARbourS), which includes data accumulated for more than 40 years in some cases, is a useful collection of wave observation data for estimating design deepwater waves. One of the characteristics of NOWPHAS is the availability of only one set of wave parameters that represents any given hour based on a 20-minute long statistical analysis of wave data measured every 2 hours or 20 minutes. However, since wind waves and swells generally coexist in the wave data observed at any given time, it is normally impossible to extract only the swell conditions from these data. Therefore, a practical solution is provided in the form of an extraction criterion (**Figure. 3.2.1.2**) which, for convenience, regards waves with a significant wave period of 8 s or more and a wave steepness of less than 0.025 as swells. For example, when this extraction criterion is applied to continuous observation records for 7 to 8 years at eight representative locations on the Japanese coast, it gives a swell occurrence ratio of 30 to 50 % on the Pacific coast and less than 10% on the Japan Sea coast, and it has been confirmed that these results are qualitatively consistent with the swell arrival trend along the Japanese coast¹⁹⁾.

As in the case of conventionally defined high waves without differentiation between wind waves and swells (hereinafter called "all waves"), when extracting high waves caused by swells, the peak wave height for swells among each representative storm should be extracted as a single extreme value dataset. When the peak wave height of all waves exists separately, it should be considered that wind waves and swells coexist in a single representative storm. For the extreme value data for all waves or swells thus obtained, when the occurrence ratio of high waves generated by swells among the total number of these data is calculated, the result is equal to the occurrence ratio of swells that appeared during the above-mentioned observation period on the Pacific side of Japan, but on the Japan Sea side, the calculated value tends to be more than twice as large as the observed values at each location (Akita and Tottori). This indicates that swells that rarely occur on the Japan Sea side tend to emerge as high waves²⁰.

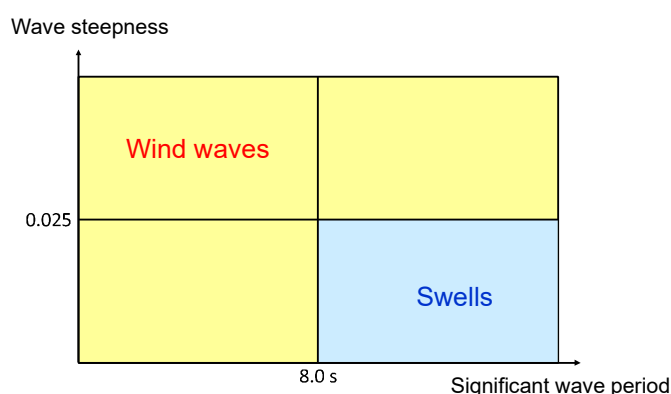


Figure. 3.2.1.2 Swell extraction criterion

The parameters of probabilistic waves can be obtained for all waves and swells by extreme statistical analysis of each of these extreme value data. When the wave data, including data obtained every 2 hours, for 11 to 22 years at the above-mentioned eight representative locations were subjected to extreme statistical analysis by wave direction, the resultant 50-year probabilistic wave height of swells was lower than the 50-year probabilistic wave height of all waves corresponding to the conventional design deepwater waves at all locations and for every wave direction¹⁾. However, the differences between wave heights of all waves and swells on the Pacific coast facing the ocean (Tomakomai, Kashima, Kochi) were relatively small. Considering the wave transformation characteristics of swells with a long period and high directional concentration, it should be noted that the wave-exciting force of swells that acts on port facilities may be larger than that of conventional design deepwater waves.

(3) Calculation of swell propagation and transformation

Because of their longer period and wavelength, swells are more susceptible than wind waves to deformation by the deeper bathymetry. For this reason, the deepwater boundary where swell propagation and transformation calculations start should generally be set far offshore from the port facilities, but this will increase the computational load in wave transformation calculations using the Boussinesq equation (see 2.1.1). Therefore, it is advisable to consider conducting coupling calculations²⁾ with a wave spectrum method, represented by third-generation wave hindcasting models (such as WAM, SWAN, and WW III) and energy balance equation methods, at the offshore boundary of the Boussinesq model set at an arbitrary water depth. When using these coupling calculation methods, the multi-directional random waves for all different

directional spectra on the connection boundary calculated by the wave spectrum method on the offshore side are generated by the single-summation method and are incident with wave absorbing method to the Boussinesq model on the shore side. Therefore, the connection boundary should be set in a sea area where there is no significant difference in the respective wave transformation results calculated by the two models.

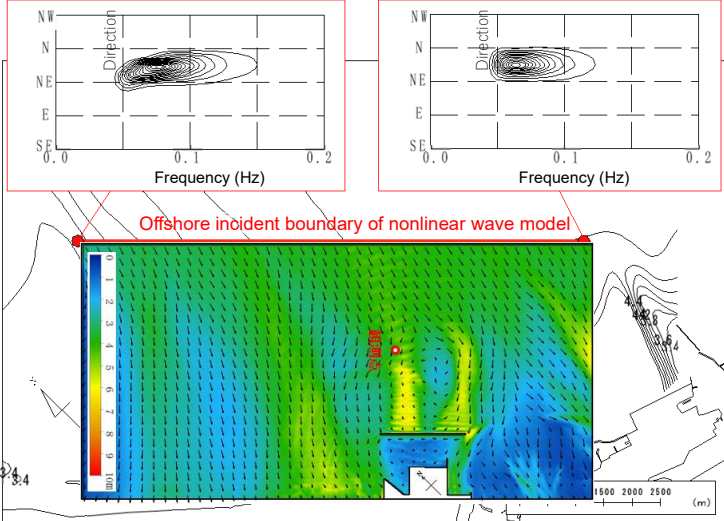


Figure. 3.2.1.3 Example of a coupling calculation using the wave spectrum method and Boussinesq model

2.2 Determination of Wave Forces

2.2.1 Wave force formulas used in performance verification and their changes

(1) Overview

Technical Standards and Commentaries for Port and Harbour Facilities in Japan (2018) (TSCPHF) categorizes and explains wave forces as shown in **Figure. 3.2.2.1**. Port and harbor structures include wall-type structures such as breakwaters and revetments and column-type or horizontal-plate-type structures such as piled piers, and it is necessary to calculate the wave forces acting on each type of structure. Since the components of those structures include armor protection work and wave-dissipating work, their stability against waves is also an important factor. This section discusses formulas for calculating the wave forces acting on upright walls and their changes.

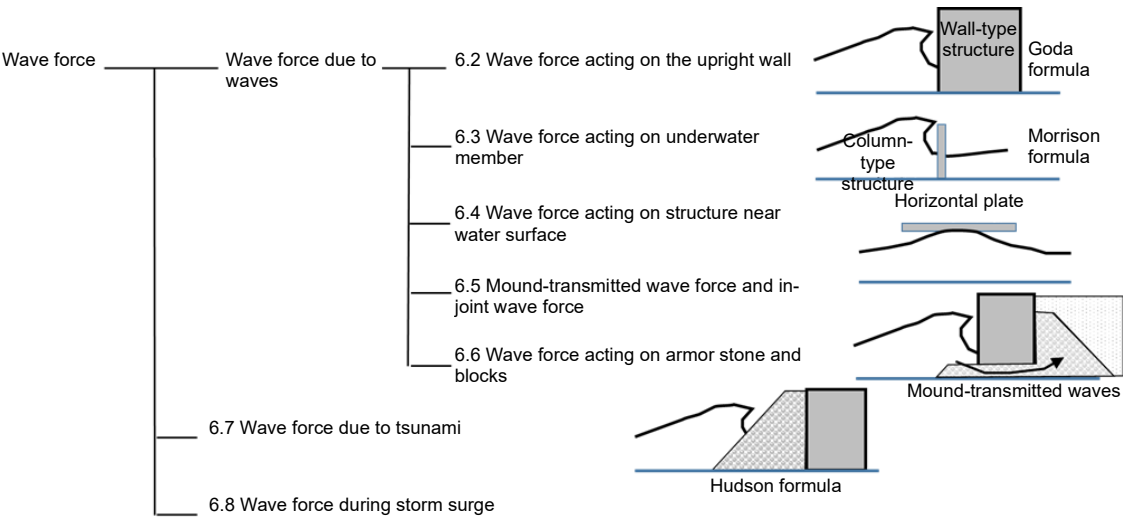


Figure. 3.2.2.1 Classification of Wave Forces

(2) Wave forces acting on upright walls

Wave forces acting on upright walls such as breakwaters and revetments are currently calculated by using the Goda formula. Before the Goda formula was proposed in 1973, wave pressure formulas such as the Sainflou formula, Minikin formula, and Hiroi formula were used to calculate wave force. However, the Goda formula (1973) has been widely used since it was first proposed. The original formula was developed based on the finite amplitude standing wave theory, the results of hydraulic model experiments on wave pressure and examples of damaged and undamaged breakwaters in the field. The formula is characterized by its ability to calculate wave forces under a wide range of conditions, from the region before wave breaking (standing wave region) to the region after wave breaking. Another feature is its use of maximum wave height (H_{max}) based on the concept of random waves. By systematizing various parameters of irregular waves, the Goda formula has made it possible to calculate the wave forces acting on upright walls more rationally for random waves, as in the case of the overtopping discharge rate calculation method.

Today’s Goda formula is the result of changes over the years, which include the incorporation of the impact of the wave direction β by Tanimoto et al. (1981) in the form of $(1 + \cos\beta)/2$ and the addition of the impulsive breaking wave force coefficient by Takahashi et al. (1992). The Goda formula is also applied to wave force calculation formulas for deformed breakwaters such as perforated wall caissons, sloping top caissons and breakwaters covered with wave-dissipating blocks. The Tanimoto formula, which is used to calculate tsunami

wave forces, is also an extension of the Goda formula.

(3) Wave force of Tsunami

The Tanimoto formula was proposed after the 1983 Nihonkai-Chubu Earthquake tsunami as a formula for calculating the tsunami wave forces acting on upright walls. In this formula, the wave forces acting on the front of a wall structure can be calculated by using Goda formula when the wave length is very long. The Tanimoto formula is also designed to consider cases after the water level behind the breakwater falls during receding tsunami. During the 2011 Great East Japan Earthquake, there were many cases where caissons slid due to tsunami overflow water overtopping breakwaters, and inland tsunami protection walls were damaged by the tsunami run-up. Therefore, as a result of many experiments, a formula for calculating the wave pressure due to tsunami overflowing and a formula for calculating the wave forces due to tsunami run-up waves were proposed and incorporated in TSCPHF.

2.2.2 Determination of wave force based on numerical analysis

With the evolution of computers, there has been an active movement toward the use of numerical analysis to calculate wave forces and overtopping waves. As a pioneering effort in that movement in Japan, the numerical simulation CADMAS-SURF was released in 2001. A number of verifications have been carried out on the calculation of wave forces on upright walls and the relevant overtopping discharge rates, resulting in significant improvements in the calculation code, and CADMAS-SURF/3D was released in 2010.

When designing breakwaters and revetments, wave forces and wave overtopping discharge rates are the most important items to consider. However, it is often difficult to estimate these items in facilities with complex shapes by Goda's wave force formula or overtopping discharge rate calculation charts. Although numerical analysis is a very useful tool for such cases, there are some difficulties in estimating the breaking wave force by numerical analysis, including spike noise that may be misinterpreted as wave force. Thus, accurate estimation of breaking wave force is still a challenge. In attempting to estimate the wave overtopping discharge rate, the results of estimations by numerical analysis are in good agreement with the experimental results when the overtopping discharge rate is large, but estimates tend to be lower than the actual value when the rate is small. Therefore, in design work, numerical analysis should be used in conjunction with hydraulic experiments.

In addition to CADMAS-SURF, several other numerical codes have been developed in recent years. For instance, OpenFOAM is often used in the grid method, and codes such as DualSPHysics and PARISPHERE have also been developed for the particle method and are expected to enjoy greater use in the future. However, each code has its own advantages and disadvantages. As with CADMAS-SURF, these codes should be used in combination with experiments to fully evaluate their performance before they are applied to design.

-
- 1) Karlsson, "Refraction of continuous ocean wave spectra," *J. Waterways and Harbors Division*, ASCE, Vol. 95, pp. 437–448, 1969.
 - 2) Takayama, T.: "Wave Diffraction and Wave Height Distribution inside a Harbor," *Report of the Port and Harbour Research Institute*, Vol. 30, No. 1, pp. 21–67, 1981.
 - 3) Hirayama, K.: "Utilization of Numerical Simulation on Nonlinear Irregular Wave for Port and Harbor Design," *Technical Note of the Port and Airport Research Institute*, No. 1036, p. 162, 2002.
 - 4) Takayama, T. and Hiraishi, T.: "Experimental Characteristics of Random Waves Generated by the Serpent Type Wave Generator —The short-crested wave generator in the Offshore Structure Experimental Basin—," *Report of the Port and Harbour Research Institute*, Vol. 26, No. 3, pp. 37–83, 1987.
 - 5) Cruz, E., Yokoki, H., Isobe, M. and Watanabe, A.: "Nonreflecting Boundary for Nonlinear Wave Equations," *Proceedings of*

- Coastal Engineering*, Vol. 40, pp. 46–50, 1993.
- 6) Hirayama, K. and Hiraishi, T.: "Development of partial reflection boundary with porous layer for Boussinesq type wave model," *Report of the Port and Harbour Research Institute*, Vol. 40, No. 1, pp. 3–30, 2001.
 - 7) Sato, S. and Kabling, M.: "Numerical Calculation of Three-dimensional Beach Deformation Using the Boussinesq Equation," *Proceedings of Coastal Engineering*, Vol. 40, pp. 386–390, 1993.
 - 8) Schaffer, H.A., Madsen, P.A., and Deigaard, R. "A Boussinesq model for waves breaking in shallow water," *Coast. Engng.*, 20, pp. 185–202, 1993.
 - 9) Kennedy, A.B., Chen, Q., Kirby, J.T., and Dalrymple, R.A. "Boussinesq modeling of wave transformation, breaking, and runup. I: 1D," *J. Wtrwy., Port, Coast., and Oc. Engng.*, Vol. 126, ASCE, pp. 48–56, 2000.
 - 10) Ohya, T and Hasebe, M.: "Modeling of Wave and Current Fields in a Breaking Zone Considering Vorticity Supply by Breaking Waves," *Proceedings of Coastal Engineering*, Vol. 48, pp. 121–125, 2001.
 - 11) Hirayama, K. and Hiraishi, T.: "Method for Calculating Wave Breaking and Run-up by a Boussinesq Model and Its Applicability," *Proceedings of Coastal Engineering*, Vol. 51, pp. 11–15, 2004.
 - 12) Shi, F., Kirby, J.T., Harris, J.C., Geiman J.D., and Grilli, S.T. "A high-order adaptive time-stepping TVD solver for Boussinesq modeling of breaking waves and coastal inundation," *Ocean Model.* 43–44, 36–51, 2012.
 - 13) Madsen, P.A., Sorensen, O.R., and Schaffer, H.A. "Surf-zone dynamics simulated by a Boussinesq-type model. Part II. Surf beat and swash oscillations for wave groups and irregular waves," *Coast. Engng.*, 32, pp. 289–319, 1997.
 - 14) Hirayama, K.: "Improvement of Porous Layer Boundary on Boussinesq-type Wave Transformation Model," *Proceedings of Civil Engineering in the Ocean*, Vol. 22, pp. 241–246, 2006.
 - 15) Hirayama, K., Hasegawa, J., and Hasegawa I.: "Numerical Calculation of Irregular Wave Overtopping by a Boussinesq Model Considering Overtopping," *Proceedings of Coastal Engineering*, Vol. 53, pp. 706–710, 2006.
 - 16) Hirayama, K. and Hasegawa, I.: "Calculation for Wave Overtopping and Inundation by Using Boussinesq-type Wave Transformation Model," *Journal of JSCE B3 (Ocean Development)*, Vol. 67, No. 2, pp. I_262–I_267, 2011.
 - 17) Hirayama, K., Iwase, H., and Kashima, H.: "Generation and Characteristics of Random Waves for Distribution of Directional Spectra on Variable Bathymetry," *Report of the Port and Airport Research Institute*, Vol. 51, No. 1, pp. 3–22, 2012.
 - 18) Hirayama, K. and Nakamura, T.: "Discussion on Real-time Estimation of Vertical Distribution of Horizontal Velocities for One-way Coupling from NOWT-PARI to CADMAS-SURF/2D," *Report of the Port and Airport Research Institute*, Vol. 54, No. 2, pp. 3–30, 2015.
 - 19) Hirayama, K., Kashima, H., Itsui, M., and Naruke, T.: "Consideration for Probability of Extreme Swell Occurrences and Characteristics of Their Regional Distribution," *Journal of JSCE B2 (Coastal Engineering)*, Vol. 71, No. 2, pp. I_85–I_90, 2015.
 - 20) Hirayama, K., Iwase, H., and Kashima, H.: "Generation and Characteristics of Random Waves for Distribution of Directional Spectra on Variable Bathymetry," *Report of the Port and Airport Research Institute*, Vol. 51, No. 1, pp. 3–22, 2012.

2.3 Setting of Actions Related to Tsunamis and Storm Surges

2.3.1 Verification for tsunamis

(1) Overview

Japan is located where several plate boundaries meet and has many volcanoes. It is also one of the world's most tsunami-prone regions. Therefore, in areas where tsunamis are prominent, one of the tsunamis that occurred in the Meiji Era (1868~1912) or later, where a relatively large amount of objective data remains, has been selected as the “design tsunami,” and disaster “prevention” countermeasures have been taken using such facilities as levees and seawalls to stop inundation. However, the tsunami following the Great East Japan Earthquake¹⁾ in 2011 greatly exceeded the height of those facilities, causing unprecedented human and material damage.²⁾ This disaster made Japan focus on various means of “disaster mitigation.” Specifically, these include estimating the “largest-class tsunami” by using a multitude of scientific methods such as surveying existing flood trace heights, examining descriptions in ancient documents and analyzing sediments; providing “resilience” to facilities against an “excess design tsunami” in order to delay the start of inundation and reduce the area prone to inundation; and combined use of structural measures such as breakwaters and seawalls and nonstructural measures such as evacuation. In other words, the new focus is on verifying the performance of each facility against both the “design tsunami” and the “excess design tsunami.”

(2) “Design tsunami” and “excess design tsunami”

To establish measures against tsunamis, a “frequently-occurring tsunami” and the “largest-class tsunami” in the region should be set first. Then, the “design tsunami” and an “excess design tsunami” should be identified in this range according to the importance of the facility. A “frequently-occurring tsunami” is defined as one that occurs once in several tens of years to around 150 years, and should be determined based on recent tsunamis for which objective data are relatively abundant, as well as tsunamis generated by scenario earthquakes in seismically blank areas. The “largest-class tsunami” should be defined by analyzing historical data, tsunami deposits and the coastal topography as far back as possible and conducting a wide range of data organization and analysis from the perspective of disaster prevention in the region, considering all possibilities. These tsunamis should be defined through sufficient coordination with local port authorities, coastal management bodies and other stakeholders so that they are consistent with local disaster management plans.

(3) Concept of tsunamis to be used for performance verifications of facilities

The “design tsunami” and “excess design tsunami” should be used for performance verifications of a facility. The “design tsunami,” as its name suggests, is used to verify the stability of the facility. The “excess design tsunami” is defined to verify that the facility can “resiliently” maintain stability through structural measures. In this context, “resilience” means that a seawall will not collapse even if hit by overtopping waves, thereby mitigating inundation by the tsunami, and a breakwater will not deform significantly, even under overtopping waves, and will generally maintain its ability to suppress waves, ensuring harbor calmness and contributing to the quick restoration of the region.

The “frequently-occurring tsunami” should be set as the “design tsunami.” However, for extremely important facilities such as power plants and facilities that protect areas where people, assets and industries

are extremely concentrated, it is still necessary to consider the “largest-class tsunami” when setting the “frequently-occurring tsunami.” The “excess-design tsunami” should be appropriately set within the range of definitions up to that of the “largest-class tsunami,” taking into account the costs of structural concepts and their effects.

It is also important to consider the changes in the settlement, deformation and residual strength of the facility induced by seismic motion and crustal movement caused by the earthquake.

2.3.2 Verification for storm surges

(1) Overview

Since Japan is located in the path of typhoons and extratropical cyclones and many of its inner bays are wide and shallow, the country has suffered many large storm surge disasters. For this reason, the design tide levels of facilities where storm surge must be considered are generally based on either (i) the highest high-water level or (ii) the mean monthly highest water level plus the past maximum tide anomaly or the tide anomaly estimated by using the model typhoon. As the model typhoon in (ii), the Isewan Typhoon of 1959 or any typhoon of equivalent scale is assumed for Tokyo Bay, Ise Bay and Osaka Bay³⁾. However, Typhoon Haiyan, which was much stronger than the Isewan Typhoon, caused a remarkable storm-surge event⁴⁾ in the Philippines in 2013. This led to a growing concern about changes in typhoon characteristics due to climate change⁵⁾, and increased recognition of the need for disaster mitigation against the “tide level exceeding the design tide level.” “Tide level exceeding the design tide level” is a new concept that was recently added in the 2018 revision of TSCPHF. Application of this new concept is expected to increase in the future.

(2) Design tide levels for storm surge protection facilities

The design tide level for storm surge protection facilities should be set as the most dangerous level between the mean monthly-lowest water level and the design “high” tide levels shown below. For the crown height, the design “high” tide level is taken as the design tide level.

[Design “high” tide levels]

- (i) Highest high-water level + some margin if necessary
- (ii) Mean monthly highest water level + past largest tidal level anomaly or tidal level anomaly estimated by using the model typhoon
- (iii) Tide level for a certain return period in the occurrence probability curve of past abnormally high tide levels
- (iv) Tide level considering the construction cost of the facility, the occurrence probability of abnormally high tide levels and the cost of damage to the hinterland

Each of these setting methods has advantages and disadvantages. For example, (i) is simple but requires data accumulated over a long period of time. Currently, (i) and (ii) are commonly used, although neither method provides a clear return period. The return period for (iii) is clearly defined but this method may lack reliability unless long-term data are available, and (iv) is an ideal method for project evaluation, but it is difficult to estimate the cost of damage.

The crown height of the facility should be determined for the worst-case condition where the design high-tide level and the design wave occur simultaneously. If the crown height becomes excessive, the design high tide level may be reconsidered based on the frequency of the simultaneous occurrence of a high astronomical

tide, the peak of the storm surge height and the peak wave height.

(3) Tide level set for accidental waves

Port facilities should not only maintain stability against variable waves (generally, 50-year-return waves in Japan) and the design tide level, but also mitigate waves within the harbor and flooding of the hinterland in case of “accidental waves” that are more severe than the above-mentioned waves and their corresponding “tide levels exceeding the design tide level.” The first step in setting the “tide level exceeding the design tide level” is to determine the “largest-class typhoon or extra-tropical cyclone” for the target region based on the record of meteorological disturbances of the country and the development limit of typhoons pursuant to meteorology. (This type of event corresponds to the “largest-class tsunami” in performance verification against tsunamis.) After this first step, the changes with time in tide levels and waves are estimated, in tide levels including storm surges as well as waves for several scenarios consisting of different routes, maximum wind velocity radii, travel speeds and other parameters of typhoons or extra-tropical cyclones as close as possible to those in the largest class. As a result, the tide level that causes the most severe damage to the port is selected as the “tide level exceeding the design tide level,” while also considering construction costs and facility expenses. It is desirable to make sure that the return period of that tide level and waves is sufficiently long by using extreme statistical analysis of the observed data, a stochastic typhoon simulation, etc.⁶⁾

(4) Impacts of rising mean sea level and countermeasures

As the sea level rises due to climate change, a facility may lose its stability, be exposed to inundation and/or become subject to restrictions on the use of under bridge routes due to reduced clearances. The solutions to the impacts of rising sea levels include developing new facilities, improving existing facilities, changing land use and enhancing the disaster prevention system. Adaptive measures that take into account the natural conditions and social characteristics of each region are necessary. When building or renewing a facility, it is advisable to review the content or cost of the countermeasures to be taken, the timing of implementation, their impacts on the surrounding environment and other factors in light of the results of sea-level monitoring and the latest future projections for sea level rise.

-
- 1) Kawai, H., Satoh, M., Kawaguchi, K. and Seki, K.: Characteristics of the 2011 Tohoku tsunami waveform acquired around Japan by NOWPHAS equipment, Coastal Engineering Journal, World Scientific Publishing Company and Japan Society of Civil Engineers, Vol. 55, No. 3, 2013.
 - 2) Tsunami Disasters in Ports due to the Great East Japan Earthquake (Appendix to Report No.112: Mitigation of Tsunami Disasters in Ports), PIANC Report No. 122, 2014.
 - 3) Kawai, H.: Lessons learned from storm surge disasters and technical issues on countermeasures in Japan, Proceedings of 29th International Ocean and Polar Engineering Conference (ISOPE2019), ISOPE, Vol. 3, pp. 3713-3720, 2019.
 - 4) Kawai, H., Seki, K. and Fujiki, T.: Storm surges in Leyte Gulf, Philippines caused by 2013 Typhoon Haiyan and major typhoons with similar tracks, Proceedings of the 24th International Offshore and Polar Engineering Conference (ISOPE2014), Vol. 3, pp. 845-852, 2014.
 - 5) Special report on the ocean and cryosphere in a changing climate, Intergovernmental Panel on Climate Change, 2019.
 - 6) Kawai, H., Hashimoto, N. and Matsuura, K.: Estimation of extreme storm water level in Japanese bays by using stochastic typhoon model and tide observation data, Proceedings of the 18th International Offshore and Polar Engineering Conference (ISOPE2008), Vol. 3, pp. 497-504, 2008.

2.4 Characteristics of Verifying Reinforcing Embankment of Breakwater

(1) Overview

Breakwaters are constructed to protect port facilities and their hinterland from waves. The composite breakwater, a structure in which concrete caissons are placed on a rubble mound, is a popular type of breakwater and is widely used in Japan, as it is especially suitable for Japanese conditions. In particular, because Japan's coasts are frequently attacked by high waves, breakwaters are constructed to a relatively great depth. Since composite breakwaters have proven useful against heavy seas, they have been widely used in Japan. However, many composite breakwaters were damaged by the unexpected huge tsunami that followed the Great East Japan Earthquake in 2011, and there were many reports of concrete caissons sliding off their mounds. Following the damage inflicted by the tsunami of 2011, many ideas for reinforcing the resilience of composite breakwaters were studied, including the addition of a reinforcing embankment by piling up rubble and concrete blocks behind caissons to increase the resilience of the breakwater. Such reinforcing embankment work is actually underway to reinforce breakwaters. This type of reinforcement makes it possible to construct composite breakwaters which are strong enough to withstand powerful wave forces. TSCPHF provides design methods and notes to assist in proper design of reinforcing embankments, as summarized in the following:

(2) General

Figure 3.2.4.1 is a schematic illustration showing a composite breakwater reinforced by a rubble reinforcing embankment. The cross-sectional design is implemented in order to satisfy the intended performance, based on the height of the reinforcing embankment and the width of the embankment top both being not less than $\frac{1}{3}$ of the caisson height. In particular, when a reinforcing embankment is small, it is desirable to determine the final cross-section through detailed reviews using, for example, centrifuge model testing or finite element analysis. Since a reinforcing embankment is a supplementary countermeasure, the basic rule is that an individual caisson should have action-strength ratio of less than 1.0. In addition, when the water level is different inside and outside the breakwater during tsunami, seepage force acts on the rubble materials of the mound and the reinforcing embankment. Since seepage force reduces the resistance of the reinforcing embankment and the caisson bearing capacity, these effects must be considered in the design.

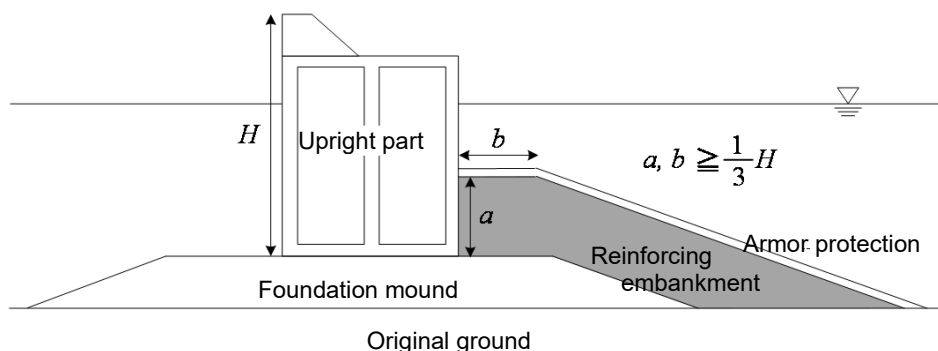


Figure 3.2.4.1 Breakwater with its port side reinforced with rubble

(3) Verification method

When designing a conventional composite breakwater, the sliding and overturning stability of the caisson and the mound bearing capacity (including the reinforcing embankment) need to be verified. The same items

must also be verified when a reinforcing embankment is installed. Since the effect of installing the reinforcing embankment on overturning of the caisson is small, the basic procedure is to disregard the effect of the reinforcing embankment on overturning. However, when a caisson may slide, the reinforcing embankment provides a large resistance force. Therefore, this resistance force is included in the stability verification equation. As shown in **Figure. 3.2.4.2**, a shallow circular slip surface that starts at the bottom-rear corner of the caisson should be assumed, and the resistance force P_{H2max} , which balances the moment, should be determined by the simplified Bishop method and used in the verification equation.

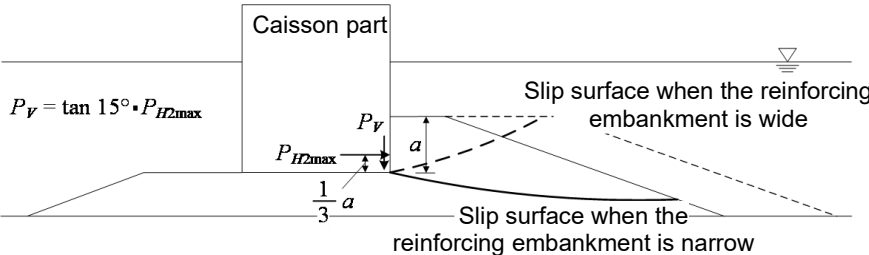


Figure. 3.2.4.2 Shallow slip surface to verify sliding failure

The effect of the reinforcing embankment on the mound bearing capacity should also be taken into account. The bearing capacity is also examined by calculation of circular slip failure using the simplified Bishop method. In this calculation, the reinforcing embankment should be treated as the ground, as in the case of the mound. Here, a deep circular slip surface with a starting point at the bottom of the caisson is assumed as shown in **Figure. 3.2.4.3**. The force from the caisson is considered to be applied not only to the mound but also to the reinforcing embankment, so that both the mound and the reinforcing embankment support the caisson.

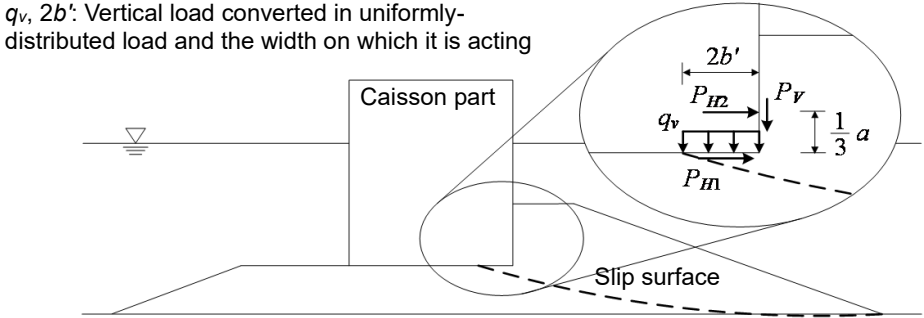


Figure. 3.2.4.3 Deep slip surface to verify bearing capacity failure

2.5 Characteristics of Class 2 Channel Design Method

(1) Overview

TSCPHF provides two design methods for performance verifications related to navigation channels. The first is specification code Class 1 design method, by which the size of a channel is calculated based on the specifications of the design ship. The second is Class 2 design method, which directly considers the ship's maneuverability and navigational conditions (navigational risk factors). A similar classification is also used in PIANC Report No. 121 - 2014, Harbour Approach Channels - Design Guidelines, where the concept design and detailed design in the guidelines in the PIANC Report correspond to Class 1 design method and Class 2 design method, respectively. While, in a sense, Class 1 design method represents a highly versatile "universal formula," Class 2 design method is effective as a tool for assessing detailed navigational risks. Class 2 design method also has other characteristics including the following:

- (i) In Class 2 design method, since it is necessary to incorporate the ship's behavior during navigation in order to evaluate the ship's maneuverability or navigational risk, methods have been developed from a mechanical perspective, incorporating knowledge of ship operation and shipbuilding.
- (ii) At the same time, Class 2 design method requires more condition settings and input information than Class 1 design method in order to verify the performance of the channel design, and the calculation process itself is also complex.
- (iii) Since Class 2 design method can directly consider risk factors such as the wind speed and tidal currents during navigation, the calculated channel specifications tend to be smaller than those obtained by Class 1 design method. Class 2 design method can also determine whether the ship can safely enter an existing navigation channel or not, and if so, the conditions under which it can enter (e.g., wind speed restrictions).

(2) Basic concept for determining navigation channel specifications in Class 2 design method

The elements of a channel design include the channel depth, channel width and channel bends. In Class 2 design method, these specifications are determined based on the following concepts:

The channel depth is primarily determined so that the ship squatting when the ship navigates at a constant speed is absorbed. Because ship squatting reduces the under-keel clearance (UKC) of the ship, which causes a risk in ship navigation, it is necessary to ensure a sufficient channel depth to keep UKC at a certain level.

The channel depth is calculated as the sum of the following elements:

- Draft of the design ship
- Ship squatting at a constant speed (squat)
- Ship motions due to swells
- Additional keel clearance (consideration of risk factors other than the above)

In actual calculations, information on specific ship speeds or swells (swell period, etc.) needs to be input as navigation conditions.

The channel width is determined so that the ship can safely navigate without touching the seabed or sidewalls. This is required because a ship tends to move obliquely due to wind or tidal currents and meander to a certain degree around the planned course as it navigates. In addition, when a ship moves close to the

sidewalls or obstacles or mutually approaches other ships, a certain hydrodynamic force acts on it, creating a risk of collision. To prevent this, "separation distance" is also considered as a factor in channel width. In reality, there are various types of channels, such as single channels and channels that allow ships to cross or overtake each other (Figure. 3.2.5.1). These varying cases may be considered in advance.

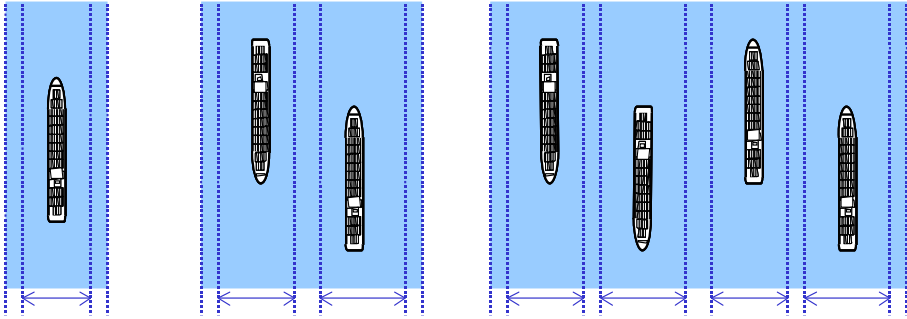


Figure. 3.2.5.1 Examples of channel width setting

Some characteristic elements of Class 2 design method are as follows. First, Class 2 design method provides for oblique navigation of a ship due to wind, where the degree of obliqueness is calculated as a balance of forces, taking into account the ship-related motion equation. In this process, the wind pressure acting on the ship and the interference coefficient of the rudder are considered as navigation conditions and the navigation performance of the ship. Second, in the degree of meandering, the accuracy of the ship's position is considered. For example, if a ship is equipped with a high-performance GPS, it may be reasonable to suppose that the degree of meandering and deviation from the planned course are small. Third, Class 2 design method does not directly consider the motion equation regarding the action against sidewalls, but specifies a safe separation distance in light of experimental results and other knowledge in the field of shipbuilding.

For channel bends, the required radius of curvature is to be determined by using the turning ability factor, which represents a ship's ability to turn. The required radius can be changed depending on the ability of the design ship.

(3) Calculation process

As explained above, in Class 2 design method, the following information needs to be determined, obtained and input according to the circumstances of the target port.

- Navigation conditions, including the wind velocity and direction, tidal current velocity and direction, swell period and direction, water depth, channel shape and the shapes of obstacles around the channel
- Ship information, including the design ship speed, ship specifications (such as draft, length, width and block coefficient), wind pressure area, rudder information (such as the rudder area) and the turning performance factor

Regarding ship information, although highly accurate channel specifications can be set by inputting information about individual design ships, it may be difficult for port stakeholders to obtain such information. Therefore, Class 2 design method provides general input values for typical ships for major types of ships. A channel calculation program (J-Fairway) is also available to improve the ease of calculations. This program is distributed to the relevant domestic and foreign parties.

3. Geotechnical Field

3.1 Strong Ground Motion Observation Network and Setting Input Seismic Motion

(1) Factors influencing seismic motion, especially site characteristics

It is generally understood that seismic motions are determined by three factors: the influence of the rupture process of the causative fault (source effects), the influence of the propagation path from the source to the seismological bedrock (path effects) and the influence of the sedimentary layers which exist on the seismological bedrock (site effects) (Figure. 3.3.1.1). Among these factors, the influence of sedimentary layers on seismic motion is particularly significant. For example, a comparison of the seismic motions observed at several points in and around a major port, Sakaiminato Port (Sakai Port, Tottori Prefecture), during the Western Tottori Earthquake in 2000 showed that the maximum velocity was four times greater at the port observation point located on the sedimentary layer of the Yumigahama Peninsula (Sakaiminato G) and a Japan Meteorological Agency (JMA) observation point than at two National Research Institute for Earth Science and Disaster Prevention (NIED) observation points located at the foot of the Shimane Peninsula (SMN001 and SMNH10)) (Figure. 3.3.1.2).

A strong ground motion observation network covering major ports and harbors in Japan has been established and is now in operation (<http://www.mlit.go.jp/kowan/kyosin/eq.htm>), and as mentioned above, strong ground motion observation is conducted by JMA and NIED. As one of the results, these efforts have clarified the importance of site characteristics.

In Technical Note of the Port and Airport Research Institute No. 1112, the site amplification factor (defined as the effects of sedimentary layers on the amplitude of seismic motion) has been determined for strong ground motion observation sites in various areas including ports and harbors. The results are available in the CD attached to Technical Note No. 1112, as well as on the website of PARI:

http://www.pari.go.jp/bsh/jbn-kzo/jbn-bst/taisin/siteamplification_jpn.html .

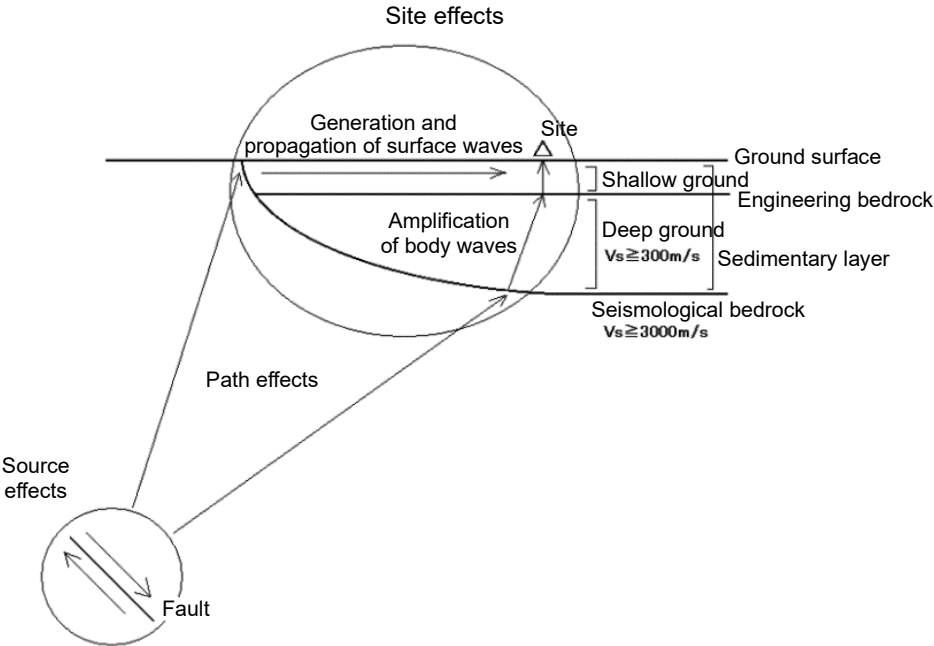


Figure. 3.3.1.1 Source, path and site effects

(2) Input seismic motion considering site characteristics

Given the importance of site characteristics, input seismic motions that reflect the site characteristics of each port and each zone within the port are used in seismic design of port facilities in Japan. This is one of the main characteristics of the design of port facilities in Japan.

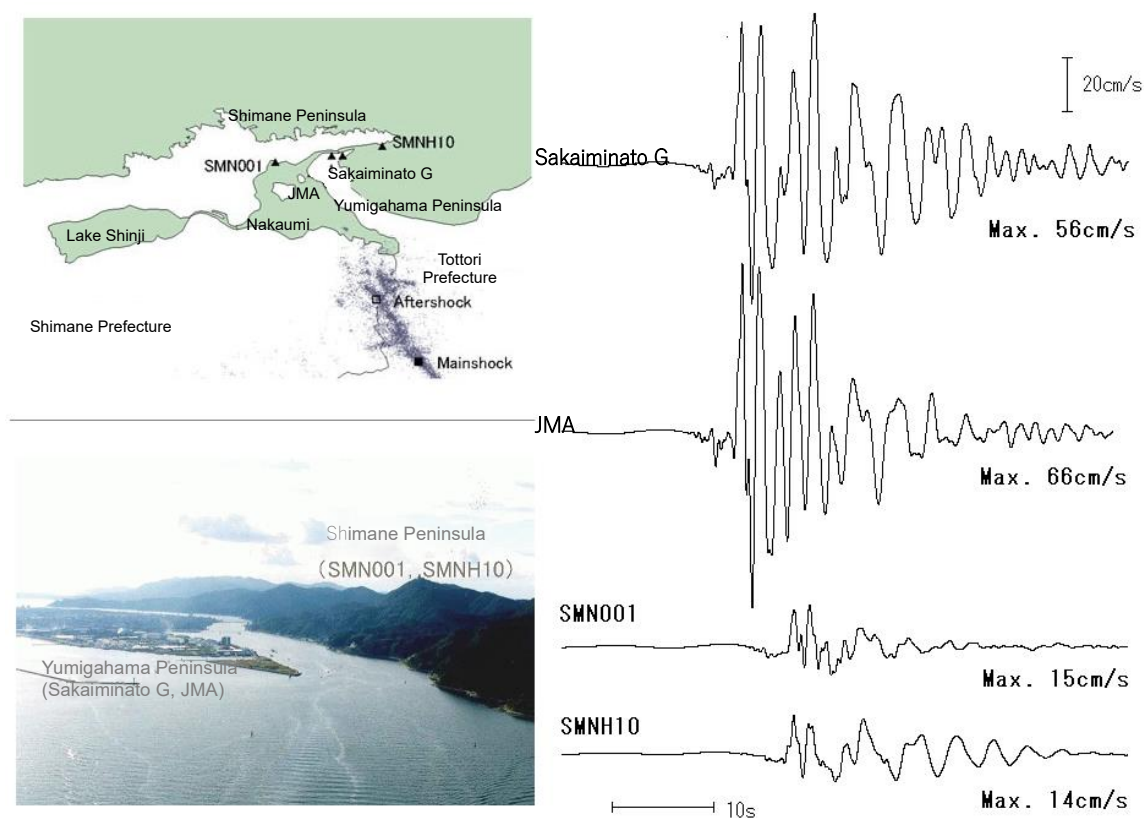


Figure. 3.3.1.2 Topography of the area around Sakaiminato Port and locations of strong ground motion observation stations (left), and the velocity waveforms observed around Sakaiminato Port during the 2000 Western Tottori Earthquake (right)

Two levels of seismic motion, Level 1 and Level 2, are used for verification of seismic design of port facilities in Japan. Level 1 refers to seismic motions with a return period of 75 years and is established by probabilistic seismic hazard analysis considering source, path and site effects. Level 1 seismic motions that reflect the site characteristics of each port and zone have been developed gradually since around 2007 and are available on the National Institute for Land and Infrastructure Management website: <http://www.ysk.nilim.go.jp/kakubu/kouwan/sisetu/sisetu.html>

However, there are cases where it has not been confirmed whether the site amplification characteristics used for calculating Level 1 seismic motions are equivalent to the site amplification characteristics at the location where the target facility is constructed. Therefore, it is necessary to determine whether these characteristics are equivalent based on the results of microtremor observation. Level 2 seismic motions are established based on scenario earthquakes and by calculating strong ground motion waveforms considering source, path and site effects. TSCPHF describes the method of setting the hypocenter parameters. The corrected empirical Green's function method is often used to calculate strong ground motion waveforms based on the source parameters. The calculation program is available in the attached CD of Technical Note of the Port and Airport Research Institute No. 1173 and on the PARI website:

http://www.pari.go.jp/bsh/jbn-kzo/jbn-bst/taisin/sourcemodel/somodel_program.html

In any case, in these evaluations, an accurate grasp of the site characteristics at the location of the target facility is important. Local seismic observation and microtremor observation are useful tools for this purpose, and TSCPHF includes guidelines for their proper use.

3.2 Changes in Performance Verification Methods Based on the Seismic Coefficient Method

(1) Changes in seismic coefficients in port design standards

In the seismic design of port structures, it is necessary to assume in advance the external forces due to seismic motions, i.e., the seismic external forces, that the structures should be able to withstand. Seismic motion is a dynamic phenomenon that changes in a complex manner from moment to moment. Considering the low degree of impact of relatively small seismic motions on a target structure, the complexity of directly incorporating seismic external forces as dynamic forces in the design of the target structure could not be justified economically, and in any case, there was no available calculation environment for achieving it in the past. The solution developed in response to this problem is to convert dynamic seismic external force to the static inertial force acting on the center of gravity of the target structure, namely, the product of the target structure's mass and the acceleration due to the seismic motion, regarding its size and acting direction as time-invariant, and to define the result as “seismic force.” Then, the magnitude of acceleration due to this seismic force is divided by gravitational acceleration, and this is defined as the “seismic coefficient.” Use of these processes has led to simpler seismic design. Seismic force and its seismic coefficient are concepts which were created by Sano (1915¹, 1916²), and the framework for seismic design that combines this approach with the allowable stress method is called the seismic coefficient method.

Seismic design based on the seismic coefficient method was introduced as a legally binding national standard for the first time in Japan in the Regulation for Enforcement of the Urban Buildings Act revised in 1924³). The following Japanese port design standards, which include various standards related to the design of ports and harbors and their facilities, starting from the Handbook of Design Specifications for Port and Harbor Work published in 1950 to the most recently updated edition of TSCPHF, which was published in 2018, are collectively referred to as “port design standards.” These port design standards have been revised approximately once every 10 years to incorporate the results of research in various fields related to ports and harbors, such as structures, materials, waves and geotechnical engineering, available at the time of each revision^{4),5),6),7),8),9),10),11}). Although the values of the seismic coefficient and its calculation method differ in the various standards and versions, the port design standards have been consistently based on a seismic design method that only considers the horizontal seismic coefficient based on the seismic coefficient method. This approach was adopted because the seismic coefficient method is applied to structures with short natural periods and low damping, and major port structures such as gravity-type quaywalls have these characteristics. When the port design standards⁴ were published in 1950, 35 years had already passed since the birth of the seismic coefficient concept, and 26 years had elapsed since the revision of the Regulation for Enforcement of the Urban Buildings Act. Considering this, it can be assumed that the concept of the seismic coefficient method was well known and was familiar to the engineers of that time for various reasons such as its simplicity.

Table 3.3.2.1 shows the changes in the seismic coefficients used in the port design standards. As set values of the seismic coefficient, uniform values ranging from 0.05 to 0.3 were adopted nationwide in the port design standards published in 1950⁴), and were set depending on the hardness of the ground, the importance of the target structure and the geographical conditions. However, the values adopted in the 1959 edition of the Handbook of Port and Harbor Construction Design³) were divided into the three categories of 0.15 to 0.25, 0.05 to 0.20, and 0.00 to 0.10, according to the degree of seismic activity throughout Japan. The seismic

coefficient was then established as a product of the region-specific seismic coefficient, the ground condition factor and the importance factor in the port design standards from the Design Standards for Port and Harbor Structures (1967)⁶⁾ to Technical Standards and Commentaries for Port and Harbour Facilities in Japan (1999)⁹⁾. Region-specific seismic coefficients have been designated; specifically, values based on the seismic coefficient corresponding to the seismic motion with an average return period of 75 years are designated by area with reference to the maximum seismic coefficient expectation distribution chart (Kawasumi, 1951)¹²⁾. This makes it possible to explicitly consider the hardness of the ground at the location where the target port structure is to be constructed or the importance of the target structure. More refined setting of seismic coefficients can now be realized than before the publication of the port design standards in 1959⁵⁾. The value to be multiplied by the seismic coefficient when calculating the actual seismic force was not specified in the port design standards published in 1950⁴⁾, but was assumed to be the self-weight of the target structure. However, the port design standards published in 1959 and 1968^{5),6)} specified it as the sum of the target structure's self-weight and superimposed load. The standards published in 1979⁷⁾ up to those published in 1999⁹⁾ specified the use of a value more disadvantageous to the target structure based on a comparison of the seismic forces for the structure's self-weight alone and for the sum of the structure's self-weight and superimposed load. The port design standards published in 1967⁶⁾ clearly stated that the buoyancy acting on a target structure should not be subtracted when calculating seismic forces, but the apparent seismic coefficient considering buoyancy should be used when calculating earth pressure.

(2) Paradigm shift in the seismic coefficient calculation method in TSCPHF (2007)

The 2007 edition of the port design standards, TSCPHF (2007)¹⁰⁾, showed a major shift from specification-based design, which is the framework of the design method adopted for the conventional port design standards, to performance-based design. This change was adopted in response to the international trend toward using performance-based design standards regardless of the field, as it was Japan's general intention to comply with the Basis of Structural Design for Buildings and Public Works¹³⁾ compiled by the Ministry of Land, Infrastructure, Transport and Tourism in 2002, in order to make the design standards used in various fields in Japan consistent with international standards including ISO and Eurocodes. This followed the regularization in ISO 2394 of the use of the performance-based design approach in structural design, including the design of port structures, based on the WTO Agreement on Government Procurement (GPA) and the Agreement on Technical Barriers to Trade. The basic intention here is to verify the performance requirements for structures based on the reliability-based design method. The edition of TSCPHF published in 2007¹⁰⁾ incorporated this concept in calculations of seismic coefficients, with gravity-type quaywalls and sheet pile quaywalls as the major targets of application. Specifically, TSCPHF (2007) adopted the seismic design method, which allows a certain level of deformation of the target structure even under a small seismic motion, and assures the safety of the structure against the said seismic motion as long as likely deformation of the structure by the expected small-scale seismic motion remains within the predetermined allowable range of deformation. However, one major problem arises here: The seismic coefficient method, which has been adopted in Japan's port design standards, is intended solely to provide the framework for determining static seismic forces regardless of whether the natural period of the target structure is considered or not. Hence, the concept of residual deformation of the target structure is not incorporated in the concept of the seismic coefficient. If the concept of residual deformation of the target structure is introduced into the framework of

seismic design, it is necessary to conduct a dynamic analysis, that is, a numerical analysis in which the dynamic seismic external force is the input and the response of the target structure to it is the output. This, however, would sacrifice the simplicity inherent in the seismic coefficient method, namely the ability to calculate the coefficient manually. To solve this problem, a method was developed to calculate the seismic coefficient from Level 1 seismic motion, which is a dynamic seismic motion predetermined probabilistically by considering the hypocenter properties, propagation path characteristics and site amplification characteristics at the engineering bedrock of each port or each location, as the case may be, according to the specifications of the target structure and the characteristics of the subsurface layer (the soil layer between the engineering bedrock surface and the ground surface)¹⁴. This method was adopted in TSCPHF (2007)¹⁰. By applying a certain signal processing to Level 1 seismic motion on the ground surface, this method can be used to calculate the frequency response characteristics of the target structure to the seismic motion, as well as the seismic coefficient corresponding to the residual deformation of the target structure according to the assumed duration of the seismic motion. In other words, a new framework of the seismic coefficient method that can take into account the residual deformation of structures, which could not be considered by the conventional seismic coefficient method, was introduced as a seismic design method for port structures.

(3) Technical Standards and Commentaries for Port and Harbour Facilities in Japan: Deepening of the seismic coefficient calculation method in 2018

Although TSCPHF (2007)¹⁰ adopted the seismic coefficient method, which enables consideration of residual deformation of the target structure, one major issue still remained. The seismic coefficient calculation formula in the 2007 edition¹⁰ is expressed as a regression equation derived only from the results of a two-dimensional seismic response analysis using FLIP for several types of numerical virtual cross-sections with different structural specifications and surface soil hardness and softness, and several types of input seismic motions. Therefore, there was no verification of whether the seismic coefficient obtained by the seismic coefficient calculation formula was reliable from the perspective of whether there was actual damage, i.e., whether the target structure could withstand actual seismic motion equivalent to Level 1 seismic motion. To resolve this issue, a new method was developed, in which the reliability of the seismic coefficient obtained from the seismic coefficient calculation formula is verified based on actual damage data¹⁵. In this approach, real damage data arising from actual seismic motion equivalent to Level 1 seismic motion acting on actual structures (mainly gravity type quaywalls) is collected, and the data showing whether the target structure suffered deformation beyond the threshold value predetermined by the port design standards under that seismic motion are compared with the results of an analysis of whether the seismic coefficient corresponding to the seismic motion exceeded the seismic coefficient that the target structure can resist in the design calculation. This method is called the damage verification method, and was used to verify the seismic coefficient calculation formula for gravity-type quaywalls in the edition of TSCPHF published in 2007¹⁰. It was then adopted as the seismic coefficient calculation formula in the most recent revision of TSCPHF published in 2018¹¹.

(4) Issues with the damage verification method and prospects for improving the seismic coefficient calculation method in the future

In TSCPHF (2018)¹¹, the reliability of the seismic coefficient obtained from the seismic coefficient

calculation formula in TSCPHF (2007)¹⁰⁾ is verified by using the damage verification method not only for gravity-type quaywalls, but also for sheet pile quaywalls with vertical pile anchorage or coupled-pile anchorage. Ultimately, the seismic coefficient calculation formula used in the 2007 edition was also adopted without modification in the 2018 edition. In fact, good results were obtained for gravity-type quaywalls by damage verification, as more than 90 % of the actual damage and the damage predicted by the design calculation were consistent, showing that the seismic coefficients obtained by the seismic coefficient calculation formula are highly reliable. However, good results were not obtained for anchored sheet pile quaywalls. This difference was due to the scarcity of data for the latter type. While 44 cases of actual damage data were used to verify the damage to gravity-type quaywalls, only 8 were available for sheet pile quaywalls with vertical pile anchorage or coupled-pile anchorage. This scarcity of damage data increased the data variance, and the number of actual damage data was insufficient to accurately judge the reliability of the seismic coefficient calculation formula by the damage verification approach. Although this is presumed to be one of the reasons for the poor results for anchored sheet pile quaywalls, because many anchored sheet pile quaywalls designed based on the seismic coefficient calculation formula have maintained their safety, it was decided that the seismic coefficient calculation formula in TSCPHF (2007)¹⁰⁾ would also be adopted without modification in the 2018 revision¹¹⁾, regardless of the damage verification results. In order to endorse the seismic coefficient obtained from the seismic coefficient calculation formula from the viewpoint of damage verification, in the future, it would be desirable to collect actual damage data for other port structures, such as anchored sheet pile quaywalls, and use the damage verification method to evaluate the reliability of the seismic coefficient obtained from the seismic coefficient calculation formula. Moreover, it would also be desirable to develop a method for modifying the seismic coefficient to improve reliability based on the evaluation.

Figure 3.3.2.1 Topography of the changes in the seismic coefficient in port design standards

Year of publication	Name of design standards	Name of seismic coefficient in the design standards	Region-specific seismic coefficient														Ground condition factor			Importance factor																						
			• Nemuro • Kushiro • Tokachi	Hidaka	• Ishikari • Shiribeshi	• Ibari • Hiyama • Oshima	Soya	Rumoi	Abashiri	• Kamikawa • Sorachi	Pacific side of Tohoku	Sea of Japan side of Tohoku	Ibaraki	• Chiba • Tokyo (other than Hachijo and Ogasawara Islands) • Kanagawa • Shizuoka • Aichi	• Hachijo Island • Ogasawara Island	• Niigata • Toyama • Ishikawa	Fukui	Kyoto	Kinki (other than Kyoto)	Class 1	Class 2	Class 3	Specific	Class A	Class B	Class C																
1950	Handbook of Design Specifications for Port and Harbor Work	Design seismic coefficient	0.05 to 0.30, depending on the hardness of the ground, importance of the structure, or geographical condition																																							
1959	Handbook of Port and Harbor Construction Design	Design seismic coefficient	0.25 to 0.15	0.20 to 0.05			0.10 to 0.00			–	0.20 to 0.05			0.25 to 0.15	0.25 to 0.15	0.20 to 0.05		0.25 to 0.15		–			–																			
1967	Design Standards for Port and Harbor Structures	Design seismic coefficient	0.15	0.10	0.10	0.10	0.05	0.10	0.05	–	0.10	0.10	0.10	0.15	0.15	0.10	0.10	0.15	0.15	–			0.5 to 1.5																			
1979	Technical Standards and Commentaries for Port and Harbour Facilities in Japan (1979)	Design seismic coefficient		–						–										–	–	–	–	–	–	–	–	–	–	–	–	–	–	–	–	–	–	–	–	–	–	–
1989	Technical Standards and Commentaries for Port and Harbour Facilities in Japan (1989)	Design seismic coefficient		0.15						–										–	–	–	–	–	–	–	–	–	–	–	–	–	–	–	–	–	–	–	–	–	–	–
1999	Technical Standards and Commentaries for Port and Harbour Facilities in Japan (1999)	Design seismic coefficient	–	0.11	0.12	0.08	0.11	0.11	0.11	0.13	0.12	0.13	–	0.08	0.12	–	–	–	–	–	–	–	–	–	–	–	–	–	–													
2007	Technical Standards and Commentaries for Port and Harbour Facilities in Japan (2007)	Seismic coefficient for verification	Follow the seismic coefficient calculation formula for verification, in principle.																																							
2018	Technical Standards and Commentaries for Port and Harbour Facilities in Japan (2018)	Seismic coefficient for verification	Follow the seismic coefficient calculation formula for verification, in principle.																																							

Year of publication	Name of design standards	Name of seismic coefficient in the design standards	Region-specific seismic coefficient														Ground condition factor			Importance factor																																				
			• Tottori • Hiroshima	Okayama	Shimane	Yamaguchi	Kochi	Tokushima	Kagawa	Ehime	Fukuoka	• Oita • Miyazaki • Kumamoto	• Saga • Nagasaki (other than Goto, Iki, and Tsushima Islands) • Kagoshima (other than the Amami Islands)	• Goto Islands • Iki Islands • Tsushima Island	Amami Islands	Okinawa (other than the Daito Islands)	Daito Islands	Class 1	Class 2	Class 3	Specific	Class A	Class B	Class C																																
1950	Handbook of Design Specifications for Port and Harbor Work	Design seismic coefficient	0.05 to 0.30, depending on the hardness of the ground, importance of the structure, or geographical condition																																																					
1959	Handbook of Port and Harbor Construction Design	Design seismic coefficient	0.20 to 0.05		0.10 to 0.00			0.20 to 0.05				0.10 to 0.00				–	–	–			–																																			
1967	Design Standards for Port and Harbor Structures	Design seismic coefficient	0.10	0.10	0.05	0.05	0.10	0.10	0.10	0.05	0.05	0.05	0.05	0.05	0.05	0.05	0.05	0.05	0.05	0.05	0.05	0.05	0.05	0.05	0.05	0.05	0.05	0.05	0.05																											
1979	Technical Standards and Commentaries for Port and Harbour Facilities in Japan (1979)	Design seismic coefficient																												–	–	–	–	–	–	–	–	–	–	–	–	–	–	–	–	–	–	–	–	–	–	–	–	–	–	–
1989	Technical Standards and Commentaries for Port and Harbour Facilities in Japan (1989)	Design seismic coefficient																												–	–	–	–	–	–	–	–	–	–	–	–	–	–	–	–	–	–	–	–	–	–	–	–	–	–	–
1999	Technical Standards and Commentaries for Port and Harbour Facilities in Japan (1999)	Design seismic coefficient	0.12	0.11	0.11	0.08	0.13	0.13	0.11	0.12	0.08	0.12	0.11	0.08	0.12	0.11	0.08	–	–	–	–	–	–	–	–	–	–	–	–	–	–																									
2007	Technical Standards and Commentaries for Port and Harbour Facilities in Japan (2007)	Seismic coefficient for verification	Follow the seismic coefficient calculation formula for verification, in principle.																																																					
2018	Technical Standards and Commentaries for Port and Harbour Facilities in Japan (2018)	Seismic coefficient for verification	Follow the seismic coefficient calculation formula for verification, in principle.																																																					

* " – " indicates that it is not mentioned in the port design standards. The background colors of cells are: light purple for a seismic coefficient between 0.05 and 0.10; purple for a seismic coefficient between 0.10 and 0.15; and dark purple for a seismic coefficient not less than 0.15. When the seismic coefficient is indicated in a range of values, the cell background color shown on the left is used according to the class value.

-
- 1) Sano, T.: "Housing Seismic Structure Handbook," Kenchiku Zasshi, Vol. 341, 1915.
 - 2) Sano, T.: "Housing Seismic Structural Theory," Report of Earthquake Damage Prevention Survey Association, 1916, Vol. 83.
 - 3) Regulation for Enforcement of the Urban Buildings Act, Home Ministry, 1924, Chapter 3, Section 2, Structural Strength, 7, Strength Calculation, Article 101-2.
 - 4) Handbook of Design Specifications for Port and Harbor Work, the Ports and Harbours Association of Japan, 1950, p. 27.
 - 5) Handbook of Port and Harbor Construction Design, the Ports and Harbours Association of Japan, 1959, p. 144.
 - 6) Design Standards for Port and Harbor Structures, Ports and Harbours Bureau, Ministry of Transport, 1967, p. 2-9-1-2-9-3.
 - 7) Technical Standards and Commentaries for Port and Harbour Facilities in Japan, 1979, the Ports and Harbours Association of Japan, 1979, p. 2-165-2-168.
 - 8) Technical Standards and Commentaries for Port and Harbour Facilities in Japan, 1989, the Ports and Harbours Association of Japan, 1989, p. 195-196.
 - 9) Technical Standards and Commentaries for Port and Harbour Facilities in Japan, 1999, the Ports and Harbours Association of Japan, 1999, p. 261-264.
 - 10) Technical Standards and Commentaries for Port and Harbour Facilities in Japan, 2007, the Ports and Harbours Association of Japan, 2007.
 - 11) Technical Standards and Commentaries for Port and Harbour Facilities in Japan, 2018, the Ports and Harbours Association of Japan, 2018.
 - 12) Kawasumi, H.: "Distribution of Earthquake Risk in Japan," Bulletin of the Earthquake Research Institute, 1951, Vol. 29, No. 3.
 - 13) Review Committee for the Basis of Structural Design for Buildings and Public Works: Basis of Structural Design for Buildings and Public Works, Ministry of Land, Infrastructure, Transport and Tourism, 2002.
http://www.mlit.go.jp/kisha/kisha02/13/131021_.html
 - 14) Nagao, T., Iwata, N., Fujimura, M., Morishita, N., Sato, H., and Ozaki, R.: "Seismic Coefficients of Caisson Type and Sheet Pile Type Quay Walls against the Level-one Earthquake Ground Motion," Technical Note of National Institute for Land and Infrastructure Management, 2007, No. 310.
 - 15) Fukunaga, Y., Takenobu, M., Miyata, M., Nozu, A., and Kohama, E.: "Validation of present seismic design method for gravity-type and sheet pile quaywalls by past earthquake-induced damage data of port facilities and reproduced seismic ground motions," Technical Note of National Institute for Land and Infrastructure Management, 2016, No. 920.

3.3 Seismic Design Based on Numerical Analysis

3.3.1 Verification of deformation by numerical analysis

(1) Overview

The earthquake-resistant performance design of port facilities specified by TSCPHF was introduced based on the lessons learned from the damage of port facilities caused by the Hyogo-ken Nanbu Earthquake in 1995. This approach requires verification that important facilities (high earthquake-resistant facilities) satisfy performance requirements against two levels of seismic motion, namely, Level 1 and Level 2 seismic motion. The seismic performance verification methods for Level 2 seismic motion, which is the strongest seismic motion estimated to occur at any given location, include numerical analysis and model vibration testing. The general procedure is to conduct deformation verification by a seismic response analysis, which is one of the numerical analysis techniques.

Verifying the deformation of port structures requires an analysis technique that can consider the interaction of the soil-water-structure and the liquefaction behavior of sandy soil by a seismic response analysis. Here, the important point is to confirm the applicability of the analysis method used to verify deformation through reproduction analysis of disaster cases. For example, one of the methods proven to be applicable to port structures such as gravity-type quaywalls is the two-dimensional seismic response analysis program FLIP,¹⁾ which is based on the finite element method and the effective stress method. This section gives an example of reproduction analysis using FLIP.

(2) Applicability of numerical analysis

A gravity-type quaywall at Kobe Port is an application example of reproduction analysis by FLIP. **Figure 3.3.3.1** shows the damage which occurred at the Port of Kobe's Rokko Island, where the caisson tilted with settlement on the sea side, suffering damage that caused a maximum horizontal displacement of 5 m and an average displacement of 3 m in the lateral direction. The waveforms of the vertical array for Port Island at GL-32m were used as the input seismic motion for the analysis. **Figure 3.3.3.2** shows the results of the analysis. The displacement mode of the caisson tilting and sinking into the rubble mound is consistent with the disaster situation, and the liquefaction that occurred in the landfill ground was also consistent with the disaster.

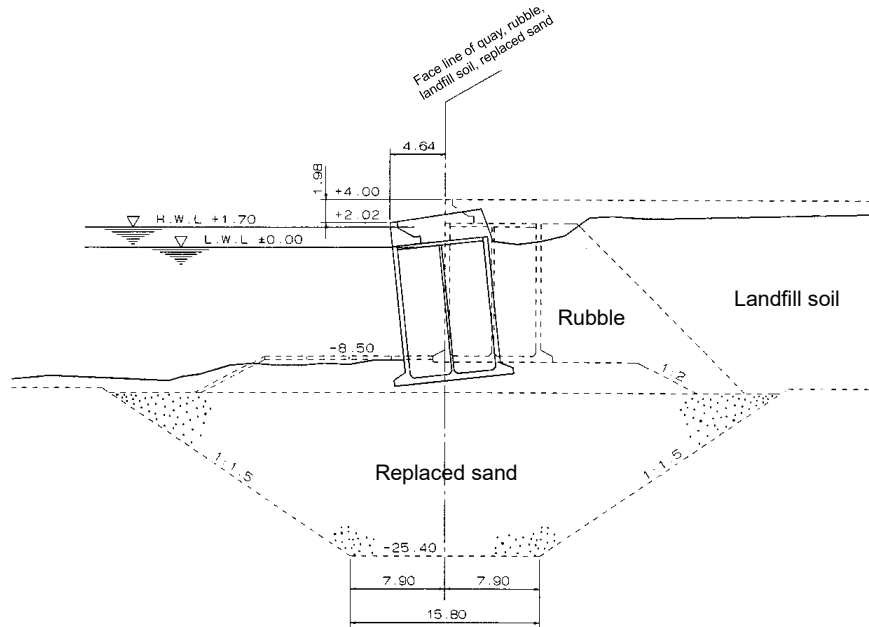


Figure. 3.3.3.1 Cross-section of damage to the RF3 quaywall on Rokko Island, Port of Kobe (water depth: 8.5 m)

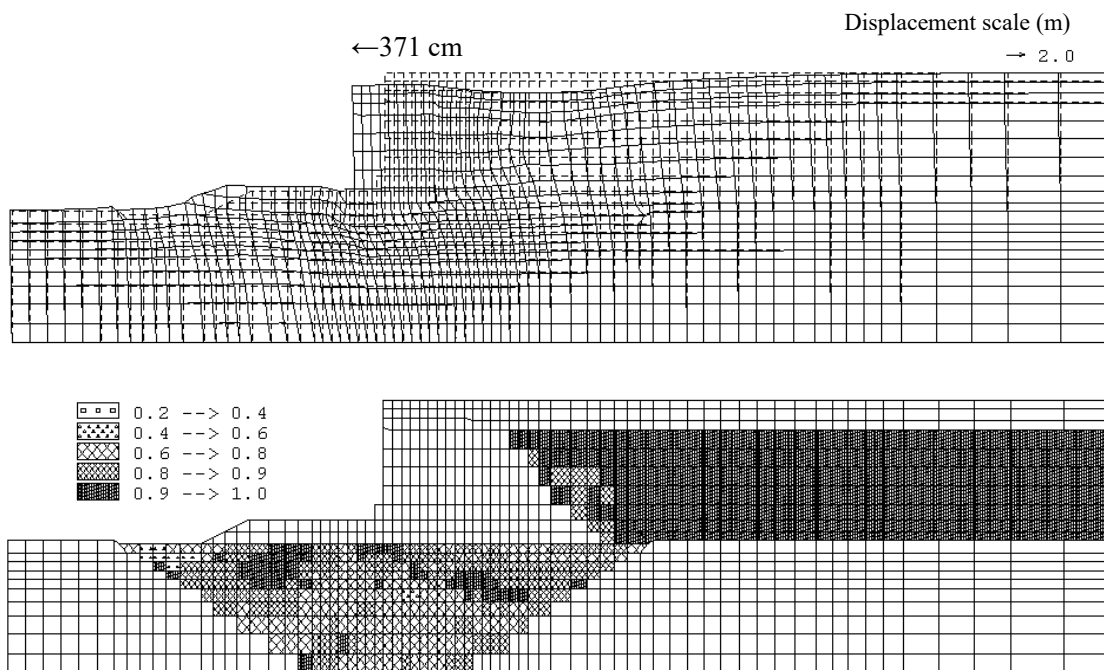


Figure. 3.3.3.2 Analysis results (Top: Residual deformation diagram; Bottom: Maximum excess pore water pressure ratio distribution diagram)²⁾

Other representative cases demonstrating the applicability of FLIP include an open-type wharf on vertical piles and gravity-type breakwater which were damaged by the 1995 Hyogo-ken Nanbu Earthquake and a sheet pile quaywall damaged by the 1983 Nihonkai-Chubu Earthquake. When there are no damage case examples sufficient for confirming the applicability of the analysis method, for example, its applicability to a newly devised type of structure, applicability can be confirmed by a suitable method such as reproduction analysis of the results of appropriate vibration experiments.

(3) Standard understanding of deformation limit values

Standard deformation limit values for a high earthquake-resistant facility against Level 2 seismic motion should be set according to the performance requirements of the facility. In the case of a high earthquake-resistant facility (specially designated (emergency supply transport)), the limit value of residual horizontal deformation and the limit value of residual inclination angle may be determined from a functional perspective as about 30 to 100 cm and about 3°, respectively. When it is judged possible to maintain the serviceability of a facility based on constant availability of materials for emergency repair and an established emergency rehabilitation system, even assuming major deformation occurs, the limit value of residual deformation can be set to about 100 cm.

3.3.2 Seismic design considering inelastic behavior of steel pipe piles

(1) Characteristics of the verification method

An example of damage due to an open-type wharf on vertical piles can be seen at the Port of Kobe, where the pier was damaged by the 1995 Hyogo-ken Nanbu Earthquake. As shown in **Figure 3.3.3.3**, damage due to local buckling occurred at the pile heads and in the underground portions of some steel pipe piles. Referring to this example of damage, one characteristic of the verification method for damage to piles of a wharf in seismic design against Level 2 seismic motion is that local buckling of some pile members is allowed and verification is based on the number of local buckling points. For example, for a wharf categorized as a specially designated high earthquake-resistant facility, one damage location is allowed per pile, but local buckling at two or more locations is not allowed.

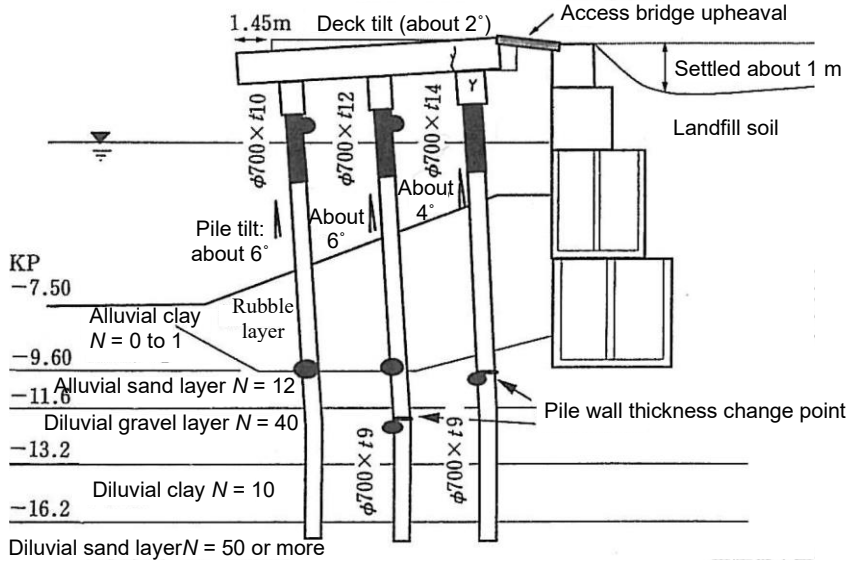


Figure 3.3.3.3 Damage to an open-type wharf on vertical piles at Kobe Port

(Local buckling occurred at the pile heads and underground portions of piles, as indicated by circles.)

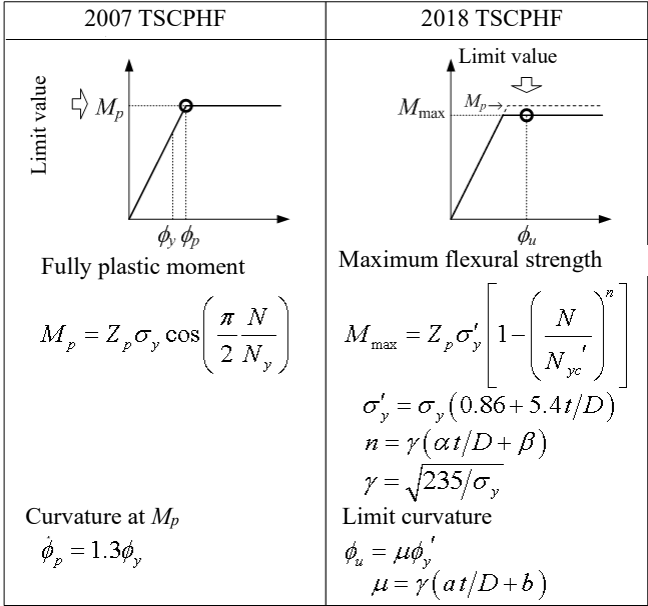
(2) Bearing strength characteristics of steel pipe members

There has been a trend toward widespread use of thin-walled large-diameter piles with a D/t ratio of about 100 in recent years. This trend has emerged from the viewpoints of economic design and the increase in the seismic action assumed in design in the 2007 revision of TSCPHF. One of the reasons for this trend is that TSCPHF (2007) specifies the fully plastic moment obtained by a cross-sectional calculation as the limit value indicating local buckling, and from the viewpoint of design, increasing the diameter of the steel pipe piles is more beneficial in design than increasing the pipe thickness. However, larger D/t ratios result in a higher risk of local buckling. That is, as D/t increases, it becomes more likely that the actual moment capacity will be lower than the fully plastic moment.

Therefore, in TSCPHF (2018), the limit curvature was adopted as the limit value instead of the fully plastic moment, which means that the type of verification changed from cross-sectional force to deformation. This made it possible to evaluate load bearing capacity and deformation performance based on the D/t ratio.

Figure 3.3.3.4 shows a comparison of the limit values in the old (2007) and new (2018) standards. The Figure presents the equations for calculating the maximum flexural strength and limit curvature using the

bilinear $M-\phi$ relation (relationship between flexural moment and curvature) as the standard methods. As the verification method, a seismic response analysis is carried out using the $M-\phi$ relationship with the maximum flexural strength as the upper limit, and local buckling is assumed to occur when the limit curvature is exceeded in the analysis results. This is the procedure for determining local buckling assumed in the method.



Note: The calculation formula given in 2018 TSCPHF is for compressive axial force.

Figure 3.3.3.4 Comparison of modeling methods and limit values for steel pipe members (Left: 2007 TSCPHF; Right: 2018 TSCPHF)

The formulas were developed based on the results of a three-dimensional finite element analysis of a steel pipe member using shell elements, with the aim of accurately evaluating the maximum flexural strength and the limit curvature, which is the curvature of the allowable limit under the maximum flexural strength. The parameters of the formulas were set to reproduce the results of the three-dimensional finite element analysis and were established to cope with loading and boundary conditions of steel pipe members of structures such as those in open-type wharf on vertical piles and steel pipe sheet pile quaywalls.

Figure 3.3.3.5 compares the $M-\phi$ relationships resulting from a beam element analysis and 3D finite element analysis using one thin-walled large-diameter pile. The flexural strength in the 3D finite element analysis in which local buckling occurred is much lower than the fully plastic moment (adopted as the limit value in the 2007 TSCPHF). The results of the calculation formula (2018 TSCPHF) accurately reproduced the maximum flexural strength and limit curvature, and the difference in the D/t ratio is neatly reflected in the $M-\phi$ relationship, although those results are a logical outcome as the formula was developed based on a finite element analysis.

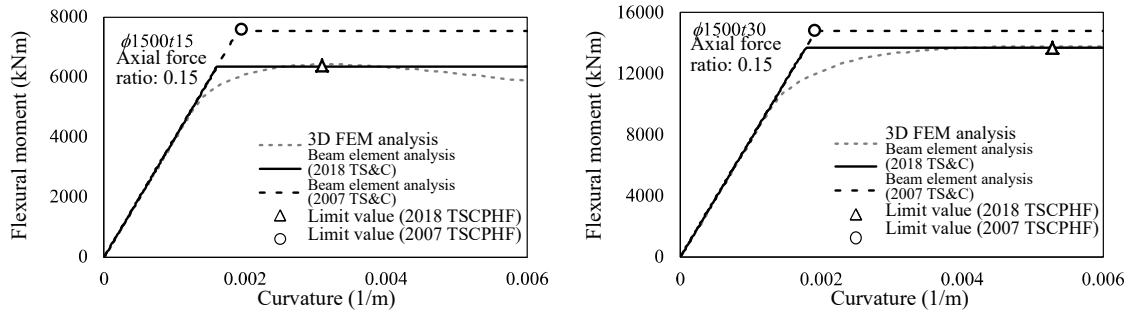


Figure. 3.3.3.5 Comparison of $M-\phi$ relationships (Left: $D/t = 100$; Right: $D/t = 50$)

-
- ¹⁾ Iai, S., Matsunaga, Y. and Kameoka, T.: Strain Space Plasticity Model for Cyclic Mobility, Report of the Port and Harbour Research Institute, Vol. 29, No. 4, pp. 27–56, 1990
- ²⁾ Iai, S., Ichii, K., Morita, T. and Miyata, M.: Seismic performance of caisson walls on loose saturated sand foundation, Proc. 14th Int. Conf. on SMFE, Hamburg, 1997

3.4 Liquefaction Prediction and Assessment

(1) Overview

The technical standards for liquefaction charts and the simplified procedures for liquefaction prediction and assessment are outlined in this section.

Liquefaction charts commonly represent the relationship between the severity of seismic loading defined in terms of the cyclic stress ratio versus the field measured soil resistance represented by the SPT N-values, CPT q-values or shear wave velocities V_s . All these charts share the same basic principle and that is an important characteristic of liquefaction charts. The soil resistance in Japanese liquefaction charts is defined by the equivalent N-value obtained from SPT N-value. The external force is defined by the equivalent acceleration α_e which is obtained from the cyclic stress ratio through seismic response analysis, generally using the code SHAKE. The equivalent N-value is adjusted for soils with fine particles in function of fines contents and plasticity index.

The occurrence and possibility of liquefaction are predicted and assessed by classifying into the four zones of the chart, where zone I means that liquefaction will occur, zone II represents a high possibility of liquefaction, zone III represents a low possibility of liquefaction and zone IV means that liquefaction will not occur. For a more accurate evaluation of liquefaction in zones II and III, one may conduct liquefaction tests in the laboratory using undisturbed soil samples, and together with the results of these tests, one can assess the occurrence or absence of liquefaction.

Before applying the liquefaction chart, soil classification by particle size distribution is performed. That is, the particle size distribution of the soil having a possibility of liquefaction will be within a certain range. If the soil has a grain size distribution that falls in the ranges with the possibility of liquefaction, it is assessed that liquefaction can occur, and if not, it is assessed that liquefaction does not occur. In cases where liquefaction can occur, the liquefaction chart is applied for liquefaction prediction and assessment.

(2) Feature of the liquefaction prediction and assessment method

The seismic motions at given sites generally have different waveforms and durations, which vary considerably depending on the ground characteristics, the routes along which seismic waves propagate and the rupture process of the hypocenter. The relevant feature of the liquefaction prediction and assessment method described above is that it is capable of considering the influence of such seismic motion waveforms and durations. The validity of the method has been verified in light of the past case histories of major earthquakes in Japan involving the 1983 Central Japan Sea Earthquake, the 1993 Kushiro offshore Earthquake, the 1995 Southern Hyogo Prefecture Earthquake, the 2009 Suruga Bay Earthquake and the 2011 off the Pacific Coast of Tohoku Earthquake (Great East Japan Earthquake).

(3) Worldwide use of the liquefaction prediction and assessment method

A unique feature of the liquefaction prediction and assessment method is its universality. Namely, the method considering the waveforms and duration of the seismic motion can be applied to various types of liquefaction charts, facilitating more rational liquefaction prediction and assessment worldwide. Details of the procedures are described by Sassa and Yamazaki (2017)¹⁾.

1) Sassa, S. and Yamazaki, H.: Simplified Liquefaction Prediction and Assessment Method Considering Waveforms and Durations of Earthquakes, Journal of Geotechnical and Geoenvironmental Engineering, ASCE, DOI:10.1061/(ASCE)

GT.1943-5606.0001597. 2017

3.5 Ground Survey

(1) Purpose and overview of ground survey

The general purpose of surveys and tests on ground is to obtain accurate information on the properties of the ground to ensure the safest and most rational design and construction, improvement and maintenance of respective structures, and to enable these structures to effectively fulfill their functions. The ground surveys which have been generally implemented mainly through boring consists of in-situ tests and geophysical logging using boreholes, sampling and laboratory soil tests, and sounding to evaluate soil parameters with measuring instruments penetrating the ground,.

(2) Planning ground survey

Detailed and accurate information on ground becomes available by appropriately planning staged surveys, from general surveys to detailed surveys, in a manner that determines the locations of the detailed surveys and tests including sampling based on the information on ground conditions obtained through general surveys. For effective and efficient ground surveys, they need to be conducted step-wisely by engineers who fully understand the roles and purposes of the survey to be implemented. In planning the detailed surveys, it is necessary to select appropriate boring points based on the distribution of bearing layers and the engineering foundation layers used in seismic resistant design, test items, etc. based on an understanding of the ground information required for design.

It is important to clarify the purpose of the ground surveys before the work begins; a vague idea that ground surveys will provide something information will bring an insufficient outcome. Ground surveys needs to be planned and conducted based on an understanding of the purposes for which the acquired data will be used.

- (i) Grasp the performance and functions required for the facility to be constructed, such as crown height, flatness, linearity and recoverability or serviceability immediately after a disaster.
- (ii) Specification of the geotechnical issues that must be solved to maintain the performance or functions in (i), such as subsidence, stability and deformation.
- (iii) Specification what ground information is necessary for measures against the geotechnical issues in (ii), such as soil profile, consolidation characteristics, strength, liquefaction resistance, and permeability.
- (iv) Specification of appropriate methods for ground surveys or soil tests to obtain the ground information in (iii), such as standard penetration test for sounding, and consolidation test, unconfined compression test and triaxial test for laboratory test.
- (v) Specification of scope, location, depth, and number of surveys and tests to be conducted with reference to the scale and type of the facility, the surrounding topography (including the shape of the coastline and undulations of the hinterland), and the results of past subsoil explorations.

The ground conditions may have changed for various reasons, such as the progress of ground settlement due to the construction of structures or landfill work conducted after the last ground surveys. It is also likely that the contractor (survey techniques) and testing engineers have changed since the last surveys. Considering this, the existence of past ground survey results does not justify omission of a new survey. However, the results of past ground surveys should be used as reference information to a great extent.

(3) Quality of subsoil exploration results

A facility is designed allowing for a margin of safety by a safety factor or partial factors. However, the purpose of this margin is to take into account modeling errors in design, uncertainty or non-homogeneity of the ground, not to compensate for inadequate tests or surveys.

Ideally, soil tests should be conducted on collected samples under conditions that are completely unchanged from the in-situ conditions, which is, however, difficult in practice. When soil samples are taken from the ground, their quality inevitably deteriorates due to mechanical disturbance or stress release. Therefore, when evaluating the results of soil tests, it is important to evaluate the quality of sampled specimens and to determine the allowable amount of decrease in quality of the specimens. It is also necessary to handle specimens used for soil tests consistently and carefully in all processes from sampling from the ground to completion of the soil tests. Vibration or changes in humidity and temperature during transportation and storage are often blind spots. These disturbances directly result in deteriorated quality of specimens, which leads to spoil the careful execution of surveys and soil tests.

On the other hand, since sounding is a survey in which the resistance of in-situ soil is measured by making a cone penetrate ground, attention must be paid to ground disturbance during the preceding drilling, but there is no need to consider the influence of disturbance or stress release of specimens during sampling, as in laboratory tests. However, if ground surveys are poorly managed, the strength and stiffness of the ground cannot be evaluated with sufficient accuracy, leading to a dangerous design or the adoption of unnecessary countermeasures.

(4) Handling of ground survey results in design

Even if the ground conditions have not changed since the last ground survey, the results of the last survey and the new survey cannot be treated as equal (e.g., by combining the two data to obtain average values) because it is highly likely that the survey techniques or testing engineers are different. However, the past data can be used as reference information to confirm trends such as the depth distribution of soil properties. In addition, for example, where there are thin layers for which no sufficient information can be obtained for statistical processing when evaluating the quality of soil test results, the past data can also be effectively used as reference information to help evaluate the quality of the soil data of such layers or to consider the need to correct such data.

Many empirical equations are introduced in design methods and technical standards, as well as theoretical equations. Empirical equations were proposed based on accumulated experiences and engineering judgments. Therefore, they have background on design specifications at that time such as type or size of structures, safety margins for expected actions, target performance and scope of application, and thus have been validated in that context. In order to achieve safe and rational design when designing a recent large-scale structure or a new type of structure, it is important to pay attention to the applicability of empirical equations, for example, by checking the background of how the equations were proposed and examining the original technical papers on which the equations were based, rather than mechanically applying the existing design methods or empirical equations.

(5) Standard penetration test and N-value

The standard penetration test is the most common sounding method in Japan. The N-value measured by

the standard penetration test has been studied, particularly in regard to its relation to the engineering properties of soil, and it is also used in the investigation and design of civil engineering facilities not limited to port facilities. The standard penetration test has a very broad scope of application to soil, and in fact, it can be applied to almost all types of soil that are normally encountered, ranging from soft clay to dense sand. Even when static penetration is not possible due to the presence of hard layers or sandy gravel layers, the standard penetration test, which uses dynamic penetration force, can often be applied to survey. This type of test is therefore more resistant to changes in ground conditions than the static cone penetration test. The standard penetration test is also advantageous in that it can collect disturbed samples in the sampler while simultaneously measuring the N -values, and it allows visual observation of the soil. In Japan, there have been no reports of defects in port facilities that could be attributed to design methods that use N -values.

However, the fact that N -values can be measured in various soil types does not mean that the accuracy of the obtained N -values is guaranteed. The above evaluation can be rephrased to say that N -values are insensitive to changes in ground conditions. It is necessary to avoid using N -values to the extent possible, or at least to pay attention to using them, particularly when evaluating ground with a very small N -value or an N -value that greatly exceeds 50. The fact that no problems have been reported with design equations using N -values may also indicate that the clarity of the structure to be designed or the scope of application of the equation compensates for the insensitivity of N -values to ground characteristics. Therefore, as with other geotechnical parameters, the standard penetration test and N -value should be applied with careful attention to the target structure and the scope of application.

3.6 Changes in Ground Improvement Techniques

(1) Overview and changes

Port and harbor zones in Japan are often located in areas with soft ground, and appropriate measures must be taken when constructing structures. Since Japan is also prone to earthquakes, liquefaction of the ground should be considered or countermeasures to cope with it need to be taken. One major solution for coping with soft ground is to improve the ground itself, and various ground improvement techniques have been developed to satisfy performance requirements. TSCPHF provides design methods and points to note concerning those techniques comprehensively.

Reviewing the history of ground improvement techniques in Japan, the replacement method, in which the original ground at a planned breakwater construction site is simply excavated and replaced with good quality soil, was adopted in the 1920s. Another early stage ground improvement technique is the preloading method, in which loads are applied to the original ground in advance. Other major ground improvement techniques were introduced from abroad or developed in Japan from the 1950s, following the end of World War II. At that time, Japan was in a period of rapid economic growth, and many large-scale development projects were underway, requiring efficient ground improvement of vast sites using large construction machinery. Typical ground improvement techniques dating from this period include the vertical drain method represented by the sand drain method, the sand compaction pile method (which involves forming columns of compacted sand) and the deep mixing method, which comprises mixing a stabilizer such as cement with soil and stirring and agitating the mixture to form stabilized soil columns in the ground. These methods remain popular as major ground improvement methods even today. The sand compaction pile method and the deep mixing method will be described in more detail later. Other ground improvement techniques in which the physical properties of the soil are improved before backfilling (e.g., the premixing method, pneumatic-flow mixing method and the lightweight treated soil method) were developed later.

As a separate problem, the Niigata Earthquake in 1964 triggered the study of measures to control ground liquefaction. This has led to the adoption of the gravel drain method, which quickly dissipates excess pore water pressure, and the sand compaction pile method for compacting loose sandy soil. In recent years, grid-type improvement by deep mixing has also been used as a countermeasure to control liquefaction. At present, there is a growing need to improve existing facilities and port infrastructure due to aging, and various techniques have been developed to improve the ground beneath existing facilities. Examples include chemical grouting, jet grouting and compaction grouting to control liquefaction. Thus, a wide variety of ground improvement techniques have been developed to meet the needs of society, and their reliability is increasing based on records of their application. The design methods and important points to note that reflect experience gained to date have been incorporated in TSCPHF.

(2) Sand compaction pile method

The sand compaction pile method is a method for improving soft ground by installing many large-diameter, well-compacted sand piles in the ground. **Figure 3.3.6.1** shows a typical execution procedure for sand pile formation by the vibro-driving method. As the diagram shows, a casing pipe is driven into the ground, sand is pressed in while the casing pipe is raised, and then the casing pipe is driven into the ground again while vibrating to expand the diameter of the sand pile. Since sand is charged into the ground by means of a casing pipe, well-compacted continuous sand piles are reliably formed in the ground. It is also possible to compact

the ground between the piles by expanding the diameter of the sand piles.

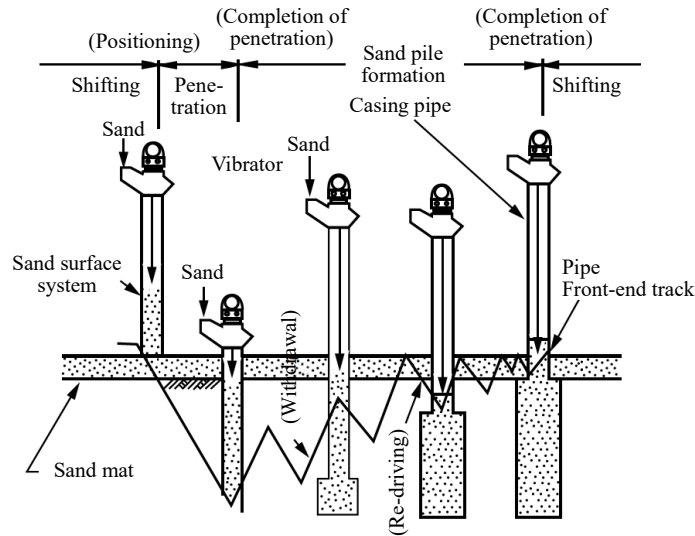


Figure. 3.3.6.1 Execution procedure for the sand compaction pile method

When clayey soil is improved, the vertical load is concentrated on highly stiff compacted sand piles, which reduces settlement, and the sand piles exert additional shear resistance, enhancing the stability of the composite ground. In most cases, 50 to 80 % of the target ground is replaced with sand, but sometimes the replacement rate is less than 50 %. The replacement rate can be selected according to the performance requirements. When loose sandy soil is improved, the surrounding soil is compacted during sand pile formation and the horizontal confining pressure in the soil rises, which eventually increases the stability of the composite ground and reduces the occurrence of liquefaction. The replacement rate is often about 7 to 20 %. The sand compaction pile method has been widely used in Japan as a solution to cope with soft ground such as clayey soil or loose and sandy ground with liquefaction potential, and is a highly reliable method.

(3) Deep mixing method

The deep mixing method involves supplying a stabilizer such as lime or cement to the ground and forcibly mixing and agitating it with the original ground to solidify the ground. Several stabilized soil columns are formed in a single process, and overlapping those columns can create a solid block or wall structure. Ground improved by deep mixing displays high stiffness and strength. This method has been widely employed when heavy structures such as caissons are to be located on the improved ground, as shown in **Figure. 3.3.6.2**. In recent years, deep mixing has been applied to improve the ground in front of sheet piles to increase the horizontal resistance force to the sheet piles. It is also applied in ground improvement techniques that prevent liquefaction of loose sandy ground in earthquakes by improving the ground in a grid-type pattern to suppress its shear deformation. The deep mixing method was developed in Japan and Scandinavia but is now used worldwide, not only in Japan, Europe and North America, but also in Asia and South America. TSCPHF explains the design method and the points to note for the deep mixing method in Japan. This method makes it possible to execute highly reliable designs.

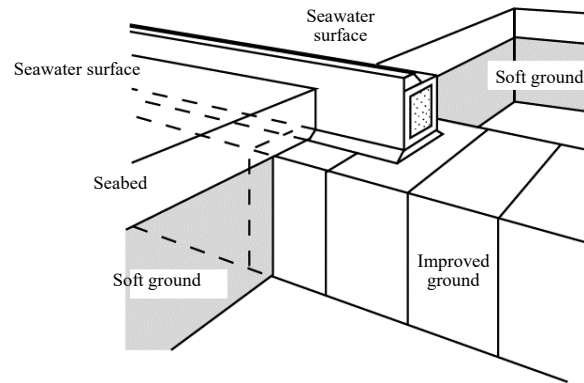


Figure. 3.3.6.2 Example of application of the deep mixing method

(4) Pneumatic flow mixing method

The pneumatic flow mixing method is a construction method in which soft ground is pumped pneumatically using a pipe, a hardener such as cement is added in the pipe, and the soil and hardener are stirred and mixed utilizing the turbulent flow effect of the plug flow generated in the conveying pipe. This method makes it possible to use a large amount of soft soil generated by channel dredging, etc. at one time as reclamation soil. Since the soft soil is hardened with cement, good quality ground with high rigidity and strength can be produced. However, the applicable types of soft soil are limited because soil is conveyed by pneumatic pumping. The most suitable soil is soft soil with a sandy fraction of no more than 30 % and a water content of 90 % to 110 % (approximately 1.3 to 1.5 times the liquid limit). Water adding is required for the soil with a low water content. This method was first used in reclamation at the Port of Nagoya in 1998. Since that time, it has been used in reclamation in port and harbor areas in Japan, and in reclamation for construction of artificial islands for offshore airports, including the Chubu Centrair International Airport in Nagoya and the Tokyo International Airport (Haneda Airport). In recent years, it has been adopted not only in Japan, but also in projects in North America and the Asian region.

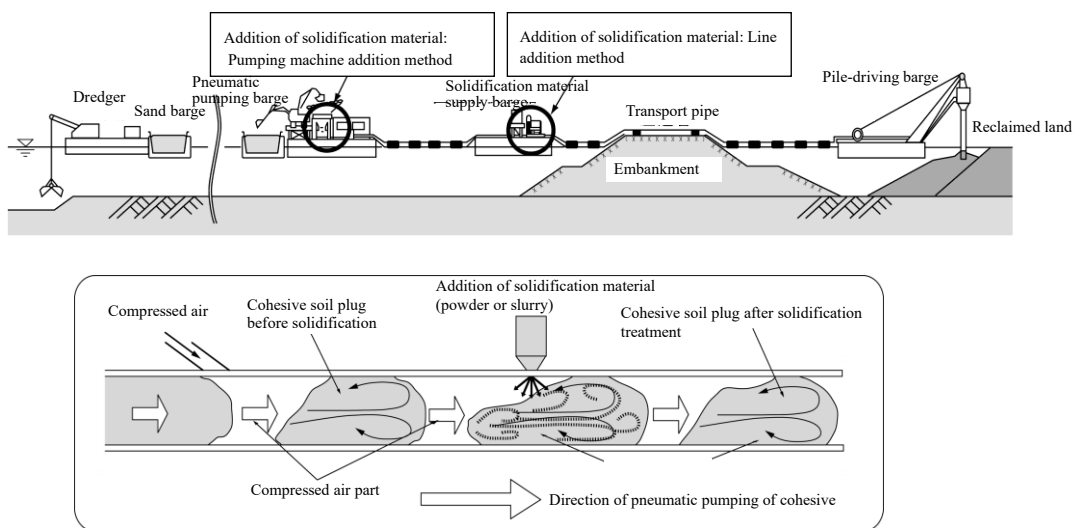


Figure. 3.3.6.3 Overview of execution by the pneumatic flow mixing method and condition of mixing in pipe

4. Structural Aspect

4.1 Examination of change in performance over time

4.1.1 Verification of corrosion of reinforcing bar in concrete structures

(1) Introduction

Since port concrete structures are located close to the sea, corrosion of reinforcing bar often occurs due to penetration of chloride ion, as shown in **Photo 3.4.1.1**. When port concrete structures were designed in the past, the conventional specification-based design approach was used. Only a few rules were applied to such construction, such as the maximum water-cement ratio (0.55 for the superstructure of a piled pier) or the minimum concrete cover (70 mm for the superstructure of a piled pier). In reality, however, there are cases where deterioration such as that shown in the photo occurred within the design service life, even when those conditions were satisfied. In response to these problems and the trend of the times, the design method for port concrete structures was changed from the conventional specification-based approach to the performance verification approach in April 2007.

In TSCPHF, verification of reinforcing bar corrosion is mandatory in the design of reinforced concrete structures (e.g., superstructure of piled pier) where chloride-induced deterioration is a concern. However, the conventional specification-based approach may be applied to other port concrete structures such as caissons, since there have been few reported cases of significant deterioration due to chloride-induced deterioration.



**Photo. 3.4.1.1 Corrosion of reinforcing bars in the superstructure (slab) of a pier
(30 years after construction)**

(2) Outline of the verification method for corrosion of reinforcing bar of port concrete structures

The basis of verification for corrosion of reinforcing bar due to penetration of chloride ion in port concrete structures is a simplified method which appropriately determines the quality or other characteristics of the concrete so that C_d , which is the design value of the chloride ion concentration at the position of reinforcing bars, will not exceed C_{lim} , the limit concentration for initiation of corrosion of reinforcing bar, during the design working life.

$$\gamma_i \frac{C_d}{C_{lim}} \leq 1.0 \quad (1)$$

Where, γ_i : structure factor.

Future predictions of C_d should be calculated by using **Eq. (2)**, which is the solution to Fick's diffusion equation.

$$C_d = \gamma_{Cl} C_0 \left(1 - \operatorname{erf} \left(\frac{0.1c}{2\sqrt{D_d t}} \right) \right) + C_i \quad (2)$$

Here,

γ_{Cl} : safety coefficient considering the C_d ,

C_0 : chloride ion concentration at the surface of the concrete (kg/m^3),

c : design value of the concrete cover (distance from the concrete surface to the reinforcing bar surface) (mm),

D_d : design diffusion coefficient for chloride ions (cm^2/year),

t : design working life, C_i : initial chloride ion concentration (kg/m^3) and

erf (s): error function.

Figure 3.4.1.1 shows the change over time in C_d , which is calculated by Eq. (2), and Figure 3.4.1.2 is a graphical representation of the chloride ion concentration distribution in concrete over time. The main parameters (C_{lim} , C_0 , and D_d) in Eq. (2) for verifying corrosion of reinforcing bar are recommended in the TSCPHF that they are by surveying actual structures or conducting laboratory tests. Also, the values of each parameters based on surveys of actual structures and long-term exposure test results are shown in the TSCPHF.

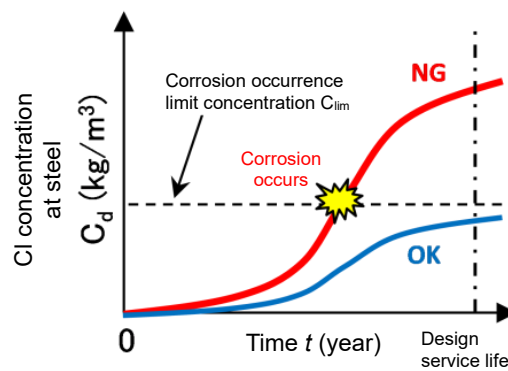


Figure. 3.4.1.1 Change over time in the design value of the chloride ion concentration C_d at the position of reinforcing bar (schematic illustration)

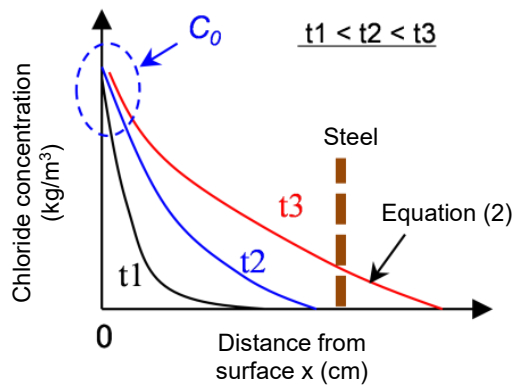


Figure.3.4.1.2 Change over time in the distribution of the chloride ion concentration in concrete (schematic illustration)

4.1.2 Corrosion protection design of steel members

Port steel structures are inherently prone to steel corrosion because they face the sea. Therefore, the design of corrosion protection for steel is crucial.

(1) Corrosion of steel

Based on survey results, the corrosion rate of steel is set at 0.1 to 0.2 mm/year in the general underwater area and 0.1 to 0.3 mm/year in the splash zone. Concentrated corrosion may occur near the L.W.L. (mean monthly-lowest water level) in vertically continuous port steel structures as shown in **Photo 3.4.1.2**, and the corrosion rate in this case may reach as much as approximately 1 mm/y. It has been believed that the concentrated corrosion are affected by the rust induced in tidal zone, the inflow of river water, and so on.



Photo 3.4.1.2 Example of concentrated corrosion in steel sheet piles near the L.W.L.

(2) Corrosion protection design of steel members

1) General (scope of application of corrosion protection)

The standard procedure in TSCPHF is to apply protective coating method up to L.W.L.-1 (m) and cathodic protection method up to the M.L.W.L. (mean low water level) as shown in **Figure. 3.4.1.3**. There are no cases where concentrated corrosion has become a problem in structures that complied with this standard.

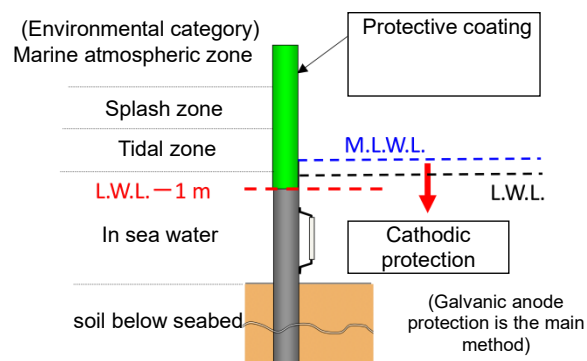


Figure. 3.4.1.3 Standard scope of application of corrosion protection

2) Design for cathodic protection

Cathodic protection is a method of corrosion protection that involves applying an inflow of a protective current to a steel structure. In Japan, the most common method is the galvanic anode method (installing aluminum alloy anodes on the steel surface) owing to its ease of maintenance (see **Figure. 3.4.1.3**). In this case, the electrons (e^-) generated by dissolution of aluminum (Al) in the sea move through the steel, causing a reduction reaction of oxygen on the steel surface to start demonstrating the effect of cathodic protection. Therefore, only the outer surface of steel pipe piles facing the seawater or soil below seabed is protected from

corrosion. Based on survey results, the protective current density flowing into the steel surface is set at about 100 to 130 mA/m² in the sea and 20 to 26 mA/m² in soil below seabed.

In designing cathodic protection for port steel structures, the standard procedure is to set the corrosion prevention percentage at or below the M.L.W.L. ($= (\text{corrosion rate without corrosion protection} - \text{corrosion rate with corrosion protection}) / \text{corrosion rate without corrosion protection}$) to 90 %. In this case, when the corrosion rate without corrosion protection is 0.2 mm/y, the corrosion rate with corrosion protection is 0.02 mm/y. Note that when the anode is completely depleted (\approx when it reaches its design lifetime), it is necessary to renew the anode (install an additional one).

3) Design of protective coating

Protective coating is a method that shields the protected material (steel) from corrosive environmental factors. There are generally five types of coating methods which are applied to port steel structures: (a) painting, (b) organic coating, (c) petrolatum coating, (d) inorganic coating and (e) metal coating. When designing protective coating, it is necessary to select the most appropriate method considering the ease of application, expected lifetime and any other relevant factors.

4.2 Methodology for Setting Fender Material Standards

(1) Overview

In selecting a fender standard, it is important to calculate the berthing energy of the design ship and verify the performance of a fender that can absorb that berthing energy. Other necessary considerations include a fender design that properly takes the mooring and unmooring operations into account and evaluation of the fender performance by a fender test.

(2) Berthing energy of vessels

The berthing energy of a vessel can be calculated by using **Eq. (4.2.1)** with the following parameters: the mass of the vessel, the berthing velocity of the vessel, the virtual mass factor, the eccentricity factor, the flexibility factor and the berth configuration factor.

$$E_{f_k} = \frac{1}{2} M_{s_k} V_{b_k}^2 C_{m_k} C_{e_k} C_{s_k} C_{c_k} \quad (4.2.1)$$

Where,

E_f : berthing energy of the vessel (kJ),

M_s : mass of the vessel (t),

V_b : berthing velocity of the vessel (m/s),

C_m : virtual mass factor,

C_e : eccentricity factor,

C_s : flexibility factor, and

C_c : berth configuration factor.

The subscript k means that the value used in a parameter is a characteristic value. Among these, the mass and berthing velocity of a vessel are especially important parameters that greatly affect the vessel's berthing energy. Here, the mass of a vessel means the full load displacement tonnage, which is the vessel's displacement at full load expressed as a weight. For the berthing velocity of vessels, when a large cargo ship or a large tanker is gently berthed parallel to the mooring facility by a few tugs, the berthing velocity is often taken as not more than 10 to 15 cm/s based on past experience. However, it is more accurate to set the berthing velocity of the design ship by referring to the actual measured value of the berthing velocity of vessels.

(3) Performance verification for fenders

Commonly used fender equipment includes rubber fenders and pneumatic fenders. **Figure 3.4.2.1** shows an example of the procedure of performance verification for fenders. When designing fenders, it should be selected fender types that can absorb the berthing energy of vessels. The berthing energy of a vessel is absorbed through deformation of the vessel's hull and the mooring facility. However, since the absorption of energy through deformation of the hull is generally small, it will not be considered. In rigid facilities such as gravity-type or sheet pile-type mooring facilities, energy absorption by deformation of the main body of the mooring facility is not permissible. For such rigid mooring facilities, the absorbed energy of the fender can be calculated by using **Eq. (4.2.2)**.

$$E_s = \phi E_{cat} \geq E_f \quad (4.2.2)$$

Where,

E_s : absorbed energy of the fender (kJ),

ϕ : performance variation factor such as manufacturing error (tolerance) of the fender,

E_{cat} : standard value of absorbed energy of the fender (kJ), and

E_f : berthing energy of the vessel (kJ).

It is common practice to use a performance tolerance of -10 % for absorbed energy in fenders. In the case of a flexible structure such as a pier-type mooring facility, the performance of the reaction force of the fender must also be verified, since the influence of the reaction force may be significant in the design of the structure.

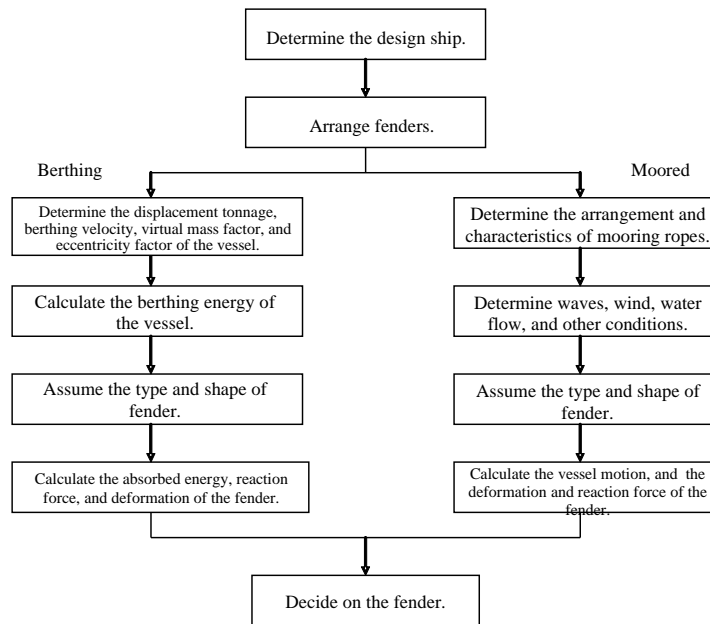


Figure. 3.4.2.1 Example of performance verification procedure for fender

At mooring facilities that are susceptible to swells and long-period waves in ports facing the open sea, it is necessary to consider not only the impact force when vessels are berthing but also when they are moored. For such mooring facilities, it is necessary to calculate the impact force acting on the fenders by simulation of moored vessel motions under external forces such as waves, and confirm the safety of the fenders.

(4) Consideration of mooring/unmooring operations

In some cases, the shape or arrangement of fenders or bollards makes the mooring and unmooring operations (delivering mooring ropes between a vessel and landside workers) difficult when vessels berth or leave the mooring facility. Especially in the case of fenders with contact panels, the mooring ropes may interfere with the upper and lower parts of the contact panel during the mooring and unmooring operations. This point needs to be considered when designing fenders. Relevant measures are usually taken in the stage of detailed design of the fender after the standards and basic specifications of the fender have been determined.

(5) Performance evaluation by fender tests

The characteristics of fenders, such as absorbed energy and reaction force, are highly dependent on their constituent materials and shapes. Therefore, it is necessary to ensure that the fenders which are to be produced will have physical properties such as aging and ozone resistance, sufficient compressive performance for absorbed energy and reaction force and durability against cyclic loading. As such, it is important to verify

the basic performance of fenders through physical tests, static compression tests and durability tests at various stages of fender production.

5. Environmental Aspect

5.1 Design Technique for Green Port Structures

(1) Overview

As consideration for preservation of the natural environment of ports and harbors, it is necessary to minimize the impact of facilities on the natural environment and to take measures that can create a good natural environment. Technologies for preservation and creation of the natural environment of ports include creation of tidal flats, creation of artificial shoals and biologically symbiotic port structures for coexistence with living organisms. These technologies are hybrid-type green infrastructure that represent a fusion of “gray” (hard-engineered structures (i.e., concrete)) and “green” (nature) in order to satisfy both the stability of the structures and the diverse functions of nature¹⁾²⁾. Tidal flats and shoals are closer to “green,” while symbiotic structures are closer to “gray.” This section describes biologically symbiotic port structures, that is, “green port structures,” which were newly added to TSCPHF in the Revision of 2018.

(2) Green port structures

A green port structure is a structure which has the basic functions of a port structure and also has the functions of a habitat for organisms, such as a tidal flat or a rocky shore (biologically symbiotic breakwater, biologically symbiotic seawall, biologically symbiotic quaywall or biologically symbiotic piled pier). There are three structural types of green port structures, the cover type, the piled pier type and the caisson type (Figure. 3.5.1.1).

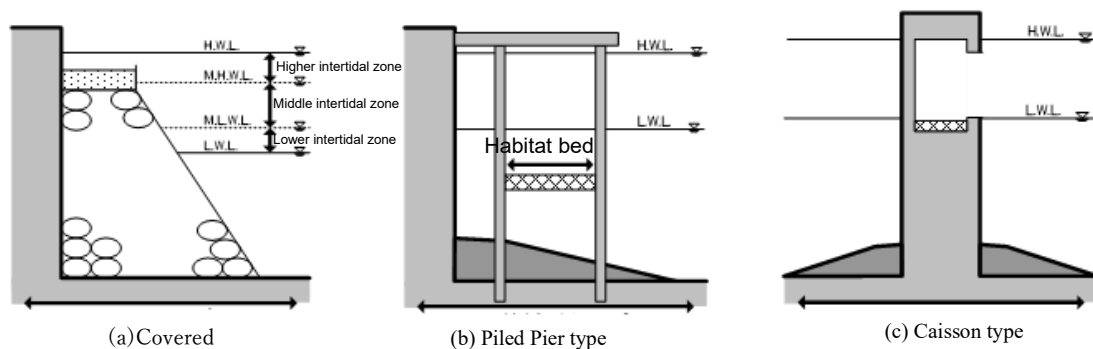


Figure. 3.5.1.1 Structural types of green port structures

There are three types of habitat, namely, the silt type, the gravel type and the block type, depending on the type of habitat for organisms to be added as a green port structure. The silt type uses sand and mud as a habitat. If the habitat is set in the intertidal zone, it is an intertidal flat, and if it is set deeper than the intertidal zone, it is a shallow area. The gravel type uses stone materials as a habitat. Depending on the water depth and environmental conditions where the habitat is placed, it can serve as a base for the growth of seaweed or as a habitat for sessile marine organisms. The block type uses blocks such as algae reefs and fishing reefs to provide a habitat. Depending on the type of block, it can be a base for seaweed growth or a habitat for fish and other animals.

(3) Development plan

Green port structures add the function of a habitat for organisms to the basic port structure and are assumed to have the originally-intended function of the port structure (Figure. 3.5.1.2). Therefore, it is necessary to

collect and organize the relevant information in advance, such as restrictions on the use of places related to navigation and vessel berthing.

Because the purpose of a green port structure is to create a habitat for living organisms, it is necessary to consider structures that match the environment of the area. To this end, designers need to grasp physical conditions such as the flow regime and waves, water quality and habitat of the surrounding sea area when reviewing the target species, habitat type and detailed shape of a green port structure. It is also important to understand in advance the needs of the marine environment required at the regional level in order to promote smooth and appropriate coordination.

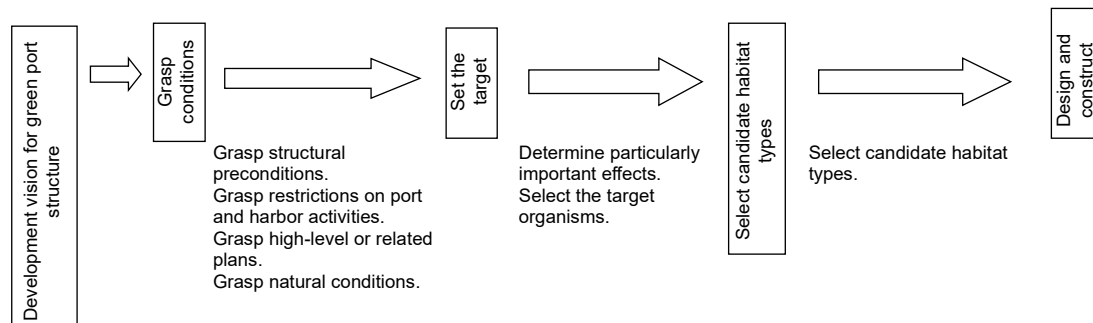


Figure. 3.5.1.2 Conceptual flow of the development plan for green port structures

(4) Selection of candidate habitat types

Candidate habitat types suitable for the intended purpose must be selected according to the structural constraints of the port structure and the expected benefits (e.g., increase in basic productivity, provision of habitat, provision of spawning and nursery grounds, circulation of nutrient salts, water purification, CO₂ reduction and sites for education and research). When there is no need to consider structural constraints and constraints on the operation and use of the port related to the target port structure, it is desirable to determine the expected effects and target species based on the natural conditions of the water area and select the type of habitat appropriate for the target. **Table 3.5.1.1** shows the main conditions for selecting habitat types.

Table 3.5.1.1 Main conditions for selecting habitat types

Habitat type	Water depth zone	Main conditions for selection
Silt type	Intertidal zone	<ul style="list-style-type: none"> ● Relatively calm waters (influence of waves and currents that may cause sand to flow out is small). ● Is not a type of water area prone to stagnant flow that may cause sedimentation of suspended matter.
Silt type	Deeper than the intertidal zone	
Gravel type	Intertidal zone	<ul style="list-style-type: none"> ● Influence of oxygen deficiency or river runoff is small, and abundant dissolved oxygen concentration suitable for a biological habitat can be expected. ● When formation of seaweed beds is expected, the light conditions (light intensity or transparency) are sufficient and salinity is suitable for seaweed growth.
Gravel type Block type	Deeper than the intertidal zone	

1) Okada, T., Mito, Y., Akiyama, Y.B., Tokunaga, K., Sugino, H., Kubo, T., Endo, T., Otani, S., Yamochi, S., Kozuki, Y., Kusakabe, T., Otsuka, K., Yamanaka, R., Shigematsu T. and Kuwae, T. 2021. Green port structures and their ecosystem services in highly urbanized Japanese bays, Coastal Engineering Journal, DOI: 10.1080/21664250.2021.1911194

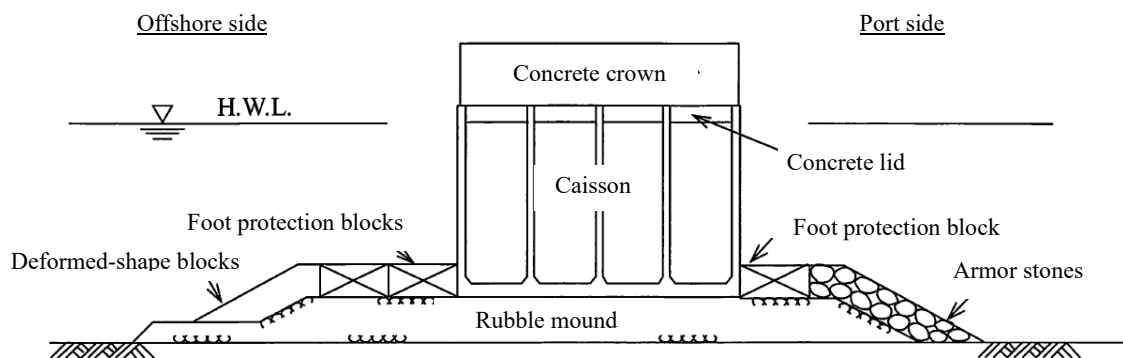
2) Kuwae, T. and Crooks, S. 2021. Linking climate change mitigation and adaptation through coastal green–gray infrastructure: a perspective, Coastal Engineering Journal, DOI: 10.1080/21664250.2021.1935581

Chapter 4 Examples of Breakwater Design

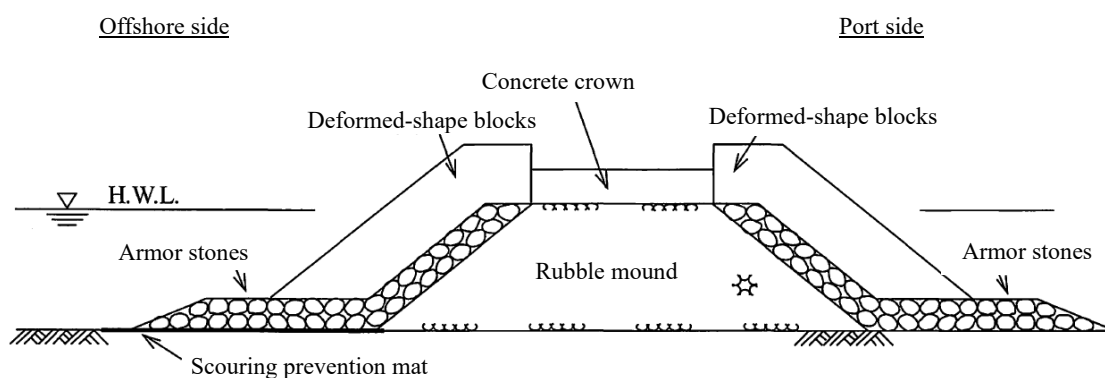
1. Typical Structural Types in Japan

The type of breakwater used in Japan was originally the rubble mound-type sloping breakwater in shallow water areas. However, as the design water depth and design wave height increased, execution of construction work for sloping breakwaters became increasingly difficult, and quick construction was also needed to meet demand for port construction accompanying the rapid economic growth of the country. Against this background, the typical structural type of breakwater in Japan has now become the “caisson-type composite breakwater,” which can be constructed quickly in areas with deep water and high wave conditions. Other structural types of breakwaters include the upright breakwater, upright wave-dissipating block breakwater, pile type breakwater, breakwater sitting on soft ground. As reference, **Figure 4.1.1** shows images of various structural types of breakwaters. (Note: This Figure also includes some structural types with no record of actual use.)

Examples of the design of the “caisson-type composite breakwater,” which is the typical structural type of breakwater in Japan, and the “rubble mound sloping breakwater,” which is also frequently used in other countries are shown below.

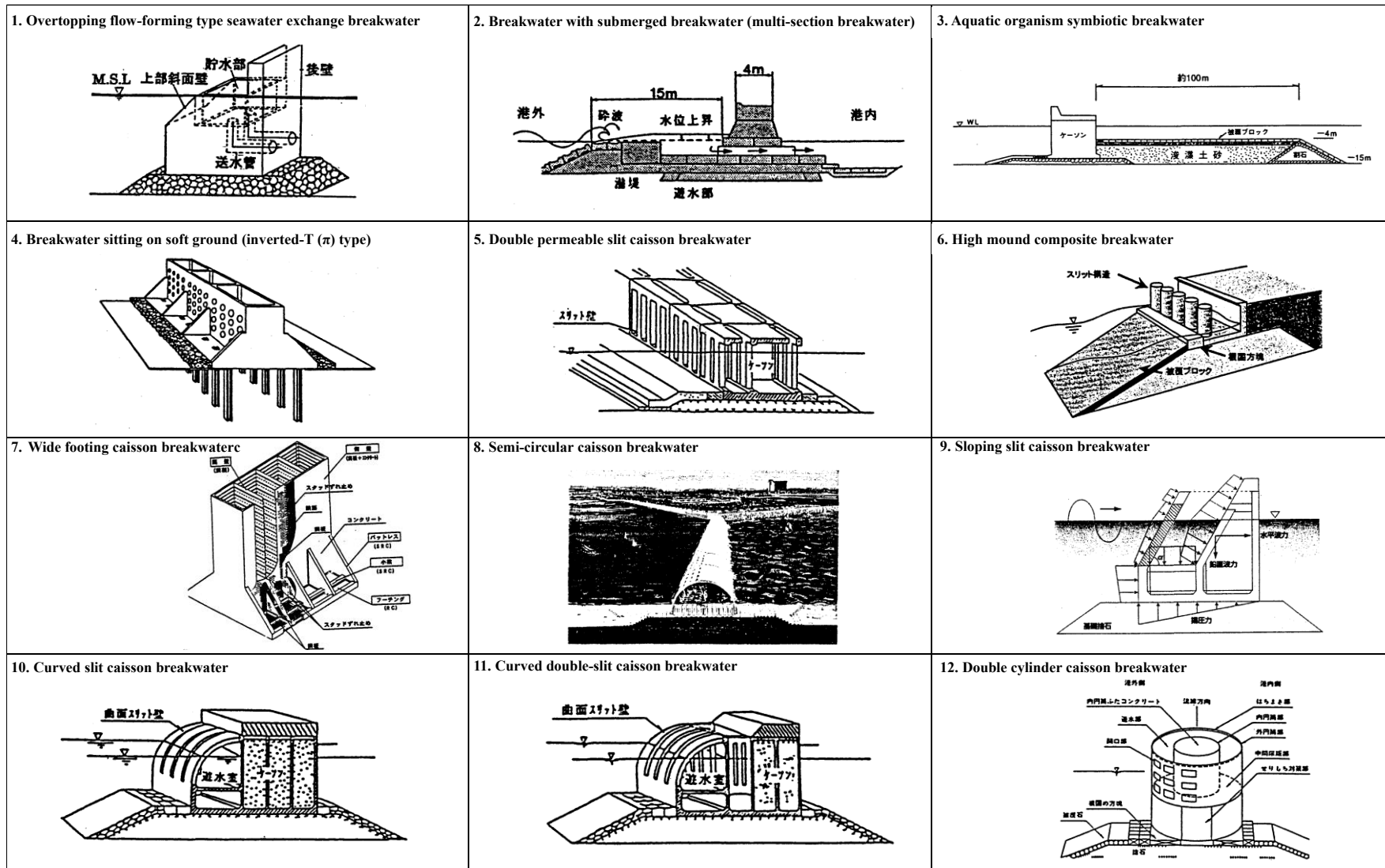


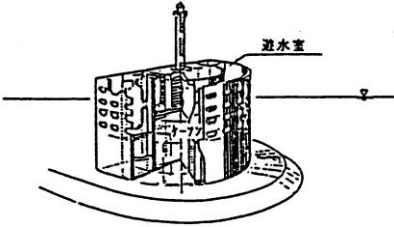
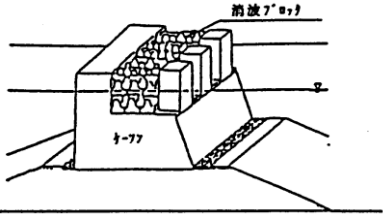
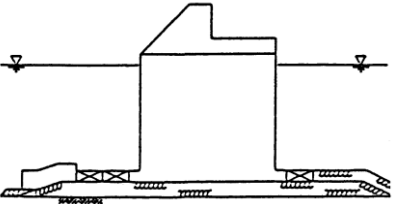
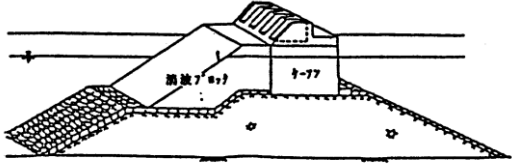
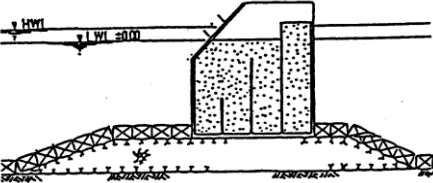
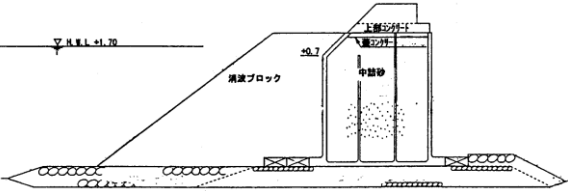
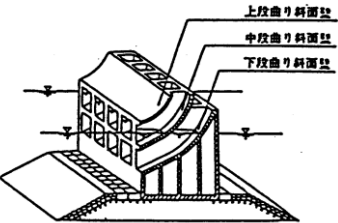
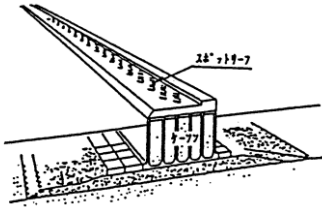
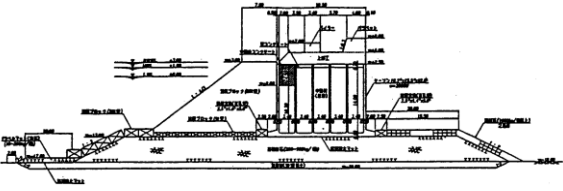
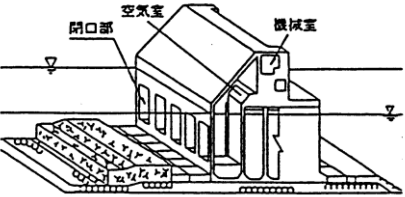
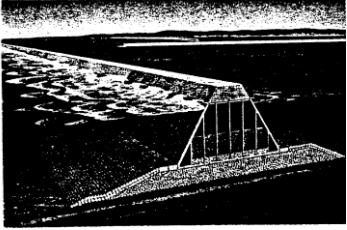
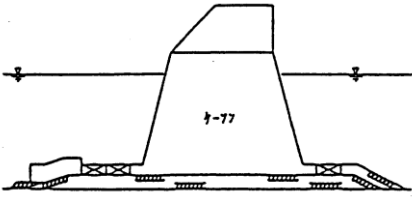
(a) Caisson-type composite breakwater



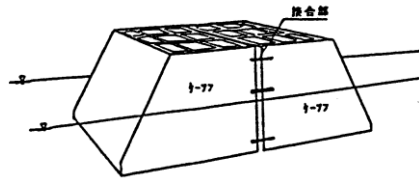
(b) Rubble mound-type sloping breakwater

Figure 4.1.1 Images of structural types of breakwaters (including structures with actual use)

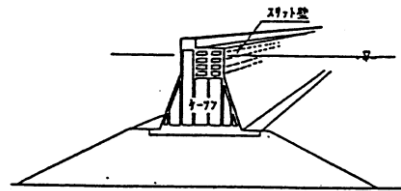


<p>13. Double semi-cylindrical caisson breakwater</p> 	<p>14. Catamaran type caisson breakwater with inner wave-dissipating blocks</p> 	<p>15. Sloping top caisson breakwater</p> 
<p>16. Wave-dissipating block covered sloping top caisson breakwater</p> 	<p>17. Semi-submerged sloping top caisson breakwater</p> 	<p>18. Wave-dissipating block covered semi-submerged sloping top caisson breakwater</p> 
<p>19. Multi-cellular caisson breakwater</p> 	<p>20. Setback parapet type spot reef composite caisson breakwater</p> 	<p>21. Top piler caisson breakwater</p> 
<p>22. Wave power extracting caisson breakwater (wave energy absorption type power-generation caisson breakwater)</p> 	<p>23. Trapezoidal caisson breakwater</p> 	<p>24. Sloping top trapezoidal caisson breakwater</p> 

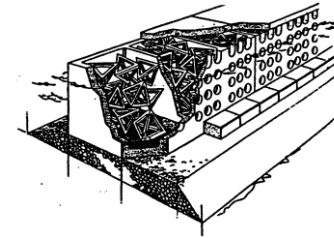
25. Offshore floating jointed caisson breakwater



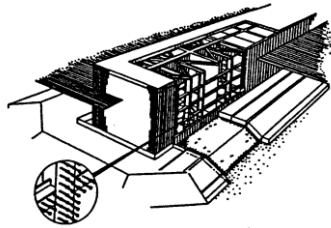
26. Bottom trapezoidal top slit caisson breakwater



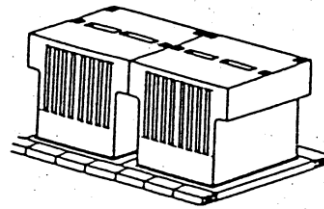
27. Block-filled porous wall caisson breakwater



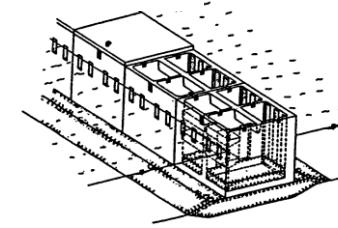
28. Long caisson breakwater



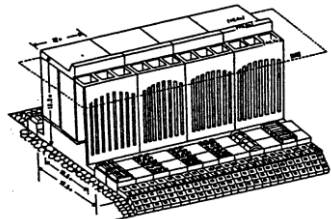
29. Permeable joint type slit caisson breakwater



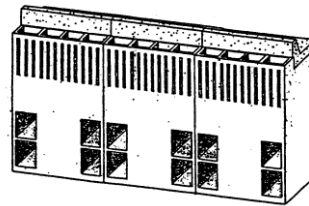
30. Slit caisson with projecting plates



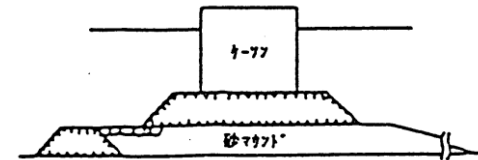
31. Vertical slit bottom permeable type caisson breakwater



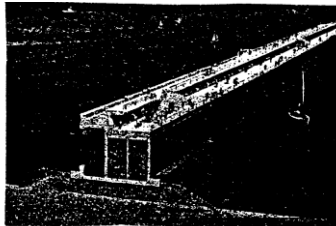
32. Upright wave-dissipating type permeable caisson breakwater



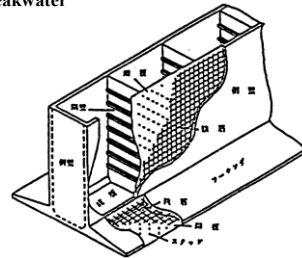
33. Sand mound type composite breakwater



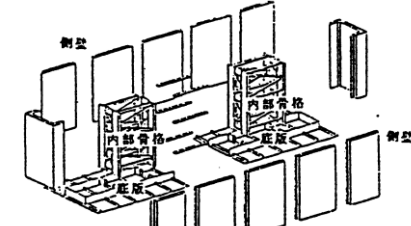
34. Amenity-oriented breakwater



35. Hybrid caisson breakwater



36. Panel system caisson breakwater



<p>37. Precast caisson breakwater</p>	<p>38. Upright wave-dissipating caisson breakwater</p>	<p>39. Suction foundation breakwater</p>
<p>40. Crenelated breakwater</p>	<p>41. Upright wave-dissipating block breakwater</p>	<p>42. Flapboard breakwater</p>
<p>43. L-shaped wave-dissipating breakwater</p>	<p>44. Curtain type breakwater</p>	<p>45. Floating breakwater</p>
<p>46. Steel pipe pile breakwater</p>	<p>47. Jacket type (pile type) breakwater</p>	<p>48. Wave absorbing system using sand liquefaction (liquefied sandbed wave barrier: LSWB)</p>

2. Caisson-type Composite Breakwater

(1) Basic section for examination

Figure 4.2.1 and 4.2.2 respectively show a typical sectional view and a caisson structural drawing.

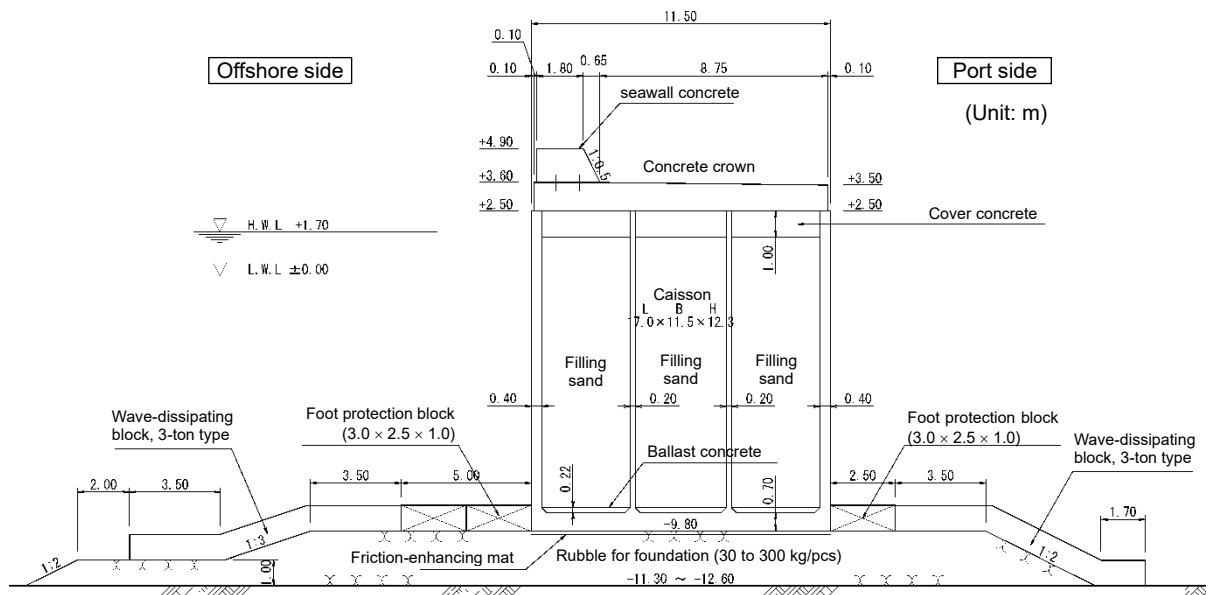
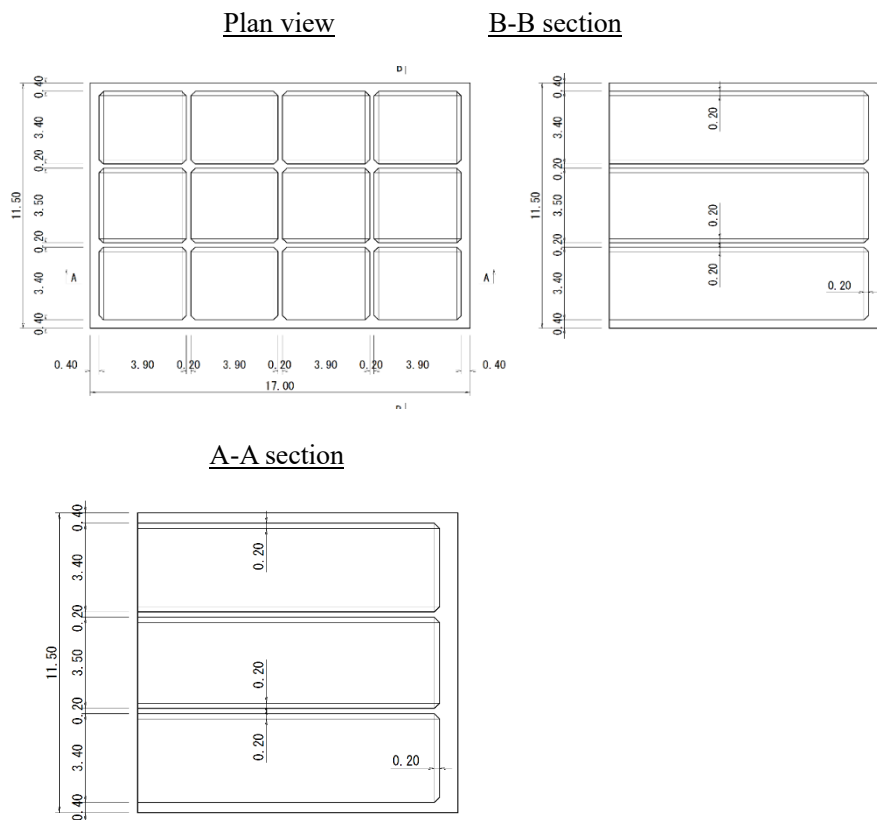


Figure 4.2.1 Basic section for examination



(Unit: m)

Figure 4.2.2 Caisson structural drawing

(2) Design conditions

1) Breakwater location

A breakwater subject to design is shown in **Figure 4.2.3**.

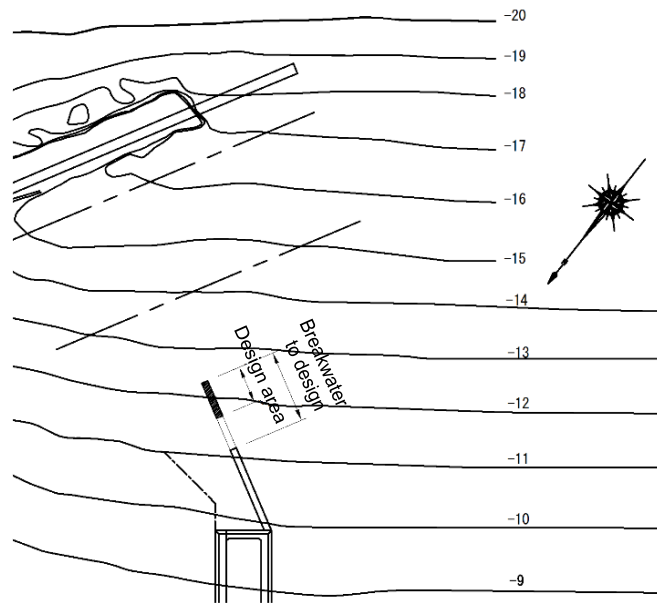


Figure 4.2.3 Breakwater location map

2) Tide level

H.W.L.: +1.70 m (based on the site conditions)

L.W.L.: 0.00 m (based on the site conditions)

3) Seabed slope

$i = 1/100$ (based on the site conditions)

4) Design wave

Table 4.2.1 Specifications of design wave

50-year probability wave		H.W.L.	L.W.L.
H_{max}	(m)	6.9	7.2
$H_{1/3}$	(m)	3.9	4.0
T	(s)	11.0	11.0
Incident angle β	(°)	21.0	21.0

Note: β is the value after directional adjustent.

i) Deepwater wave

- Estimated value

Two cases per year where high waves occurred were extracted from surface weather chart data from 1987 to 2016 (hence 60 cases in total), the gradient wind was calculated, and deepwater waves were estimated using the spectral method (third generation model: SWAN). Some of the estimation results are shown in **Table 4.2.2**.

Table 4.2.2 Results of wave forecast

Case	Period	SE		SSE	
		H_0	T_0	H_0	T_0
1	1987.1.15~1.16	4.9	8.7	3.0	6.1
↓					
30	2001.1.30~1.31	7.2	10.7	5.0	8.9
↓					
60	2016.10.19~10.20	6.3	7.1	6.2	10.0

To calculate the probability wave height, conduct statistical processing using the wave direction based on the estimated wave height data. For the probability distribution of wave height, select waves with a high correlation coefficient as the probability wave height using the Gumbel distribution and Weibull distribution.

Table 4.2.3 Correlation coefficient and probability wave height (wave direction: SSE)

Distribution form	Gumbel distribution	Weibull distribution						
		0.75	0.85	1.00	1.10	1.25	1.50	2.00
Correlation factor	0.986	0.957	0.969	0.979	0.982	0.984	0.982	0.973
Probability wave height	7.6	8.1	8.1	8.0	7.9	7.8	7.6	7.3

As shown above, use the value of the Gumbel distribution, which has the highest correlation factor. **Table 4.2.4** summarizes the estimation results by probability year. (Only the SSE data are shown, as this direction is where the impact on the breakwater is estimated to be greatest.)

To calculate the cycle, the relationship between wave height and cycle was summarized, and the value was calculated from the linear regression equation.

Table 4.2.4 Estimation result (wave direction: SSE)

Probability year	Deepwater wave height H_0 (m)	Deepwater wave cycle T_0 (s)
5 years	5.6	9.0
10 years	6.2	10.0
20 years	6.8	10.0
30 years	7.2	11.0
50 years	7.6	11.0

ii) Equivalent deepwater wave

Refraction coefficient (Kr): 0.979 (based on the site conditions)

Diffraction coefficient (Kd): 0.530 (based on the site conditions)

Wave direction: N173° (after refraction or diffraction)

Equivalent deepwater wave: $H_0' = Kr \cdot K_d \cdot H_0 = 0.979 \times 0.530 \times 7.6 = 3.94$ (m)

iii) Design wave

- Judgment on the inside and outside of the breaker zone

Tide level: H.W.L. +1.70 m

Depth of the original ground: D.L. -11.30 m (based on the site conditions)

Water depth: $h = 13.00$ m (based on the site conditions)

$$L_0 = 1.56T^2 = 1.56 \times 11.0^2 = 188.76 \text{ m}$$

$$H_0'/L_0 = 3.94/188.760 = 0.021$$

$$h/H_0' = 13.00/3.94 = 3.299$$

Charts with a seabed slope of 1/100 were used, as the seabed slope i is 1/100.

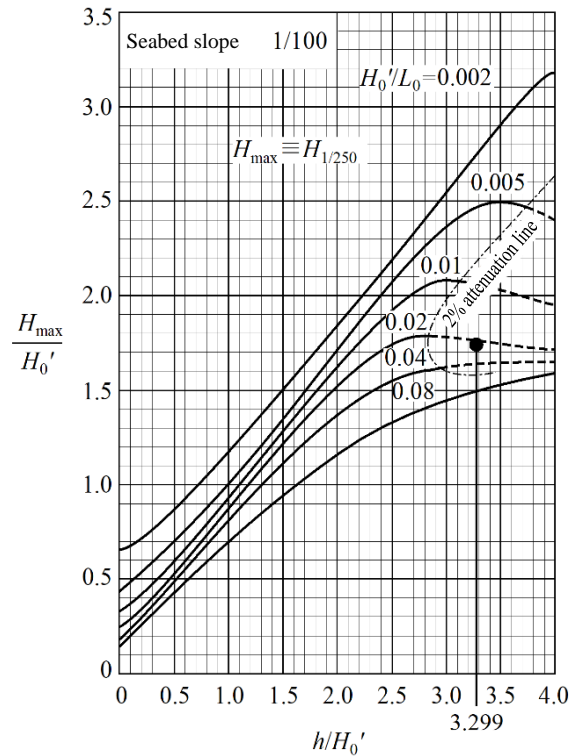


Figure 4.2.4 Judgment on the inside and outside of the breaker

Since the design wave is plotted in the area on the right-hand side of the 2% attenuation line as shown in **Figure.4.2.4**, it is thus judged to be located outside the breaker zone.

- Significant wave height $H_{1/3}$

$$h/L_0 = 13.00/188.760 = 0.069$$

$$H_0'/L_0 = 3.94/188.760 = 0.021$$

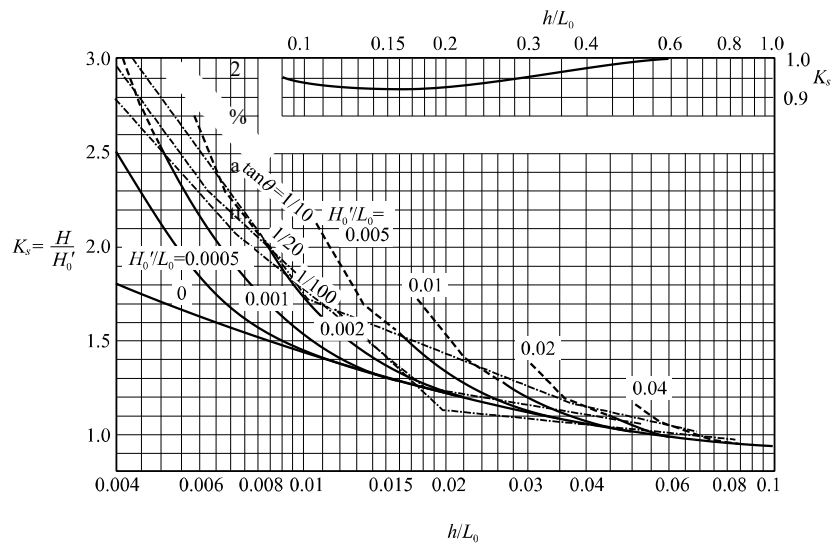


Figure 4.2.5 Calculation of shoaling coefficient

$$K_s = 0.97$$

$H_{1/3} = K_s \times H_0' = 0.97 \times 3.94 = 3.82 = 3.9$ (m) (The solution should be rounded up, as rounding it down is dangerous.)

- Design wave height H_D (maximum wave height H_{max})

$$H_D = 1.8 \times H_{1/3} = 1.8 \times 3.82 = 6.88 = 6.9 \text{ (m)}$$

5) Ground conditions

The boring survey shows that the foundation ground is composed of sandy soil. Therefore, it is divided into sandy soil (1) and sandy soil (2) according to the vertical distribution of N-values.

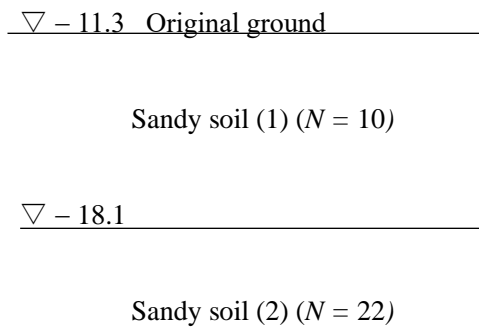


Figure 4.2.6 Soil strata according to the boring

- i) Angle of shear resistance for sandy soil

Calculate the angle of shear resistance for sandy soil using the following equation:

$$\phi = 25 + 3.2 \sqrt{\frac{100N}{\sigma'_{v0} + 70}} \quad (1)$$

ϕ : Angle of shear resistance for sand ($^\circ$)

N: Standard penetration test value

σ'_{v0} : Effective overburden pressure at a depth where the standard penetration test value was measured (kN/m²)

- ii) Summary of characteristic values of ground conditions

The ground conditions of sandy soil and rubble for foundation are shown in **Table 4.2.5**.

Table 4.2.5 Ground conditions

	Angle of shear resistance ϕ_k' ($^\circ$)	Saturated weight γ'_{satk} (kN/m ³)	Wet weight γ'_{ak} (kN/m ³)
Rubble for foundation	40	20.0	18.0
Sandy soil (1)	34	20.0	18.0
Sandy soil (2)	36	20.0	18.0

6) Maximum acceleration of engineering bedrock

The maximum acceleration of L1 seismic motion at the said location based on the engineering bedrock is 110.6 (cm/s²).

7) Friction coefficient

Although the coefficient of friction between friction-enhancing mats and rubble (f_k) is 0.75, 0.70 is used, taking the recorded values in cold areas into consideration.

8) Unit weight

Table 4.2.6 Unit weight

Material	Weight per unit volume (kN/m ³)
Reinforced concrete	24.0
Plain concrete	22.6
Filling sand (saturated weight)	18.9
Seawater	10.1

* The value for the filling sand is based on the result of the weight per unit volume test.

(3) Design specifications

1) Determination of the crown height of caisson

The crown height of a caisson in the offshore area will be D.L. + 2.50 m, as it is generally desirable to make it the mean monthly highest-water level (H.W.L.) + 1.70 m or more to facilitate concrete casting of the crown.

2) Review of stability during floating

Since these caissons are to be towed to a breakwater construction position, examine their stability during floating to ensure they do not overturn or tilt. Use ballast materials to ensure stability during floating.

- Caisson's center of gravity

Use asphalt mats as friction-enhancing mats. These asphalt mats comprise asphalt mixture molded in a mattress shape and integrated with reinforcements and wire ropes for hoisting.

Unit weight of each asphalt mat: 22.6 kN/m³

Thickness of asphalt mat: 0.08 m

$$W_m = 17.00 \times 11.50 \times 0.08 \times 22.6$$

$$= 353.464 \text{ kN/caisson}$$

Table 4.2.7 shows the caisson weight including mats and the moment.

Table 4.2.7 Caisson weight and moment

Description	$W(\text{kN})$	$y^*(\text{m})$	$W_y(\text{kN}\cdot\text{m})$
Bottom slab	3,284.400	0.380	1,248.072
Front wall/rear wall	3,786.240	6.530	24,724.147
Side wall	2,383.104	6.530	15,561.669
Bulkhead (parallel to the face line)	1,804.032	6.530	11,780.329
Bulkhead (vertical to the face line)	1,720.512	6.530	11,234.943
Vertical haunch	267.264	6.530	1,745.234
Horizontal haunch (parallel to the face line)	40.320	0.797	32.135
Horizontal haunch (vertical to the face line)	34.944	0.797	27.850
Corner haunch	3.072	0.805	2.473
Friction-enhancing mat	353.464	0.040	14.139
Total	13,677.352		66,370.991

* Set the bottom of the friction-enhancing mat as the basis.

Concrete (unit weight w_s : 22.6 kN/m³) is used as ballast, and the ballast thickness is assumed to be 0.22 m.

Table 4.2.9(b) gives:

$$W' = 720.374 \text{ (kN)}$$

Table 4.2.8 gives:

$$W_y' = 26.915 \times 22.6 = 608.279 \text{ (kN}\cdot\text{m)}$$

Table 4.2.8 Ballast volume and moment

Description	$V(\text{m}^3)$	$y(\text{m})$	$V_y(\text{m}^4)$
Ballast	35.350	0.840	29.694
Vertical haunch	-0.211	0.840	-0.177
Horizontal haunch (parallel to the face line)	-1.680	0.797	-1.339
Horizontal haunch (vertical to the face line)	-1.456	0.797	-1.160
Corner haunch	-0.128	0.805	-0.103
Total	31.875		26.915

Caisson's center of gravity G' is given as follows:

$$G' = (W_y + W_y') / (W + W') = (66,370.991 + 608.279) / (13,677.352 + 720.374) = 4.652 \text{ (m)}$$

- Draft of caisson

Assuming the draft is d'

$$d' = (W + W') / (B \times L \times w) = (13,677.352 + 720.374) / (11.50 \times 17.00 \times 10.1) = 7.292 \text{ (m)}$$

- Caisson's center of buoyancy

Caisson's center of buoyancy C' is given as follows:

$$C' = V_y' / V'$$

$$V' = B \times L \times d' = 11.50 \times 17.00 \times 7.292 = 1,425.586 \text{ (m}^3\text{)}$$

$$V_y' = B \times L \times d' \times d' / 2 = 11.50 \times 17.00 \times 7.292 \times 7.292 / 2 = 5,197.687 \text{ (m}^4\text{)}$$

$$C' = 5,197.687 / 1,425.586 = 3.646 \text{ (m)}$$

- Metacenter position

$$I = L \times B^3 / 12 = 17.00 \times 11.50^3 / 12 = 2,154.573 \text{ (m}^4\text{)}$$

The distance between the metacenter and the center of buoyancy is given as follows:

$$\overline{MC'} = I / V' = 2,154.573 / 1,425.586 = 1.511 \text{ (m)}$$

- Stability review

$$\overline{GM'} = \overline{MC'} - \overline{CG'} = 1.511 - (4.652 - 3.646) = 0.505 \text{ (m)} \geq 0.05 \times 7.148 = 0.357 \text{ (m)} \text{ -O.K.-}$$

3) Thickness of lid concrete

The thickness of lid concrete shall be 1.0 m, considering cases where caissons are placed in severe wave conditions and may remain with their crown concrete uncompleted for a long time (carried over to the next year).

4) Shape of crown concrete

Set the crown height to control overtopping waves as much as possible, since the area behind the breakwater is small in this harbor. Therefore, set the crown height of the breakwater to +4.9 m (H.W.L. + $0.8H_{1/3} = 1.7 + 0.8 \times 3.9$) by setting the coefficient of wave transmission to 0.2, according to the experimental value of the coefficient of wave transmission and crown height.

Construct the crown concrete in two stages. The first stage places concrete up to D.L. + 3.6 m (or D.L. + 3.5 m for the port side), and the second stage to a required crown height of D.L. + 4.90 m. Shape the crown concrete like a parapet to ensure stability of the breakwater body.

5) Scouring prevention work

For the offshore side of the breakwater, since it is likely to be scoured by flows from the upright part, provide scouring prevention works measuring 1.0 m thick and 2.0 m wide (gravel mat).

6) Foot protection block

Place two foot-protection blocks at the sea side of the upright part, and one on the port side. Provide holes in the blocks with an aperture ratio of about 10% to reduce uplift pressure. Use the following equation to determine the shape of the blocks:

$$t = d_f(h'/h)^{-0.787} \times H_{1/3} \quad (1)$$

Where:

t : required thickness of foot protection block (m)

$H_{1/3}$: Significant wave height (m)

d_f : 0.18 at the breakwater trunk and 0.21 at the breakwater head

h' : depth at the mound crown (excluding blocks) (m)

h : design depth (m)

(applicable depth: $h'/h = 0.4$ to 1.0)

The required thickness t is checked at the LWL which is critical for the determination of thickness, as follows:

$$\begin{aligned} t &= d_f(h'/h)^{-0.787} \times H_{1/3} & (2) \\ &= 0.18 \times (9.80/11.30)^{-0.787} \times 4.0 = 0.805 \end{aligned}$$

From the above results, the dimensions of the foot protection block are determined as follows:

Dimension: $L(\text{m}) \times b(\text{m}) \times t(\text{m}) = 3.0 \times 2.5 \times 1.0$

Porous type, $W = 15.64$ (t/piece)

7) Review of armor units

The required weight of armor units is calculated using the Hudson formula with the stability number N_s , as shown below:

$$M = \frac{\rho_r H^3}{N_s^3 (S_r - 1)^3} \tag{3}$$

Where:

M : required mass of rubble or concrete blocks (t)

ρ_r : density of rubble or concrete blocks (2.30 t/m³)

ρ_o : density of seawater (1.03 t/m³)

H : wave height used in stability calculation (m)

$$H_d = \gamma_H H_k = 1.0 \times 3.9 = 3.9 \text{ (m)}$$

N_s : stability number, which shall be $N_s^3 = 112$ according to the brochure

S_r : specific gravity of rubble or concrete blocks against water ($\rho_r/\rho_o = 2.30/1.03 = 2.233$)

$$M = (2.30 \times 3.9^3) / \{ 112 \times (2.233 - 1)^3 \} = 0.650 \text{ (t/piece)}$$

As above, while the required minimum weight of concrete blocks against waves is that of the 1-ton type, the 3-ton type will be used based on the requirement that 2 upper grade from the required minimum weight shall be adopted.

(4) Characteristic value of design load

1) Breakwater body weight and moment

Body weights and moments are shown in **Tables 4.2.9 (b), (c) and (d)**. The weight W_k' and moment $W_k'x$ per meter are as given in **Table 4.2.9 (a)**.

Table 4.2.9(a) Body weight and moment per meter

Portion	W_k' (kN/m)	$W_k'x$ (kN·m/m)
Caisson	783.758	4,506.609
Cover concrete	212.334	1,220.918
Filling sand	1,843.187	10,598.325
Ballast	42.375	243.656
Superstructure	333.464	2,224.088
Total	3,215.118	18,793.596

Table 4.2.9 (b) Breakwater weight and moment (caisson, cover concrete, filling sand, and ballast)

Description	Calculation equation	V(m ³)	w(kN/m ³)	W _k (kN)	x(m)	W _k x(kN·m)
Caisson						
Bottom slab	11.50 × 17.00 × 0.70 × 1	136.850	24.00	3,284.400	5.750	18,885.300
Front wall/rear wall	0.40 × 17.00 × 11.60 × 2	157.760	24.00	3,786.240	5.750	21,770.880
Side wall	10.70 × 0.40 × 11.60 × 2	99.296	24.00	2,383.104	5.750	13,702.848
Bulkhead (parallel to the face line)	0.20 × 16.20 × 11.60 × 2	75.168	24.00	1,804.032	5.750	10,373.184
Bulkhead (vertical to the face line)	10.30 × 0.20 × 11.60 × 3	71.688	24.00	1,720.512	5.750	9,892.944
Vertical haunch	0.20 × 0.20 × 11.60 × 1/2 × 48	11.136	24.00	267.264	5.750	1,536.768
Horizontal haunch (parallel to the face line)	0.20 × 0.20 × 14.00 × 1/2 × 6	1.680	24.00	40.320	5.750	231.840
Horizontal haunch (vertical to the face line)	0.20 × 0.20 × 9.10 × 1/2 × 8	1.456	24.00	34.944	5.750	200.928
Corner haunch	0.20 × 0.20 × 0.20 × 1/3 × 48	0.128	24.00	3.072	5.750	17.664
Subtotal		555.162		13,323.888		76,612.356
Cover concrete	3.40 × 3.90 × 1.00 × 8	106.080	22.60	2,397.408	5.750	13,785.096
	3.50 × 3.90 × 1.00 × 4	54.600	22.60	1,233.960	5.750	7,095.270
Vertical haunch reduction	0.20 × 0.20 × 1.00 × 1/2 × 48	-0.960	22.60	-21.696	5.750	-124.752
Subtotal		159.720		3,609.672		20,755.614
Filling sand	3.40 × 3.90 × 10.38 × 8	1,101.110	18.90	20,810.979	5.750	119,663.129
	3.50 × 3.90 × 10.38 × 4	566.748	18.90	10,711.537	5.750	61,591.338
Vertical haunch reduction	0.20 × 0.20 × 10.38 × 1/2 × 48	-9.965	18.90	-188.339	5.750	-1,082.949
Subtotal		1,657.893		31,334.177		180,171.518
Ballast	3.40 × 3.90 × 0.22 × 8	23.338	22.60	527.439	5.750	3,032.774
	3.50 × 3.90 × 0.22 × 4	12.012	22.60	271.471	5.750	1,560.958
Vertical haunch	0.20 × 0.20 × 0.22 × 1/2 × 48	-0.211	22.60	-4.769	5.750	-27.422
Horizontal haunch (parallel to the face line)	0.20 × 0.20 × 14.00 × 1/2 × 6	-1.680	22.60	-37.968	5.750	-218.316
Horizontal haunch (vertical to the face line)	0.20 × 0.20 × 9.10 × 1/2 × 8	-1.456	22.60	-32.906	5.750	-189.210
Corner haunch	0.20 × 0.20 × 0.20 × 1/3 × 48	-0.128	22.60	-2.893	5.750	-16.635
Subtotal		31.875		720.374		4,142.149
Total		2,404.650		48,988.111		281,681.637

Table 4.2.9 (c) Breakwater weight and moment (superstructure) *per meter

Description	Calculation equation	W _k (kN/m)	x(m)	W _k x(kN·m/m)
Superstructure	2.55 × 1.10 × 1 × 22.60	63.393	8.85 + 2.55 × 1/2 = 10.125	641.854
	1/2 × 8.75 × 0.10 × 1 × 22.60	9.888	0.10 + 8.75 × 2/3 = 5.933	58.666
	8.75 × 1.00 × 1 × 22.60	197.750	0.10 + 8.75 × 1/2 = 4.475	884.931
	1.80 × 1.30 × 1 × 22.60	52.884	9.50 + 1.80 × 1/2 = 10.400	549.994
	1/2 × 0.65 × 1.30 × 1 × 22.60	9.549	8.85 + 0.65 × 2/3 = 9.283	88.643
Total		333.464		2,224.088

Table 4.2.9 (d) Breakwater weight and moment (superstructure (parapet)) *per meter

Description	Calculation equation	W _k (kN/m)	x(m)	W _k x(kN·m/m)
	1.80 × 1.30 × 1 × 22.60	52.884	0.65 + 1.80 × 1/2 = 1.550	81.970
	1/2 × 0.65 × 1.30 × 1 × 22.60	9.549	0.65 × 2/3 = 0.433	4.135
Total		62.433		86.105

2) Buoyancy and moment

The buoyancy per meter is shown below:

- H.W.L.

$$W_{Bk} = 11.5 \times 11.5 \times 1.0 \times 10.1 = 1,335.725 \text{ (kN/m)}$$

Buoyancy moment

$$W_{Bk}x = 1,335.725 \times 5.750 = 7,680.419 \text{ (kN·m/m)}$$

- L.W.L.

$$W_{Bk} = 11.5 \times 9.8 \times 1.0 \times 10.1 = 1,138.270 \text{ (kN/m)}$$

Buoyancy moment

$$W_{Bkx} = 1,138.270 \times 5.750 = 6,545.053 \text{ (kN} \cdot \text{m/m)}$$

3) Wave force and moment

Wave force can be calculated using Goda's formula. A calculation example at the time of H.W.L. is shown below:

The design wave height H_D and the period in Goda's formula are the wave height and period of the highest wave, respectively. The design wave height is given by:

$$H_D = 1.8 \times H_{1/3} = 1.8 \times 3.82 = 6.88 = 6.9 \text{ (m)}$$

According to **Table 4.2.9(e)**, since the period of the design wave is 11.0 s and the water depth is 13.00 m, the wavelength $L = 115.163 \text{ m}$.

Table 4.2.9(e) Water depth, period, wavelength and wave celerity

	11.0		12.0		13.0		14.0		15.0	
1.0	34.2	3.11	37.4	3.12	40.5	3.12	43.7	3.12	46.8	3.12
2.0	48.2	4.38	52.6	4.39	57.1	4.39	61.6	4.40	66.0	4.40
3.0	58.6	5.33	64.2	5.35	69.6	5.36	75.1	5.37	80.6	5.37
4.0	67.3	6.12	73.7	6.14	80.1	6.16	86.5	6.18	92.8	6.19
5.0	74.9	6.81	82.0	6.84	89.2	6.86	96.3	6.88	103.4	6.90
6.0	81.5	7.41	89.4	7.45	97.3	7.48	105.1	7.51	113.0	7.53
7.0	87.6	7.96	96.1	8.01	104.7	8.05	113.2	8.08	121.6	8.11
8.0	93.1	8.46	102.3	8.52	111.4	8.57	120.6	8.61	129.6	8.64
9.0	98.1	8.92	108.0	9.00	117.7	9.05	127.4	9.10	137.1	9.14
10.0	102.8	9.35	113.2	9.44	123.6	9.50	133.8	9.56	144.1	9.60
11.0	107.2	9.75	118.2	9.85	129.1	9.93	139.9	9.99	150.6	10.04
12.0	111.3	10.12	122.8	10.24	134.2	10.33	145.6	10.40	156.8	10.45
13.0	115.2	10.47	127.2	10.60	139.1	10.70	151.0	10.78	162.7	10.85
14.0	118.8	10.80	131.3	10.95	143.8	11.06	156.1	11.15	168.3	11.22
15.0	122.2	11.11	135.3	11.27	148.2	11.40	161.0	11.50	173.7	11.58
16.0	125.5	11.41	139.0	11.58	152.4	11.72	165.7	11.83	178.8	11.92
17.0	128.5	11.68	142.6	11.88	156.4	12.03	170.1	12.15	183.8	12.25
18.0	131.4	11.95	145.9	12.16	160.3	12.33	174.4	12.46	188.5	12.57
19.0	134.2	12.20	149.2	12.43	163.9	12.61	178.6	12.75	193.0	12.87
20.0	136.8	12.44	152.3	12.69	167.5	12.88	182.5	13.04	197.4	13.16
22.0	141.7	12.89	158.1	13.17	174.1	13.39	190.0	13.57	205.7	13.72
24.0	146.2	13.29	163.4	13.61	180.3	13.87	197.0	14.07	213.5	14.23
26.0	150.2	13.66	168.3	14.02	186.0	14.31	203.5	14.53	220.8	14.72
28.0	153.9	13.99	172.8	14.40	191.3	14.72	209.6	14.97	227.6	15.17
30.0	157.3	14.30	176.9	14.74	196.2	15.10	215.3	15.38	234.1	15.60
35.0	164.4	14.95	186.0	15.50	207.2	15.94	228.1	16.29	248.7	16.58
40.0	170.1	15.46	193.5	16.12	216.5	16.65	239.1	17.08	261.4	17.43
45.0	174.5	15.86	199.6	16.64	224.4	17.26	248.7	17.76	272.6	18.17
50.0	178.0	16.18	204.7	17.06	231.0	17.77	256.9	18.35	282.5	18.83
55.0	180.7	16.42	208.8	17.40	236.6	18.20	264.1	18.86	291.1	19.41
60.0	182.7	16.61	212.1	17.68	241.4	18.57	270.3	19.31	298.8	19.92
70.0	185.5	16.86	216.9	18.08	248.7	19.13	280.3	20.02	311.6	20.77
80.0	187.0	17.00	220.0	18.33	253.7	19.52	287.7	20.55	321.5	21.43
90.0	187.8	17.07	221.9	18.49	257.2	19.78	293.1	20.93	329.1	21.94
100.0	188.3	17.11	223.0	18.58	259.5	19.96	297.0	21.21	334.9	23.32
120.0	188.6	17.15	224.1	18.67	261.9	20.15	301.6	21.54	342.5	22.83
140.0	188.7	17.15	224.4	18.70	262.9	21.70	303.8	21.70	346.6	23.11
160.0	188.7	17.16	224.5	18.71	263.3	20.26	304.9	21.78	348.7	23.25
180.0	188.7	17.16	224.6	18.72	263.5	20.27	305.3	21.81	349.8	23.32
200.0	188.7	17.16	224.6	18.72	263.6	20.27	305.5	21.82	350.4	23.36
	188.7	17.16	224.6	18.72	263.6	20.28	305.7	21.84	350.9	23.40

$$h_b = 13.000 + 5 \times 3.9 \times 1/100 = 13.195 \text{ (m)}$$

$$d = 11.500 - 1.000 = 10.500 \text{ (m) (top of foot protection block)}$$

$$\alpha_1 = 0.6 + \frac{1}{2} \left\{ \frac{4\pi h/L}{\sinh(4\pi h/L)} \right\}^2 \quad (4)$$

$$= 0.6 + \frac{1}{2} \left\{ \frac{4 \times \pi \times 13.000 / 115.163}{\sinh(4 \times \pi \times 13.000 / 115.163)} \right\}^2 = 0.866$$

$$\alpha_2 = \min \left\{ \frac{h_b - d}{3h_b} \left(\frac{H_D}{d} \right)^2, \frac{2d}{H_D} \right\} \quad (5)$$

$$= \min \left\{ \frac{13.195 - 10.500}{3 \times 13.195} \times \left(\frac{6.9}{10.500} \right)^2, \frac{2 \times 10.500}{6.9} \right\}$$

$$= \min \{0.029, 3.043\} = 0.029$$

Where the mound is high and waves are breaking against it, α_2 of **Eq. (5)** is generalized to α^* , and either α_2 or α_1 , whichever is larger, should be used.

$$\alpha^* = \max \{ \alpha_2, \alpha_1 \}$$

In this example calculation, since α_1 is zero according to the following review, the following value is given:

$$\alpha^* = \alpha_2 = 0.029$$

Where B_M is the mound width and L is the wavelength at the depth where the breakwater is installed.

$$B_M = 8.50 \text{ (m)}$$

$$B_M/L = 8.50/115.163 = 0.074$$

$$(h - d)/h = (13.00 - 10.50)/13.00 = 0.192$$

$$\alpha_{H1} \leq 0 \text{ gives } \alpha_{H1} = 0 \text{ as}$$

$$\begin{aligned} \alpha_3 &= 1 - \frac{h'}{h} \left\{ 1 - \frac{1}{\cosh(2\pi h/L)} \right\} \\ &= 1 - \frac{11.50}{13.00} \times \left\{ 1 - \frac{1}{\cosh(2 \times \pi \times 13.00 / 115.163)} \right\} \\ &= 0.816 \end{aligned}$$

$$\begin{aligned} \eta^* &= 0.75(1 + \cos\beta)\lambda_1 H_D \\ &= 0.75 \times (1 + \cos 21) \times 1.00 \times 6.90 = 10.006 \text{ (m)} \end{aligned}$$

$$\begin{aligned} p_1 &= 0.5(1 + \cos\beta)(\alpha_1 \lambda_1 + \alpha_2 \lambda_2 \cos^2\beta) w_o H_D \\ &= 0.5 \times (1 + \cos 21)(0.866 \times 1.000 + 0.029 \times 1.000 \times \cos^2 21) \times 1.03 \times 9.81 \times 6.90 = 60.076 \\ &\text{(kN/m}^2\text{)} \end{aligned}$$

$$\begin{aligned} p_2 &= p_1 / \cosh(2\pi h/L) \\ &= 60.076 / \cosh(2 \times \pi \times 13.00 / 115.163) = 47.594 \text{ (kN/m}^2\text{)} \end{aligned}$$

$$p_3 = \alpha_3 p_1 = 0.816 \times 60.076 = 49.022 \text{ (kN/m}^2\text{)}$$

$$p_4 = 60.076 \times (10.006 - 3.20) / 10.006 = 40.863 \text{ (kN/m}^2\text{)}$$

$$\begin{aligned} p_u &= 0.5(1 + \cos\beta)\alpha_1 \alpha_3 \lambda_3 w_o H_D = 0.5 \times (1 + \cos 21) \times 0.866 \times 0.816 \times 1.000 \times 1.03 \times 9.81 \times 6.90 \\ &= 47.632 \text{ (kN/m}^2\text{)} \end{aligned}$$

Figure 4.2.7 shows the wave pressure distribution calculated from Goda's formula. The wave force and

moment are given in **Table 4.2.10**.

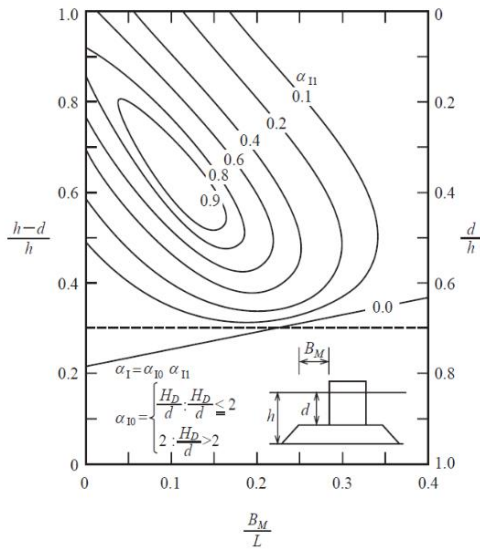


Figure 4.2.6 Impulsive breaking wave pressure coefficient

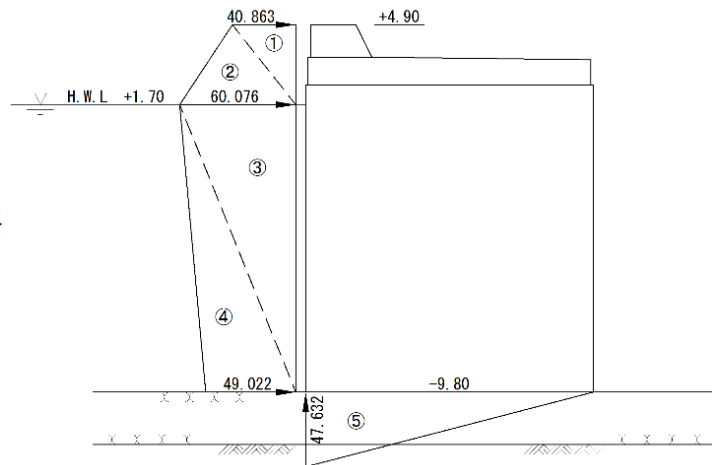


Figure 4.2.7 Wave pressure distribution

Table 4.2.10 Wave force and moment

		P_{Ik} (kN/m)	y (m)	$P_{Ik}y$ (kN·m/m)
①	$40.863 \times 3.20 \times 1/2$	65.381	13.633	891.339
②	$60.076 \times 3.20 \times 1/2$	96.122	12.567	1,207.965
③	$60.076 \times 11.50 \times 1/2$	345.437	7.667	2,648.465
④	$49.022 \times 11.50 \times 1/2$	281.877	3.833	1,080.435
		788.817		5,828.204

		P_{Ik} (kN/m)	x (m)	$P_{Ik}x$ (kN·m/m)
⑤	$47.632 \times 11.50 \times 1/2$	273.884	7.667	2,099.869
		273.884		2,099.869

4) Eccentric inclined loading

An example of a calculation at the time of H.W.L. is shown below (see **Table 4.2.11**):

i) Check of the distribution profile of the bottom reaction force

Calculate the bottom reaction force using the characteristic value of each design element, and check its distribution profile. The bottom reaction force calculated here will be used to verify the performance of structural members.

$$x = \frac{\Sigma M}{\Sigma V} = \frac{3,185.104}{1,605.509} = 1.984(\text{m})$$

$$e = \frac{B}{2} - x = \frac{11.50}{2} - 1.984 = 3.766(\text{m})$$

$$e > B / 6 = 1.917(\text{m})$$

∴ The bottom reaction force is distributed in a triangular pattern.

$$P_1 = \frac{2\Sigma V}{3\left(\frac{B}{2} - e\right)} = \frac{2 \times 1,605.509}{3 \times \left(\frac{11.50}{2} - 3.766\right)} = 539.486(\text{kN/m}^2)$$

$$b = 3(B/2 - e) = 3 \times (11.50/2 - 3.766) = 5.952(\text{m})$$

Where:

e : eccentricity of total resultant force (m)

B : width of bottom (m)

P_1 : characteristic value of bottom reaction at the hind toe (kN/m^2)

b : action width of bottom reaction when $e > B/6$ (m)

V : total vertical force (kN/m)

Table 4.2.11 Characteristic value of each design

	Characteristic value V_k (kN/m)	Characteristic value M_k ($\text{kN} \cdot \text{m/m}$)
Caisson weight	783.758	4,506.609
Cover concrete weight	212.334	1,220.918
Filling sand weight	1,843.187	10,598.325
Ballast weight	42.375	243.656
Superstructure weight	333.464	2,224.088
Horizontal wave force	—	-5,828.204
Uplift pressure	-273.884	-2,099.869
Buoyancy	-1,335.725	-7,680.419
Total	1,605.509	3,185.104

ii) Calculation of surcharge load and its loading width

Table 4.2.11 gives:

$$2b' = \frac{2\Sigma M}{\Sigma V} = \frac{2 \times 3,185.104}{1,605.509} = 3.968(\text{m})$$

$$q = \frac{\Sigma V}{2b'} = \frac{1,605.509}{3.968} = 404.614(\text{kN/m}^2)$$

5) Ground conditions used in the simplified Bishop method

Ground conditions (characteristic values) used in the simplified Bishop method are as shown in **Table 4.2.12**.

Table 4.2.12 Ground conditions

	Angle of shear resistance $\phi'_k (^\circ)$	Saturated weight W'_{satk} (kN/m^3)	Wet weight W'_{tk} (kN/m^3)	Cohesion	
				C'_k (kN/m^2)	First-order coefficient of cohesion
Rubble for foundation	35.00	20.00	18.00	20.00	0.00
Sandy soil (1)	45.00	20.00	18.00	0.00	0.00
Sandy soil (2)	45.00	20.00	18.00	0.00	0.00

(5) Stability verification

Verify each design condition as follows based on the characteristic value of each design element determined in (3). The verification process at H.W.L. is described here.

1) Variable situation related to waves

i) Sliding of the upright part

- Body weight $W_k = 3,215.118$ (kN/m)
- Buoyancy $P_{Bk} = 1,335.725$ (kN/m)
- Wave force and uplift pressure $P_{Hk} = 788.817$ (kN/m), $P_{uk} = 273.884$ (kN/m)
- Verification

Resistance value

$$R_k = f_k(W_k - P_{Bk} - P_{uk}) = 0.70 \times (3,215.118 - 1,335.725 - 273.884) = 1,123.856 \text{ (kN/m)}$$

$$R_d = \gamma_R R_k = 0.83 \times 1,123.856 = 932.800 \text{ (kN/m)}$$

Load value

$$S_k = P_{Hk} = 788.817 \text{ (kN/m)}$$

$$S_d = \gamma_s S_k = 1.08 \times 788.817 = 851.922 \text{ (kN/m)}$$

Verification

$$m(S_d/R_d) = 1.00 \times (851.922/932.800) = 0.913 \leq 1.0 \text{ -O.K.-}$$

ii) Overturning of the upright part

- Moment of body weight $a_1 W_k = 18,793.596$ (kN·m/m)
- Buoyancy moment $a_2 P_{Bk} = 7,680.419$ (kN·m/m)
- Moments of wave force and uplift pressure
 $a_4 P_{Hk} = 5,828.204$ (kN·m/m), $a_3 P_{Uk} = 2,099.869$ (kN·m/m)
- Verification

Resistance value $R_k = a_1 W_k - a_2 P_{Bk} - a_3 P_{Uk}$

$$= 18,793.596 - 7,680.419 - 2,099.869$$

$$= 9,013.308 \text{ (kN·m/m)}$$

$$R_d = \gamma_R R_k = 0.95 \times 9,013.308 = 8,562.643 \text{ (kN·m/m)}$$

Load value

$$S_k = a_4 P_{Hk} = 5,828.204 \text{ (kN·m/m)}$$

$$S_d = \gamma_s S_k = 1.14 \times 5,828.204 = 6,644.153 \text{ (kN·m/m)}$$

Verification

$$m(S_d/R_d) = 1.00 \times (6,644.153/8,562.643) = 0.776 \leq 1.0 \text{ -O.K.-}$$

iii) Bearing capacity of the foundation ground

- Eccentric and inclined load

Characteristic values of horizontal wave force, surcharge load, and distribution width determined in (3) are shown below:

$$P_{Hk} = 788.817 \text{ (kN/m)}$$

$$q_k = 404.614 \text{ (kN/m}^2\text{)}$$

$$2b' = 3.968 \text{ (m)}$$

- Ground conditions

Ground conditions are shown in **Table 4.2.13**.

- Verification

Verification results are shown below:

$$\text{Acting moment: } S_k = 28,153.31 \text{ (kN} \cdot \text{m)}$$

$$\text{Resisting moment: } R_k = 28,288.42 \text{ (kN} \cdot \text{m)}$$

$$S_d = \gamma_s S_k = 1.00 \times 28,153.31 = 28,153.31 \text{ (kN} \cdot \text{m)}$$

$$R_d = \gamma_R R_k = 1.00 \times 28,288.42 = 28,288.42 \text{ (kN} \cdot \text{m)}$$

$$m = 1.00$$

$$m(S_d/R_d) = 1.00 \times (28,153.31/28,288.42) = 0.995 \leq 1.0 \text{ -O.K.-}$$

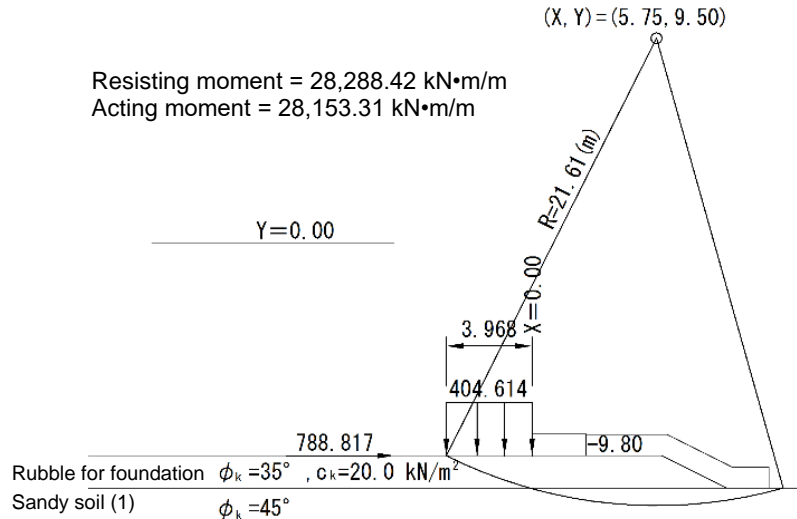


Figure 4.2.8 Examination of eccentric and inclined load

2) Verification of the permanent situation

i) Slip of the foundation ground

An examination of the slip failure of the foundation ground is made here using the modified Fellenius method.

• Surcharge

$$\Sigma M = W_k'x - W_{Bk}x = 18,793.596 - 6,545.053 = 12,248.543 \text{ (kN} \cdot \text{m/m)}$$

$$\Sigma V = W_k' - W_{Bk} = 3,215.118 - 1,138.270 = 2,076.848 \text{ (kN/m)}$$

$$x = \Sigma M / \Sigma V = 12,248.543 / 2,076.848 = 5.898 \text{ (m)}$$

$$e = (B/2) - x = (11.50/2) - 5.898 = -0.148 \text{ (m)}$$

Since $e < B/6 = 1.917 \text{ (m)}$, the bottom reaction force is distributed in a trapezoidal pattern.

$$p_1 = \left(1 + \frac{6e}{B}\right) \frac{\Sigma V}{B}$$

$$= \left(1 - \frac{6 \times 0.148}{11.50}\right) \times \frac{2,076.848}{11.50} = 166.650 \text{ (kN/m}^2\text{)}$$

$$p_2 = \left(1 - \frac{6e}{B}\right) \frac{\Sigma V}{B}$$

$$= \left(1 + \frac{6 \times 0.148}{11.50}\right) \times \frac{2,076.848}{11.50} = 194.541 \text{ (kN/m}^2\text{)}$$

3. Sloping Breakwater

(1) Basic section for review

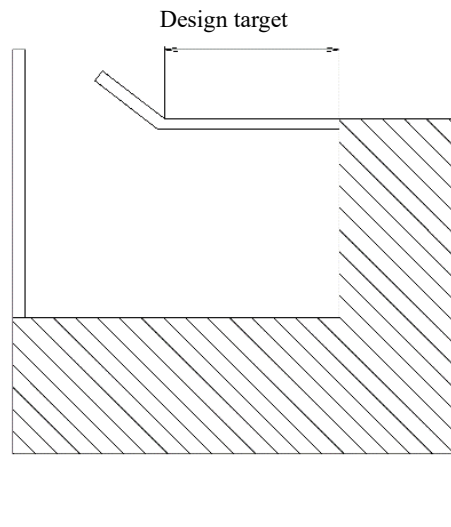


Figure 4.3.1 Location of breakwater

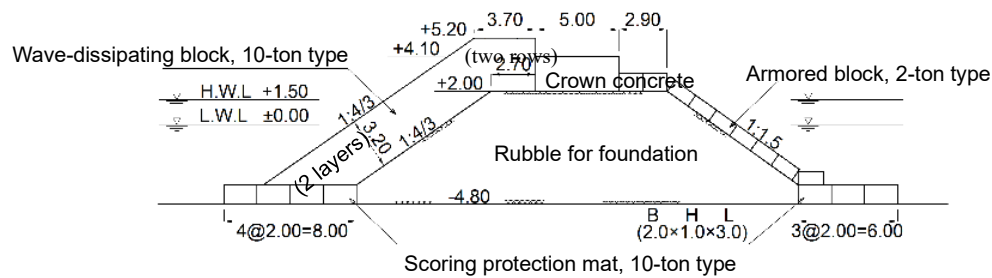


Figure 4.3.2 Basic section for review

(2) Design conditions

1) Design wave

$$H_{1/3} = 4.3 \text{ m}, \quad H_D = H_{\max} = 5.6 \text{ m}, \quad T = 14.0 \text{ s}, \quad \beta = 40^\circ$$

2) Tide level

$$\text{H.W.L.: } +1.5 \text{ m}; \quad \text{L.W.L.: } \pm 0.0 \text{ m}$$

3) Depth of installation

$$-4.8 \text{ m}$$

4) Soil characteristics

-4.8 to -7.8 m: cohesive soil with $c = 30 \text{ kN/m}^2$

(Coefficient of variation C_V is 0.25 or more.)

$$\gamma = 16 \text{ kN/m}^3, \quad \gamma' = 6 \text{ kN/m}^3$$

-7.8 and under: bedrock

5) Friction coefficient

$$\text{Concrete and rubble: } f = 0.6$$

6) Unit weight

Concrete: $\gamma_c = 22.6 \text{ kN/m}^3$ (above water)

Rubble: $\gamma_t = 18 \text{ kN/m}^3$ (above water), $\gamma' = 10 \text{ kN/m}^3$ (under water)

7) Partial factor

(Variable situation caused by variable waves)

Sliding of superstructure

$\gamma_R = 1.00$ (partial factor that is to be multiplied with the resistance term)

$\gamma_S = 1.00$ (partial factor that is to be multiplied with the load term)

$m = 1.20$ (adjustment factor)

Overturning of superstructure

$\gamma_R = 1.00$ (partial factor that is to be multiplied with the resistance term)

$\gamma_S = 1.00$ (partial factor that is to be multiplied with the load term)

$m = 1.20$ (adjustment factor)

Bearing capacity for the eccentric and inclined action

$\gamma_R = 1.00$ (partial factor that is to be multiplied with the resistance term)

$\gamma_S = 1.00$ (partial factor that is to be multiplied with the load term)

$m = 1.00$ (adjustment factor)

(Permanent situation)

Circular slip failure (cohesive ground, when $CV > 0.25$)

$\gamma_R = 1.00$ (partial factor that is to be multiplied with the resistance term)

$\gamma_S = 1.00$ (partial factor that is to be multiplied with the load term)

$m = 1.30$ (adjustment factor)

(3) Determination of structural dimensions

1) Crown height of the breakwater (superstructure)

$$\text{H.W.L.} + 0.6 H_{1/3} = +1.5 + 0.6 \times 4.3 = +4.08 \rightarrow +4.1 \text{ m}$$

Note: The crown height needs to be greater than the height of the center of gravity of wave-dissipating blocks at the top part in order to prevent the block from falling behind the superstructure.

2) Crown height of rubble for foundation

It shall be 0.5 m above H.W.L., (i.e. +2.0 m) with assumption that the rubble is spreading from the land toward to the sea by heavy construction machineries.

3) Crown height of superstructure

It shall be 5.0 m, considering the service width of heavy construction machinery.

4) Required mass of wave-dissipating blocks

Use wave-dissipating blocks with a K_D value of 8.3, and calculate required mass with the Hudson formula using 1:4/3 for the slope gradient.

Since both γ_{N_s} and γ_H are 1.0, this makes the characteristic value and the design value the same.

$$N_{sd}^3 = N_{sk}^3 = K_D \cot \alpha = 8.3 \times 4/3 = 11.07$$

$$H_d = H_k = 4.3 \text{ m}$$

$$\begin{aligned}
M_d &= \frac{\rho_r H_d^3}{N_{s_d}^3 (S_r - 1)^3} \\
&= \frac{2.3 \times 4.3^3}{11.07 \times (2.3/1.03 - 1)^3} \\
&= 8.81 \text{ t}
\end{aligned}$$

Therefore, use 10-ton type wave-dissipating blocks (with an actual mass of 9.20 t).

5) Required mass of port-side armor units

Calculate the port-side design wave using 0.60 for K_d . Since γ_H is 1.0, the characteristic value and the design value are the same.

$$H_d = H_k = K_d H_i = 0.60 \times 4.3 = 2.58 \rightarrow 2.6 \text{ m}$$

H_i : Offshore-side design wave height (m)

Use armored blocks with a K_D value of 13.6, and calculate the required mass with the Hudson formula using 1:1.5 for the slope gradient.

$$\begin{aligned}
N_{s_d}^3 &= N_{s_k}^3 = 13.6 \times 1.5 = 20.40 \\
M_d &= \frac{\rho_r H_d^3}{N_{s_d}^3 (S_r - 1)^3} \\
&= 1.0 \times \frac{2.3 \times 2.6^3}{20.4 \times (2.3/1.03 - 1)^3} \\
&= 1.06 \text{ t}
\end{aligned}$$

Therefore, use the 2-ton type armored blocks.

6) Mass of rubble for foundation

The mass shall be 1/10 to 1/15 that of the wave-dissipating blocks.

$$M_d = (1/10 \sim 1/15) \times 9.20 = 0.61 \sim 0.92 \text{ t/piece}$$

(4) Calculation of the design external force

1) Body weight and resisting moment

$$\begin{aligned}
W_k &= 5.0 \times 2.1 \times 22.6 = 237.30 \text{ kN/m} \\
M_{W_k} &= 237.30 \times (1/2 \times 5.0) = 593.25 \text{ kN} \cdot \text{m/m}
\end{aligned}$$

2) Wave force and overturning moment

i) Intensity of wave pressure

$$\begin{aligned}
\lambda &= \exp[-10(h/L)^{1.5}(1-h'/h)^5] \\
&= \exp[-10 \times (6.3/107.6)^{1.5} \times \{1 - (-0.5/6.3)\}^5] = 0.81 \\
L &= \frac{gT^2}{2\pi} \tanh \frac{2\pi h}{L} \\
&= \frac{9.81 \times 14.0^2}{2\pi} \tanh \frac{2\pi \times 6.3}{L}
\end{aligned}$$

Hence, $L = 107.6 \text{ m}$

$$\eta^* = 0.75(1 + \cos \beta) \lambda H_D = 0.75 \times (1 + \cos 40^\circ) \times 0.81 \times 5.6 = 6.01 \text{ m}$$

$$\alpha_1 = 0.6 + \frac{1}{2} \left[\frac{4\pi h/L}{\sinh(4\pi h/L)} \right]^2$$

$$= 0.6 + \frac{1}{2} \left[\frac{4\pi \times 6.3/107.6}{\sinh(4\pi \times 6.3/107.6)} \right]^2 = 1.019$$

$$\alpha_3 = 1 + \frac{h'}{\eta^*} = 1 + \frac{-0.5}{6.01} = 0.917$$

$$h_c^* = \min \{ \eta^*, h_c \} = \min \{ 6.01, 2.6 \} = 2.6$$

$$\alpha_4 = 1 - \frac{h_c^*}{\eta^*} = 1 - \frac{2.6}{6.01} = 0.567$$

$$p_1 = 1/2(1 + \cos \beta) \lambda a_1 \rho_0 g H_D = 1/2 \times (1 + \cos 40^\circ) \times 0.81 \times 1.019 \times 1.03 \times 9.81 \times 5.6 = 41.24 \text{ kN/m}^2$$

$$p_3 = p_u = \alpha_3 p_1 = 0.917 \times 41.24 = 37.82 \text{ kN/m}^2$$

$$p_4 = \alpha_4 p_1 = 0.567 \times 41.24 = 23.38 \text{ kN/m}^2$$

$$\ell_u = \min \left\{ B, 0.2 \cdot \frac{(\eta^* + h')^2}{|h'|} \right\} = \min \left\{ 5.0, 0.2 \times \frac{(6.01 - 0.5)^2}{|-0.5|} \right\} = \min \{ 5.0, 12.14 \} = 5.0 \text{ m}$$

ii) Wave pressure distribution

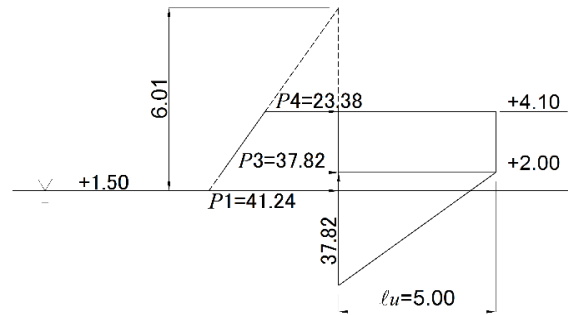


Figure 4.3.3 Wave pressure distribution

iii) Resultant force of wave pressure and overturning moment

$$P_{Hk} = 1/2 \times (23.38 + 37.82) \times 2.1$$

$$= 64.26 \text{ kN/m}^2$$

$$M_{Pk} = \frac{2.1^2}{6} \times (2 \times 23.38 + 37.82) = 62.17 \text{ kN} \cdot \text{m/m}$$

iv) Uplift pressure and overturning moment

$$P_{Uk} = 1/2 \times 37.82 \times 5.0 = 94.55 \text{ kN/m}$$

$$M_{Uk} = 94.55 \times (2/3 \times 5.0) = 315.17 \text{ kN} \cdot \text{m/m}$$

(5) Stability verification

1) Examination of sliding

$$m \cdot \frac{S_d}{R_d} \leq 1.0 \quad R_d = \gamma_R R_k \quad S_d = \gamma_S S_k \quad (1)$$

$$R_k = f_k (W_k - P_{Uk})$$

$$S_k = P_{Hk}$$

$$\begin{aligned}
m \cdot \frac{S_d}{R_d} &= m \frac{\gamma_S \times P_{Hk}}{\gamma_R \times (f_k \times (W_k - P_{Uk}))} \\
&= 1.20 \times \frac{1.00 \times 64.26}{1.00 \times (0.6 \times (237.3 - 94.55))} \\
&= 0.90 < 1.0
\end{aligned}$$

2) Examination of overturning

$$m \cdot \frac{S_d}{R_d} \leq 1.0 \quad R_d = \gamma_R R_k \quad S_d = \gamma_S S_k \quad (2)$$

$$R_k = M_{Wk} - M_{Uk}$$

$$S_k = M_{Pk}$$

$$\begin{aligned}
m \cdot \frac{S_d}{R_d} &= \frac{\gamma_S \times M_{Pk}}{\gamma_R \times (M_{Wk} - M_{Uk})} \\
&= 1.20 \times \frac{1.00 \times 62.17}{1.00 \times (593.25 - 315.17)} \\
&= 0.26 < 1.0
\end{aligned}$$

3) Bearing capacity of the foundation against eccentric and inclined load

Examine this using the simplified Bishop method.

The performance verification equation is shown in (3).

$$\begin{aligned}
m \cdot \frac{S_d}{R_d} &\leq 1.0 \\
R_d &= \gamma_R R_k \quad S_d = \gamma_S S_k
\end{aligned} \quad (3)$$

Where:

R_k ; characteristic value of resistance (resisting moment)

S_k ; characteristic value of load (acting moment)

γ_R ; partial factor by which the resistance term is multiplied

γ_S ; partial factor by which the load term is multiplied

m ; adjustment factor

Table 4.3.1 Standard lower limit value of the adjustment factor (m) in analysis of the bearing capacity against eccentric and inclined action

	Quaywall, etc.	Breakwater
Permanent situation	1.20 or more	-
Variable situation related to Level 1 earthquake ground motion	1.00 or more	-
Variable situation related to waves	-	1.00 or more

The standard value of adjustment factor (m) will be determined as the lower limit value of the minimum value of (m) obtained from the simplified Bishop method.

Calculate the distribution width of the end-toe pressure and bottom reaction force should be calculated as follows:

$$\begin{aligned}
M_k &= M_{Wk} - M_{Uk} - M_{Pk} \\
&= 593.25 - 315.17 - 62.17 = 215.91 \text{ kN} \cdot \text{m/m}
\end{aligned}$$

$$V_k = W_k - U_k = 237.30 - 94.55 = 142.75 \text{ kN/m}$$

$$\chi = M_k / V_k = 215.91 / 142.75$$

$$= 1.51 \text{ m} < b/3 = 5.0/3 = 1.67 \text{ m}$$

∴ The bottom reaction force is distributed in a triangular pattern.

$$p_1 = \frac{2}{3} \cdot \frac{V}{x} = \frac{2}{3} \times \frac{142.75}{1.51} = 63.02 \text{ kN/m}^2$$

$$b' = 3x = 3 \times 1.51 = 4.53 \text{ m}$$

Calculate the equivalent uniformly-distributed load and distribution width as follows:

$$q = \frac{p_1 b'}{4x} = \frac{63.02 \times 4.53}{4 \times 1.51} = 47.27 \text{ kN/m}^2$$

$$B = 2x = 2 \times 1.51 = 3.02 \text{ m}$$

Horizontal force H ($=P=64.26 \text{ kN/m}$) should be caused to act on the bottom of the breakwater body.

The strength constants of the foundation shall take the following values:

Rubble for foundation:

$$\phi = 35^\circ \text{ and } c = 20 \text{ kN/m}^2$$

Foundation ground: $c = 30 \text{ kN/m}^2$

A computer was used to calculate the above values, and the results are shown in **Figure 4.3.4**.

Minimum m value = $1.84 \geq$ set m value = 1.00

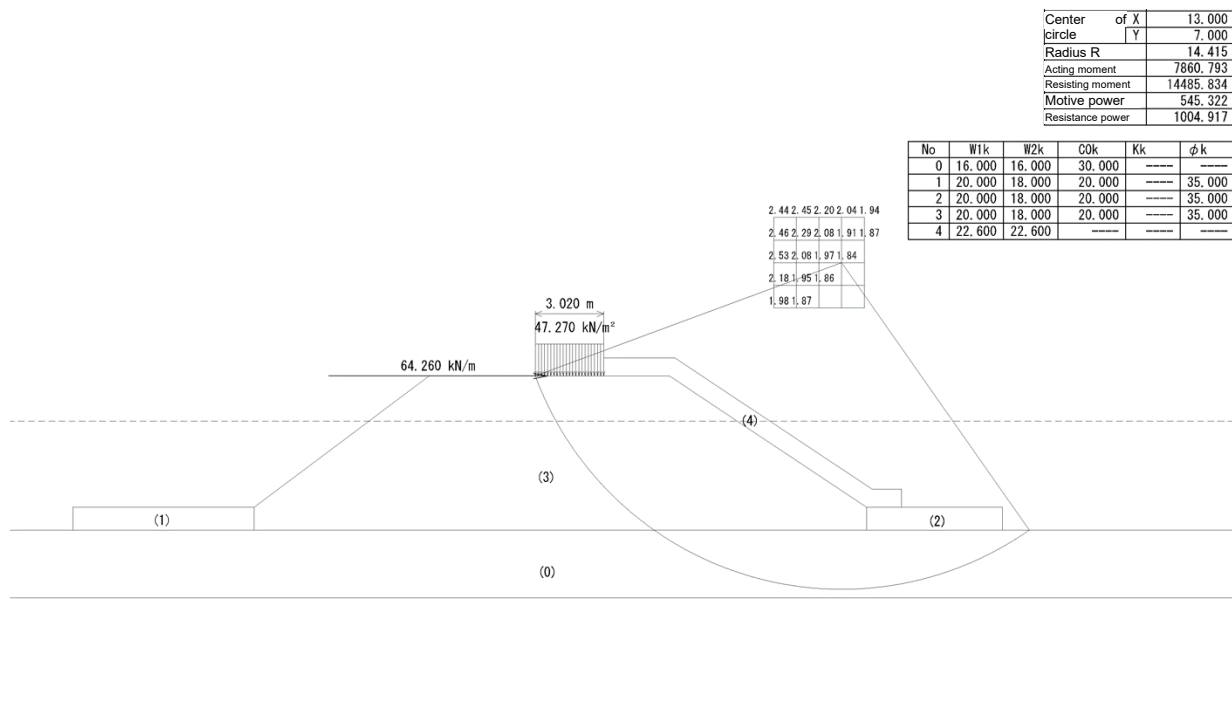


Figure 4.3.4 Calculation results for the bearing capacity against eccentric and inclined load

The performance verification equation is shown as **Eq. (4)**.

$$m \cdot \frac{S_d}{R_d} \leq 1.0 \quad (4)$$

$$R_d = \gamma_R R_k \quad S_d = \gamma_S S_k$$

Where:

R_k ; characteristic value of resistance (resisting moment)

S_k ; characteristic value of load (acting moment)

γ_R ; partial factor by which the resistance term is multiplied

γ_S ; partial factor by which the load term is multiplied

m ; adjustment factor

Determine the value of the partial factor as in the case of the breakwater. The coefficient of variation (CV) of cohesive soil shall have a value not smaller than 0.25.

The verification results are shown in **Figure 4.3.5**

Offshore side → Port side

$$m \cdot \frac{S_d}{R_d} = 1.30 \times 8891.815 / 12688.084$$

$$= 0.91 \leq 1.0$$

Port side → Offshore side

$$m \cdot \frac{S_d}{R_d} = 1.30 \times 9638.553 / 13573.066$$

$$= 0.91 \leq 1.0$$

Offshore side → Port side

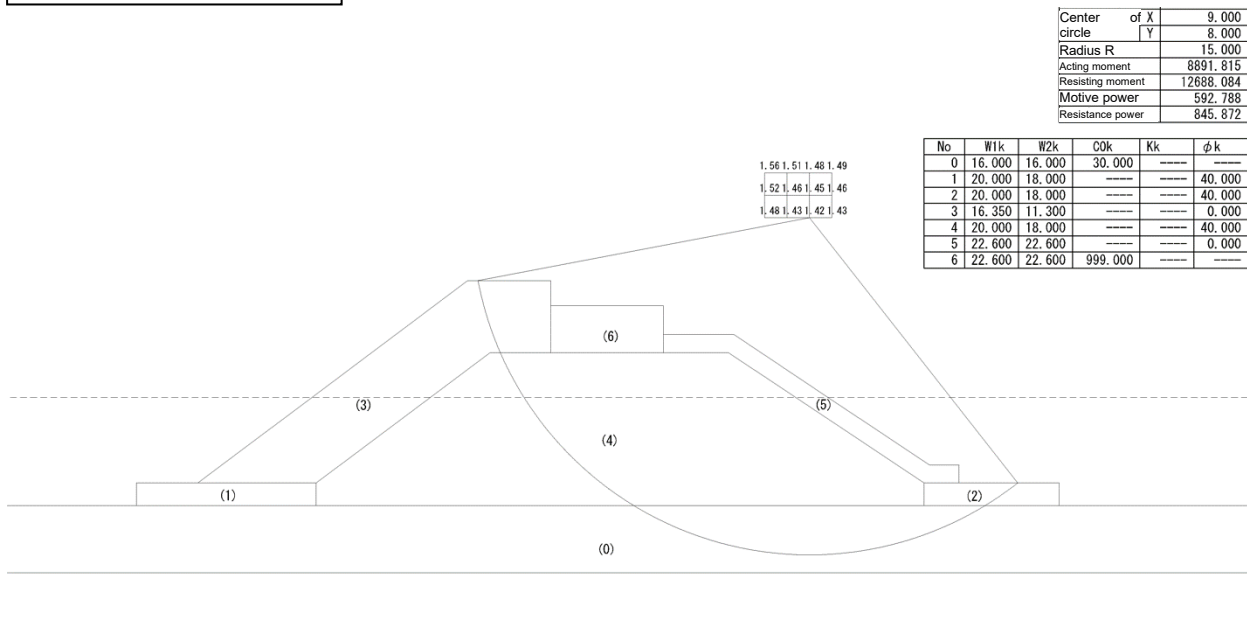


Figure 4.3.5 Calculation results of bearing capacity against inclined and eccentric load

Port side → Offshore side

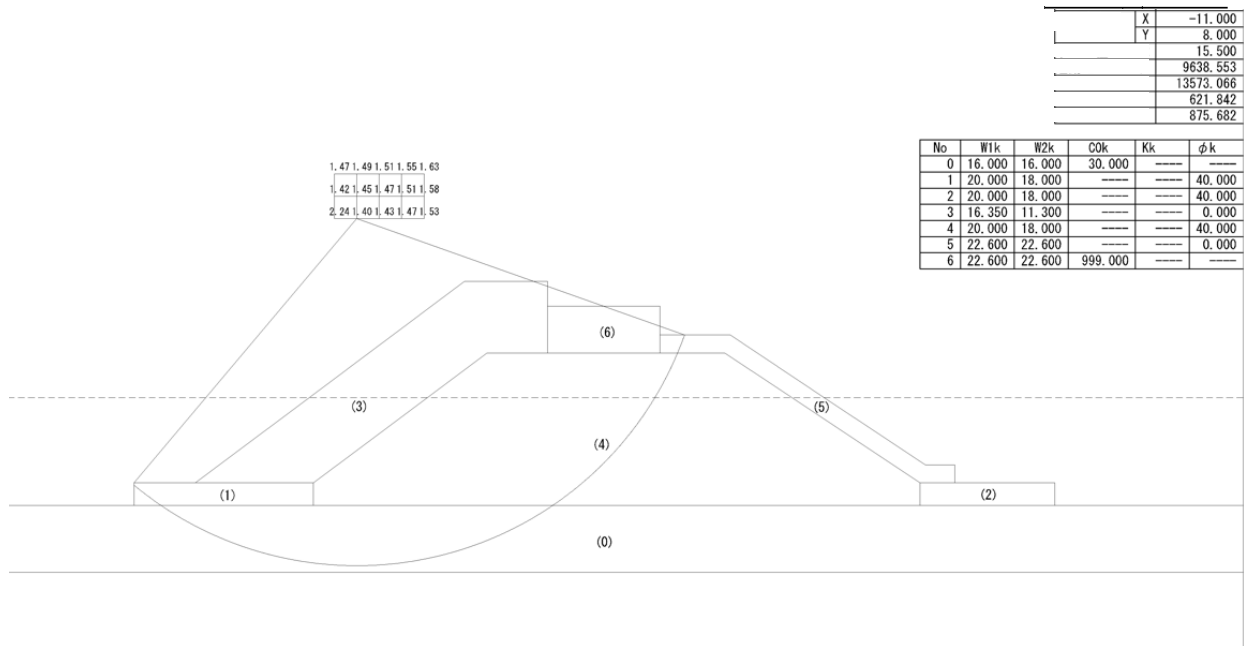


Figure 4.3.6 Calculation results of circular slip failure

(6) Calculation of consolidation settlement

There are three methods of calculating the final consolidation settlement of the foundation, namely the m_v method, the $e-\log p$ curve method, and the C_c method. Use the m_v method for this calculation.

When the m_v method is used, the final consolidation settlement can be determined using the following equation. Determine the design value for m_v by correcting the dispersion of data and correcting the number of data.

$$S = m_v \Delta \rho h \quad (5)$$

Where:

S : final consolidation settlement (m)

m_v : coefficient of volume compressibility when the consolidation pressure is $\rho_0 + 1/2\Delta\rho$
(m^2 / kN)

ρ_0 : overburden pressure of the ground in situ (kN/m^2)

$\Delta\rho$: pressure increment (kN/m^2)

h : layer thickness (m)

1) Calculation model

The section to calculate shall be the one after completion of the foundation work and superstructure work as shown in **Figure 4.3.7**.

The coefficient of volume compressibility m_v can be determined from the curve $\rho-m_v$ obtained from compression testing, and is set to $2.5 \times 10^{-4} \text{m}^2/\text{kN}$ in this example.

Calculation subject is the center of the breakwater body.

2) Calculation of pressure increment

i) Pressure increment due to the rubble for foundation

The vertical underground stress due to strip load can be calculated from (6) using the calculation diagram of influence values shown in **Figure 4.3.8**.

$$\sigma_z = \rho I_\sigma \quad (6)$$

Where:

σ_z : vertical underground stress due to strip load (kN/m²)

ρ : loading intensity (kN/m²)

I_σ : influence value

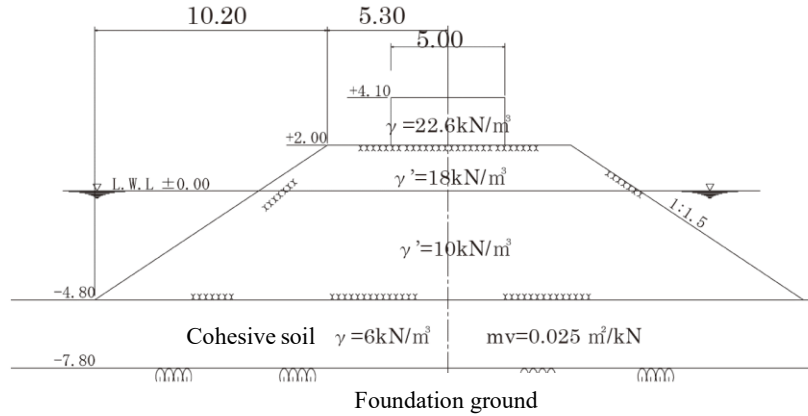


Figure 4.3.7 Calculation model

$$a/z = 10.20/1.50 = 6.80$$

$$b/z = 5.30/1.50 = 3.53$$

z : Depth from the ground surface at the target point (m)

Figure 4.3.8 gives: I_σ : 0.5

Double the loading intensity, assuming that the shape is bilaterally symmetrical.

$$\rho = 2\sum r_i h_i = 2 \times (18 \times 2.00 + 10 \times 4.80)$$

$$= 168.00 \text{ kN/m}^2$$

$$\therefore \sigma_z = \rho I_\sigma = 168.00 \times 0.5 = 84.00 \text{ kN/m}^2$$

ii) Pressure increment due to the superstructure

The vertical underground stress due to the uniformly distributed strip load can be calculated from (7) using the calculation diagram of influence values shown in **Figure 4.3.9**.

$$\sigma_z = \rho I_\sigma \quad (7)$$

Where:

σ_z : vertical underground stress due to a uniformly distributed strip load (kN/m²)

ρ : loading intensity (kN/m²)

I_σ : influence value

$$x/B = 0.00/5.00 = 0.00$$

$$z/B = 8.30/5.00 = 1.66$$

z : Depth from the ground surface at the target point (m)

In this calculation, it shall be the depth from the underside of the superstructure.

That is, $z = 6.80 + 1.50 = 8.30$ m

Figure 4.3.9 gives: I_σ : 0.36

$$\rho = \gamma h = 22.6 \times 2.10 = 47.46 \text{ kN/m}^2$$

$$\therefore \sigma_z = \rho I_\sigma = 47.46 \times 0.36 = 17.09 \text{ kN/m}^2$$

iii) Total pressure increment

$$\Delta p = 84.00 + 17.09 = 101.09 \text{ kN/m}^2$$

3) Calculation of final consolidation settlement

According to the above calculations, the final consolidation settlement shall take the following value:

$$S = m_v \Delta p h = 2.5 \times 10^{-4} \times 101.09 \times 3.00$$

$$= 0.0758 \text{ m} = 7.58 \text{ cm}$$

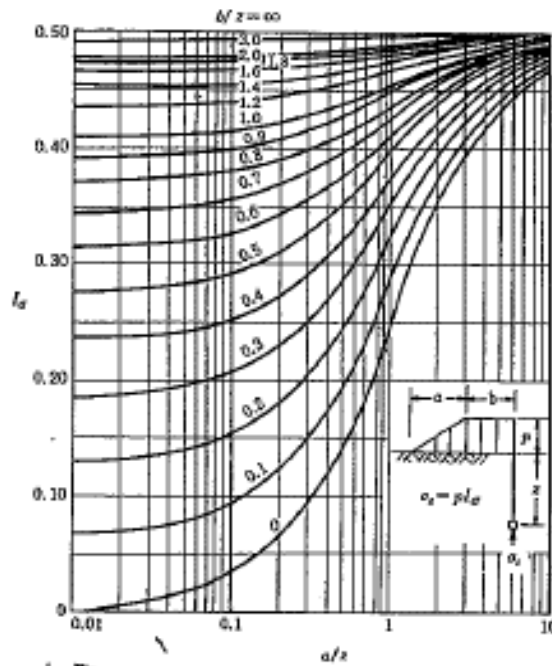


Figure 4.3.8 Influence values of the vertical underground stress due to strip load

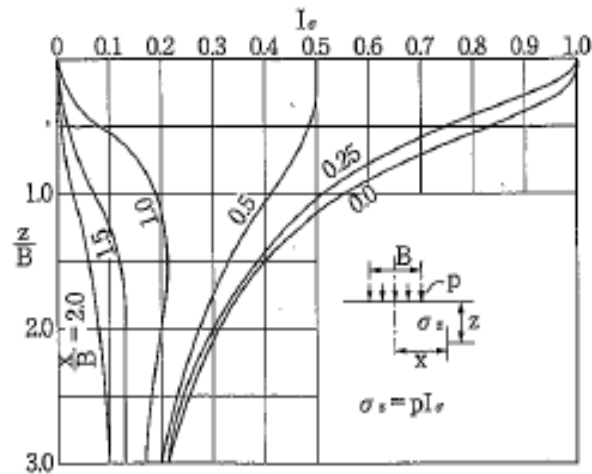


Figure 4.3.9 Influence values of the vertical underground stress due to uniformly distributed strip load

Chapter 5 Examples of Mooring Facility Design

1. Typical Structural Types in Japan

The optimum structural type for mooring facilities is largely governed by the ground conditions at the design location. The “gravity type,” “sheet pile type,” “cellular-bulkhead type” and similar types are suitable for locations where the ground conditions are good, while the “open-type wharf on vertical piles” is suitable when the bearing capacity of the ground is inadequate or the bearing stratum is deep.

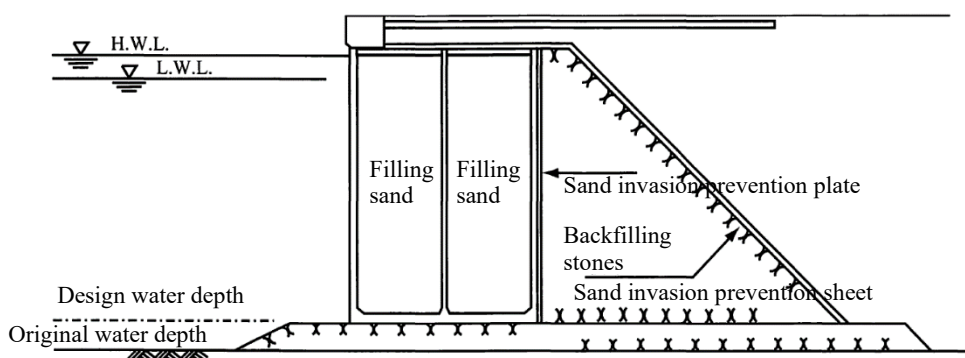
Gravity-type quaywalls include the “caisson type,” “block type,” “L-shaped block type,” “cellular block type” and others. In Japan, however, the “caisson type” is frequently used, as this type can also be applied to quaywalls at locations with a large water depth.

For sheet pile type quaywalls, in addition to the use of ready-made U-shaped sheet piles in the body of the structure, steel pipe sheet piles with connectors attached to the pipes are used in many large-scale quaywalls. The types of anchorage include anchor plates, sheet piles, piles and others. Piles are widely used in large-scale quaywalls.

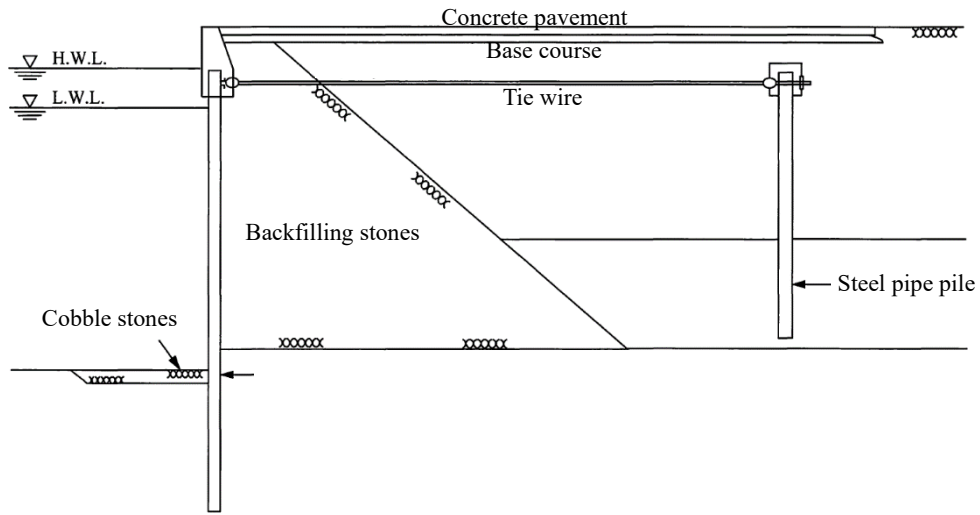
The structural types of piles used in open-type wharfs on vertical piles are the vertical pile type and the open-type wharf on coupled raking piles. The latter is used in cases where large horizontal forces, such as seismic forces, etc., are assumed to act on the structure, as this type has large horizontal resistance capacity.

Structurally, the cellular-bulkhead type quaywall is close to the gravity type. The structure consists of cylindrical cells made of steel sheet piles or steel plates, which are filled with an appropriate filling material. An advantage of this type is that the wall body can be constructed at low cost in calm waters.

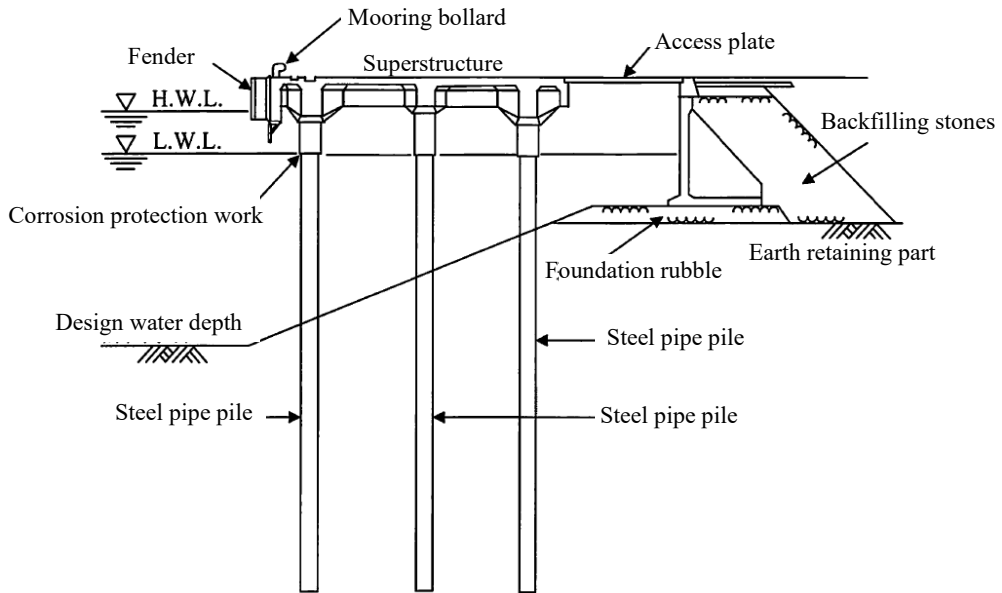
As design examples, this chapter introduces the “gravity-type quaywall (caisson type),” “anchored sheet pile quaywall,” “open-type wharf on vertical piles” and “steel plate cellular-bulkhead quaywall,” as shown in the following Figures. These four types of quaywalls are widely used not only in Japan, but also overseas.



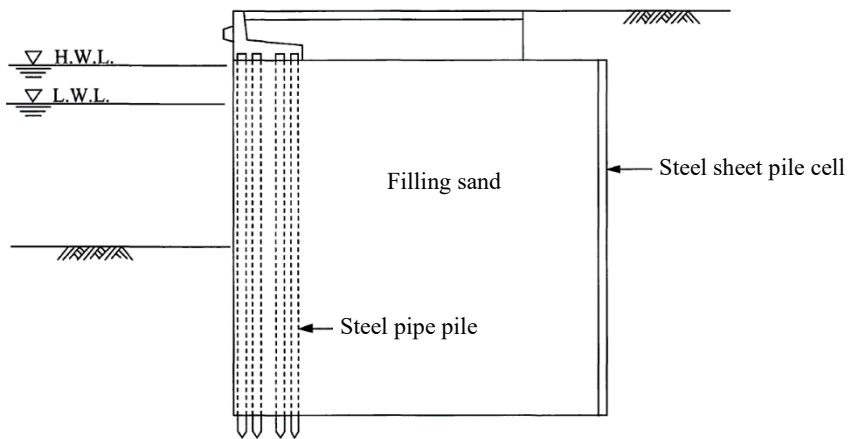
(a) Example of cross section of gravity-type quaywall



(b) Example of cross section of sheet pile type quaywall



(c) Example of cross section of open-type quaywall on vertical piles



(d) Example of section of steel plate cellular-bulkhead quaywall

2. Gravity Type Quaywall

(1) Examination of typical cross section

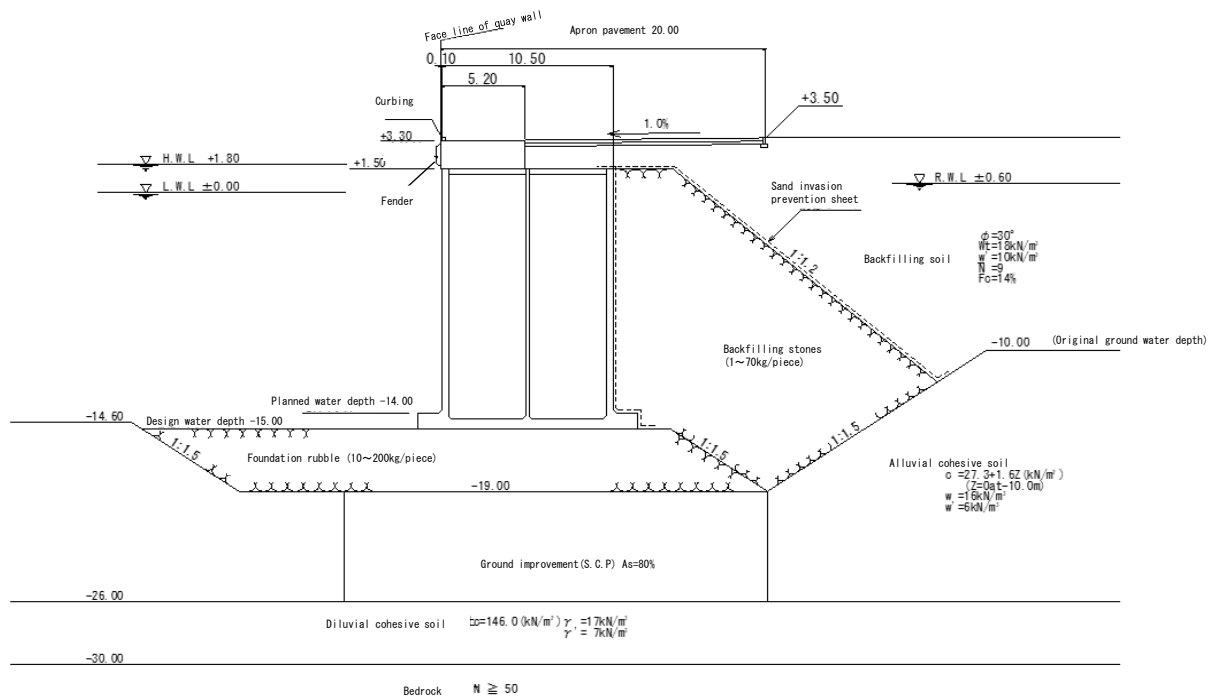


Figure 5.2.1 Typical cross section for examination

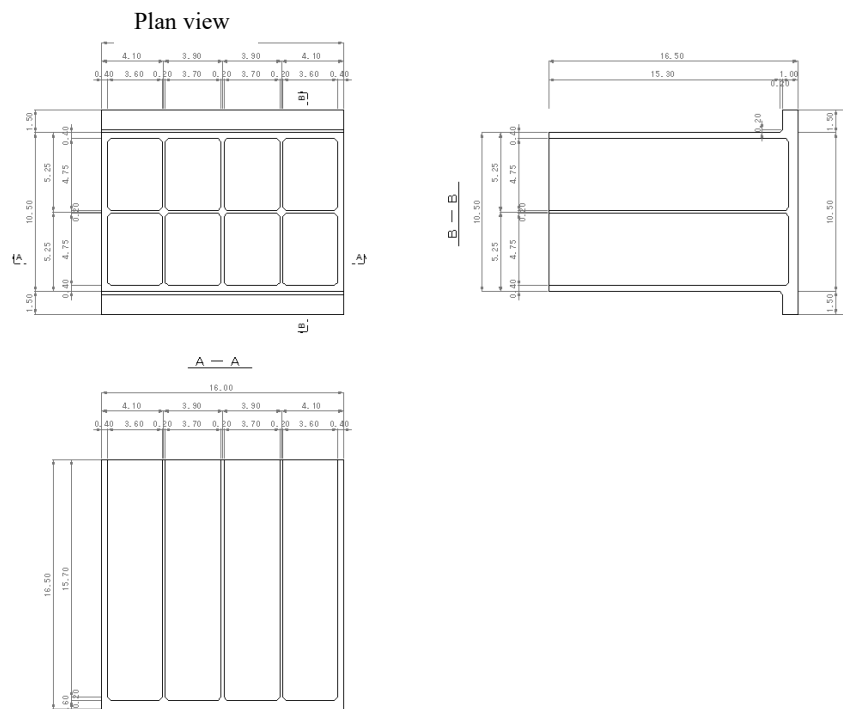


Figure 5.2.2 Cross section of caisson (Unit: m)

(2) Design conditions

1) Planning and use conditions

i) Design ship

Container ship, heavy cargo carrier (multi-purpose berth)

50,000 DWT

Berthing velocity $V = 0.10$ m/s

ii) Type of quay wall

Large-scale quay wall of major port (high earthquake-resistance facility (standard))

iii) Water depth and crown height

Planned water depth -14.00 m

Design water depth -15.00 m (considering footing thickness of 1.0 m)

Crown height +3.30 m (1.5 m above H.W.L.)

Apron width 20.0 m

iv) Surcharges

As surcharges, the following values are used for permanent states and earthquake action (variable states of Level 1 earthquake ground motion and accidental states of Level 2 earthquake ground motion).

Permanent state	Earthquake action
30 kN/m ²	15 kN/m ²

v) Limit values of residual deformation

Level 1 earthquake ground motion	Level 2 earthquake ground motion
10cm	1.5m

• Variable states associated with Level 1 earthquake ground motion

Because this wharf is classified as a “high earthquake-resistance facility,” the limit of residual deformation for variable states associated with Level 1 earthquake ground motion is set at 0.1 m and a verification of deformation is conducted.

• Accidental states associated with Level 2 earthquake ground motion

Gravity-type quay walls of high earthquake-resistance facilities are required to maintain structural stability under accidental states associated with Level 2 earthquake ground motion, with residual deformation limited to a degree that enables cargo handling for emergency supplies, etc. after a certain time.

Here, an example of a design calculation assuming a residual deformation limit of 1.5 m is presented.

2) Natural conditions

i) Tide levels

H.W.L. + 1.80 m

L.W.L. ±0.00 m

R.W.L. +0.60 m (1/3 of tide level difference)

ii) Ground conditions

Planned crown

Backfilling soil	$\phi = 30^\circ$ $w_t = 18 \text{ kN/m}^3, w = 20 \text{ kN/m}^3$ $w' = 10 \text{ kN/m}^3$ $\bar{N} = 9$
Original ground	-10.00
Alluvial cohesive soil	$c = 27.3 + 1.6Z \text{ (kN/m}^2)$ $(Z = 0 \text{ at } -10.0 \text{ m})$ $W = 16 \text{ kN/m}^3, w' = 6 \text{ kN/m}^3$
	-26.00
Diluvial cohesive soil	$c = 146.0 \text{ kN/m}^2$ $W = 17 \text{ kN/m}^3, w' = 7 \text{ kN/m}^3$
	-30.00
Bedrock	$\bar{N} > 50$

• Foundation rubble

$$\phi = 40^\circ$$

$$w = 20 \text{ kN/m}^3, w' = 10 \text{ kN/m}^3$$

• Backfilling stones

$$\phi = 40^\circ$$

$$w_t = 18 \text{ kN/m}^3, w = 20 \text{ kN/m}^3$$

$$w' = 10 \text{ kN/m}^3$$

• Sand compaction pile improved ground (S.C.P. method)

As the ground constant of the sand piles, the standard value for treated soil of 70 % or more is used.

Treatment ratio of sand pile $A_s = 80 \%$

Shear resistance angle of sand pile $\phi_s = 35^\circ, n = 1$

$$w_t = 18 \text{ kN/m}^3, w = 20 \text{ kN/m}^3$$

$$w' = 10 \text{ kN/m}^3$$

3) Friction coefficient between rock and caisson

$$f = 0.6 \text{ (case of no friction enhancement mat)}$$

4) Materials

Reinforced concrete (caisson)

$$\text{Standard design strength } f'_{ck} = 30 \text{ N/mm}^2$$

$$\text{Unit weight } w_c = 24.0 \text{ kN/m}^3$$

Non-reinforced concrete (crown concrete, lid concrete)

$$\text{Standard design strength } f'_{ck} = 18 \text{ N/mm}^2$$

$$\text{Unit weight } w_c = 22.6 \text{ kN/m}^3$$

Filling sand and ballast

$$w_t = 18 \text{ kN/m}^3, w = 20 \text{ kN/m}^3$$

(3) Seismic Coefficient for Verification

For calculation of the characteristic value of the seismic coefficient for verification for Level 1 earthquake ground motion, the Level 1 earthquake ground motion is input to the engineering bedrock of the ground model, and the acceleration wave profile of the ground surface is calculated by one-dimensional seismic response analysis (FLIP).

- The acceleration wave profile is obtained by filtering the above-mentioned acceleration wave profile (FFT → multiplication by a filter function → IFFT), and the maximum value obtained by filtering is defined as α_f .
- The corrected maximum value of acceleration at the ground surface α_c is calculated by multiplying the maximum value of acceleration α_f by the reduction factor p , which considers the effect of the duration of the earthquake ground motion.
- The characteristic value of the seismic coefficient for verification is calculated by using the maximum corrected acceleration α_c and the allowable deformation D_a at the crown of the quay wall.

1) Filter

$$a(f) = \begin{cases} b & 0 < f \leq 1.0 \\ \frac{b}{1 - [0.34(f-1)]^2 + 6.8[0.34(f-1)]^4} & 1.0 \leq f \end{cases} \quad (1)$$

$$b = 1.05 \frac{H}{H_R} - 0.88 \frac{T_b}{T_{bR}} + 0.96 \frac{T_u}{T_{uR}} - 0.23 \quad (2)$$

where

H : wall height (m)

H_R : standard wall height (= 15 m)

T_b : initial natural frequency of hinterland ground (s)

T_{bR} : standard initial natural frequency of hinterland ground (= 0.8 s)

T_u : initial natural frequency of ground underneath wall (s)

T_{uR} : standard initial natural frequency of ground underneath wall (= 0.4 s)

The value of b is set in the range shown by **Eq. (3)** using the wall height H .

$$0.04H + 0.08 \leq b \leq 0.04H \quad \text{Provided, however, } b \geq 0.28.$$

where

H : wall height (m)

2) Correction

$$p = 0.36 \cdot \ln(RSS / \alpha_f) - 0.29 \quad (4)$$

Provided, however, $p \leq 1.0$.

$$\alpha_c = p \cdot \alpha_f \quad (5)$$

3) Calculation of seismic coefficient for verification

The characteristic value k_h of the seismic coefficient for verification of caisson type quaywalls is calculated by **Eq. (6)**.

$$k_h = 1.78 \left(\frac{D_a}{D_r} \right)^{-0.55} \frac{\alpha_c}{g} + 0.04 \quad (6)$$

where

k_h : characteristic value of seismic coefficient for verification

α_c : maximum correction acceleration (Gal)

g : acceleration of gravity (= 980 Gal)

D_a : allowable deformation of quaywall crown (= 10 cm)

D_r : standard deformation (= 10 cm)

The seismic coefficient for verification k_h is calculated based on the acceleration wave profile at the surface of the backfill soil behind a caisson type quaywall. It should be noted that what is obtained here is the characteristic value. The acceleration wave profile is obtained by conducting one-dimensional seismic response analysis of the backfilling soil ground.

4) Setting of analysis conditions

The analysis program must be capable of accurately evaluating the amplitude of the frequency band, which is important in calculations of the seismic coefficient for verification. In this example, the effective stress analysis program FLIP is used, as this program has a proven record of use in damage analysis and verification of earthquake-resistant performance of a large number of port and harbor structures, and its adaptability and reliability have been confirmed.

5) Input seismic motion

Figure 5.2.3 shows an accelerogram of Level 1 earthquake ground motion. Seismic ground motion with a return period of 75 years is used. This ground motion is a 2E wave and has a maximum acceleration of 220 (Gal). In the analysis, this is input from the lower edge of the bottom viscous boundary of the free ground.

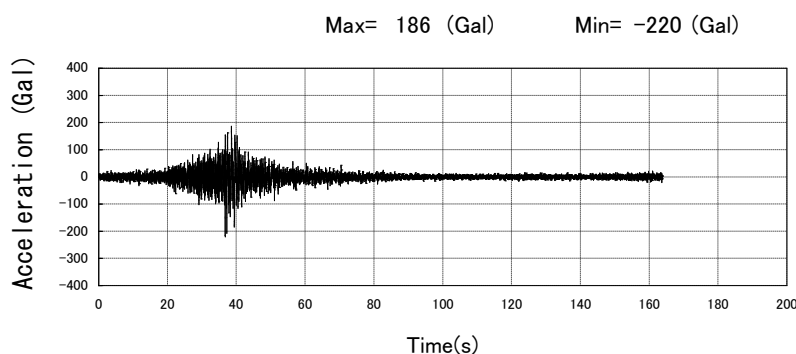


Figure 5.2.3 Time-series seismic wave profile of Level 1 Earthquake Ground Motion

6) Analysis parameters

The setting of analysis parameters is omitted here.

7) Calculation of seismic coefficient for verification of variable states (Level 1 earthquake ground motion)

The natural periods T_b and T_u are calculated from V_S and the layer thickness H using Eq. (7).

$$T = \Sigma \frac{4 \cdot H}{V_s} \quad (7)$$

where

T : fundamental natural period of ground (s)

H : thickness of layer (m)

V_s : shear wave velocity in layer (m/s)

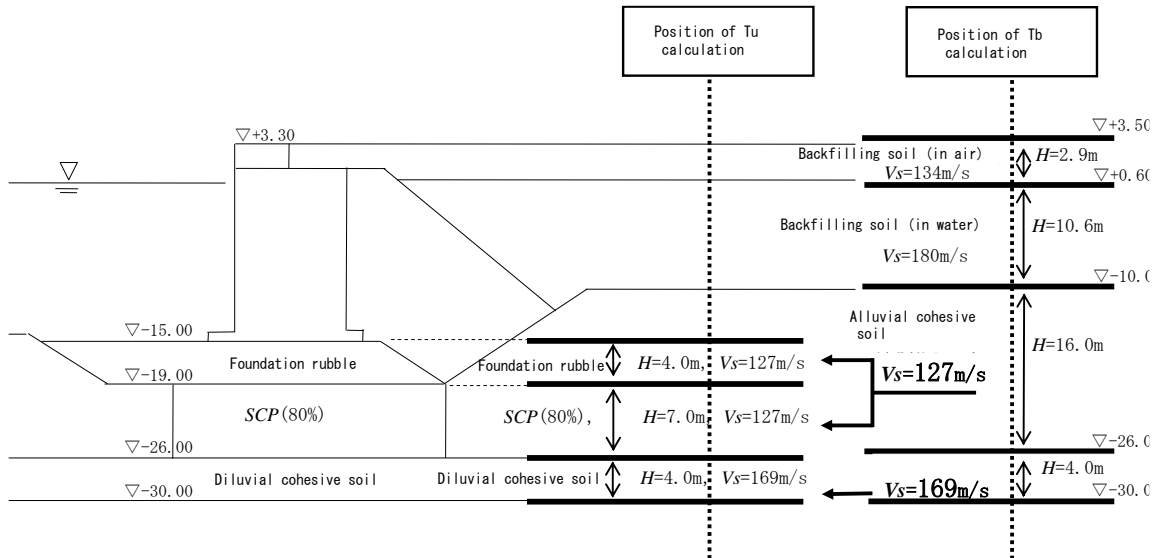


Figure 5.2.4 V_s used in calculation of natural period T_u of ground underneath caisson

Table 5.2.1 Calculation of natural periods T_b and T_u

Hinterland ground

Soil layer	Layer thickness(m)	Shear wave velocity V_s (m/s)	$4H/V_s$
Backfilling soil (above water)	2.9	134	0.0866
Backfilling soil (below water)	10.6	180	0.2356
Alluvial cohesive soil	16.0	127	0.5039
Diluvial cohesive soil	4.0	169	0.0947
		$\Sigma =$	0.9208

● Ground underneath wall

Soil layer	Layer thickness(m)	Shear wave velocity V_s (m/s)	$4H/V_s$
Rubble mound	4.0	127	0.1260
SCP (80%)	7.0	127	0.2205
Diluvial cohesive ground	4.0	169	0.0947
		$\Sigma =$	0.4412

● H (wall height) [m]	18.3
● T_b (initial natural period of hinterland ground) [s]	0.921
● T_u (initial natural period of ground underneath wall) [s]	0.441

T_b and T_u were obtained as follows from Table 5.2.1.

- Natural period of hinterland ground $T_b = 0.921$ (s)
- Natural period of ground underneath wall $T_u = 0.441$ (s)

The following value of b was obtained by **Eq. (2)** from the wall height $H = 18.3$ (m) of the caisson and T_b and T_u .

$$b = 1.05 \frac{18.3}{15.0} - 0.88 \frac{0.921}{0.8} + 0.96 \frac{0.441}{0.4} - 0.23$$

$$= 1.0963$$

From **Eq. (3)**, the range of b limited by the wall height $H = 18.3$ m is from 0.732 to 1.172.

$$0.04H + 0.08 \leq b \leq 0.04H + 0.44$$

$$0.04 \times 18.3 + 0.08 \leq b \leq 0.04 \times 18.3 + 0.44$$

$$0.732 \leq b (= 1.0963) \leq 1.172$$

In addition, $b \geq 0.28$.

Because the value of $b = 1.0963$ obtained here is within the limit range, $b = 1.0963$ is set.

The reduction factor p is obtained from by $\alpha_f = 94$ (Gal) and $RSS = 1,804$ (Gal) calculated by the wave profile processing process shown in **Figure 5.2.5** and **Eq. (4)**.

$$p = 0.36 \ln(1804 / 94) - 0.29$$

$$= 0.77361$$

$$\alpha_c = 0.77361 \times 94$$

$$= 73(\text{Gal})$$

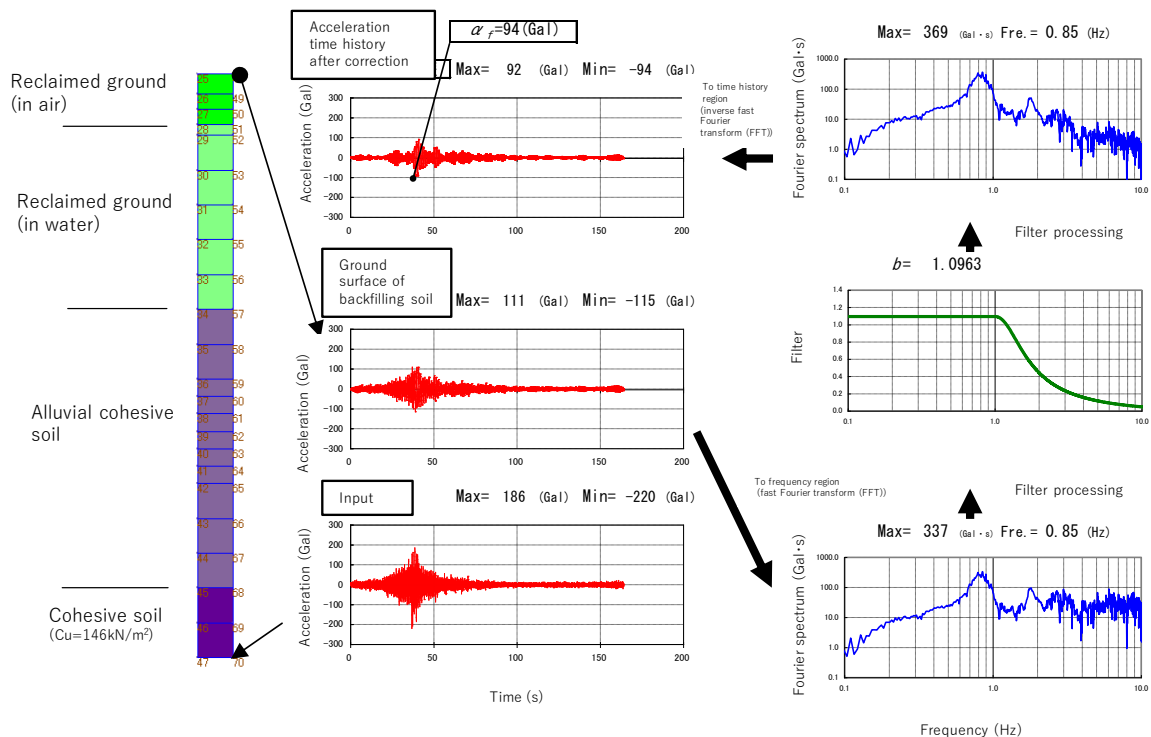


Figure 5.2.5 Processing of wave profile in Calculation Process of Seismic Coefficient (k_h) for Verification (Level 1 earthquake ground motion)

The ground under the wall is improved by the sand compaction pile method (S.C.P. method) with a improvement ratio of 80 %. In case ground improvement is carried out by the sand compaction method with an improvement ratio of 70 %, the seismic coefficient (k_h) for verification can be calculated by using the value obtained by multiplying the maximum corrected acceleration α_c by an appropriately-set reduction coefficient α_s . The reduction coefficient for the sand compaction method with an improvement ratio of 70 %

or more can generally be set as $\alpha_s = 0.75$. Therefore, the maximum corrected acceleration to be used in the calculation of the seismic coefficient for verification k_h is $\alpha_{cs} = 55$ Gal.

$$\begin{aligned}\alpha_{cs} &= \alpha_s \times \alpha_c \\ &= 0.75 \times 73 \\ &= 55(\text{Gal})\end{aligned}\quad (8)$$

Accordingly, the characteristic value of the seismic coefficient (k_h) for verification can be calculated as $k_h = 0.14$, assuming the allowable deformation $D_a = 10$ (cm) of Eq. (6).

Table 5.2.2 Calculation of seismic coefficient for verification k_h (Level 1 earthquake ground motion)

Input acceleration (Gal)	Response acceleration of ground surface (Gal)	b	Maximum acceleration after filter processing α_f (Gal)	Root sum square RSS (Gal)	Reduction factor p	Maximum corrected acceleration α_c (Gal)	Reduction coefficient for SCP of 70 % or more α_s	Maximum corrected acceleration considering SCP reduction coefficient (Gal)	k_h
220	115	1.09630	94	1804	0.77361	73	0.75	55	0.14

$$\begin{aligned}k_h &= 1.78 \times \left(\frac{10}{10}\right)^{-0.55} \times \frac{55}{980} + 0.04 \\ &= 0.139 \\ &= 0.14 \quad (\text{level 1})\end{aligned}$$

(4) Wall Specifications

1) Calculation of characteristic values

i) Characteristic values of caisson weight and moment

Table 5.2.3 Characteristic values of caisson weight and moment

Part	Dimensions (m)	Number	Volume V (m ³)	Unit weight w (kN/m ³)	Weight W_k (kN)	Center of gravity		Moment	
						x(m)	y(m)	$W_k \cdot x$ (kN·m)	$W_k \cdot y$ (kN·m)
Bottom slab	10.50 × 16.00 × 0.60	1	100.80	24.00	2,419.20	6.75	0.30	16,329.60	725.76
Front/back walls	0.40 × 16.00 × 15.90	2	203.52	24.00	4,884.48	6.75	8.55	32,970.24	41,762.30
Side wall	0.40 × 9.70 × 15.90	2	123.38	24.00	2,961.12	6.75	8.55	19,987.56	25,317.58
Normal parallel partition wall	0.20 × 15.20 × 15.90	1	48.34	24.00	1,160.16	6.75	8.55	7,831.08	9,919.37
Normal perpendicular partition wall	0.20 × 9.50 × 15.90	3	90.63	24.00	2,175.12	6.75	8.55	14,682.06	18,597.28
Vertical haunch	1/2 × 0.20 ² × 15.90	32	10.18	24.00	244.32	6.75	8.55	1,649.16	2,088.94
Normal parallel haunch	1/2 × 0.20 ² × 13.00	4	1.04	24.00	24.96	6.75	0.67	168.48	16.72
Normal perpendicular haunch	1/2 × 0.20 ² × 8.70	8	1.39	24.00	33.36	6.75	0.67	225.18	22.35
Corner angle haunch	1/3 × 0.20 ³	32	0.09	24.00	2.16	6.75	0.68	14.58	1.47
Footing	1.50 × 16.00 × 1.00	2	48.00	24.00	1,152.00	6.75	0.50	7,776.00	576.00
Footing haunch	1/2 × 0.20 ² × 16.00	2	0.64	24.00	15.36	6.75	1.07	103.68	16.44
Total			628.01		15,072.24	6.75	6.57	101,737.62	99,044.21

ii) Verification of stability under buoyancy

Because stability against buoyancy is not secured with the shape of this caisson, ballast material is used.

- Volume of ballast

Ballast thickness $t = 1.55$ (m)

Ballast-containing compartments: All compartments

- Position of center of gravity G' of caisson

According to **Table 5.2.4**,

$$G' = \frac{M_y}{W} = \frac{W_k \cdot y}{W_k} = \frac{104,310.08}{18,878.79} = 5.53 \text{ (m)}$$

- Draft D' of caisson

When the draft of the caisson is D' ,

$$D' = \frac{W_k - V_f \rho_0 g}{BL \rho_0 g} = \frac{18,878.79 - 48.64 \times 10.1}{10.50 \times 16.00 \times 10.1} = 10.84 \text{ (m)}$$

- Position of center of buoyancy C'

$$C' = \frac{Vy'}{V'} = \frac{9,895.15}{1,869.76} = 5.29 \text{ (m)}$$

$$\begin{aligned} V' &= BLD' + V_f \\ &= 10.50 \times 16.00 \times 10.84 + 48.64 \\ &= 1,869.76 \text{ (m}^3\text{)} \end{aligned}$$

$$\begin{aligned} Vy' &= \frac{BLD'^2}{2} + V_f y \\ &= \frac{10.50 \times 16.00 \times 10.84^2}{2} + 24.68 \\ &= 9,895.15 \text{ (m}^4\text{)} \end{aligned}$$

- Position of metacenter

$$I' = I = 1,543.50 \text{ (m}^4\text{)}$$

Distance between the metacenter and the buoyancy is

$$\overline{MC'} = \frac{I'}{V'} = \frac{1,543.50}{1,869.76} = 0.83 \text{ (m)}$$

- Verification of stability

$$\overline{G'M'} = \frac{I'}{V'} - \overline{C'G'} = 0.83 - (5.53 - 5.29) = 0.59 \text{ (m)}$$

$$0.05D' = 10.84 \times 0.05 = 0.54 \leq \overline{G'M'} = 0.59$$

Therefore, in case the ballast thickness is 1.55 m, the structure is stable because $\overline{G'M'}$ is at least 5 % of draft.

Table 5.2.4 Position of center of gravity of caisson

Item	Dimensions (m)	Number	Unit weight w_k (kN/m ³)	Weight W_k (kN/m ³)	Center of gravity	Moment
					y (m)	$W_k \cdot y$ (kN · m)
Caisson		1		15,072.24	6.57	99,044.21
Ballast	$14.60 \times 9.50 \times 1.55$	1	18.00	3,869.73	1.38	5320.88
Ballast (vertical haunch)	$1/2 \times 0.20^2 \times 1.55$	32	18.00	-17.86	1.38	-24.65
Ballast (normal parallel haunch)	$1/2 \times 0.20^2 \times 13.00$	4	18.00	-18.72	0.67	-12.54
Ballast (normal perpendicular haunch)	$1/2 \times 0.20^2 \times 8.70$	8	18.00	-25.06	0.67	-16.79
Ballast (corner angle haunch)	$1/3 \times 0.20^3$	32	18.00	-1.54	0.67	-1.03
Total				18,878.79		104,310.08

iii) Wall body weight and moment

The characteristic values of the wall body weight and moment are shown in **Table 5.2.5**.

Table 5.2.5 Characteristic values of wall body moment and weight

Part name	Volume V (m ³)	Weight W_k (kN)	Center of gravity		Moment	
			X (m)	y (m)	$W_k \cdot x$ (kN · m)	$W_k \cdot y$ (kN · m)
Caisson concrete	628.01	15,072.24	6.75	6.57	101,737.62	99,044.21
Filling material	2,151.22	43,024.40	6.75	8.41	290,414.70	361,835.20
Lid concrete	41.42	936.09	6.75	16.35	6,318.60	15,305.07
Superstructure	149.68	3,382.77	4.00	17.40	13,535.73	58,861.77
Fill soil	198.72	3,576.96	10.05	17.40	35,948.45	62,239.10
Backfilling material	371.68	7,390.40	12.75	8.71	94,231.95	64,399.79
Total	3,540.73	73,382.86	7.39	9.02	542,187.05	661,685.14
*Per unit length	221.30	4,586.43			33,886.69	41,355.32

iv) Buoyancy and moment

The characteristic values of buoyancy and moment are shown in **Table 5.2.6**.

Table 5.2.6 Characteristic values of buoyancy and moment

Part name	Calculation formula (m)	Number	Volume V (m ³ /m)	Unit weight of water $\rho_w g$ (kN/m ³)	Buoyancy P_{Bk} (kN)	Center of gravity	Moment
						x (m)	$P_{Bk} \cdot x$ (kN · m/m)
Caisson	12.00×15.60	1	187.20	10.10	1,890.72	7.50	14,180.40
Footing	1.50×1.00	1	1.50	10.10	15.15	0.75	11.36
Footing haunch	$1/2 \times 0.20^2$	1	0.02	10.10	0.20	1.43	0.29
Total			188.72		1,906.07	7.45	14,192.10

5) Surcharge and moment

The characteristic values of surcharges and moments are shown in **Table 5.2.7**.

Table 5.2.7 Characteristic Values of Surcharges and Moments

State	Surcharge w (kN/m ²)	Load width b (m)	Vertical force (P_{vk}) $w \cdot b$ (kN/m)	Inertia force (P_{HK}) $Kh \cdot P_{vk}$ (kN/m)	Center of gravity		Moment	
					x (m)	y (m)	$P_{vk} \cdot x$ (kN· m/m)	$P_{HK} \cdot y$ (kN· m/m)
Permanent state	30.00	12.10	363.00	-	7.45	18.30	2,704.40	-
Variable states associated with Level 1 earthquake ground motion	15.00	12.10	181.50	25.41	7.45	18.30	1,352.20	465.00

6) Earth pressure and moment

Earth pressure is calculated by the following equation.

$$P_a = K_a \left[\sum w_i h_i + \frac{\omega}{\cos \beta} \right] \quad (9)$$

$$K_a = \frac{\cos^2(\phi - \theta)}{\cos \theta \cos(\delta + \theta) \left[1 + \sqrt{\left(\frac{\sin(\phi + \theta) \sin(\phi - \beta - \theta)}{\cos(\delta + \theta) \cos \beta} \right)^2} \right]}$$

where

P_a : intensity of active earth pressure (kN/m²)

ϕ : shear resistance angle of soil (°)

w_i : unit weight of soil (kN/m³)

h_i : thickness of a layer (m)

K_a : coefficient of active earth pressure

β : angle of ground surface to the horizontal (°)

δ : angle of wall friction (°)

ω : load per unit area of ground surface (kN/m²)

θ : composite seismic angle (°)

$$\theta = \tan^{-1} k \text{ or } \theta = \tan^{-1} k'$$

(In the permanent state, $\theta=0$)

k : seismic coefficient

k' : apparent seismic coefficient

The apparent seismic coefficient is given by the following equation.

$$k' = \frac{2(\sum w_i h_i + \sum w h_j + \omega) + w h}{2\{\sum w_i h_i + \sum (w - 10) h_j + \omega\} + (w - 10) h} k$$

where

h_i : thickness of i-th soil layer above residual water level (m)

h_j : thickness of j-th soil layer above the layer where a soil layer below the residual water level is to be obtained (m)

h : thickness of a soil layer below the residual water level, where the soil layer is to be obtained (m)

w_t : unit weight of soil above the residual water level (kN/m³)

w : unit weight in air of soil saturated with water (kN/m³)

ω : load per unit area of ground surface (kN/m²)

k : seismic coefficient

k' : apparent seismic coefficient

- Permanent state

Surcharge: $\omega = 30$ (kN/m²)

Friction angle of wall: $\delta = 15$ (°)

Characteristic value of vertical soil pressure

$$P_{Vk} = 510.92 \times \tan 15^\circ = 136.90 \text{ (kN/m)}$$

Characteristic value of moment

$$P_{Vk} \cdot x = 136.90 \times (10.5 + 1.5 \times 2) = 1,848.15 \text{ (kN} \cdot \text{m/m)}$$

- Variable states associated with Level 1 earthquake ground motion

Surcharge: $\omega = 15$ (kN/m²)

Friction angle of wall: $\delta = 15$ (°)

Characteristic value of vertical soil pressure

$$P_{Vk} = 741.84 \times \tan 15^\circ = 198.78 \text{ (kN/m)}$$

Characteristic value of moment

$$P_{Vk} \cdot x = 198.78 \times (10.5 + 1.5 \times 2) = 2,683.53 \text{ (kN} \cdot \text{m/m)}$$

- Characteristic values of inertia force and moment

Inertia force acting on wall body: P_{Fk}

$$P_{Fk} = W_k \cdot k_h = 4586.43 \times 0.14 = 642.10 \text{ (kN)}$$

Moment of inertia force acting on wall body: $W_k \cdot y \cdot k_h$

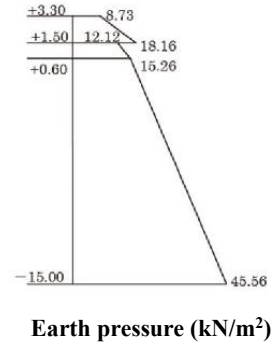
$$W_k \cdot y \cdot k_h = 41,355.32 \times 0.14 = 5,789.74 \text{ (kN} \cdot \text{m/m)}$$

Table 5.2.8 Characteristic values of intensity of active earth pressure (permanent state)

Layer No.	Elevation (m)	Layer thickness h_i (m)	w_i (kN/m ³)	$w_i h_i$ (kN/m ³)	$\Sigma w_i h_i + \omega$ (kN/m ²)	ϕ (°)	$K_{a \cos \delta}$	P_a (kN/m ²)
1	3.30	1.80	18.00	32.40	30.00	30.00	0.2911	8.73
	1.50				62.40		0.2911	18.16
2	1.50	0.90	18.00	16.20	62.40	40.00	0.1942	12.12
	0.60				78.60		0.1942	15.26
3	0.60	15.60	10.00	156.00	78.60	40.00	0.1942	15.26
	-15.00				234.60		0.1942	45.56

**Table 5.2.9 Characteristic values of resultant force of earth pressure and moment
(permanent state)**

Section	Horizontal earth pressure P_{HK} (kN/m)		Height of action y (m)		Moment $P_{HK} \cdot y$ (kN·m/m)
	Calculation formula	P_{HK} (kN/m)	Calculation formula	y (m)	
1	$1/2 \times 1.80 \times 8.73$	7.86	$2/3 \times 1.80 + 16.50$	17.70	139.12
	$1/2 \times 1.80 \times 18.16$	16.34	$1/3 \times 1.80 + 16.50$	17.10	279.41
2	$1/2 \times 0.90 \times 12.12$	5.45	$2/3 \times 0.90 + 15.60$	16.20	88.29
	$1/2 \times 0.90 \times 15.26$	6.87	$1/3 \times 0.90 + 15.60$	15.90	109.23
3	$1/2 \times 15.60 \times 15.26$	119.03	$2/3 \times 15.60 + 0.00$	10.40	1,237.91
	$1/2 \times 15.60 \times 45.56$	355.37	$1/3 \times 15.60 + 0.00$	5.20	1,847.92
Total	$\Sigma P_{HK} = 510.92$		$\Sigma P_{HK} \cdot y = 3,701.88$		

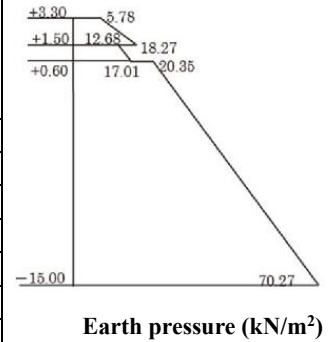


**Table 5.2.10 Characteristic value of intensity of active earth pressure
(variable states of Level 1 earthquake ground motion)**

Layer No.	Elevation (m)	Layer thickness h_i (m)	w_i (kN/m³)	$w_i h_i$ (kN/m²)	$w_i h_i + \omega$ (kN/m²)	k, k'	Angle of resultant force θ (°)	ϕ (°)	Kacos δ	Pa (kN/m²)
1	3.30	1.80	18.00	32.40	15.00	0.14	7.97	30.00	0.3855	5.78
	1.50				47.40	0.14	7.97		0.3855	18.27
2	1.50	0.90	18.00	16.20	47.40	0.14	7.97	40.00	0.2675	12.68
	0.60				63.60	0.14	7.97		0.2675	17.01
3	0.60	15.60	10.00	156.00	63.60	0.22	12.41	40.00	0.3200	20.35
	-15.00				219.60	0.22	12.41		0.3200	70.27

**Table 5.2.11 Characteristic values of resultant force of earth pressure and moment
(variable states of Level 1 earthquake ground motion)**

Section	Horizontal earth pressure P_{HK} (kN/m)		Height of action (m)		Moment $P_{HK} \cdot y$ (kN·m/m)
	Calculation formula	P_{HK} (kN/m)	Calculation formula	y (m)	
1	$1/2 \times 1.80 \times 5.78$	5.20	$2/3 \times 1.80 + 16.50$	17.70	92.04
	$1/2 \times 1.80 \times 18.27$	16.44	$1/3 \times 1.80 + 16.50$	17.10	281.12
2	$1/2 \times 0.90 \times 12.68$	5.71	$2/3 \times 0.90 + 15.60$	16.20	92.50
	$1/2 \times 0.90 \times 17.01$	7.65	$1/3 \times 0.90 + 15.60$	15.90	121.64
3	$1/2 \times 15.60 \times 20.35$	158.73	$2/3 \times 15.60 + 0.00$	10.40	1,650.79
	$1/2 \times 15.60 \times 72.27$	548.11	$1/3 \times 15.60 + 0.00$	5.20	2,850.17
Total	$\Sigma P_{HK} = 741.84$		$\Sigma P_{HK} \cdot y = 5,088.26$		



7) Residual water pressure and moment

Residual water pressure considers the water pressure due to the difference of the water levels between the frontal water level (L.W.L.) and the residual water level (R.W.L.).

$$P_w = w_w h_w$$

where

P_w : residual water pressure (kN/m)

h_w : residual water level; in case the water level in the backfilling material or the backfilling soil is higher than the water level on the front side of the structure, the maximum water level difference at that

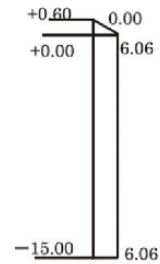
time is used

w_w : unit weight of water (kN/m³)

$w_w = \rho_{0g} = 10.1$ (kN/m³)

Table 5.2.12 Characteristic value of residual water pressure and moment

Section	Residual water pressure P _{wk} (kN/m)		Height of action y (m)		Moment P _{wk} · y (kN · m/m)
	Calculation formula	P _{wk} (kN/m)	Calculation formula	y (m)	
1	$1/2 \times 0.60 \times 6.06$	1.82	$1/3 \times 0.60 + 15.00$	15.20	27.66
	15.00×6.06	90.90	$1/2 \times 15.00$	7.50	681.75
Total	$\Sigma P_{wk} = 92.72$		$\Sigma P_{wk} \cdot y = 709.41$		



Residual water pressure (kN/m²)

8) Dynamic water pressure and moment

Under variable situations associated with Level 1 earthquake ground motion, the dynamic water pressure at the front side of the quaywall is directed toward the sea. Dynamic water pressure is obtained by the following equation (Westergaard's approximate formula).

$$P_{dw} = \frac{7}{8} k w_w \sqrt{Hy}$$

$$P_{dw} = \pm \frac{7}{12} k w_w H^2, \quad h_{dw} = \frac{3}{5} H$$

where

P_{dw} : dynamic water pressure (kN/m²)

k : horizontal seismic coefficient

w_w : unit weight of water (seawater) (kN/m³)

H : height of structure below the still water level (m) (caisson installation water depth at L.W.L.)

y : depth of the hydrodynamic pressure calculation level from the still water level (m)

P_{dvw} : resultant force of dynamic water pressure (kN/m)

h_{dw} : depth of the acting point of the dynamic water pressure resultant force from the still water level (m)

i) Design dimensions

Frontal water depth $H = 15.00$ (m)

ii) Resultant force of dynamic water pressure (L.W.L.)

The design value of the dynamic water pressure under variable situations associated with Level 1 earthquake ground motion is as follows.

- Resultant force of hydrodynamic pressure

$$P_{dvw} = 7 \times 0.14 \times 10.1 \times 15.00^2 / 12 = 185.59 \text{ (kN/m)}$$

- Position of action

$$h_{dw} = 3 \times 15.00 / 5 = 9.00 \text{ (m) (elevation -9.00 m)}$$

- Moment

$$P_{dwk} \cdot y = 185.59 \times (15.00 - 9.00) = 1,113.54 \text{ (kN} \cdot \text{m/m)}$$

(5) Verification of Stability

1) Examination of sliding/overturning of wall body

- Permanent state (not considering surcharge on wall body)

a) Verification of sliding

Load	Vertical force $V(\text{kN/m})$	Load	Horizontal force $H(\text{kN/m})$
Weight of wall body	4,586.43	Horizontal earth pressure	510.92
Buoyancy	-1,906.07	Residual water pressure	92.72
Vertical earth pressure	136.90	Total	603.64
Total	2,817.26		

The design values for the resistance term is calculated considering the friction coefficient between the bottom side of the caisson and the foundation, and the partial factor γ_R .

$$\gamma_R = 0.87$$

$$R_d = \gamma_R \cdot f \cdot V = 0.87 \times 0.60 \times 2,817.26 = 1,470.61 \text{ (kN/m)}$$

The design value for the load term is calculated considering the partial factor γ_S to the horizontal force acting on the wall body.

$$\gamma_S = 1.06$$

$$S_d = \gamma_S \cdot H = 1.06 \times 603.64 = 639.86 \text{ (kN/m)}$$

From the above,

$$m \frac{S_d}{R_d} = 1.0 \cdot \frac{639.86}{1,470.61} = 0.44 \leq 1.00.$$

Therefore, it is stable.

b) Examination of the stability against overturning

Load	Moment $V \cdot x(\text{kN} \cdot \text{m/m})$	Load	Moment $H \cdot y(\text{kN} \cdot \text{m/m})$
Weight of wall body	33,886.69	Horizontal earth pressure	3,701.88
Buoyancy	-14,192.10	Residual water pressure	709.41
Vertical earth pressure	1,848.15	Total	4,411.29
Total	21,542.74		

The design value for the load term is calculated considering the partial factor γ_R to the vertical moment.

$$\gamma_R = 0.99$$

$$R_d = \gamma_R \cdot V \cdot x = 0.99 \times 21,542.74 = 21,327.31 \text{ (kN} \cdot \text{m/m)}$$

The design value for the load term is calculated considering the partial factor γ_S to the moment in the horizontal direction.

$$\gamma_S = 1.23$$

$$S_d = \gamma_S \cdot H \cdot y = 1.23 \times 4,411.29 = 5,425.89 \text{ (kN} \cdot \text{m/m)}$$

From the above,

$$m \frac{S_d}{R_d} = 1.0 \cdot \frac{5,425.89}{21,327.31} = 0.26 \leq 1.00.$$

Therefore, it is stable.

• **Permanent state (considering surcharge on wall body)**

a) Verification of sliding of wall body

Load	Vertical force $V(\text{kN/m})$	Load	Horizontal force $H(\text{kN/m})$
Weight of wall body	4,586.43	Horizontal earth pressure	510.92
Buoyancy	-1,906.07	Residual water pressure	92.72
Vertical earth pressure	136.90	Total	603.64
Surcharge	363.00		
Total	3,180.26		

The design value for the load term is calculated considering the coefficient of friction between the bottom surface of the vertical wall body and the foundation, and the partial factor γ_R which is multiplied with the load term.

$$\gamma_R = 0.87$$

$$R_d = \gamma_R \cdot f \cdot V = 0.87 \times 0.60 \times 3,180.26 = 1,660.10 \text{ (kN/m)}$$

The design value for the load term is calculated considering the partial factor γ_S to the horizontal force acting on the wall body.

$$\gamma_S = 1.06$$

$$S_d = \gamma_S \cdot H = 1.06 \times 603.64 = 639.86 \text{ (kN/m)}$$

From the above,

$$m \frac{S_d}{R_d} = 1.0 \cdot \frac{639.86}{1,660.10} = 0.39 \leq 1.00.$$

Therefore, it is stable.

b) Verification of overturning

Load	Moment $V \cdot x(\text{kN} \cdot \text{m/m})$	Load	Moment $H \cdot y(\text{kN} \cdot \text{m/m})$
Weight of wall body	33,886.69	Horizontal earth pressure	3,701.88
Buoyancy	-14,192.10	Residual water pressure	709.41
Vertical earth pressure	1,848.15	Total	4,411.29
Surcharge	2,704.40		
Total	24,247.14		

The design value for the load term is calculated considering the partial factor γ_R to the vertical moment.

$$\gamma_R = 0.99$$

$$R_d = \gamma_R \cdot V \cdot x = 0.99 \times 24,247.14 = 24,004.67 \text{ (kN} \cdot \text{m/m)}$$

The design value for the load term is calculated considering the partial factor γ_S to the horizontal moment.

$$\gamma_S = 1.23$$

$$S_d = \gamma_S \cdot H \cdot y = 1.23 \times 4,411.29 = 5,425.89 \text{ (kN} \cdot \text{m/m)}$$

From the above,

$$m \frac{S_d}{R_d} = 1.0 \cdot \frac{5,425.89}{24,004.67} = 0.23 \leq 1.00.$$

Therefore, it is stable.

• **Variable states associated with Level 1 earthquake ground motion (not considering surcharge on wall body)**

a) Verification of sliding/overturning of wall body

Load	Vertical force $V(\text{kN/m})$	Moment $V \cdot x(\text{kN} \cdot \text{m/m})$
Weight of wall body	4,586.43	33,886.69
Buoyancy	-1,906.07	-14,192.10
Vertical earth pressure	198.78	2,683.53
Total	2,879.14	22,378.12

Load	Horizontal load $H(\text{kN/m})$	Moment $H \cdot y(\text{kN} \cdot \text{m/m})$
Inertia force	642.10	5,789.74
Horizontal earth pressure	741.84	5,088.26
Residual water pressure	92.72	709.41
Dynamic water pressure	185.59	1,113.54
Total	1,662.25	12,700.95

b) Verification of sliding

The design value for the load term is calculated considering the coefficient of friction between the bottom surface of the vertical wall body and the foundation, and the partial fact γ_R which is multiplied with the load term.

$$\gamma_R = 1.00$$

$$R_d = \gamma_R \cdot f \cdot V = 1.00 \times 0.60 \times 2,879.14 = 1,727.48 \text{ (kN/m)}$$

The design value for the load term is calculated considering the partial factor γ_S to the horizontal load acting on the wall body.

$$\gamma_S = 1.00$$

$$S_d = \gamma_S \cdot H = 1.00 \times 1,662.25 = 1,662.25 \text{ (kN/m)}$$

From the above,

$$m \frac{S_d}{R_d} = 1.0 \cdot \frac{1,662.25}{1,727.48} = 0.97 \leq 1.00.$$

Therefore, it is stable.

c) Verification of overturning

The design value for the load term is calculated considering the partial factor γ_R to the vertical moment.

$$\gamma_R = 1.00$$

$$R_d = \gamma_R \cdot V \cdot x = 1.00 \times 22,378.12 = 22,378.12 \text{ (kN} \cdot \text{m/m)}$$

The design value for the load term is calculated considering the partial factor γ_S to the horizontal moment.

$$\gamma_s = 1.00$$

$$S_d = \gamma_s \cdot H \cdot y = 1.00 \times 12,700.95 = 12,700.95 \text{ (kN} \cdot \text{m/m)}$$

From the above,

$$m \frac{S_d}{R_d} = 1.1 \cdot \frac{12,700.95}{22,378.12} = 0.63 \leq 1.00.$$

Therefore, it is stable.

• **Variable states associated with Level 1 earthquake ground motion (considering surcharge on wall body)**

a) Verification of sliding/overturning of wall body

Load	Vertical load $V(\text{kN/m})$	Moment $V \cdot x(\text{kN} \cdot \text{m/m})$
Weight of wall body	4,586.43	33,886.69
Buoyancy	-1,906.07	-14,192.10
Vertical earth pressure	198.78	2,683.53
Surcharge	181.50	1,352.20
Total	3,060.64	23,730.32

Load	Horizontal load $H(\text{kN/m})$	Moment $H \cdot y(\text{kN} \cdot \text{m/m})$
Inertia force	642.10	5,789.74
Horizontal earth pressure	741.84	5,088.26
Residual water pressure	92.72	709.41
Dynamic water pressure	185.59	1,113.54
Inertia force of surcharge	25.41	465.00
Total	1,687.66	13,165.95

b) Verification of sliding

The design value for the load term is calculated considering the coefficient of friction between the bottom surface of the vertical wall body and the foundation, and the partial fact γ_R which is multiplied with the load term.

$$\gamma_R = 1.00$$

$$R_d = \gamma_R \cdot f \cdot V = 1.00 \times 0.60 \times 3,060.64 = 1,836.38 \text{ (kN/m)}$$

The design value for the load term is calculated considering the partial factor γ_S to the horizontal load acting on the wall body.

$$\gamma_s = 1.00$$

$$S_d = \gamma_s \cdot H = 1.00 \times 1,687.66 = 1,662.25 \text{ (kN/m)}$$

From the above,

$$m \frac{S_d}{R_d} = 1.0 \cdot \frac{1,687.66}{1,836.38} = 0.92 \leq 1.00.$$

Therefore, it is stable.

c) Verification of overturning

The design value for the load term is calculated considering the partial factor γ_R to the vertical moment.

$$\gamma_R = 1.00$$

$$R_d = \gamma_R \cdot V \cdot x = 1.00 \times 23,730.32 = 23,370.32 \text{ (kN} \cdot \text{m/m)}$$

The design value for the load term is calculated considering the partial factor γ_S to the horizontal moment.

$$\gamma_S = 1.00$$

$$S_d = \gamma_S \cdot H \cdot y = 1.00 \times 13,165.95 = 13,165.95 \text{ (kN} \cdot \text{m/m)}$$

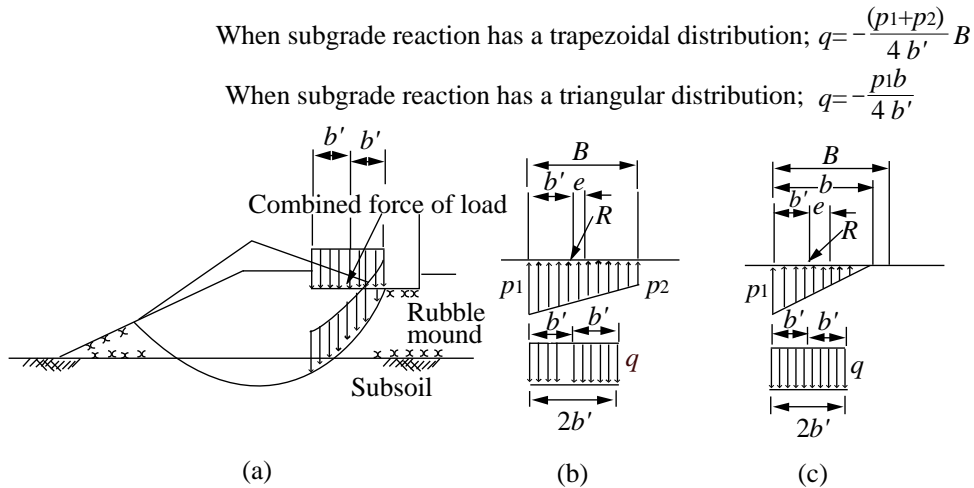
From the above,

$$m \frac{S_d}{R_d} = 1.1 \cdot \frac{13,165.95}{23,370.32} = 0.62 \leq 1.00.$$

Therefore, it is stable.

2) Examination of stability against bearing capacity failure of foundation ground

Verification for failure of the bearing capacity of the foundation ground is conducted by Bishop's method.



Analysis of Bearing Capacity for Eccentric and Inclined Actions

i) Ground conditions

Table 5.2.13 Characteristic values of ground conditions for verification of bearing capacity

	Saturated weight w (kN/m ³)	Weight in water w' (kN/m ³)	Shear resistance angle ϕ'_k (°)	Cohesion	
				c'_k (kN/m ²)	Primary coefficient of cohesion
Foundation rubble	20.00	10.00	35.00 ($\tan \phi'_k = 0.700$)	20.00	0.00
Alluvial cohesive soil	16.00	6.00	0.00 ($\tan \phi'_k = 0.000$)	27.30	1.60
SCP improved ground	19.20	9.20	38.66 ($\tan \phi'_k = 0.800$)	5.46	0.32

* As the characteristic values of the strength parameters of foundation rubble for verification of bearing capacity, apparent cohesion $c'_k = 20$ (kN/m²) and $\phi'_k = 35$ (°) are used as standard strength parameters.

** For SCP sand piles, the characteristic value of the shear resistance angle $\phi' = 45$ (°) is used, regarding the N -value as 10 or more.

Therefore, shear resistance angle ϕ'_k of SCP improved ground (improvement ratio: 80 %) is estimated

as below;

$$\phi'_k = \tan^{-1} (0.8 \times \tan 45^\circ) = 38.66 (^\circ)$$

Cohesion c'_k of SCP improved ground (20 % unimproved)

$$c'_k = 0.2 (27.3 + 1.6Z) = 5.46 + 0.32Z (Z = 0 \text{ at } -10.0 \text{ m})$$

ii) Load conditions

In analyses of bearing capacity for eccentric and inclined loads by Bishop's method, the vertical load acting on the bottom surface of the wall body is converted to a uniformly distributed load.

• **Permanent state (not considering surcharge on wall body)**

Confirmation of shape of distribution of vertical subgrade reaction of caisson bottom slab

$$x = \frac{\Sigma M}{\Sigma V} = \frac{\Sigma V \cdot x - \Sigma H \cdot y}{\Sigma V} = \frac{21,542.74 - 4,411.29}{2,817.26} = 6.08 \text{ (m)}$$

$$e = \frac{B}{2} - x = \frac{13.50}{2} - 6.08 = 0.67 \text{ (m)}$$

$$e < B/6 = 2.25 \text{ (m)}$$

Accordingly, the distribution is trapezoidal, and

$$p_1 = \frac{\Sigma V}{B} \left(1 + \frac{6e}{B} \right) = \frac{2,817.26}{13.50} \left(1 + \frac{6 \times 0.67}{13.50} \right) = 270.83 \text{ (kN/m}^2\text{)}$$

$$p_2 = \frac{\Sigma V}{B} \left(1 - \frac{6e}{B} \right) = \frac{2,817.26}{13.50} \left(1 - \frac{6 \times 0.67}{13.50} \right) = 146.54 \text{ (kN/m}^2\text{)}$$

Distribution width $b = 13.50$ (m) (width of caisson bottom)

Calculation of load width

$$\overline{2b'} = \frac{2 \Sigma \overline{M}}{\Sigma \overline{V}} = \frac{2(\Sigma \overline{V} \cdot x - \Sigma \overline{H} \cdot y)}{\Sigma \overline{V}} = \frac{2 \times (21,542.74 - 4,411.29)}{2,817.26} = 12.16 \text{ (m)}$$

Calculation of uniformly-distributed load

$$\overline{q} = \frac{\Sigma \overline{V}}{\overline{2b'}} = \frac{2,817.261}{12.16} = 231.68 \text{ (kN/m}^2\text{)}$$

Horizontal force

$$H = 603.64 \text{ (kN/m)}$$

Load	Characteristic value	
	Vertical force V (kN/m)	Moment $V \cdot x$ (kN·m/m)
Weight of wall body	4,586.43	33,886.69
Buoyancy	-1,906.07	-14,192.10
Vertical earth pressure	136.90	1,848.15
Total	2,817.26	21,542.74

Load	Characteristic value	
	Horizontal force $H(\text{kN/m})$	Moment $H \cdot y(\text{kN} \cdot \text{m/m})$
Horizontal earth pressure	510.92	3,701.88
Residual water pressure	92.72	709.41
Total	603.64	4,411.29

• **Permanent state (case in which surcharge on the wall body is considered)**

Confirmation of shape of distribution of vertical subgrade reaction at caisson bottom

$$x = \frac{\Sigma M}{\Sigma V} = \frac{\Sigma V \cdot x - \Sigma H \cdot y}{\Sigma V} = \frac{24,247.14 - 4,411.29}{3,180.26} = 6.24 \text{ (m)}$$

$$e = \frac{B}{2} - x = \frac{13.50}{2} - 6.24 = 0.51 \text{ (m)}$$

$$e < B/6 = 2.25 \text{ (m)}$$

Accordingly, the distribution is trapezoidal, and

$$p_1 = \frac{\Sigma V}{B} \left(1 + \frac{6e}{B}\right) = \frac{3,180.26}{13.50} \left(1 + \frac{6 \times 0.51}{13.50}\right) = 288.97 \text{ (kN/m}^2\text{)}$$

$$p_2 = \frac{\Sigma V}{B} \left(1 - \frac{6e}{B}\right) = \frac{3,180.26}{13.50} \left(1 - \frac{6 \times 0.51}{13.50}\right) = 182.18 \text{ (kN/m}^2\text{)}$$

Distribution width $b = 13.50$ (m) (width of caisson bottom)

Calculation of load width

$$\overline{2b} = \frac{2\Sigma \overline{M}}{\Sigma \overline{V}} = \frac{2(\Sigma \overline{V} \cdot x - \Sigma \overline{H} \cdot y)}{\Sigma \overline{V}} = \frac{2 \times (24,247.14 - 4,411.29)}{3,180.26} = 12.47 \text{ (m)}$$

Calculation of uniformly-distributed load

$$\overline{q} = \frac{\Sigma \overline{V}}{\overline{2b}} = \frac{3,180.26}{12.47} = 255.03 \text{ (kN/m}^2\text{)}$$

Horizontal force for use in verification

$$H = 603.64 \text{ (kN/m)}$$

Load	Characteristic value	
	Vertical force $V(\text{kN/m})$	Moment $V \cdot x(\text{kN} \cdot \text{m/m})$
Weight of wall body	4,586.43	33,886.69
Buoyancy	-1,906.07	-14,192.10
Vertical earth pressure	136.90	1,848.15
Surcharge	363.00	2,704.40
Total	3,180.26	24,247.14

Load	Characteristic value	
	Horizontal force $H(\text{kN/m})$	Moment $H \cdot y(\text{kN} \cdot \text{m/m})$
Horizontal earth pressure	510.92	3,701.88
Residual water pressure	92.72	709.41
Total	603.64	4,411.29

• **Variable states associated with Level 1 earthquake ground motion**

(not considering surcharge on wall body)

Confirmation of shape of distribution of vertical subgrade reaction of caisson bottom slab

$$x = \frac{\Sigma M}{\Sigma V} = \frac{\Sigma V \cdot x - \Sigma H \cdot y}{\Sigma V} = \frac{22,378.12 - 12,700.95}{2,879.14} = 3.36 \text{ (m)}$$

$$e = \frac{B}{2} - x = \frac{13.50}{2} - 3.36 = 3.39 \text{ (m)}$$

$$e > B/6 = 2.25 \text{ (m)}$$

Therefore, the distribution is triangular, and

$$p_1 = \frac{2\Sigma V}{3(B/2 - e)} = \frac{2 \times 2,879.14}{3(13.50/2 - 3.39)} = 571.26 \text{ (kN/m}^2\text{)}$$

$$\text{Width of distribution } b = 3(B/2 - e) = 3(13.50/2 - 3.39) = 10.08 \text{ (m)}$$

Calculation of width of load

$$2b' = \frac{2\Sigma M}{\Sigma V} = \frac{2(\Sigma V \cdot x - \Sigma H \cdot y)}{\Sigma V} = \frac{2 \times (22,378.12 - 12,700.95)}{2,879.14} = 6.72 \text{ (m)}$$

Calculation of average value of uniformly-distributed load

$$q = \frac{\Sigma V}{2b'} = \frac{2,879.14}{6.72} = 428.44 \text{ (kN/m}^2\text{)}$$

Load	Characteristic value	
	Vertical force V (kN/m)	Moment $V \cdot x$ (kN·m/m)
Weight of wall body	4,586.43	33,886.69
Buoyancy	-1,906.07	-14,192.10
Vertical earth pressure	198.78	2,683.53
Total	2,879.14	22,378.12

Load	Characteristic value	
	Horizontal force H (kN/m)	Moment $H \cdot y$ (kN·m/m)
Inertia force	642.10	5,789.74
Horizontal earth pressure	741.84	5,088.26
Residual water pressure	92.72	709.41
Dynamic water pressure	185.59	1,113.54
Total	1,662.25	12,700.95

Variable states associated with Level 1 earthquake ground motion (considering surcharge on wall body)

Confirmation of shape of distribution of vertical subgrade reaction of caisson bottom slab

$$x = \frac{\Sigma M}{\Sigma V} = \frac{\Sigma V \cdot x - \Sigma H \cdot y}{\Sigma V} = \frac{23,730.32 - 13,165.95}{3,060.64} = 3.45 \text{ (m)}$$

$$e = \frac{B}{2} - x = \frac{13.50}{2} - 3.45 = 3.30 \text{ (m)}$$

$$e > B/6 = 2.25 \text{ (m)}$$

Therefore, the distribution is triangular, and

$$p_1 = \frac{2\Sigma V}{3(B/2 - e)} = \frac{2 \times 3,060.64}{3(13.50/2 - 3.30)} = 591.43 \text{ (kN/m}^2\text{)}$$

$$\text{Width of distribution } b = 3(B/2 - e) = 3(13.50/2 - 3.30) = 10.35 \text{ (m)}$$

Calculation of width of load

$$2b' = \frac{2\Sigma M}{\Sigma V} = \frac{2(\Sigma V \cdot x - \Sigma H \cdot y)}{\Sigma V} = \frac{2 \times (23,730.32 - 13,165.95)}{3,060.64} = 6.90 \text{ (m)}$$

Calculation of uniformly-distributed load

$$q = \frac{\Sigma V}{2b'} = \frac{3,060.64}{6.90} = 443.57 \text{ (kN/m}^2\text{)}$$

Load	Characteristic value	
	Vertical force V (kN/m)	Moment $V \cdot x$ (kN · m/m)
Weight of wall body	4,586.43	33,886.69
Buoyancy	-1,906.07	-14,192.10
Vertical earth pressure	198.78	2,683.53
Surcharge	181.50	1,352.20
Total	3,060.64	23,730.32

Load	Characteristic value	
	Horizontal force H (kN/m)	Moment $H \cdot y$ (kN · m/m)
Inertia force	642.10	5,789.74
Horizontal earth pressure	741.84	5,088.26
Residual water pressure	92.72	709.41
Dynamic water pressure	185.59	1,113.54
Inertia force of surcharge	25.41	465.00
Total	1,687.66	13,165.95

iii) Verification results

In verification of bearing capacity of the foundation ground, the adjustment factor m is considered.

Table 5.2.14 shows the load conditions and verification results. **Figure 5.2.6** shows the verification results for the case of variable states associated with Level 1 earthquake ground motion not considering surcharge, which is the most dangerous condition.

Table 5.2.14 Load Conditions and Verification Results for Verification of Bearing Capacity of Foundation Ground

State		Converted uniformly-distributed load q (kN/m ²)	Load width $2b'$ (m)	Horizontal load H (kN)	Resistance term R_d (kN · m)	Load term S_d (kN · m)	Adjustment factor m	Load-resistance ratio $m \cdot S_d / R_d$
Permanent state	Without surcharge	231.68	12.16	603.64	81,551.460	39,066.391	1.20	0.57
	With surcharge	255.03	12.47	603.64	89,572.109	43,541.679	1.20	0.58
Variable states of Level 1 earthquake ground motion	Without surcharge	428.44	6.72	1,662.25	55,014.015	53,671.524	1.00	0.98
	With surcharge	443.57	6.90	1,687.66	57,332.990	55,338.014	1.00	0.97

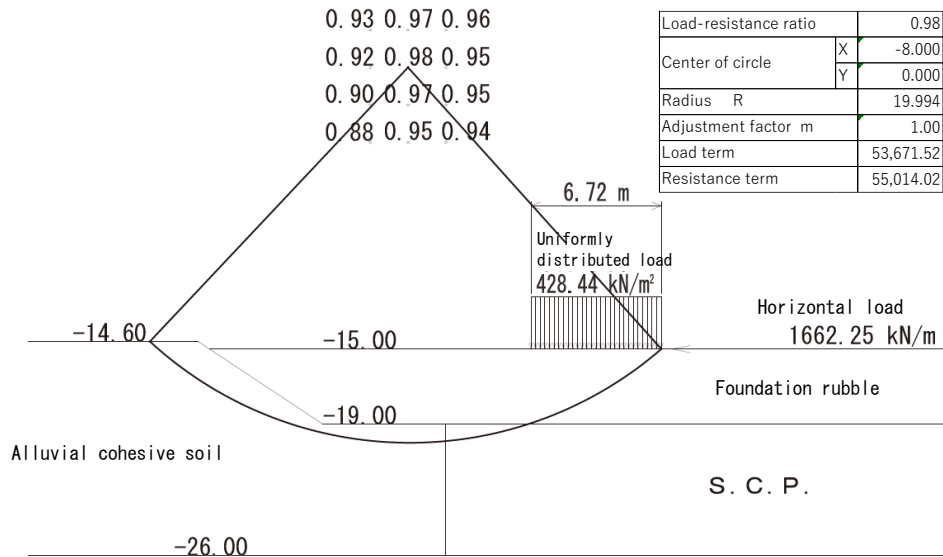


Figure 5.2.6 Example of verification of bearing capacity by Bishop's method

3) Example of circular slip failure of foundation ground

Verification is performed for circular slip failure of the foundation ground in the permanent state.

- Unit weight of wall body (caisson + filling sand + lid concrete): W'

$$W' = \frac{15,072.27 + 43,024.40 + 936.09}{628.01 + 2,151.22 + 41.42} = 20.93 \text{ (kN/m}^3\text{)}$$

- Surcharge

$$\omega = 30.0 \text{ (kN/m}^2\text{)}$$

- Residual water level

$$\text{R.W.L} = 0.60 \text{ (m)}$$

- Ground conditions

The following equation, which has the largest record of actual use, was used as the calculation formula for the shear strength τ of improved ground.

$$\tau = (1 - a_s)(c_0 + kz + \Delta\sigma_z \mu_c \Delta c / \Delta p U) + (\gamma_s z + \mu_s \Delta\sigma_z) a_s \tan \phi_s \cos^2 \theta$$

where

a_s : replacement ratio of sand pile (0.8)

$c_0 + kz$: undrained shear strength of original ground (kN/m²)

n : stress sharing ratio (because $a_s \geq 0.7$, $n = 1$)

U : average degree of consolidation (0.8)

z : vertical coordinate (m)

τ : shear strength demonstrated at position of slip line (kN/m²)

μ_s : coefficient of stress concentration on sand pile

$$(\mu_s = n / \{1 + (n - 1)a_s\}) = 1.0$$

μ_c : coefficient of stress reduction on cohesive soil

$$(\mu_c = 1 / \{1 + (n - 1)a_s\}) = 1.0$$

γ_s : unit weight of sand pile (below the surface level of ground water, unit weight in water) (kN/m³)

γ_c : unit weight of cohesive soil (below the surface level of ground water, unit weight in water) (kN/m³)

φ_s : shear resistance angle of sand pile (because $a_s \geq 0.7$, $\varphi_s = 35^\circ$)

θ : angle of slip line to horizontal line (°)

$\Delta \sigma_z$: average value of vertical stress increment due to external force at position of object slip line (kN/m²)

$\Delta c / \Delta p$: strength increase rate of original ground

$$(\Delta c / \Delta p = k / w' = 1.6 / 6.00 = 0.27)$$

Table 5.2.16 shows the verification results. Figure 5.2.7 shows the verification results for the case of the permanent state considering surcharge on the wall body, which is the most dangerous condition.

Table 5.2.15 Characteristic values of ground conditions for verification of circular slip failure stability of foundation ground

	Saturated weight w (kN/m ³)	Wet weight w_t (kN/m ³)	Weight in water w' (kN/m ³)	Shear resistance angle ϕ'_k (°)	Cohesion	
					c'_k (kN/m ²)	Primary coefficient of cohesion
Foundation rubble	20.00	18.00	10.00	40.00	0.00	0.00
Alluvial cohesive soil	16.00	16.00	6.00	0.00	27.30	1.60
SCP sand pile	20.00	18.00	10.00	35.00	0.00	0.00
Diluvial cohesive ground	17.00	17.00	7.00	40.00	146.00	0.00
Wall body	20.93	20.93	10.93	40.00	0.00	0.00
Superstructure	22.60	22.60	-	40.00	0.00	0.00
Backfilling stones	20.00	18.00	10.00	40.00	0.00	0.00
Backfilling soil	20.00	18.00	10.00	40.00	0.00	0.00

Table 5.2.16 Characteristic values of ground conditions for verification of circular slip failure stability of foundation ground

State		Resistance term R_d (kN · m)	Load term S_d (kN · m)	Adjustment factor m	Action-resistance ratio $m \cdot S_d / R_d$
Permanent state	Without surcharge	92,257.29	47,606.28	1.0	0.52
	With surcharge	99,040.80	54,592.78	1.0	0.55

Minimum action resistance ratio $m \cdot S_d / R_d = 0.55$
 Center of ark $X = -7.00$ (m)
 $Y = 1.00$ (m)
 Radius $R = 24.839$ (m)

Resistance term $R_d = 99,040.80$ (kN·m)
 Initiation term $S_d = 54,592.78$ (kN·m)

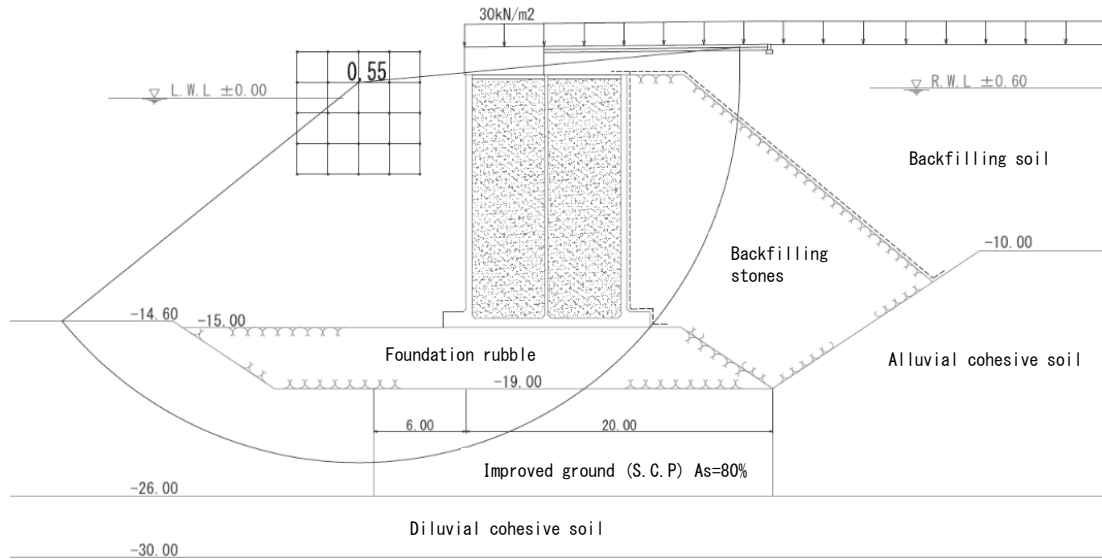


Figure 5.2.7 Verification of circular slip failure stability of foundation ground (permanent state, with surcharge)

4) Load-resistance ratio

Table 5.2.17 shows the load-resistance ratios obtained in a stability verification considering partial factors based on the study presented above.

Table 5.2.17 Load-resistance ratios

*Shaded cells show the smallest load-resistance ratio of each verification.

State		Unit	Resistance term	Load term	Adjustment factor	Load-resistance ratio
Permanent state (without surcharge)	Sliding of wall body	kN/m	1,470.61	639.86	1.0	0.44 ≤ 1.0
	Overturning of wall body	kN·m/m	21,327.31	5,425.89	1.0	0.26 ≤ 1.0
	Bearing capacity failure of foundation ground	kN·m	19,164.93	11,442.36	1.2	0.72 ≤ 1.0
	Circular slip failure of foundation ground	kN·m	92,257.29	47,606.28	1.0	0.52 ≤ 1.0
Permanent state (with surcharge)	Sliding of wall body	kN/m	1,660.10	639.86	1.0	0.39 ≤ 1.0
	Overturning of wall body	kN·m/m	21,327.31	5,425.89	1.0	0.26 ≤ 1.0
	Bearing capacity failure of foundation ground	kN·m	20,498.42	12,048.04	1.2	0.71 ≤ 1.0
	Circular slip failure of foundation ground	kN·m	99,040.80	54,592.78	1.0	0.55 ≤ 1.0
Variable states for Level 1 earthquake ground motion (without surcharge)	Sliding of wall body	kN/m	1,727.48	1,662.25	1.0	0.97 ≤ 1.0
	Overturning of wall body	kN·m/m	21,327.31	5,425.89	1.0	0.26 ≤ 1.0
	Bearing capacity failure of foundation ground	kN·m	54,970.93	50,445.91	1.0	0.92 ≤ 1.0
Various states for Level 1 earthquake ground motion (with surcharge)	Sliding of wall body	kN/m	1,836.38	1,687.66	1.0	0.92 ≤ 1.0
	Overturning of wall body	kN·m/m	21,327.31	5,425.89	1.0	0.26 ≤ 1.0
	Bearing capacity failure of foundation ground	kN·m	56,111.47	51,778.74	1.0	0.92 ≤ 1.0

5) Examination by dynamic analysis

The following shows the results of verification of the amount of deformation obtained by a dynamic analysis for Level 2 earthquake ground motion. (The calculation method, parameter setting method and other details have been omitted.)

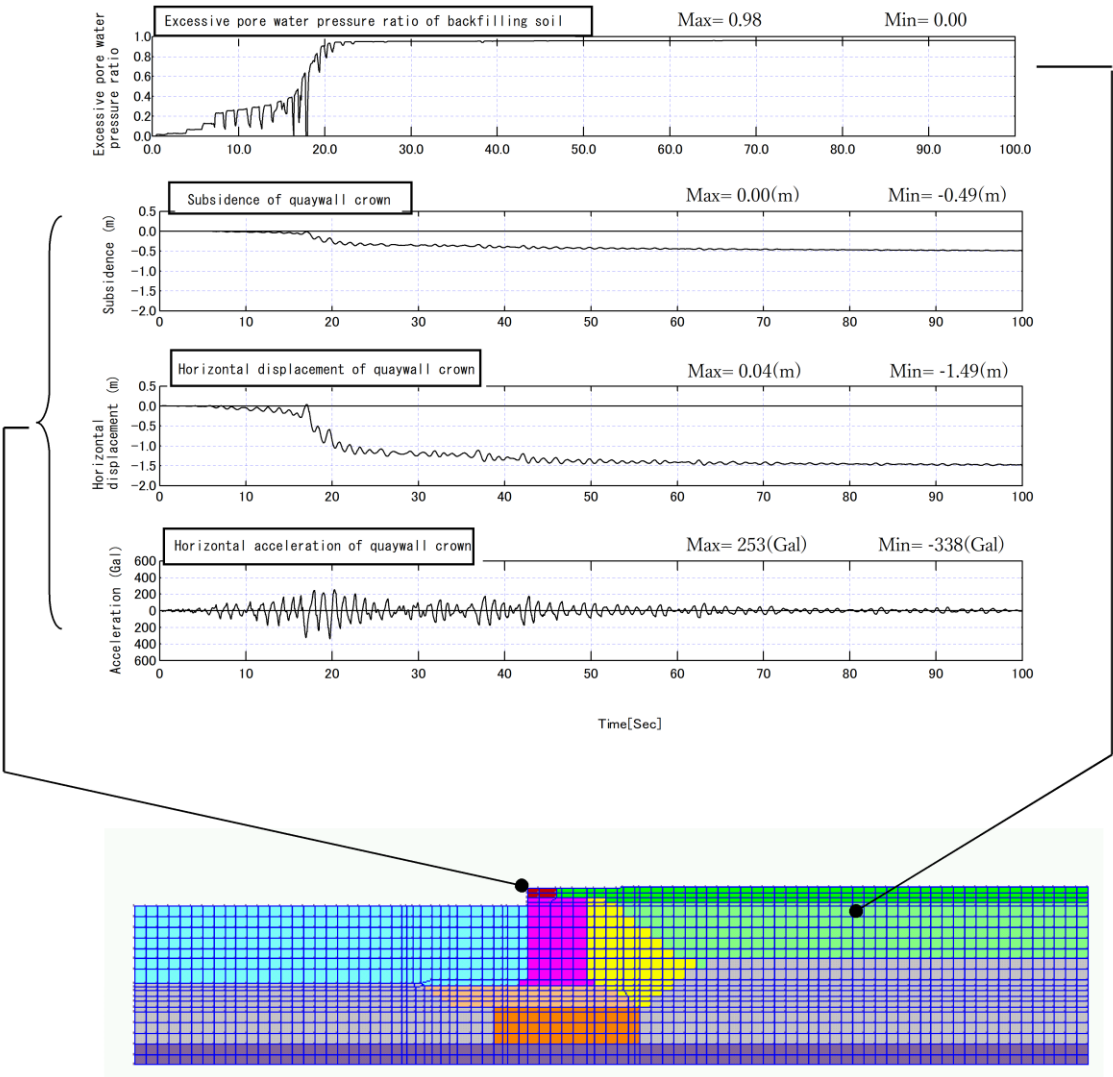


Figure 5.2.8 Time history of horizontal acceleration, horizontal displacement and settlement of quaywall crown and excessive pore water pressure ratio of backfilling soil (Level 2)

3. Anchored Sheet-pile Quaywall

(1) Basic section for examination

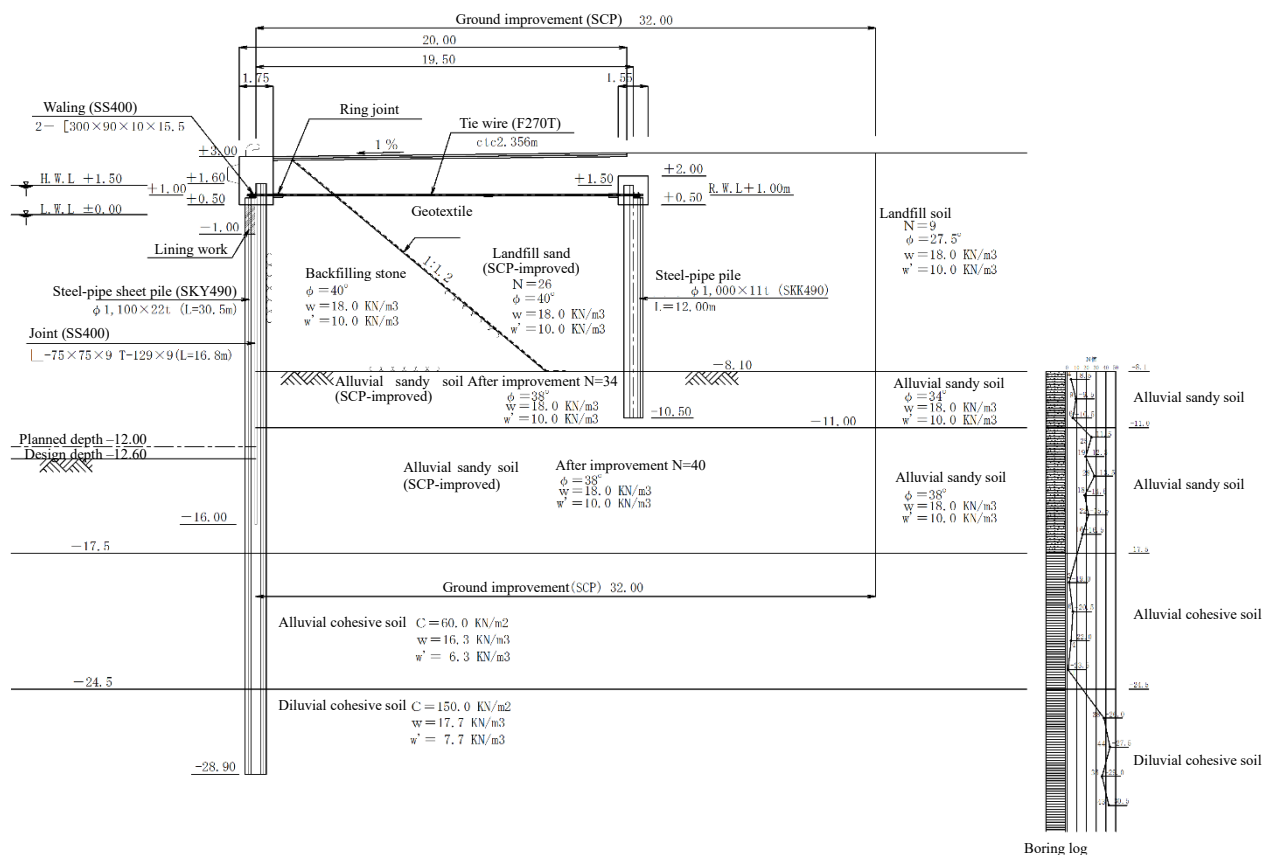


Figure 5.3.1 Basic section for examination

(2) Design conditions

1) Specifications of quaywall

- Crown height of quaywall: +3.00 m
- Crown height of sheet pile: +1.60 m
- Tie wire installation height: +1.00 m
- Planned depth: -12.00 m
- Depth for quaywall verification: -12.60 m
- Seabed slope in front of the quaywall: 0.0°

The depth for verification, described above, shall be -12.60 m relative to the planned depth of -12.0 m by considering mooring basin dredging (over-dredging).

2) Natural condition

- Tide level

H.W.L.: +1.50 m

L.W.L.: 0.00 m

Residual water level (R.W.L.): +1.0 m

$[2/3 (H.W.L. - L.W.L.)] + L.W.L.$

- Ground conditions

Figure 5.3.2 shows the status of original ground stratification and the soil conditions after ground improvement (SCP method).

- Unit weight of seawater

$$w_w = 10.1 \text{ kN/m}^3$$

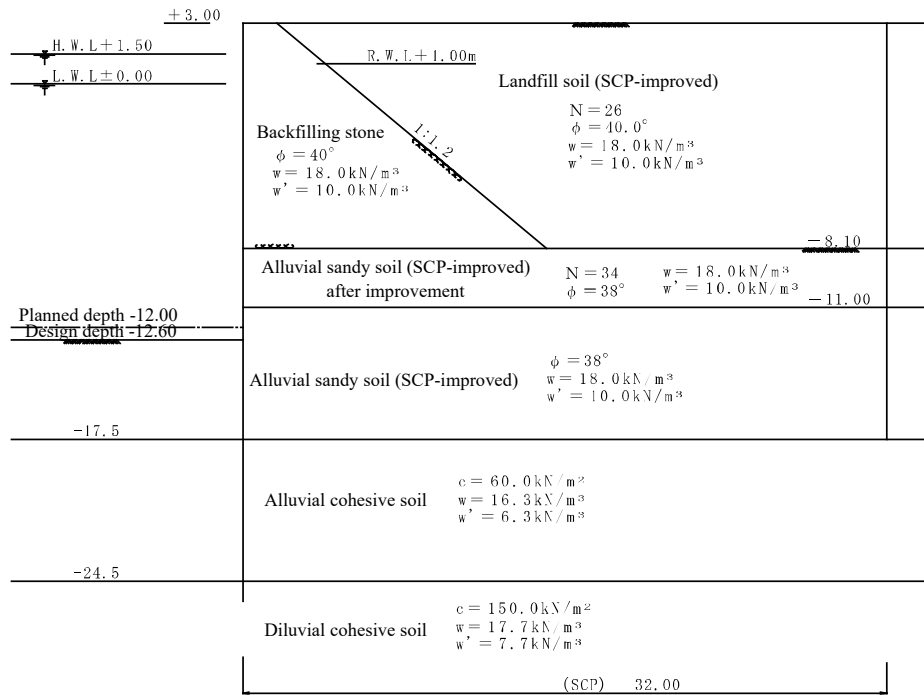


Figure 5.3.2 Soil conditions after ground improvement

3) Use conditions

- Target vessel: 30,000 DWT
- Live load (characteristic value)
 - Permanent situation: 30.0 kN/m^2
 - Variable situation: 15.0 kN/m^2
- Mooring force (characteristic value)
 - Mooring force (characteristic value): 700.0 kN/post
 - Service height: $+3.37 \text{ m}$
- Design service life: 50 years
- Allowable displacement

The allowable displacement tolerance is determined for this verification example as follows while considering various relevant factors, including the conditions at the location where the facility is to be constructed and the functions required of the facility:

Variable situation related to Level 1 earthquake ground motion: 15 cm or less

Accidental situation related to Level 2 earthquake ground motion: about 100 cm

4) Design earthquake ground motion

Figure 5.3.3 and Figure 5.3.4 show waveforms of Level 1 and Level 2 earthquake ground motions respectively.

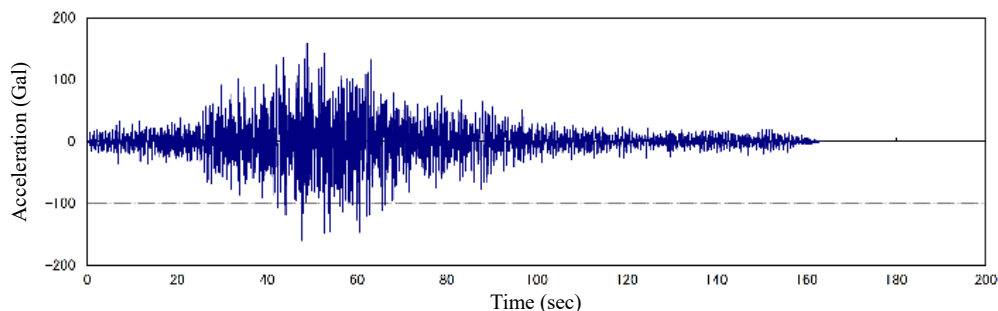


Figure 5.3.3 Level 1 earthquake ground motion

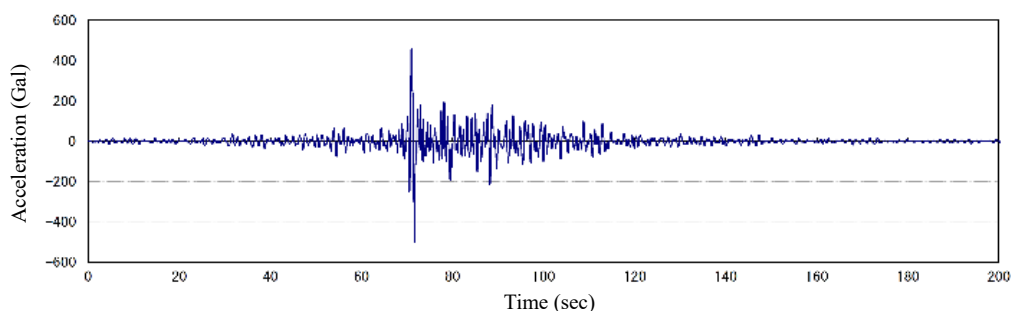


Figure 5.3.4 Level 2 earthquake ground motion

5) Corrosion allowance for steels (treated with corrosion protection)

Service life: 50 years

Corrosion rate μ : 90%

- Steel-pipe sheet pile

Corrosion speed: $1 - \mu$

$$t_1 = 0.10 \text{ mm/year} \times 0.1 \times 50 \text{ years} = 0.50 \text{ mm (sea side)}$$

$$t_2 = 0.02 \text{ mm/year} \times 50 \text{ years} = 1.00 \text{ mm (land side)}$$

- Tie wire

$$t = 2 \times 0.03 \text{ mm/year} \times 50 \text{ years} = 3.00 \text{ mm}$$

- Waling (to be provided in the superstructure)

$$t = 0.00 \text{ mm}$$

- Vertical anchor pile

$$t = 0.02 \text{ mm/year} \times 50 \text{ years} = 1.00 \text{ mm}$$

6) Characteristic values of steel yield stress

Table 5.3.1 shows the characteristic values for steel yield stress.

Table 5.3.1 Characteristic values for steel yield stress

	Material	Unit	Yield stress
Steel-pipe sheet pile	SKY490	N/mm ²	315.0
General steel	SS400	N/mm ²	235.0
(waling)	SKK490	N/mm ²	315.0

(3) Seismic coefficient for verification

1) Procedure to calculate the seismic coefficient for verification

Figure 5.3.5 shows the general procedure for calculating the seismic coefficient for verification.

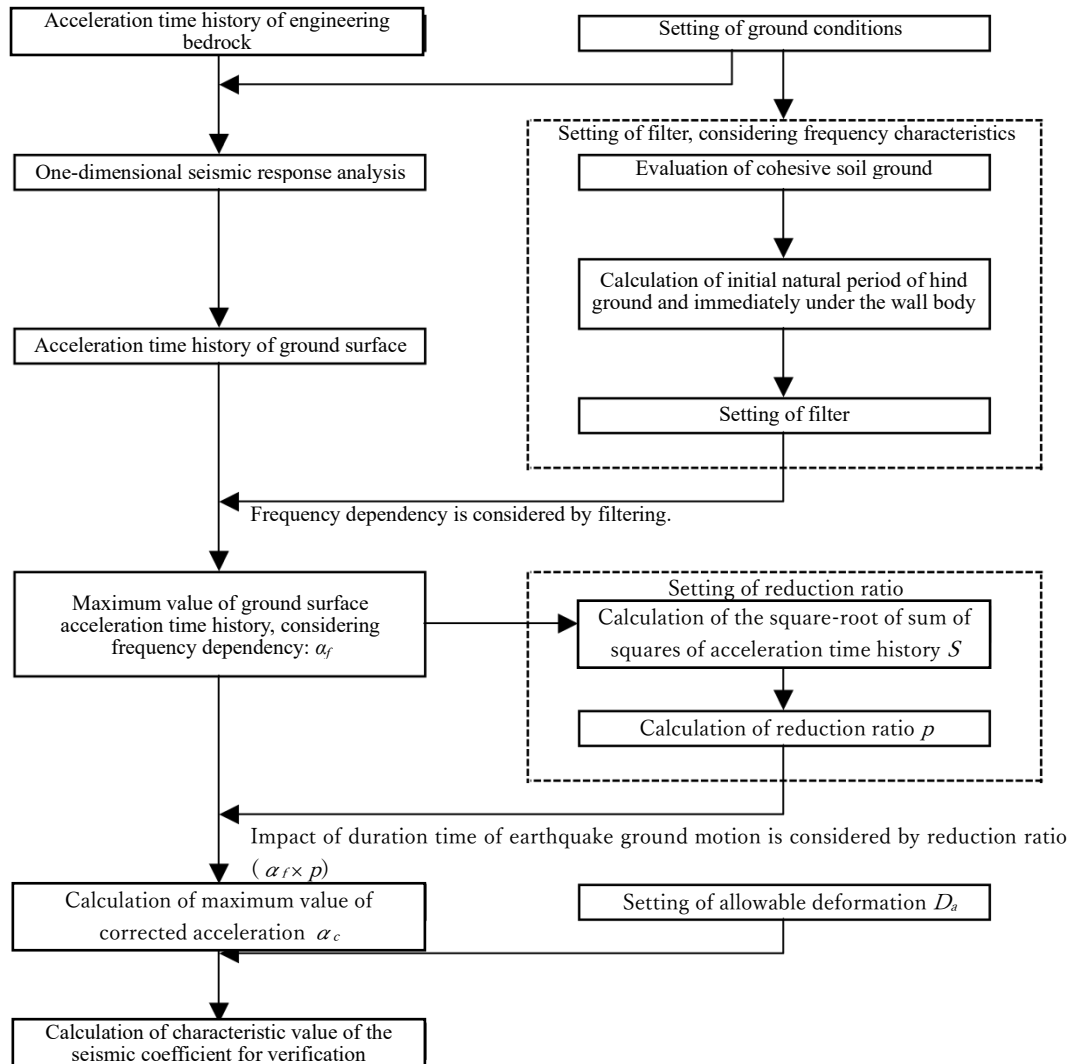


Figure 5.3.5 Procedure to calculate seismic coefficient for verification

- Input the Level 1 earthquake ground motion of the port to be verified in the engineering bedrock, and calculate the acceleration waveform on the ground surface in the surrounding ground by one-dimensional seismic response analysis (FLIP is used in this case example).
- Apply filter processing to the obtained acceleration waveform (FFT "Fourier transformation" → spectral waveform of frequency → filter processing with the frequency characteristics taken into consideration → IFFT "reverse Fourier transformation") to obtain time history acceleration waveforms. The maximum value of this time history acceleration is taken as α_f .
- Calculate the square-root of the sum of squares S of the filtered acceleration waveform to standardize

the maximum acceleration value α_f . Calculate the reduction ratio p from S/α_f to calculate the corrected maximum acceleration value α_c .

- Calculate the characteristic value of the seismic coefficient for verification using the corrected maximum acceleration value α_c and the deformation D_a allowed at the top of the quaywall.

a) Setting of the filter, with the frequency characteristics taken into consideration

$$a(f) = \begin{cases} b & f \leq 1.0\text{Hz} \\ \frac{b}{1 - \left(\frac{f-1.0}{1/0.34}\right)^2 + 11\left(\frac{f-1.0}{1/0.34}\right)i} & 1.0\text{Hz} < f \end{cases} \quad (1)$$

$$b = 2.25 \frac{H}{H_R} - 0.88 \frac{T_b}{T_{b_R}} + 0.96 \frac{T_u}{T_{u_R}} - 0.96 \quad (2)$$

Set the value of b as a value in the range shown by **Eq. (3)** using the wall height H of the wall structure. However, the lowest value set for b shall be 0.41 in any case, regardless of the range set by **Eq. (3)**.

$$0.12H - 0.78 \leq b \leq 0.12H - 0.24 \quad (3)$$

Provided that $b \geq 0.41$

Where:

H : wall height (15.6 m in this verification example)

H_R : standard wall height (15 m)

T_b : initial natural period of the surrounding ground (s)

T_u : standard initial natural period of the surrounding ground (0.8 s)

T_{b_R} : Initial natural period of the ground under the seabed (s)

T_{u_R} : Standard initial natural period of the ground under the seabed (0.4 s)

b) Correction of the effect of duration

Correct the effect of duration using **Eq. (4)** to **Eq. (6)** as follows:

$$p = 0.35 \times \text{Ln}(S / \alpha_f) - 0.20 \quad (4)$$

$$\alpha_c = p \times \alpha_f \quad (5)$$

$$S = \sqrt{\sum acc^2} \quad (6)$$

Where:

p : reduction ratio ($p \leq 1.0$)

S : square-root of the sum of squares of the acceleration time history after filtering (Gal)

α_f : maximum acceleration value after filtering (Gal)

α_c : corrected value of the maximum acceleration of the ground at the ground surface (Gal)

acc : acceleration after filtering each time (Gal)

iii) Calculation of the characteristic values of seismic coefficient for verification

Calculate the characteristic values of seismic coefficient for verification using **Eq. (7)** as follows:

$$k_{h_k} = 1.91 \left(\frac{D_a}{D_r} \right)^{-0.69} \frac{\alpha_c}{g} + 0.03 \quad (7)$$

Where:

k_{h_k} : characteristic value of the seismic coefficient for verification

α_c : corrected value of the maximum acceleration of the ground at the ground surface (Gal)

g : gravitational acceleration (980 Gal)

D_a : allowable amount of deformation at the top of the quaywall (15 cm)

D_r : standard deformation amount (10 cm)

2) Level 1 earthquake ground motion

Level 1 earthquake ground motion is the acceleration time history waveform at the engineering bedrock, determined by considering the characteristics of the ground at the target point based on the actual measurement of earthquake ground motion in the area around the target facility. **Figure 5.3.6** shows the acceleration waveform of Level 1 earthquake ground motion used as the earthquake ground motion input to the engineering bedrock in the target ground model (2E wave)

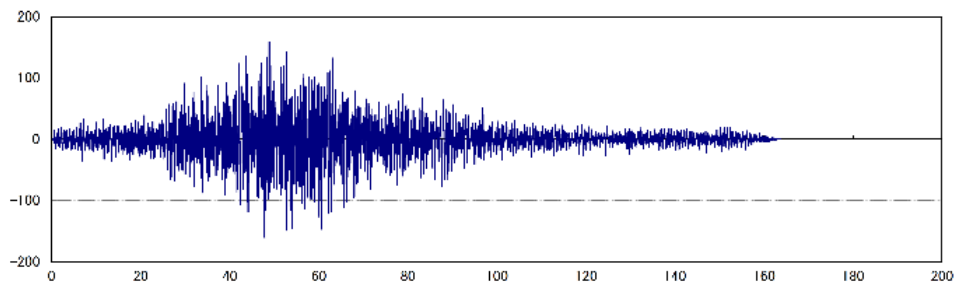


Figure 5.3.6 Input acceleration (Level 1 earthquake ground motion)

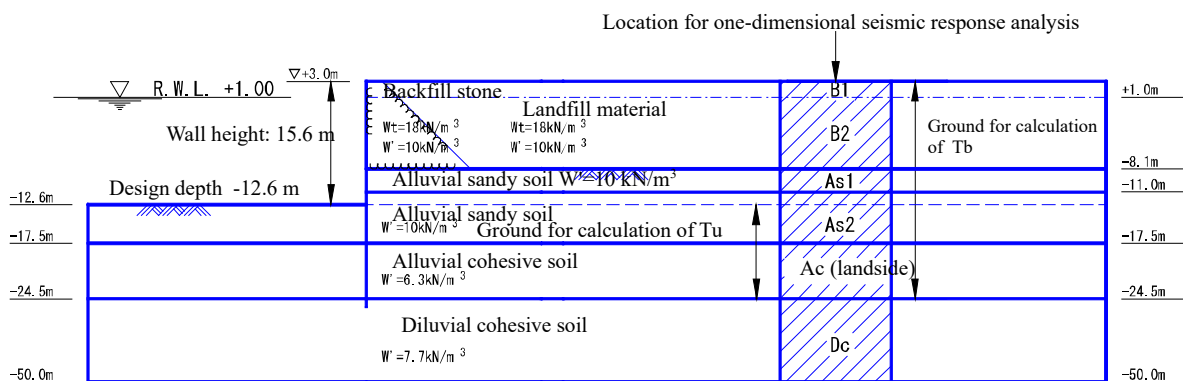


Figure 5.3.7 Calculation location of initial natural period

3) Calculation of the seismic coefficient for verification

i) Calculation of the time history acceleration waveform on the ground surface

Figure 5.3.8 shows the ground surface time history response acceleration waveform, determined by inputting the original waveform of the target port for verification into the engineering bedrock using one-dimensional seismic response analysis (FLIP).

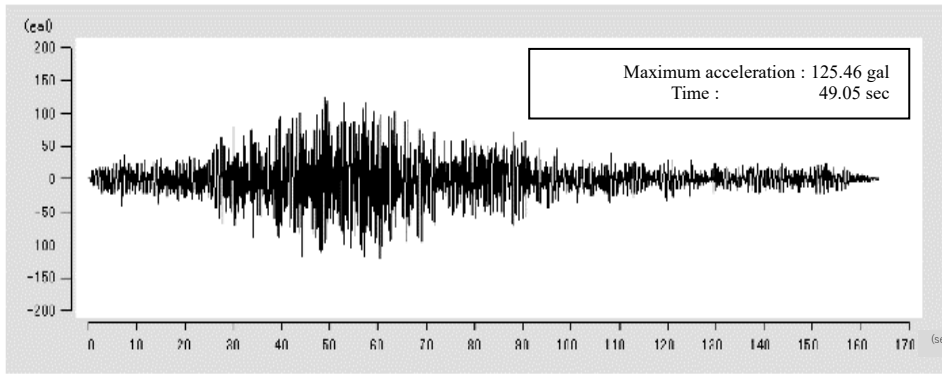


Figure 5.3.8 Acceleration of ground surface time history response

ii) Calculation of the natural period of the ground

Calculate the natural period of the ground using Eq. (8).

$$T_g = 4 \sum_{i=1} \frac{H_i}{V_i} \quad (8)$$

Where:

T_g : natural period of the ground (s)

H_i : thickness of the soil layer (m)

V_i : speed of S wave (m/s)

Tables 5.3.2 (1) and (2) show the calculation results for the natural period of the ground.

Table 5.3.2 (1) Initial natural period of the ground under the seabed

Soil layer	H (m)	V _s (m/s)	$T_u = 4 \sum_i \frac{H_i}{V_{s_i}}$
As2_l	4.9	284	0.274(s)
Ac_l	7.0	136	

Table 5.3.2 (2) Initial natural period of the surrounding ground

Soil layer	H (m)	V _s (m/s)	$T_b = 4 \sum_i \frac{H_i}{V_{s_i}}$
B1	2.0	125	0.629(s)
B2	9.1	173	
As1	2.9	200	
As2_l	6.5	284	
Ac_l	7.0	136	

iii) Filtering of the time history acceleration waveform on the ground surface

The results of Fourier spectral processing of ground surface time history acceleration using the filters shown in Eq. (1) and Eq. (2) and the limit equation of Eq. (3) are shown below.

$$b = 2.25 \frac{15.6}{15.0} - 0.88 \frac{0.629}{0.80} + 0.96 \frac{0.274}{0.40} - 0.96$$

$$= 1.346 \quad (1.092 \leq b \leq 1.632)$$

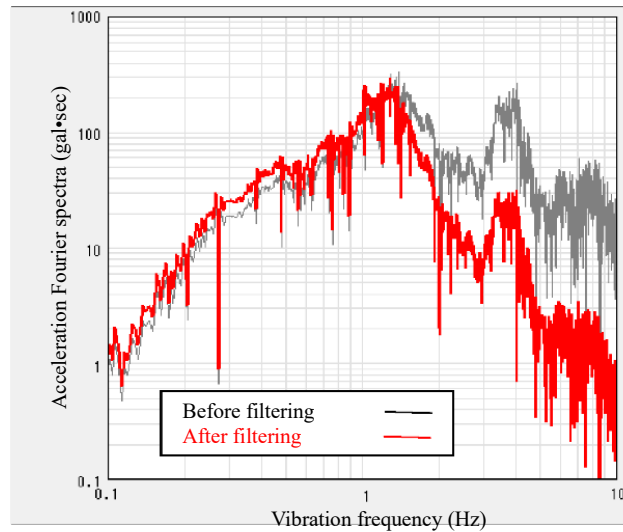


Figure 5.3.9 Acceleration Fourier spectra

iv) Ground surface time history acceleration waveform after filtering

Reverse Fourier conversion is conducted on the acceleration Fourier spectra after filtering in **Figure 5.3.9** to obtain the acceleration time history after filtering, as shown in **Figure 5.3.10**. The following values are calculated as the maximum acceleration value after filtering α_f and the square-root of the sum of squares of acceleration time history S .

$$\alpha_f = 83.5 \text{ Gal}$$

$$S = 2121.3 \text{ Gal}$$

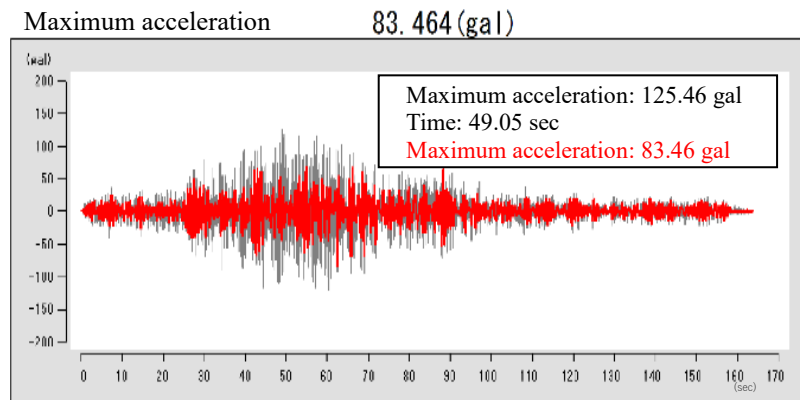


Figure 5.3.10 Ground surface time history acceleration (after filtering)

v) Correction of the maximum acceleration

Calculate the reduction ratio p using **Eq. (4)** as follows:

$$p = 0.35 \times \text{Ln}(S / \alpha_f) - 0.20$$

$$= 0.35 \times \text{Ln}(2121.3 / 83.5) - 0.20$$

$$= 0.932$$

Calculate the maximum acceleration after correction using **Eq. (5)** as follows:

$$\alpha_c = p \times \alpha_f = 0.932 \times 83.5 = 77.8 \text{ Gal}$$

vi) Determination of the seismic coefficient for verification

Calculate the characteristic value of the seismic coefficient for verification using **Eq. (7)** as follows:

$$\begin{aligned}
 k_{hk} &= 1.91 \left(\frac{D_a}{D_r} \right)^{-0.69} \frac{\alpha_c}{g} + 0.03 \\
 &= 1.91 \times (15.0 / 10.0)^{-0.69} \times 77.8 / 980 + 0.03 \\
 &= 0.144
 \end{aligned}$$

Where:

k_{hk} : characteristic value of the seismic coefficient for verification

α_c : corrected value of the maximum acceleration of the ground at the ground surface (Gal)

g : gravitational acceleration (980 Gal)

D_a : allowable amount of deformation at the top of the quaywall (15 cm)

D_r : standard deformation amount (10 cm)

Based on the above calculation results, the following value is used as the characteristic value of the seismic coefficient for verification:

$$k_{hk} = 0.144 \Rightarrow 0.14$$

vii) Prediction and judgment of liquefaction

Figure 5.3.11 is used to predict and judge liquefaction. In this example, it confirmed that no liquefaction will occur in any layer of sandy soil located under the groundwater level as shown in **Table 5.3.3**.

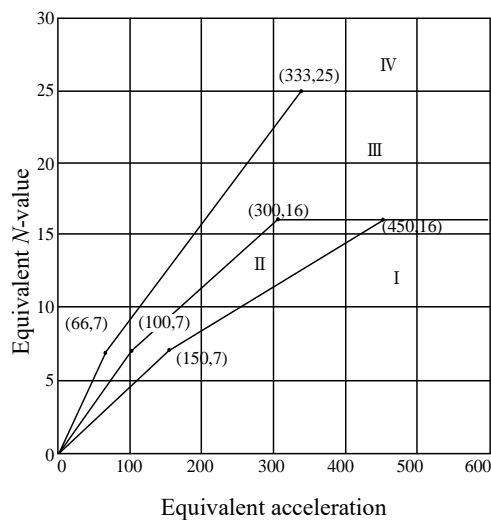


Figure 5.3.11 Classification of soil layers with equivalent N -value and equivalent acceleration

Table 5.3.3 Prediction and judgment results for liquefaction with equivalent N -value and equivalent acceleration

Soil layer	No.	Layer thickness h (m)	Depth (m)	Elevation (m)	Weight per unit volume		Effective stress (kN/m ²)	Equivalent N -value		Maximum shear stress (kN/m ²)	Equivalent acceleration (cm/s)	Judgment result
					Saturated (kN/m ³)	Wet (kN/m ³)		Before correction	After correction			
B1	1	2.000	2.00	1.00	20.00	18.00	18.0			2.1	78.6	IV No liquefaction will occur.
B2	2	2.275	4.28	-1.28	20.00	18.00	47.4	8.60	15.70	6.6	95.8	IV No liquefaction will occur.
B2	3	2.275	6.55	-3.55	20.00	18.00	70.1	8.60	15.70	10.9	107.5	IV No liquefaction will occur.
B2	4	2.275	8.83	-5.83	20.00	18.00	92.9	8.60	15.70	14.4	106.9	IV No liquefaction will occur.
B2	5	2.275	11.10	-8.10	20.00	18.00	115.6	8.60	15.70	16.6	99.4	IV No liquefaction will occur.
As1	6	2.900	14.00	-11.00	20.00	18.00	141.5	8.80	16.00	17.6	86.1	IV No liquefaction will occur.
As2	7	3.250	17.25	-14.25	20.00	18.00	172.3	21.40	38.90	18.3	73.6	IV No liquefaction will occur.
As2	8	3.250	20.50	-17.50	20.00	18.00	204.8	21.40	38.90	21.8	73.6	IV No liquefaction will occur.

(4) Outline of verification

In this verification example, performance verification of a sheet-pile quaywall is conducted for three design situations, namely the permanent situation, the variable situation due to Level 1 earthquake ground motion, and the accidental situation due to Level 2 earthquake ground motion, depending on the service condition of the quaywall and the related action conditions.

Verification items for the permanent and variable situations are shown below:

- Verification of the embedded length of front steel sheet piles
- Verification of the stress of front steel sheet piles
- Verification related to circular slip failure (only for the permanent situation)
- Verification of the tensile load on tie wires
- Verification of the waling stress
- Verification of the stress of anchorage, embedded length, and placement position

Use FLIP to verify the accidental situation for the following items:

- Verification of quaywall displacement
- Verification of the stress intensity of the steels (front steel sheet piles, tie wires, and raked steel pipe piles)

(5) Performance verification of sheet-pile wall in the permanent situation

1) Verification of the embedded length of sheet pile

- i) Calculation of earth pressure and residual water pressure service on the sheet-pile wall

Tables 5.3.4 and 5.3.5 show the calculation results for active earth pressure, residual water pressure and passive earth pressure in the permanent situation.

Table 5.3.4 Distribution of active earth pressure and residual water pressure in the permanent situation

Active side					Surcharge $\omega = 30.00$ (KN/m ²)						
Elevation	Characteristic value				Layer thickness (m)	w·h KN/m ²	$\Sigma wh + \omega$ KN/m ²	ka·cos δ	1) Earth pressure intensity KN/m ²	2) Residual water pressure KN/m ²	①+② $P_a + P_w$ KN/m ²
	w KN/m ³	ϕ (°)	δ (°)	c KN/m ²							
+3.00	18.00	40.0	15.0		1.50	27.00	30.00	0.1942	5.826		5.826
+1.50							57.00	0.1942	11.069		11.069
+1.50	18.00	40.0	15.0		0.50	9.00	57.00	0.1942	11.069		11.069
+1.00							66.00	0.1942	12.817	0.000	12.817
+1.00	10.00	40.0	15.0		0.50	5.00	66.00	0.1942	12.817	0.000	12.817
+0.50							71.00	0.1942	13.788	5.050	18.838
+0.50	10.00	40.0	15.0		0.50	5.00	71.00	0.1942	13.788	5.050	18.838
+0.00							76.00	0.1942	14.759	10.100	24.859
+0.00	10.00	40.0	15.0		8.10	81.00	76.00	0.1942	14.759	10.100	24.859
-8.10							157.00	0.1942	30.489	10.100	40.589
-8.10	10.00	38.0	15.0		2.90	29.00	157.00	0.2115	33.206	10.100	43.306
-11.00							186.00	0.2115	39.339	10.100	49.439
-11.00	10.00	38.0	15.0		1.60	16.00	186.00	0.2115	39.339	10.100	49.439
-12.60							202.00	0.2115	42.723	10.100	52.823
-12.60	10.00	38.0	15.0		4.90	49.00	202.00	0.2115	42.723	10.100	52.823
-17.50							251.00	0.2115	53.087	10.100	63.187
-17.50	6.30			60.00	5.10	32.13	251.00		131.000	10.100	141.100
-22.60							283.13		163.130	10.100	173.230
-22.60	6.30			60.00	1.90	11.97	283.13		163.130	10.100	173.230
-24.50							295.10		175.100	10.100	185.200
-24.50	7.70			150.00	0.64	4.90	295.10		0.000	10.100	10.100
-25.14							300.00		0.000	10.100	10.100
-25.14	7.70			150.00	24.86	191.45	300.00		0.000	10.100	10.100
-50.00							491.45		191.450	10.100	201.550

Table 5.3.5 Distribution of passive earth pressure in the permanent situation

Passive side					Surcharge $\omega = 0.00$ (KN/m ²)					
Elevation	Characteristic value				Layer thickness (m)	w·h KN/m ²	$\Sigma wh + \omega$ KN/m ²	kp·cos δ	Earth pressure intensity P_p KN/m ²	
	w KN/m ³	ϕ (°)	δ (°)	c KN/m ²						
-12.60							0.00	7.5633	0.000	
-17.50	10.00	38.0	-15.0		4.90	49.00	49.00	7.5633	370.602	
-17.50							49.00		169.000	
-22.60	6.30			60.00	5.10	32.13	49.00		201.130	
-22.60							81.13		201.130	
-24.50	6.30			60.00	1.90	11.97	81.13		213.100	
-24.50							93.10		393.100	
-25.14	7.70			150.00	0.64	4.93	93.10		398.030	
-25.14							98.03		398.030	
-50.00	7.70			150.00	24.86	191.42	98.03		589.450	

The calculation results of **Table 5.3.4** and **Table 5.3.5** are shown in **Figure 5.3.12**.

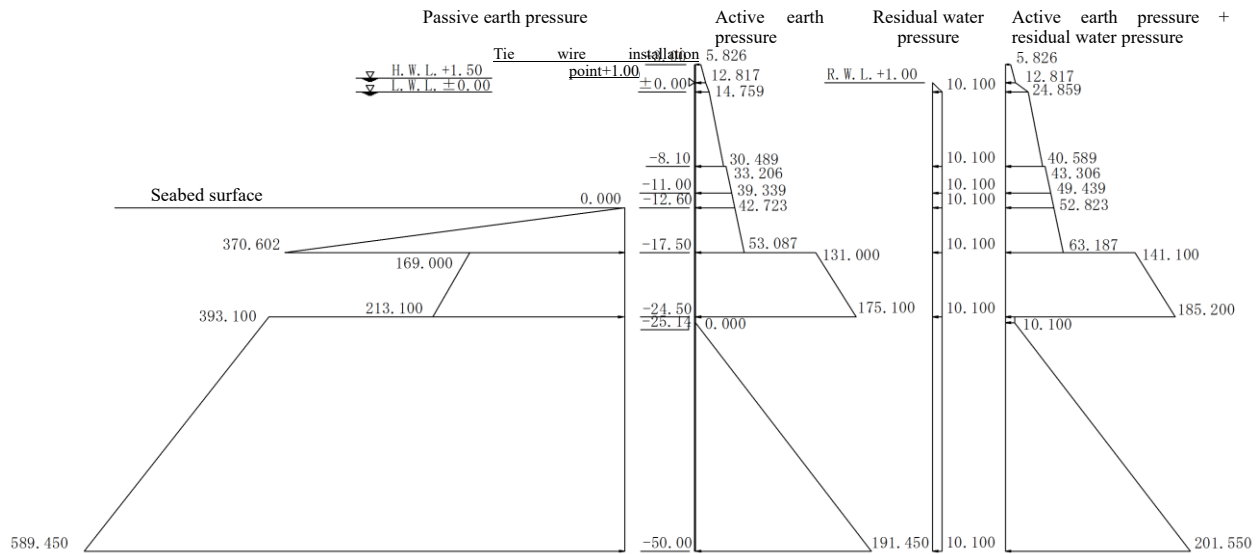


Figure 5.3.12 Distribution of active earth pressure, residual water pressure and passive earth pressure

ii) Verification of the embedded length of sheet-pile wall

The embedded length of the steel sheet-pile wall in the permanent situation is verified here using the free earth support method (**Eq. (9)**) and Rowe's method.

$$m \cdot \frac{S_d}{R_d} \leq 1.0, \quad R_d = \gamma_R R_k, \quad S_d = \gamma_s S_k$$

$$R_k = a P_{pk}$$

$$S_k = b P_{ak} + c P_{wk} + d P_{dwk} \quad (9)$$

Where:

R_k : characteristic value related to the resistance term (kN/m)

S_k : characteristic value related to the load term (kN/m)

P_p : passive earth pressure resultant force acting on the sheet-pile wall (kN/m)

P_a : active earth pressure resultant force acting on the sheet-pile wall (kN/m)

P_w : residual water pressure resultant force acting on the sheet-pile wall (kN/m)

P_{dw} : dynamic water pressure resultant force acting on the sheet-pile wall (kN/m)

(only in the case of an earthquake)

a to d : distance from the position of tie wire installation to the resultant force's point of action (m)

γ_R : partial factor by which the resistance term is multiplied

γ_s : partial factor by which the load term is multiplied

m : adjustment factor

a) Verification by the free earth support method

- Calculation of the active moment of the active earth pressure and residual water pressure on the tie wire installation point

Table 5.3.6 shows the calculation results for the active moment of the active earth pressure and residual

water pressure on the tie wire installation point.

Table 5.3.6 Calculation results for the active moment of the active earth pressure and residual water pressure on the tie wire installation point

Elevation	Layer thickness h (m)	①+② P_a+P_w KN/m ²	Horizontal force S_{pa+pw} KN/m	ΣS_{pa+pw} KN/m	Service position	Arm length l_{pa+pw} (m)	Moment $M_{pa}+M_{pw}$ KN·m/m	$\Sigma(M_{pa}+M_{pw})$ KN·m/m
+3.00	1.50	5.826	12.671		2.172	-1.172	-14.856	
+1.50		11.069		12.671				-14.856
+1.50	0.50	11.069	5.972		1.244	-0.244	-1.456	
+1.00		12.817		18.643				-16.312
+1.00	0.50	12.817	7.914		0.734	0.266	2.104	
+0.50		18.838		26.557				-14.209
+0.50	0.50	18.838	10.924		0.239	0.761	8.319	
±0.00		24.859		37.481				-5.890
±0.00	8.10	24.859	265.064		-4.374	5.374	1,424.579	
-8.10		40.589		302.545				1,418.689
-8.10	2.90	43.306	134.480		-9.582	10.582	1,423.065	
-11.00		49.439		437.025				2,841.754
-11.00	1.60	49.439	81.810		-11.809	12.809	1,047.885	
-12.60		52.823		518.835				3,889.639
-12.60	4.90	52.823	284.225		-15.123	16.123	4,582.540	
-17.50		63.187		803.060				8,472.179
-17.50	5.10	141.100	801.542		-20.137	21.137	16,942.090	
-22.60		173.230		1,604.601				25,414.269
-22.60	1.90	173.230	340.509		-23.561	24.561	8,363.085	
-24.50		185.200		1,945.110				33,777.354
-24.50	0.64	10.100	6.464		-24.820	25.820	166.900	
-25.14		10.100		1,951.574				33,944.254
-25.14	24.86	10.100	2630.810		-41.318	42.318	111,330.310	
-50.00		201.550		4,582.383				145,274.564

Note: The arm length l_{pa+pw} in the above table is the distance from the point where dynamic water pressure resultant force S_{pa+pw} acts on the tie wire installation point. When the dynamic water service position is higher than the installation point, the arm length is expressed with a "-."

b) Calculation of the resisting moment of the passive earth pressure on the tie wire installation point

Table 5.3.7 shows the calculation results for the resisting moment of the passive earth pressure on the tie wire installation point.

Table 5.3.7 Calculation results for the resisting moment of the passive earth pressure on the tie wire installation point

Location of tie wire installation point: +1.00 m								
Elevation	Layer thickness h (m)	P_p KN/m ²	Horizontal force S_p KN/m	ΣS_p KN/m ²	Service position	Arm length ℓ_p (m)	Moment M_p KN·m/m	ΣM_p KN·m/m
-12.60	4.90	0.000	907.974		-15.867	16.867	15,314.498	
-17.50		370.602		907.974				15,314.498
-17.50	5.10	169.000	943.832		-20.124	21.124	19,937.295	
-22.60		201.130		1,851.806				35,251.792
-22.60	1.90	201.130	393.519		-23.559	24.559	9,664.480	
-24.50		213.100		2,245.324				44,916.273
-24.50	0.64	393.100	253.162		-24.821	25.821	6,536.801	
-25.14		398.030		2,498.486				51,453.073
-25.14	24.86	398.030	12,274.376		-38.373	39.373	483,281.140	
-50.00		589.450		14,772.862				534,734.214

Note: The arm length ℓ_p in the above table is the distance from the point where dynamic water pressure resultant force S_p acts on the tie wire installation point. When the dynamic water service position is higher than the installation point, the arm length is expressed with a "-".

Figure 5.3.13 shows the calculation results from Tables 5.3.6 and 5.3.7.

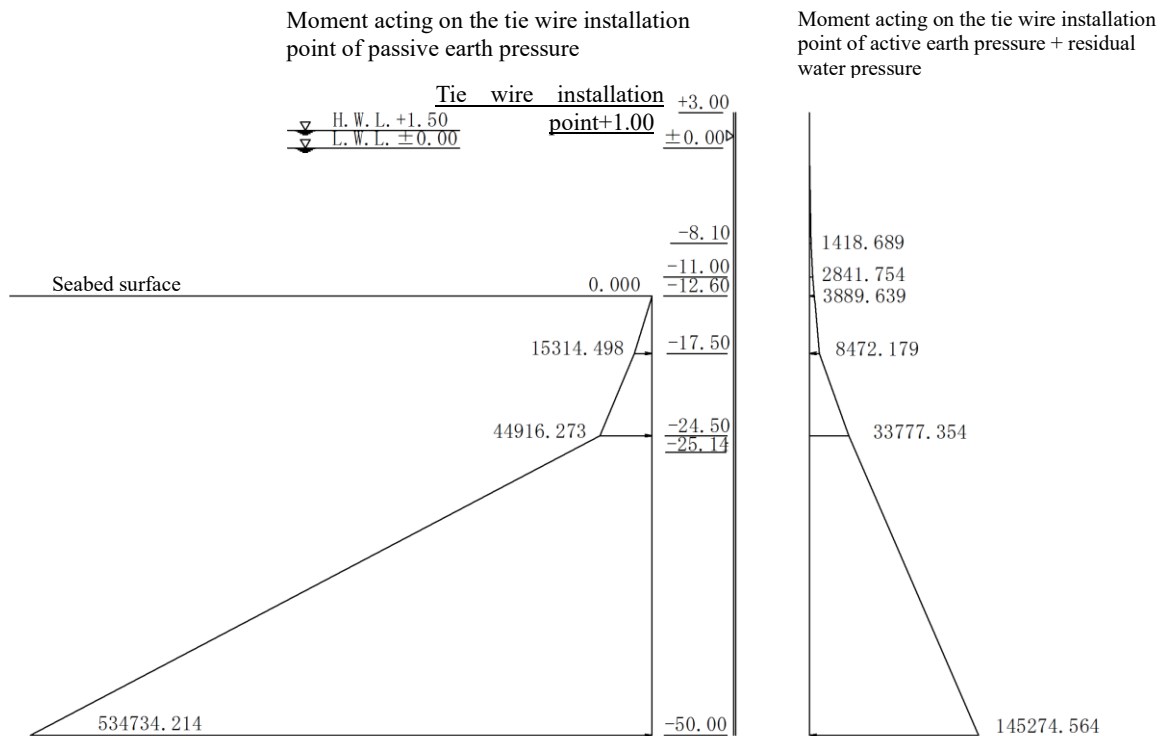


Figure 5.3.13 Moment distribution due to active earth pressure, residual water pressure and passive earth pressure (verification of the embedded length of sheet pile)

c) Verification of the embedded length

Table 5.3.8 shows the verification results for the embedded length. The partial factors related to the embedded length of sheet piles (γ_R and γ_S) shall be 0.77 and 1.11, respectively, since cohesive soil is partly

included in the soil composition from the ground surface to the bottom of the embedded length. The adjustment factor (m) shall be 1.00.

Table 5.3.8 Verification results for embedded length

Elevation	Passive side			Active side			Performance verification	Judgment
	R_k KN·m/m	γ_R	$R_k \cdot \gamma_R$ KN·m/m	S_k KN·m/m	γ_s	$S_k \cdot \gamma_s$ KN·m/m	$m \cdot S_d/R_d$ $= 1.00 \cdot S_d/R_d$	
-12.60								
-17.50	15,314.498	0.77	11,792.163	8,472.179	1.11	9,404.118	0.797	OK
-17.50								
-22.60	35,251.792	0.77	27,143.880	25,414.269	1.11	28,209.838	1.039	OUT
-22.60								
-24.50	44,916.273	0.77	34,585.530	33,777.354	1.11	37,492.862	1.084	OUT
-24.50								
-25.14	51,453.073	0.77	39,618.866	33,944.254	1.11	37,678.122	0.951	OK
-25.14								
-50.00	534,734.214	0.77	411,745.345	145,274.564	1.11	161,254.766	0.392	OK

The above calculation therefore shows that the required embedded length for a sheet-pile wall is in the range from -24.5 to -25.14 m.

Then, performance verification will be conducted with the bottom of embedded length being -24.9 m, and the verification result is shown below:

Verification result : $m \cdot S_d/R_d \leq 1.0$

The required embedded length bottom of the sheet-pile wall using the free earth support method is -24.90 m.

Tables 5.3.9 and 5.3.10 show the verification details when the bottom of embedded length is set to -24.90 m.

Table 5.3.9 Calculation of the service moment of the active earth pressure and residual water pressure on the tie wire installation point

Location of tie wire installation point: +1.00 m

Elevation	Layer thickness h (m)	①+② P_a+P_w KN/m ²	Horizontal force S_{pa+pw} KN/m		Arm length l_{pa+pw} (m)	Moment $S_k=M_{pw}+M_{pw}$ KN·m/m	$\Sigma S_k=$ $\Sigma (M_{pa}+M_{pw})$ KN·m/m	Partial factor γ_s	$S_d=S_k \cdot \gamma_s$ KN·m/m
+3.00 ~ -24.50	27.50						33,777.354		
-24.50	0.40	10.100	4.040	-24.700	25.700	103.828			
-24.90		10.100					33,881.182	1.11	37,608.112
-24.90	0.24	10.100	2.424	-25.020	26.020	63.072	33,944.254		
-25.14		10.100							

Table 5.3.10 Calculation of the resisting moment of the passive earth pressure on the tie wire installation point

Location of tie wire installation point: +1.00 m									
Elevation	Layer thickness h (m)	P_p KN/m ²	Horizontal force S_p KN/m	Acting position	Arm length ℓ_p (m)	Moment $R_k=M_p$ KN·m/m	$\Sigma R_k=\Sigma M_p$ KN·m/m	Partial factor γ_R	$R_d=R_k \cdot \gamma_R$ KN·m/m
+3.00	27.50								
-24.50							44,916.273		
-24.50	0.40	393.100	157.856	-24.700	25.700	4,056.940	48,973.213	0.77	37,709.374
-24.90		396.180							
-24.90	0.24	396.180	95.305	-25.020	26.020	2,479.850	51,453.073		
-25.14		398.030							

Shown below are the verification results when the bottom of the embedded length of sheet pile is set to -24.90 m, based on the calculation results in **Tables 5.3.9** and **5.3.10**:

Active-side service moment S_d : 37,608.112 (kN·m/m)

Passive-side resisting moment R_d : 37,709.374 (kN·m/m)

$$m \cdot S_d/R_d = 1.0 \times (37,608.112/37,709.374) = 0.997 \leq 1.0$$

Therefore, -24.90 m is given as the required embedded length of sheet pile using the free earth support method.

- Verification of the embedded length of sheet pile using Rowe's method

The following is verification of the embedded length of the sheet-pile wall using Rowe's method.

$$\delta_s = D_F/H_T \geq 4.9510 \times \omega^{-0.2} - 0.2486 \quad (10)$$

Where:

δ_s : ratio of the embedded length of sheet pile to the height from the tie wire installation point to the seabed surface (permanent situation)

D_F : embedded length of sheet pile (m)

H_T : Height from the tie wire installation point to the seabed surface (m)

ω : similarity number ($\rho \times \ell_h$)

ρ : flexibility number (H_T^4/EI) (m³/MN)

E : young's modulus of sheet pile (MN/m²)

I : geometrical moment of inertia per unit width of sheet pile (m⁴/m)

ℓ_h : modulus of the subgrade reaction of sheet-pile wall (MN/m³)

a) Structural details

Table 5.3.11 shows the specifications of steel pipe sheet-pile wall.

Table 5.3.11 Specifications of steel pipe sheet-pile wall (permanent situation)

	Unit	
Type of sheet pile		φ1,100×t22
Young's modulus (E)	MN/m ²	2.00E+05
Geometrical moment of inertia of cross-section (I)	m ⁴ /m	9.1906E-03
Embedded length of sheet pile (D_f) (free earth support method)	m	12.30
Sheet-pile wall height (H_f)	m	13.60
Average N -value of ground under seabed surface		21

- Modulus of the subgrade reaction of sheet-pile wall (ℓ_h)

Since ground improvement is not conducted on the sea side of the quaywall, determine the modulus of the subgrade reaction ℓ_h based on the soil specifications of the original ground.

Also, since the average N -value from the seabed surface -12.6 m to -17.5 m is 21, using **Figure 5.3.14**, ℓ_h should have a value of 28.0 MN/m³.

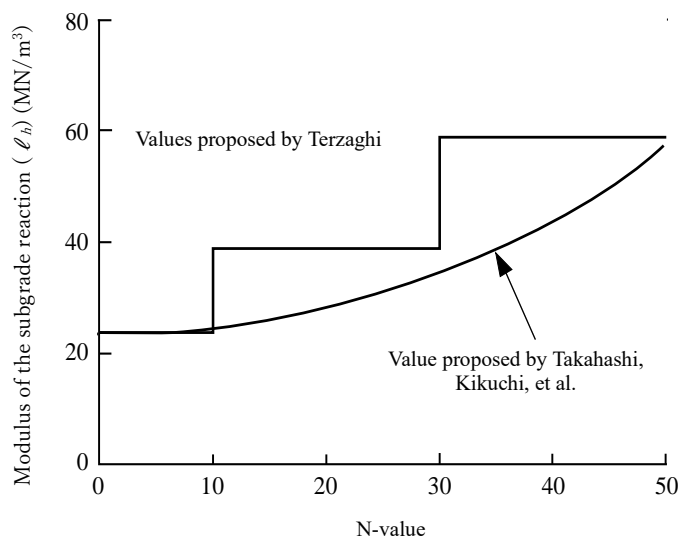


Figure 5.3.14 Relationship between modulus of the subgrade reaction (ℓ_h) and N -value

- Calculation of δ_N , ρ , and ω

Table 5.3.12 shows the calculation results for δ_N , ρ , and ω .

Table 5.3.12 Calculation results for δ_N , ρ , and ω

	Unit	
Type of sheet pile		φ1,100×t22
Young's modulus (E)	MN/m ²	2.00E+05
Geometrical moment of inertia of cross-section (I)	m ⁴ /m	9.1906E-03
Sectional rigidity (EI)	MN · m ² /m	1.8381E+03
Embedded length of sheet pile (D_F) (free earth support method)	m	12.30
Sheet-pile wall height (H_T)	m	13.60
$\delta_N = D_F / H_T$		0.904
$\rho = H_T^4 / EI$	m ³ /MN	18.612
ℓ_h	MN/m ³	28
$\omega = \rho \times \ell_h$		521.136

d) Verification of the embedded length of sheet pile using Rowe's method

Calculate the required embedded length using **Eq. (10)** as follows:

$$\delta_N = D_F / H_T = 0.904 < 4.9510 \times (521.136)^{-0.2} - 0.2486 = 4.9510 \times 521.136^{-0.2} - 0.2486 = 1.168$$

The above calculation shows that the embedded length by the free earth support method does not satisfy the requirement when verified using Rowe's method.

Therefore, calculate the corrected embedded length with Rowe's method.

$$D_F = H_T \times 1.168 = 13.60 \times 1.168 = 15.89 \text{ m}$$

Bottom of the embedded length of sheet pile:

$$-12.60 - 15.89 = -28.49 \text{ m} \Rightarrow -28.90 \text{ m (Rowe's method)}$$

As shown above, the height of the bottom of the required embedded length of the sheet-pile wall in the permanent situation is thus -28.90 m.

2) Stress verification of sheet-pile wall

i) Calculation of earth pressure and residual water pressure acting on the sheet-pile wall

Table 5.3.13 shows the calculation results for the active earth pressure and residual water pressure in the permanent situation.

The calculation results of **Table 5.3.13** are shown in **Figure 5.3.15**.

Table 5.3.13 Calculation results for the active earth pressure and residual water pressure (permanent situation; for sheet-pile stress verification)

Elevation	Characteristic value				Layer thickness h (m)	w·h KN/m ²	Σwh+ω KN/m ²	ka·cos δ	Surcharge ω = 30.00 (KN/m ²)		
	w KN/m ³	φ (°)	δ (°)	c KN/m ²					⊕ Earth pressure intensity Pa KN/m ²	⊖ Residual water pressure Pw KN/m ²	Ⓛ+Ⓜ Pa+Pw KN/m ²
+3.00							30.00	0.1942	5.826		5.826
+1.50	18.00	40.0	15.0		1.50	27.00	57.00	0.1942	11.069		11.069
+1.50							57.00	0.1942	11.069		11.069
+1.00	18.00	40.0	15.0		0.50	9.00	66.00	0.1942	12.817	0.000	12.817
+1.00							66.00	0.1942	12.817	0.000	12.817
+0.50	10.00	40.0	15.0		0.50	5.00	71.00	0.1942	13.788	5.050	18.838
+0.50							71.00	0.1942	13.788	5.050	18.838
+0.00	10.00	40.0	15.0		0.50	5.00	76.00	0.1942	14.759	10.100	24.859
+0.00							76.00	0.1942	14.759	10.100	24.859
-8.10	10.00	40.0	15.0		8.10	81.00	157.00	0.1942	30.489	10.100	40.589
-8.10							157.00	0.2115	33.206	10.100	43.306
-11.00	10.00	38.0	15.0		2.90	29.00	186.00	0.2115	39.339	10.100	49.439
-11.00							186.00	0.2115	39.339	10.100	49.439
-12.60	10.00	38.0	15.0		1.60	16.00	202.00	0.2115	42.723	10.100	52.823

Distribution of the active earth pressure and residual water pressure in the permanent situation

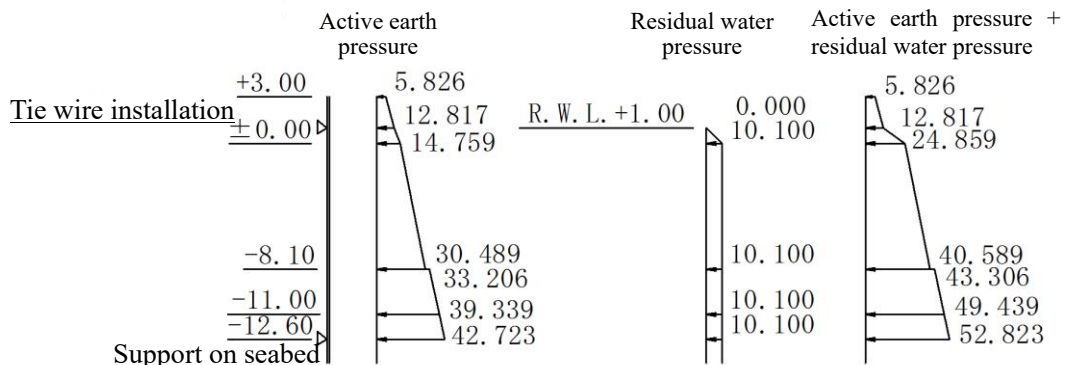


Figure 5.3.15 Distribution of the active earth pressure, residual water pressure and passive earth pressure (permanent situation; for sheet-pile stress verification)

ii) Calculation of the maximum flexural moment occurring in the quaywall sheet-pile wall and the reaction force generated at the tie wire installation point

Calculate the flexural moment acting on the sheet-pile wall and the reaction at the tie wire installation point assuming that the tie wire installation point and the seabed surface serve as the support, and that this system is a simple beam with the earth pressure above the seabed surface and the residual water pressure acting on the beam.

a) Specifications of the structural model

- Crown height of quaywall: +3.00 m
- Tie wire installation height: +1.00 m
- Support on the seabed surface: -12.60 m

The calculation model is shown in **Figure 5.3.16**.

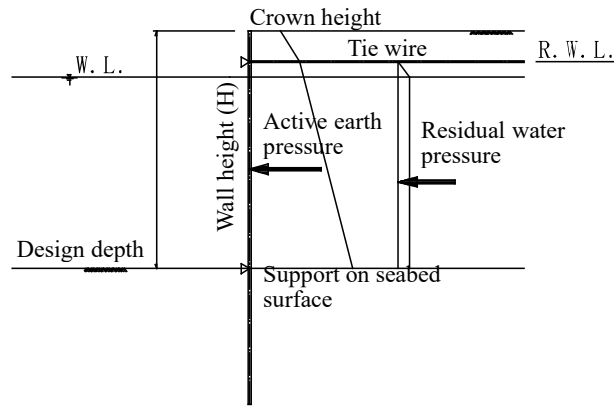


Figure 5.3.16 Calculation model (permanent situation)

b) Calculation of the flexural moment related to the tie wire installation point (permanent situation)

Table 5.3. 14 shows the calculation results for the flexural moment related to the tie wire installation point.

Table 5.3. 14 Calculation results for the flexural moment related to the tie wire installation point

Height of tie wire installation point

Elevation	Location of tie wire installation	Support interval (m)	Active side	
			$\sum S_a$ KN/m	$\sum M_a$ KN · m/m
+3.00 ~ -12.60	+1.00	13.60	518.836	3,890

c) Calculation result for the reaction at the tie wire installation point

Reaction at the support on the seabed surface: R_0

$$R_0 = \sum M_a \div \ell = 3,889.633 \div 13.60 = 286.002 \text{ kN/m}$$

Reaction at the tie wire installation point: A_P

$$A_P = \sum S_a - R_0 = 518.836 - 286.002 = 232.834 \text{ kN/m}$$

d) Calculation of the maximum flexural moment at the sheet-pile wall

The maximum flexural moment acting on the sheet-pile wall occurs at a location where shear force Q is zero. The shear force is calculated using $Q = A_P - \sum S_{Pa+Pw}$, giving the position of $Q = \text{zero}$ as -6.305 m

The calculation results are shown in **Table 5.3.15**.

Table 5.3.15 Calculation results for shear force $Q = 0$

Elevation	Layer thickness h (m)	A_p KN/m	①+② P_a+P_w KN/m ²	S_{pa+pw} KN/m	ΣS_{pa+pw}	Q KN/m
+3.000 ~ +0.000	3.000					
+0.000		232.834			37.482	195.35
+0.000 -6.305	6.305	232.834	24.859			
-6.305		232.834	37.103	195.352		
-6.305 -8.100	1.795	232.834	37.103		232.834	0.00
-8.100		232.834	40.589	69.729		
					302.563	-69.73

The flexural moment related to the position of $Q = 0$ for the earth pressure and residual water pressure from the breakwater top, or +3.00 m, to -6.305 m, is calculated as in **Table 5.3.16**.

Table 5.3.16 Calculation results for the flexural moment (permanent situation)

Height of tie wire installation point: +1.00m

Elevation	Layer thickness h (m)	①+② P_a+P_w KN/m ²	Horizontal force S_{pa+pw} KN/m	Moment M_a KN · m/m
+3.000		5.826		
-6.305	9.305	37.103	-232.834	-854.942

The calculation shown in **Table 5.3.16** gives the flexural moment at the position in the sheet-pile wall with shear force $Q = 0$ (-6.305 m) as follows:

Distance from the tie wire installation point to the zero shear-force point

$$h = 1.000 - (-6.305) = 7.305 \text{ m}$$

Maximum flexural moment

$$M_{a(Q=0)} = \Sigma M_a = A_p \times h - \Sigma M = 232.834 \times 7.305 - 854.942 = 845.910 \text{ k N} \cdot \text{m/m}$$

e) Correction of the maximum flexural moment and reaction force at the tie wire installation point using Rowe's method

Figure 5.3.17 and **Table 5.3.17** show the calculation results for the maximum flexural moment and the reaction at the tie wire installation point using the virtual beam method.

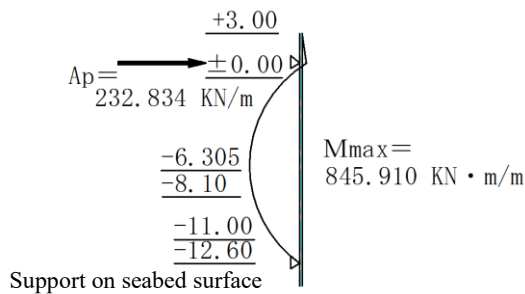


Figure 5.3.17 Maximum moment (permanent situation)

Table 5.3.17 Maximum flexural moment and reaction force at the tie wire installation point

	Sign	Unit	Permanent situation
Maximum flexural moment	M_{max}	KN · m/m	845.910
Location of occurrence		DL.m	-6.305
Reaction force at tie wire installation point	A_p	KN/m	232.834

Given the above results, the maximum flexural moment and the reaction force at the tie wire installation point are corrected using **Eq. (11)** and **Eq. (12)** as follows:

Permanent situation, correction of the maximum flexural moment

$$\mu_N = M_F / M_T = 3.8625 \times \omega^{-0.2} + 0.2255 \quad (11)$$

Permanent situation, correction of the reaction force at the tie wire installation point

$$\tau_N = T_F / T_T = 1.8259 \times \omega^{-0.2} + 0.6232 \quad (12)$$

Where:

μ_N : correction factor for the maximum moment (permanent situation)

M_F : maximum flexural moment after correction

M_T : maximum flexural moment before correction

τ_N : correction factor for the reaction force at the installation point (permanent situation)

T_F : reaction force at the installation point after correction

T_T : reaction force at the installation point before correction

ω : similarity number ($\rho \times \ell_h$)

$$\omega = 521.136$$

The correction results are given as follows:

Correction factor for maximum moment: $\mu_N = 1.3308$

$$M_F = 1.3308 \times 845.910 = 1,125.737 \text{ kN}\cdot\text{m/m}$$

Correction factor for the reaction force at the installation point: $\tau_N = 1.1457$

$$T_F = 1.1457 \times 232.834 = 266.758 \text{ kN/m}$$

The above corrected values will be used to verify the sheet-pile stress intensity, the tensile stress intensity of tie wires, the stress intensity of waling, and the anchorage.

iii) Verification of stress intensity of sheet piles

a) Cross-sectional performance of sheet piles

Verify the stress intensity of a steel-pipe sheet pile shown in **Table 5.3.18** as follows:

Table 5.3.18 Specifications of steel-pipe sheet pile

	Unit		Remarks
Type of sheet pile		φ1,100×t22	
Material		SKY490	
Section modulus (Z _o)	cm ³ /m	16,710	Before corrosion
Section modulus (Z)	cm ³ /m	16,011	After corrosion
Bending yield stress of steel (σ _{yc})	N/mm ²	315.0	

Corrosion allowance for steel-pipe sheet pile (corrosion rate μ : 90%)

$$1 - \mu = 0.1$$

$$\text{Sea side: } t_1 = 0.100 \text{ mm/year} \times 0.1 \times 50 \text{ years} = 0.50 \text{ mm}$$

$$\text{Land side: } t_2 = 0.020 \text{ mm/year} \times 50 \text{ years} = 1.00 \text{ mm}$$

The cross-sectional performance of a steel-pipe sheet pile after corrosion as shown above is the result of calculations done with 0.75 mm given as the average corrosion allowance.

b) Verification of stress intensity of sheet piles

Verify the bending stress intensity of a sheet using the following equation:

$$m \cdot \frac{S_d}{R_d} \leq 1.0, \quad R_d = \gamma_R R_k, \quad S_d = \gamma_s S_k$$

$$R_k = \sigma_{yk}$$

$$S_k = \frac{M_{max k}}{Z}$$

Where:

σ_y : bending yield stress of steel (N/mm²)

M_{max} : maximum flexural moment occurring in the sheet-pile wall (N•mm/m)

Z : section modulus of steel (mm³/m)

γ_R : partial factor by which the resistance term is multiplied (0.84)

γ_s : partial factor by which the load term is multiplied (1.18)

m : adjustment factor (1.00)

The verification result for bending stress intensity of a sheet pile is shown below:

$$m \cdot \frac{S_d}{R_d} = m \times \frac{\gamma_s S_k}{\gamma_R R_k} = 1.00 \times \frac{1.18 \times 1,125.737 \times 10^6 / (16,011 \times 10^3)}{0.84 \times 315.0} = 0.314 \leq 1.0$$

iv) Verification of the tensile load on tie wires

a) Tie wire specifications

Verify the tensile load for a tie wire shown in **Table 5.3.19** as follows:

Table 5.3.19 Specifications of tie wire

Tie wire		Taiburu	
Name		F270T	
Sectional area (A)	mm ² /pcs	1,409.6	
Diameter (φ)	mm	75.5	
Installation interval (L)	m	2.356	
Tilt angle of tie wire (θ)	°	0.00	
Yield-point load on tie wire (T _{yd})	KN	1,748.0	

b) Calculation of tie wire tension

Calculate the tie wire tension T_d using the following equation:

$$T_k = A_{pk} \times L \times \sec(\theta)$$

Where:

T_k : tension acting on the tie wire (kN/pcs)

A_{pk} : sheet-pile reaction force at the tie wire installation point (kN/m)

$A_{pk} = 266.758$ kN/m

L : tie wire installation spacing (m)

θ : tilt angle of tie wire (°)

The calculation result for tie wire tension T is shown as follows:

$$T_d = 266.758 \times 2.356 \times \sec(0.0^\circ) = 628.482 \text{ kN/pcs}$$

c) Verification of the tensile load on tie wires

Verify the tie wire tensile load using the following equation:

$$m \cdot \frac{S_d}{R_d} \leq 1.0, \quad R_d = \gamma_R R_k, \quad S_d = \gamma_s S_k$$

$$R_k = T_{yk}$$

$$S_k = T_k \quad (13)$$

Where:

T_y : tie wire yield-point load (kN)

T : tie wire tensile load (kN)

γ_R : partial factor by which the resistance term is multiplied (0.64)

γ_s : partial factor by which the load term is multiplied (1.29)

m : adjustment factor (1.00)

The verification results for the tie wire tensile load are then given as follows:

$$m \cdot \frac{S_d}{R_d} = m \times \frac{\gamma_s S_k}{\gamma_R R_k} = 1.00 \times \frac{1.29 \times 628.482}{0.64 \times 1,748.0} = 0.720 < 1.0$$

v) Verification of the stress intensity of waling

a) Waling specifications

Verify the stress intensity for a channel section shown in **Table 5.3.20** as follows:

Table 5.3.20 Waling specifications

	Unit	
Type of waling (channel steel)		2[-380 × 100 × 10.5 × 16.0
Material		SS400
Section modulus (Z) (after corrosion)	cm ³	763.0
Bending yield stress of steel (σ _y)	N/mm ²	235.0
Tie wire installation interval (L)	m	2.356
	KN	628.482

b) Calculation of the maximum flexural moment

Calculate the maximum flexural moment acting on waling $M_{max k}$ using the following equation:

$$M_{max k} = T_k \times L/10$$

Where:

T_k : tie wire tension (kN)

L : tie wire installation spacing (m)

The calculation results for the maximum flexural moment acting on waling $M_{max k}$ are shown below:

$$M_{max k} = 628.482 \times 2.356 \div 10 = 148.070 \text{ kN}\cdot\text{m}$$

c) Verification of the stress intensity of waling

Verify the bending stress intensity of waling using the following equation:

$$m \cdot \frac{S_d}{R_d} \leq 1.0, \quad R_d = \gamma_R R_k, \quad S_d = \gamma_s S_k$$

$$R_k = \sigma_{yk}$$

$$S_k = \frac{M_{max k}}{Z}$$

Where:

σ_y : bending yield stress of waling (N/mm²)

M_{max} : maximum flexural moment acting on waling (N•mm/m)

Z : section modulus of waling (mm³)

γ_R : partial factor by which the resistance term is multiplied (1.00)

γ_s : partial factor by which the load term is multiplied (1.00)

m : adjustment factor (1.67)

The verification result of bending stress intensity of waling (channel section) is shown below:

$$m \cdot \frac{S_d}{R_d} = m \times \frac{\gamma_s S_k}{\gamma_R R_k} = 1.67 \times \frac{1.00 \times 148.070 \times 106 / (2 \times 763.0 \times 10^3)}{1.00 \times 235.0} = 0.690 < 1.0$$

3) Verification of the stress intensity of anchorage in the permanent situation

i) Anchorage specifications

Table 5.3.21 shows the anchorage specifications and the tie wire tension.

Table 5.3.21 Anchorage specifications and tie wire tension

	Unit		
Anchorage crown height	m	+2.00	
Tie wire installation height	m	+1.00	
Type of anchorage (steel-pipe pile)		φ1,000×t11	
Effective width of anchorage (<i>B</i>)	mm	1,000	
Material		SKK490	
Young's modulus (<i>E</i>)	KN/m ²	200.0	
Geometrical moment of inertia (<i>I_o</i>)	cm ⁴	417,922	Before corrosion
Geometrical moment of inertia (<i>I</i>)	cm ⁴	378,770	After corrosion
Section modulus (<i>Z_o</i>)	cm ³	8,358.0	Before corrosion
Section modulus (<i>Z</i>)	cm ³	7,591.0	After corrosion
Tie wire tension (<i>T</i>)	KN	628.482	

Note: Corrosion allowance for steel-pipe pile
 $t = 1 \times 0.020 \text{ mm/year} \times 50 \text{ years} = 1.00 \text{ mm}$

ii) Lateral resistance constant k_c

The soil condition where anchor piles are installed is filling soil (after ground improvement), and the N -value is considered to be constant in the depth direction. Therefore, it is taken as C-type ground.

Average N -value: 26 (after ground improvement)

Calculate the lateral resistance constant using **Figure. 5.3.18**.

$$k_c = 540N^{0.648} = 540 \times 26^{0.648} = 4,460.0 \text{ kN/m}^{2.5}$$

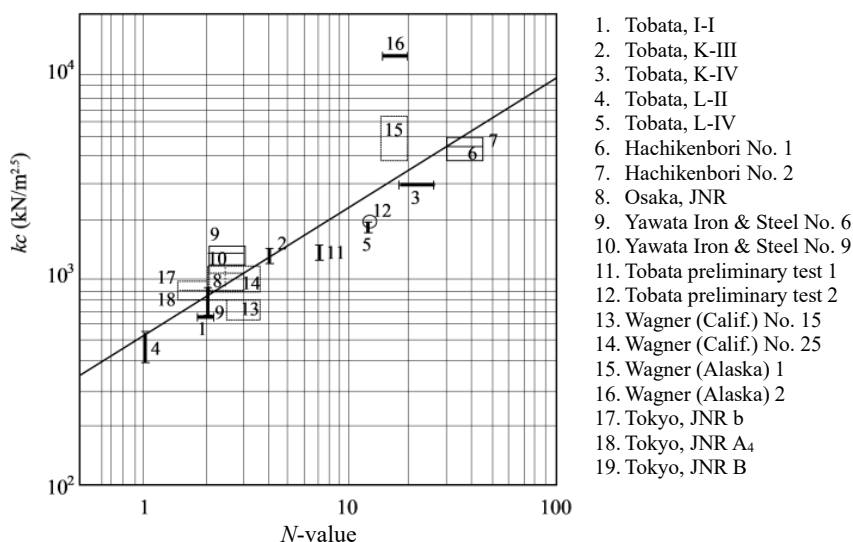


Figure. 5.3.18 Relationship between N -value and k_c

iii) Calculation results for the maximum flexural moment, pile cap displacement, and embedded length

The maximum flexural moment, pile cap displacement, and embedded length calculated using the "Koken Method (PHRI Method)" are shown in **Table 5.3.22**.

Table 5.3.22 Calculation results for anchor pile design values (permanent situation)

	Symbol	After corrosion	Before corrosion	
Pile-cap displacement	Y_{top}	0.725	0.696	cm
Ground surface displacement	Y_o	0.725	0.696	cm
Pile-cap moment	M_{top}	0.000	0.000	KN · m
Maximum underground moment	M_{max}	610.923	622.555	KN · m
Depth of moment $M = 0$	ℓ_{ml}	6.733	6.861	m
Angle of deflection at pile cap	i_{top}	0.003	0.003	rad
Angle of deflection on ground surface	i_o	0.003	0.003	rad
$\ell_{ml}/3$		2.244	2.287	m
$1.5 \times \ell_{ml}$		10.100	10.292	m

iv) Verification of the bending stress intensity of anchor pile

Use the following equation to verify the stress of an anchor pile for the result after corrosion:

$$m \cdot \frac{S_d}{R_d} \leq 1.0, \quad R_d = \gamma_R R_k, \quad S_d = \gamma_s S_k$$

$$R_k = \sigma_{yk}$$

$$S_k = \frac{M_{max k}}{Z}$$

Where:

- σ_y : bending yield stress intensity of the anchor pile (N/mm²)
- M_{max} : maximum flexural moment acting on the anchor pile (N•mm/m)
- Z : section modulus of anchor pile (mm³/m)
- γ_R : partial factor by which the resistance term is multiplied (1.00)
- γ_s : partial factor by which the load term is multiplied (1.00)
- m : adjustment factor (1.67)

The verification result for bending stress intensity of an anchor pile is then given as follows:

$$m \cdot \frac{S_d}{R_d} = m \times \frac{\gamma_s S_k}{\gamma_R R_k} = 1.67 \times \frac{1.00 \times 610.923 \times 106 / (7,591 \times 10^3)}{1.00 \times 315.0} = 0.427 < 1.0$$

v) Depth of the bottom of an anchor pile

Calculate the depth of the bottom of an anchor pile using the pre-corrosion result, considering safety, as follows:

$$\begin{aligned} \text{Depth of the bottom of the anchor pile} &= \text{height of tie wire installation} - 1.5 \times \ell_{ml} \\ &= +1.00 - 10.292 = -9.292 \text{ m} \Rightarrow -9.50 \text{ m (permanent situation)} \end{aligned}$$

vi) Review of the anchorage installation position (permanent situation)

Place a vertical anchor pile at a location where the active failure plane of the front sheet pile drawn from the seabed surface does not intersect the passive failure plane of the anchorage drawn from the position of $\ell_{ml}/3$ down the anchorage-side tie wire installation point to the tie wire installation height.

- Foundation ground height (design height): -12.60 m

- Tie wire installation height (DL): +1.00 m
- Anchorage $\ell_{m1}/3$ position (DL): -1.287m
(+1.000 - 6.861/3 = -1.287 m)
- Front sheet-pile-side soil specification: See **Figure 5.3.19**.
- Anchorage-side soil specification: See **Figure 5.3.19**.

The anchorage installation position in the permanent situation is as follows:

An installation distance of 0.854 m + 1.548 m + 3.723 m + 0.873 m + 7.672 m = 14.670 m or more is required.

⇒ Use 19.50 m (although this depends on the variable situation result).

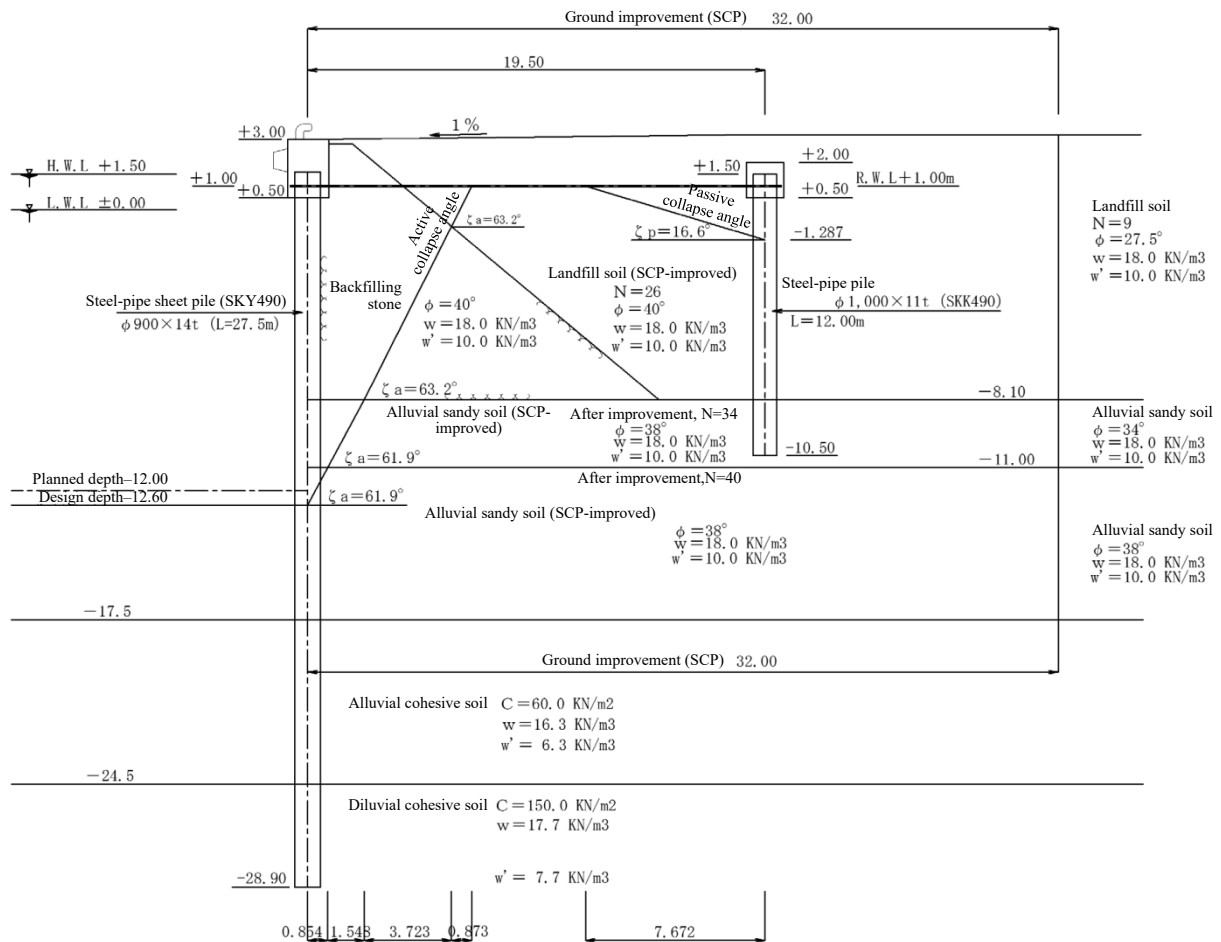


Figure 5.3.19 Anchorage installation position (permanent situation)

4) Performance verification related to circular slip failure of the foundation ground

i) Performance verification equation for circular slip failure

Verification related to circular slip failure of the foundation ground of the sheet-pile quaywall is performed for the permanent state. Verification is to be performed by the modified Fellenius' method, in which a slip circle is assumed.

$$m \cdot \frac{S_d}{R_d} \leq 1.0, \quad R_d = \gamma_R R_k, \quad S_d = \gamma_S S_k$$

$$R_k = \Sigma \{ [c' + (w'_k + q_k) \cos^2 \theta] \cdot \tan \phi' \cdot s \cdot \sec \theta \}$$

$$S_k = \Sigma [(w_k + q_k) \cdot \sin \theta]$$

Where,

S_k : characteristic value of load (acting moment) (kN · m/m)

R_k : characteristic value of load (resisting moment) (kN · m/m)

γ_S : partial factor multiplied with load term

γ_R : partial factor multiplied with resistance term

m : adjustment factor

c : in case of cohesive soil ground, the undrained shear strength, and in case of sandy soil, the apparent cohesion in the drained condition (kN/m²).

w' : effective weight of a slice (kN/m)

w : total weight of slices (kN/m)

ϕ' : apparent shear resistance angle based on effective stress (°)

s : width of slice (m)

q : surcharge acting on a slice (kN/m)

θ : angle formed by the bottom surface of a slice and the horizontal plane (°)

ii) Application of partial factor

The applicable types of ground and partial factors used in verification for circular slip failure are as follows.

Partial factors used in performance verification of foundation ground for circular slip failure

Failure mode	Coefficient of variation of cohesive soil for representative layer CV	Partial factor multiplied with resistance term γ_R	Partial factor multiplied with load term γ_S	Adjustment factor m
Circular slip failure of foundation ground (permanent situation)	In case cohesive soil does not exist in a layer through which the circle passes	0.83	1.01	
	<0.10	0.86	1.05	
	≥ 0.10 to <0.15	0.85	1.04	
	≥ 0.15 to <0.25	0.80	1.02	
	≥ 0.25	—	—	1.30

iii) Result of verification related to circular slip failure of the foundation ground

A circular slip failure diagram is shown in **Figure 5.3.20**.

The partial factor is verified with a coefficient of variation (CV) greater than 0.25, the load factor γ_s being

1.00, the resistance factor γ_R being 1.00, and the adjustment factor m being 1.30.

The verification results related to circular slip failure of the foundation ground of the sheet-pile quaywall are given as follows:

- Characteristic value of load (acting moment)

$$S_k = 118,087.781 \text{ (KN}\cdot\text{m/m)}$$

- Characteristic value of resistance (resisting moment)

$$R_k = 260,154.089 \text{ (KN}\cdot\text{m/m)}$$

$$m \cdot \frac{S_d}{R_d} = 1.30 \times \frac{1.00 \times 118,087.781}{1.00 \times 260,154.089} = 0.590 < 1.0$$

The stability verification gives a value of not more than 1.0, which therefore satisfies the performance requirement.

Block	Saturated weight W1 (KN/m ³)	Wet weight W2 (KN/m ³)	Weight in water W' (KN/m ³)	Angle of internal friction ϕ (°)	Standard cohesion Co (KN/m ²)	Cohesion gradient K	Cohesion reference height Yo (m)
1	20.0	18.0	10.0	40	0.0	0.0	0.0
2	20.0	18.0	10.0	40	0.0	0.0	0.0
3	20.0	18.0	10.0	38	0.0	0.0	0.0
4	20.0	18.0	10.0	38	0.0	0.0	0.0
5	20.0	18.0	10.0	38	0.0	0.0	0.0
6	16.3	16.3	6.3	0	60.0	0.0	0.0
7	17.7	17.7	7.7	0	150.0	0.0	0.0

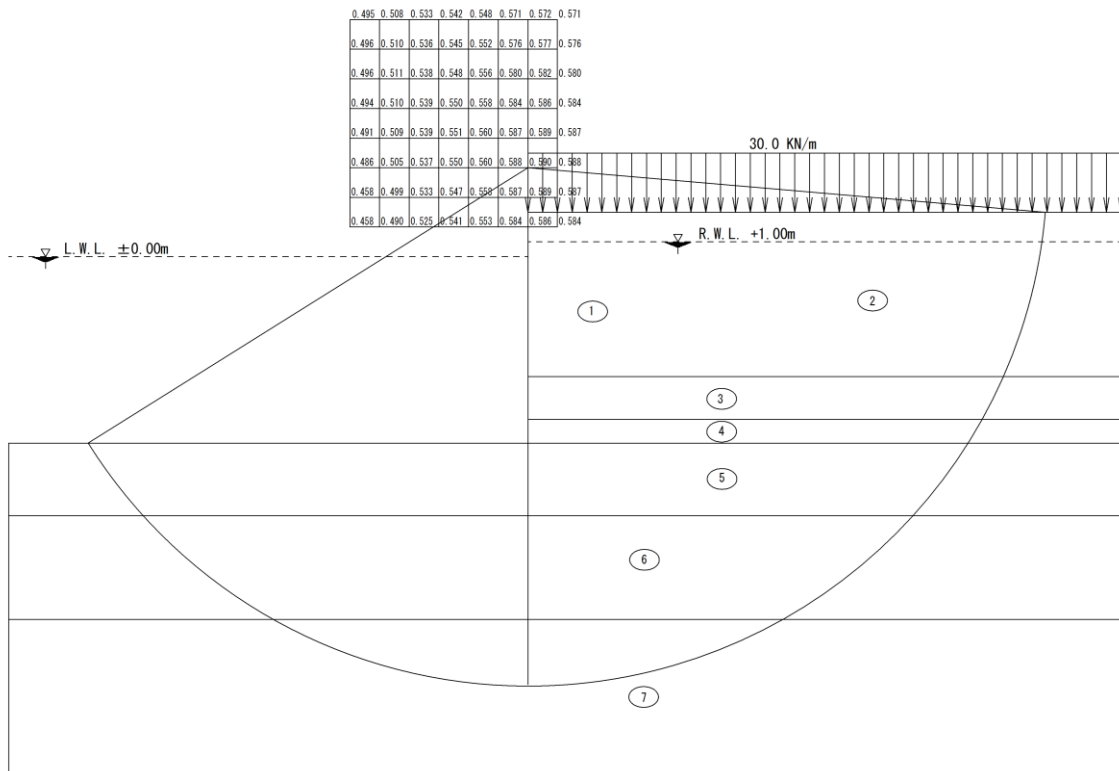


Figure 5.3.20 Verification results for circular slip failure

(6) Performance verification of sheet-pile wall in the variable situation related to Level 1 earthquake ground motion

1) Earth pressure and dynamic water pressure

Calculate the acting force and service moment caused by the dynamic water pressure on the tie wire installation point should be calculated as follows.

The dynamic water pressure distribution, dynamic water pressure service force, and service position are calculated as follows:

$$\text{Dynamic water pressure distribution: } p_{dw} = 7/8 \times k_h \times w_w \times (H \cdot y)^{1/2} \quad (14)$$

$$\text{Resultant force of dynamic water pressure: } P_{dw} = 7/12 \times k_h \times w_w \times H^2 \quad (15)$$

$$\text{Location where the resultant force acts: } h_{dw} = 3/5 \times H \quad (16)$$

Where:

p_{dw} : dynamic water pressure (kN/m²)

k_h : seismic coefficient for verification

w_w : unit weight of seawater (kN/m³)

H : water depth (m)

y : depth from the water surface to the location where the dynamic water pressure is calculated (m)

P_{dw} : resultant force of dynamic water pressure (kN/m)

h_{dw} : distance from the water surface to the location where the dynamic water pressure resultant force acts (m)

Table 5.3.23 shows the calculation results for the acting force and service moment on the tie wire installation point caused by the dynamic water pressure.

Seismic coefficient for verification: 0.14

Unit weight of seawater: 10.10 kN/m³

Location of tie wire installation point: +1.00 m

Table 5.3.23 Calculation results for dynamic water pressure, dynamic water pressure resultant force, and moment

Elevation	Dynamic water pressure P_{dw} KN/m ²	Active water pressure P_{dw} KN/m	Acting position m	Arm length ℓ_{dw} m	Moment M_{dw} KN·m/m
±0.00	0.000	0.000			
-1.00	4.392	2.928	-0.600	1.600	4.685
-2.00	6.211	8.281	-1.200	2.200	18.219
-3.00	7.607	15.214	-1.800	2.800	42.598
-4.00	8.784	23.423	-2.400	3.400	79.638
-5.00	9.820	32.735	-3.000	4.000	130.938
-6.00	10.758	43.031	-3.600	4.600	197.941
-7.00	11.620	54.225	-4.200	5.200	281.969
-8.00	12.422	66.250	-4.800	5.800	384.251
-9.00	13.175	79.052	-5.400	6.400	505.936
-10.00	13.888	92.587	-6.000	7.000	648.111
-11.00	14.566	106.817	-6.600	7.600	811.809
-12.00	15.214	121.709	-7.200	8.200	998.015
-12.60	15.589	130.951	-7.560	8.560	1,120.937

The arm length ℓ_{dw} in the above table is the distance from the point where dynamic water pressure resultant force P_{dw} acts on the tie wire installation point. When the dynamic water service position is higher than the installation point, the arm length is expressed with a "-."

Figure 5.3.21 shows the distribution of dynamic water pressure.

Distribution of dynamic water pressure

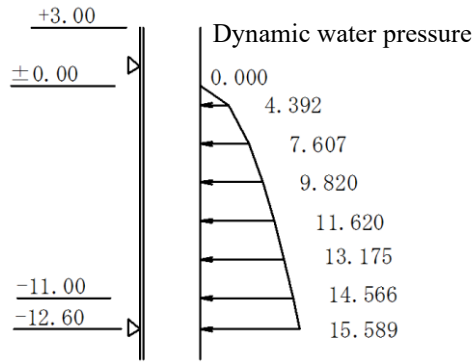


Figure 5.3.21 Distribution of dynamic water pressure

2) Verification of stress intensity of sheet piles

i) Cross-sectional performance of sheet piles

Verify the stress intensity of a steel-pipe sheet pile shown in **Table 5.3.24** as follows:

Table 5.3.24 Specifications of steel-pipe sheet pile

	Unit	Remarks	
Type of sheet pile		φ1,100×t22	
Material		SKY490	
Section modulus (Z_0)	cm ³ /m	16,710	Before corrosion
Section modulus (Z)	cm ³ /m	16,011	After corrosion
Bending yield stress of steel (σ_{yd})	N/mm ²	315.0	

ii) Verification of stress intensity of sheet pile

Verify the bending stress intensity of a sheet pile using the following equation:

$$m \cdot \frac{S_d}{R_d} \leq 1.0, \quad R_d = \gamma_R R_k, \quad S_d = \gamma_s S_k$$

$$R_k = \sigma_{yk}$$

$$S_k = \frac{M_{max k}}{Z}$$

Where:

σ_{yk} : bending yield stress intensity of steel (N/mm²)

$M_{max k}$: maximum flexural moment occurring in the sheet-pile wall (N•mm/m)

Z : section modulus of steel (mm³/m)

γ_R : partial factor by which the resistance term is multiplied (1.00)

γ_s : partial factor by which the load term is multiplied (1.00)

m : adjustment factor (1.12)

The verification result of bending stress intensity of a sheet pile is shown below:

$$m \cdot \frac{S_d}{R_d} = m \times \frac{\gamma_s S_k}{\gamma_R R_k} = 1.12 \times \frac{1.00 \times 1,964.871 \times 10^6 / 16,011 \times 10^3}{1.00 \times 315.0} = 0.436 \leq 1.0 \quad \text{OK}$$

3) Verification of the tensile load on tie wires

i) Tie wire specifications

Verify the tensile load for a tie wire shown in **Table 5.3.25** as follows:

Table 5.3.25 Tie-wire specifications

	Unit		Remarks
Tie wire		Taiburu	
Name		F270T	
Sectional area (A)		1,409.6	
Diameter (ϕ)	mm	75.5	
Installation interval (L)	m	2.356	
Tilt angle of tie wire (θ)	°	0.00	
Yield-point load on steel (T_{yd})	KN	1,748.0	

ii) Calculation of tie wire tension

Calculate tie wire tension T_d using the following equation:

$$T_d = A_{pd} \times L \times \sec(\theta)$$

Where:

T_d : tension service on the tie wire (kN/pcs)

A_{pd} : sheet-pile reaction force at the tie wire installation point (kN/m)

$A_{pd} = 410.890$ kN/m

L : tie wire installation spacing (m)

θ : tilt angle of the tie wire (°)

The calculation result for tie wire tension T is shown as follows:

$$T_d = 410.890 \times 2.356 \times \sec(0.0^\circ) = 967.890 \text{ kN/pcs}$$

iii) Verification of the tensile load on tie wires

Tie wire tensile load should be verified using the following equation:

$$m \cdot \frac{S_d}{R_d} \leq 1.0, \quad R_d = \gamma_R R_k, \quad S_d = \gamma_s S_k$$

$$R_k = T_{yk}$$

$$S_k = T_k \quad (17)$$

Where:

T_y : tie wire yield-point load (kN)

T : tensile load on tie wires (kN)

γ_R : partial factor by which the resistance term is multiplied (1.00)

γ_s : partial factor by which the load term is multiplied (1.00)

m : adjustment factor (1.67)

The verification results for tie wire tensile load are then given as follows:

$$m \cdot \frac{S_d}{R_d} = m \times \frac{\gamma_s S_k}{\gamma_R R_k} = 1.67 \times \frac{1.00 \times 967.890}{1.00 \times 1,748.0} = 0.925 \leq 1.0$$

4) Verification of the waling stress

i) Waling specifications

Verify the stress intensity for channel steel shown in **Table 5.3.26** as follows:

Table 5.3.26 Waling specifications

	Unit	
Type of waling (channel steel)		2[-380×100×10.5×16.0
Material		SS400
Section modulus (Z) (after corrosion)	cm ³	763.0
Bending yield stress of steel (σ _{yd})	N/mm ²	235.0
Tie wire installation interval (L)	m	2.356
Tie wire tension (T)	KN	967.89

ii) Calculation of the maximum flexural moment

Calculate the maximum flexural moment acting on waling M_{maxd} using the following equation:

$$M_{maxd} = T_d \times L/10$$

Where:

T_d : tie wire tension (kN)

L : tie wire installation spacing (m)

The calculation results for the maximum flexural moment acting on waling M_{maxd} are shown below:

$$M_{maxd} = 967.89 \times 2.356 \div 10 = 228.035 \text{ kN}\cdot\text{m}$$

iii) Verification of the stress intensity of waling

Verify the bending-stress intensity of waling using the following equation:

$$m \cdot \frac{S_d}{R_d} \leq 1.0, \quad R_d = \gamma_R R_k, \quad S_d = \gamma_s S_k$$

$$R_k = \sigma_{yk}$$

$$S_k = \frac{M_{maxk}}{Z}$$

Where:

σ_y : bending yield-stress intensity of waling (N/mm²)

M_{max} : maximum flexural moment acting on waling (N•mm/m)

Z : section modulus of waling (mm³)

γ_R : partial factor by which the resistance term is multiplied (1.00)

γ_s : partial factor by which the load term is multiplied (1.00)

m : adjustment factor (1.12)

The verification result for the bending-stress intensity of waling (channel steel) is shown below:

$$m \cdot \frac{S_d}{R_d} = m \times \frac{\gamma_s S_k}{\gamma_R R_k} = 1.12 \times \frac{1.00 \times 228.035 \times 10^6 / 2 \times 763.0 \times 10^3}{1.00 \times 235.0} = 0.712 \leq 1.0$$

5) Verification of the anchorage stress intensity

i) Anchorage specifications

Table 5.3.27 shows the anchorage specifications and tie wire tension.

Table 5.3.27 Anchorage specifications and tension
(Variable situation due to Level 1 earthquake ground motion)

	Unit		Remarks
Anchorage crown height	m	+2.00	
Tie wire installation height	m	+1.00	
Type of anchorage (steel-pipe pile)		φ1,000×t11	
Effective width of anchorage (<i>B</i>)	mm	1,000	
Material		SKK490	
Young's modulus (<i>E</i>)	KN/m ²	200.0	
Geometrical moment of inertia (<i>I_o</i>)	cm ⁴	417,922	Before corrosion
Geometrical moment of inertia (<i>I</i>)	cm ⁴	378,770	After corrosion
Section modulus (<i>Z_o</i>)	cm ³	8,358.0	Before corrosion
Section modulus (<i>Z</i>)	cm ³	7,591.0	After corrosion
Tie wire tension (<i>T</i>)	KN	967.89	

Note: Corrosion allowance for steel-pipe pile
 $t = 1 \times 0.020 \text{ mm/year} \times 50 \text{ years} = 1.00 \text{ mm}$

ii) Lateral resistance constant k_c

The soil condition where anchor piles are driven is filling soil (after ground improvement), and the *N*-value is considered to be constant in the depth direction. Therefore, it is taken as *C*-type ground.

Average *N*-value: 26 (after ground improvement)

Calculate the lateral resistance constant using **Figure 5.3.18**.

$$k_c = 540 N^{0.648} = 540 \times 26^{0.648} = 4,460.0 \text{ kN/m}^{2.5}$$

iii) Calculation results for maximum flexural moment, pile-cap displacement, and embedded length

The maximum flexural moment, pile cap displacement, and embedded length are calculated using the "Koken Method (PHRI Method)" as shown in **Table 5.3.28**.

Table 5.3.28 Calculation results for anchor-pile design values

	Sign	After corrosion	Before corrosion	
Pile-cap displacement	Y_{top}	1.448	1.389	cm
Ground-surface displacement	Y_o	1.448	1.389	cm
Pile cap moment	M_{top}	0.000	0.000	KN · m
Maximum underground moment	M_{max}	1,025.714	1,045.254	KN · m
Depth of moment $M = 0$	ℓ_{m1}	7.340	7.480	m
Angle of deflection at pile cap	i_{top}	0.005	0.005	rad
Angle of deflection on ground surface	i_o	0.005	0.005	rad
$\ell_{m1} / 3$		2.447	2.493	m
$1.5 \times \ell_{m1}$		11.010	11.220	m

iv) Verification of the bending stress intensity of anchor piles

Verify the stress of an anchor pile using the result after corrosion as follows:

$$m \cdot \frac{S_d}{R_d} \leq 1.0, \quad R_d = \gamma_R R_k, \quad S_d = \gamma_s S_k$$

$$R_k = \sigma_{yk}$$

$$S_k = \frac{M_{max\ k}}{Z}$$

Where:

σ_y : bending yield-stress intensity of the anchor pile (N/mm²)

M_{max} : maximum flexural moment acting on the anchor pile (N•mm/m)

Z : section modulus of the anchor pile (mm³/m)

γ_R : partial factor by which the resistance term is multiplied (1.00)

γ_s : partial factor by which the load term is multiplied (1.00)

m : adjustment factor (1.12)

The verification result for the bending-stress intensity of a sheet pile is shown below:

$$m \cdot \frac{S_d}{R_d} = m \times \frac{\gamma_s S_k}{\gamma_R R_k} = 1.12 \times \frac{1.00 \times 1,025.714 \times 10^6 / 7,591 \times 10^3}{1.00 \times 315.0} = 0.480 \leq 1.0$$

v) Height of the bottom of an anchor pile

Calculate the height of the bottom of an anchor pile using the pre-corrosion result, taking the dangerous side into consideration, as follows:

$$\begin{aligned} \text{Height of the bottom of the anchor pile} &= \text{height of tie wire installation} - 1.5 \times \ell_{m1} \\ &= +1.00 - 11.220 = -10.220 \Rightarrow -10.50 \text{ m} \end{aligned}$$

(Variable situation related to Level 1 earthquake ground motion)

As described above, in the variable situation due to Level 1 earthquake ground motion, the required bottom height of embedment for a vertical anchor pile is -10.50 m, and the bottom height of embedment for a vertical anchor pile thus takes the value of -10.50 (for the permanent situation, it is -9.50 m).

vi) Review of the anchorage installation position

A vertical anchor pile is placed at a location where the active failure plane of the front sheet pile drawn from the seabed surface does not intersect the passive failure plane of the anchorage drawn from the position of $\ell_{m1}/3$ down the anchorage-side tie wire installation point to the tie wire installation height.

- Foundation ground height (design height): -12.60 m
- Tie wire installation height (DL): $+1.000$ m
- Anchorage $\ell_{m1}/3$ position (DL): -1.493 m
($+1.000 - 7.480/3 = -1.493$ m)
- Front sheet-pile-side soil specification: See **Figure 5.3.19**.
- Anchorage-side soil specification: See **Figure 5.3.19**.

The anchorage installation distance in the variable situation is as follows:

An installation distance of $1.338\text{ m} + 2.374\text{ m} + 4.304\text{ m} + 2.455\text{ m} + 8.989\text{ m} = 19.460\text{ m}$ or more is required.
⇒ Ultimately, use 19.50 m.

(7) Verification for Level 2 earthquake ground motion

This section presents the results of a dynamic analysis of Level 2 earthquake ground motion. (The calculation method, parameter setting method, etc. are omitted.) The time-series horizontal displacement of the quaywall crown, the residual deformation diagram and the distribution of excessive pore water pressure after earthquake excitation are shown in **Figure 5.3.22** to **Figure 5.3.24**, respectively, and the results of verification of the section force of structural members (sheet piles, anchor piles, tie wires) are shown in **Table 5.3.29**.

The results of the verification of deformation satisfied the performance requirement as the residual deformation of the quaywall crown (= 98.0 cm) was held to not more than the allowable displacement of 100 cm. The results for the section force of the structural members also confirmed that the damage of the sheet piles and anchor piles was within the limit curvature, and because the generated tensile load of the tie wires did not exceed the yield point load, it was also possible to confirm that these members satisfy the performance criterion in the accidental situation for Level 2 earthquake ground motion.

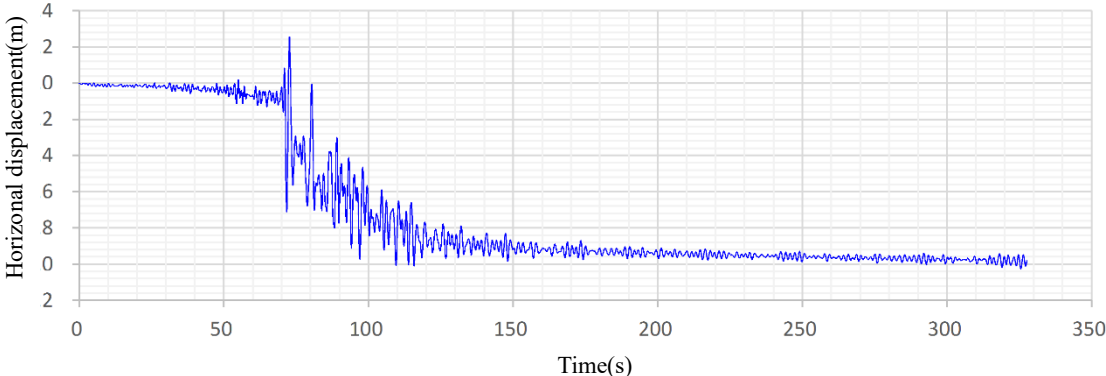


**Figure 5.3.22 Time-series horizontal displacement at quaywall crown
(Level 2 earthquake ground motion)**



Figure 5.3.23 Residual deformation diagram (Level 2 earthquake ground motion)

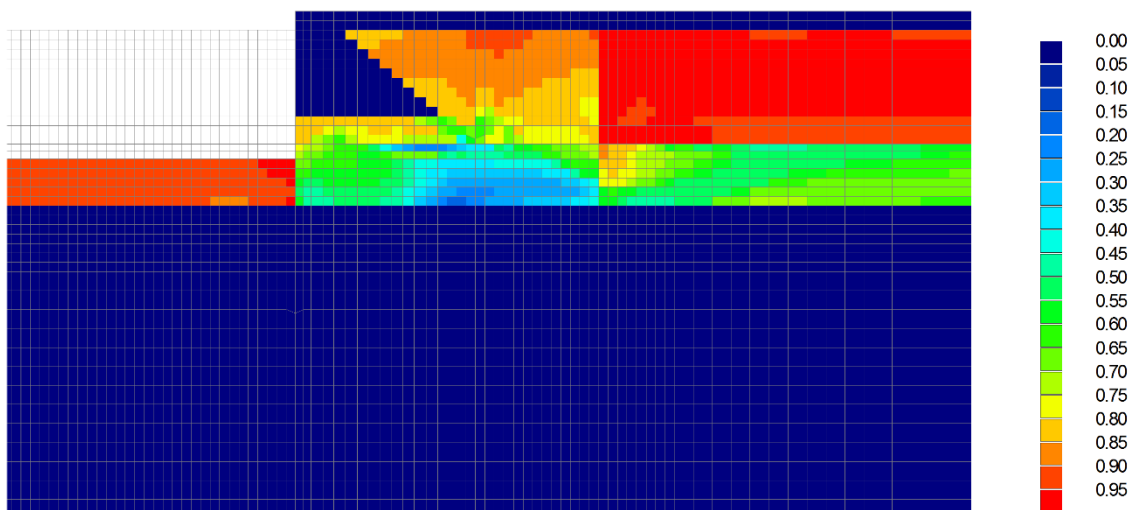


Figure 5.3.24 Distribution of excessive pore water pressure (Level 2 earthquake ground motion)

Table 5.3.29 Results of verification of section force (Level 2 earthquake ground motion)

	Maximum generation curve rate (1/m)	Limit curve rate (1/m)	Judgement
Steel pipe sheet pile (SKY490) t=22	0.0025	0.0142	OK
Anchor pile (SKK490) t=11	0.0032	0.0046	OK

	Maximum generation tensile strength(kN)	Yield load (kN)	Judgement
Tie wire (F270T)	465	1,748	OK

(8) Performance verification of tie wires and waling in the variable situation related to action by a vessel

As specified in **Figure 5.3.5**, "stress occurring in a tie wire" and "stress occurring in waling" are verified

as follows:

1) Verification of the tensile load on tie wires

i) Tie wire specifications

Verify the tensile load for a tie wire shown in **Table 5.3.30** as follows:

Table 5.3.30 Tie-wire specifications

	Unit		Remarks
Tie wire		Taiburu	
Name		F270T	
Sectional area (A)	mm ² /pcs	1,409.6	
Diameter (φ)	mm	75.5	
Installation interval (L)	m	2.356	
Tilt angle of tie wire (θ)	°	0.00	
Yield point load on tie wire (T _{yd})	KN	1,748.0	

ii) Calculation of tie wire tension

Calculate tie wire tension T_k using the following equation:

$$T_k = (A_{pk} \times L + P/4) \times \sec(\theta)$$

Where:

T_k : tension acting on the tie wire (kN/pcs)

A_{pk} : sheet-pile reaction force at the tie wire installation point (kN/m)

$A_{pk} = 266.758$ kN/m

L : tie wire installation spacing (m)

P : mooring force; it will be shared evenly by four tie wires; $P = 700.0$ kN/post

θ : tilt angle of tie wire (°)

The calculation result for tie wire tension T is shown as follows:

$$T_d = (266.758 \times 2.356 + 700.00 \div 4) \times \sec(0.0^\circ) = 803.482 \text{ kN/piece}$$

iii) Verification of the tensile load on tie wires

Verify the tensile load on tie wires using the following equation:

$$m \cdot \frac{S_d}{R_d} \leq 1.0, \quad R_d = \gamma_R R_k, \quad S_d = \gamma_s S_k$$

$$R_k = T_{yk}$$

$$S_k = T_k$$

Where:

T_y : tie wire yield-point load (kN)

T : tensile load on the tie wires (kN)

γ_R : partial factor by which the resistance term is multiplied (1.00)

γ_s : partial factor by which the load term is multiplied (1.00)

m : adjustment factor (1.67)

The verification results for tie wire tensile load are then given as follows:

$$m \cdot \frac{S_d}{R_d} = m \times \frac{\gamma_s S_k}{\gamma_R R_k} = 1.67 \times \frac{1.00 \times 803.482}{1.00 \times 1,748.0} = 0.768 \leq 1.0$$

(9) Cathodic protection

1) Design conditions

- Sheet pile (steel-pipe sheet pile)-type quaywall
Length: 230 m
- High anti-corrosion
Bottom of coping (+0.50) to -1.00 m
- Average seawater surface
+1.00 m
- Marine environment
Clean sea water
- Target of corrosion protection (steel-pipe sheet pile)
 $\phi 1,100 \times 22 \text{ t } \ell = 30.5 \text{ m}$ (193 pipes)
- Target length for protection
230 m
- Water depth
Plan -12.00 m, Design -12.60 m
- Target area for cathodic protection
M.L.W.L. +0.50 m or under
(It is assumed that the area is the center of M.S.L. (+1.00 m) and L.W.L. (± 0.00 m).)
- Area to be protected (high anti-corrosion)
+0.50 to -1.00 m
(It is assumed that the unprotected area of the joints of steel-pipe sheet piles is 10%.)
- Protective current density
Underwater: 0.10 A/m², In seabed soil: 0.02 A/m²
- Cathodic protection method
Galvanic anode method using aluminum alloy anodes
- Design service life of anode
50 years
- Seawater resistance ratio
 $30 \times 10^{-2} \Omega \cdot \text{m}$
- Current loss reviewed or not
Not reviewed

2) Design of cathodic protection

i) Target area for protection

Calculate the target area for steels to be protected in each type of environment using **Eq. (18)** as follows:

$$S_n = \alpha \times I_n \times L \quad (18)$$

Where:

S_n : target area for protection, by environment (m^2)

α : circumference factor of steel (pipe) sheet pile

l_n : length of steel for each environment (m)

L : length in the face line direction (facility length) (m)

Note that "n" indicates each relevant type of environment.

The target area for protection is thus calculated as follows:

Underwater (joint)

$$1.57^{*1} \times \{+0.5 \text{ m} - (-1.0 \text{ m})\} \times 230 \text{ m} \times 0.1 = 54.2 \text{ m}^2$$

Underwater (exposed)

$$1.57^{*1} \times \{-1.0 \text{ m} - (-12.6 \text{ m})\} \times 230 \text{ m} = 4,188.8 \text{ m}^2$$

In seabed soil

$$1.57^{*1} \times \{-12.6 \text{ m} - (-28.9 \text{ m})\} \times 230 \text{ m} = 5,885.9 \text{ m}^2$$

Note: *1 Circumference factor of steel-pipe sheet pile

ii) Initial required protective current

Calculate the initial required protective using **Eq. (19)** as follows:

$$I_{p_n} = S_n \times i_n \quad (19)$$

Where:

I_{p_n} : initial required protective current by environment (A)

S_n : target area for protection, by environment (m^2)

i_n : initial required protective current density, by environment (A/m^2)

Note that "n" indicates each relevant type of environment.

The initial required protective current by environment is thus calculated as follows:

$$\text{Underwater: } (54.2 \text{ m}^2 + 4,188.8 \text{ m}^2) \times 0.10 \text{ A/m}^2 = 424.3 \text{ A}$$

$$\text{In seabed soil: } 5,885.9 \text{ m}^2 \times 0.02 \text{ A/m}^2 = 117.7 \text{ A}$$

Therefore, the total of the initial required protective current is:

$$423.3 \text{ A} + 117.7 \text{ A} = 542.0 \text{ A}$$

iii) Required anode mass

Calculate the required anode mass using **Eq. (20)** as follows:

$$W_T = (I_p \times T \times r_l \times 8760) / Q \quad (20)$$

Where:

W_T : required anode mass (kg)

T : design service life of anode (years)

r_l : current reduction ratio

Q : effective electric quantity of anode ($A \cdot \text{hr/kg}$)

The calculated required anode mass is thus as follows:

Required anode mass:

$$= (542.0 \text{ A} \times 50 \text{ y} \times 0.5^{*1} \times 8,760 \text{ h/y}^{*2}) / (2,600 \text{ A} \cdot \text{h/kg}^{*3}) = 4,5653.1 \text{ kg}^{*4}$$

Notes:

- *1: Current reduction ratio when the design service life is 15 years or longer.
- *2: Number of hours in a year
- *3: Effective electric quantity of aluminum alloy anode
- *4: Round up to the first or second decimal place

iv) Selection of anodes to use

- Anode selection conditions

Select aluminum alloy anodes (design service life: 50 years) from among four types of standard anodes, which differ in the generated current by 0.5 A, as shown in **Table 5.3.31**.

The selection conditions shown from a) to c) should also be considered.

- a) Choose the appropriate number of anodes that ensure the proper arrangement (anode installation interval or arrangement that ensures the appropriate protective effect).
- b) The design generated current per anode shall be no less than the initial required protective current required of one anode.
- c) The highest economic efficiency shall be guaranteed if the conditions of a) and b) are satisfied.

Table 5.3.31 Standard anode items (service life of 50 years)

Design generated current (A/pcs)	Aluminum alloy anode			
	2.0	2.5	3.0	3.5
Theoretically calculated net mass (kg/pc)	168.5	210.6	252.7	294.9

- Selection process

For condition a), the guideline on the appropriate arrangement in the horizontal and depth directions is shown in **Tables 5.3.32** and **5.3.33**.

Table 5.3.32 Circumference factor and the basic concept of anode arrangement in the horizontal direction

Circumference factor conditions	Anode installation interval
When circumference factor ≤ 1.2	5 m or less
When $1.2 < \text{circumference factor} \leq 1.75$	4 m or less
When $1.75 < \text{circumference factor}$	3.2 m or less

Using these as references, review the appropriate arrangement and quantity as shown below:

Considering the fact that the circumference factor of a steel-pipe sheet pile is 1.57, the right anode installation interval (arrangement interval) is "4 m" as shown in **Table 5.3.32** when arranging in the horizontal direction.

Table 5.3.33 Water depth conditions and the basic idea of anode arrangement

Type of protection in the tidal zone	Water depth conditions	Anode arrangement (depth direction)
Organic coating	From the bottom of organic coating to 5 m below	1 stage
	From the bottom of organic coating to over 5 m to 10 m below	2 stages
	From the bottom of organic coating to over 10 m to 15 m below	3 stages

"Three-stage arrangement" is shown as the appropriate anode arrangement based on **Table 5.3.33** because the distance from the bottom of the high anti-corrosion coating for this facility (-1.00 m) to the design depth (-12.60 m) is 11.60 m.

These results show that the minimum required number of anodes that can ensure the proper arrangement is 173 as shown below:

$$(230.00 \text{ m}/4.00 \text{ m/pc}) \times 3 \text{ stages} = 172.5 \text{ pcs} \Rightarrow 173 \text{ pcs}$$

However, the above quantity is the result of calculation without considering the interval of steel-pipe sheet piles. It is necessary to consider that the actual spacing arrangement will be a multiple of the interval of steel-pipe sheet piles.

To be specific,

$$\text{Length equivalent to three times steel-pipe sheet pile interval: } 1.19 \text{ m/pc} \times 3 \text{ pcs} = 3.57 \text{ m}$$

$$\text{Length equivalent to four times steel-pipe sheet pile interval: } 1.19 \text{ m/pc} \times 4 \text{ pcs} = 4.76 \text{ m}$$

(The interval of steel-pipe sheet piles is assumed to be 1.19 m per pile.)

When considering these lengths, it is necessary to take that the interval be less than the length equivalent to three times steel pipe sheet piles interval (3.57 m) to achieve 4.00 m as the appropriate anode arrangement, as calculated above.

Therefore, using this interval, the minimum required quantity of anodes is thus given as follows:

$$(230.00 \text{ m}/3.57 \text{ m/pc}) \times 3 \text{ stages} = 193.2 \text{ pcs} \Rightarrow 194 \text{ pcs}$$

v) Judgment of selection conditions

i) Judgment of condition a)

Satisfy the minimum required quantity of anodes (194) or make sure the standard anode items are as follows:

[Type 2.0A]

$$4,5653.1 \text{ kg} / 168.5 \text{ kg/pc} = 270.9 \text{ pcs} \Rightarrow 271 \text{ pcs} > 194 \text{ pcs}$$

[Type 2.5A]

$$4,5653.1 \text{ kg} / 210.6 \text{ kg/pc} = 216.8 \text{ pcs} \Rightarrow 217 \text{ pcs} > 194 \text{ pcs}$$

[Type 3.0A]

$$4,5653.1 \text{ kg} / 252.7 \text{ kg/pc} = 180.7 \text{ pcs} \Rightarrow 181 \text{ pcs} < 194 \text{ pcs}$$

[Type 3.5A]

$$4,5653.1 \text{ kg} / 294.9 \text{ kg/pc} = 154.8 \text{ pcs} \Rightarrow 155 \text{ pcs} < 194 \text{ pcs}$$

According to the above results, the anode that satisfies these conditions is Type 2.0A or Type 2.5A.

ii) Judgment of condition b)

In light of the results given in (8) above, each standard item must satisfy the initial required protection

current provided by each anode or satisfy the following condition:

[Type 2.0A]

$$542.0 \text{ A} / 271 \text{ pcs} = 2.00 \text{ A/pc} = 2.00 \text{ A/pc (standard item)}$$

[Type 2.5A]

$$542.0 \text{ A} / 217 \text{ pcs} = 2.497 \text{ A/pc} < 2.50 \text{ A/pc (standard item)}$$

According to the above results, the anode that satisfies these conditions is Type 2.0A or Type 2.5A.

iii) Judgment of condition c)

According to the judgment results for conditions a) and b), the candidate anodes are narrowed down to two types. Ultimately, 217 Type-2.5A anodes were selected based on the review of economic efficiency in this section and the final decision on what anode to use.

vi) Instruments to measure potential measurement

Regarding the instruments used to measure potential (terminal), they must be installed in a quaywall structure in intervals of one every 20 m to 50 m.

When the potential of steels measured after installation of anodes is not more than the protection potential according to the sea water silver chloride reference electrode (Ag/AgCl) standard (-780 mV), it is judged that corrosion protection remains effective.

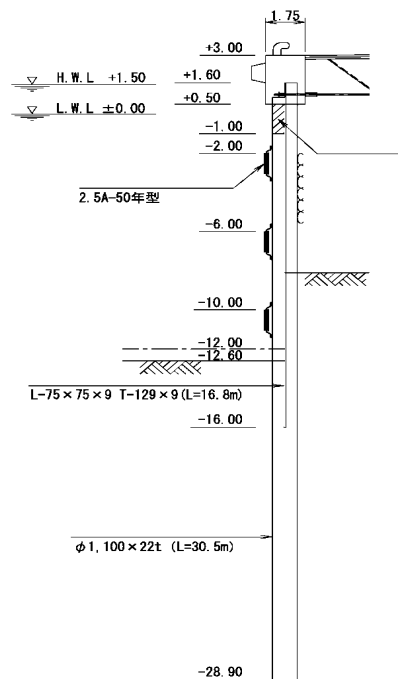


Figure 5.3.25 Arrangement of anodes

Design service life 50 years

Corrosion countermeasures

Cathodic protection for 50 years is assumed. The assumed corrosion protection efficiency is 90 %.

Coating

Heavy anticorrosion coating is applied to the intertidal zone of steel pipe piles from L.W.L. -1.00 m to the bottom of the deck beams. The assumed corrosion protection efficiency in this case is 100 %.

2) Natural conditions

i) Tide levels

- Mean-monthly highest water level H.W.L. D.L. +2.36 m
- Mean sea level M.S.L. D.L. +1.30 m
- Mean-monthly lowest water level L.W.L. D.L. ±0.00 m

ii) Geotechnical (ground) conditions

Original soil D.L. -7.00 m to D.L. -10.00 m

Cohesive soil layer $c = 10.6 + 2.33 Z$ (kN/m²)

$Z = 0$ at -10.00 m, $\gamma' = 5.4$ kN/m³

D.L. -29.50 m

Sandy soil layer $\gamma' = 10.0$ kN/m³

$N = 4$ to 50 (ave. $N = 25$), $\phi = 33^\circ$

D.L. -33.00 m

Sandy soil layer (bearing stratum) $\gamma' 10.0$ kN/m³

$N \geq 50$, $\phi = 40^\circ$

• Rubble layer

When calculating the coefficient of the lateral subgrade reaction, $k_{CH} = 3,000$ kN/m³ is assumed in the evaluation. Although there are various approaches to the skin friction of piles in rubble, including disregarding skin friction, in this example, N value = 2 (= 3,000/1,500) was set by back-calculation from $k_{CH} = 1,500$ N.

$\gamma' = 10.0$ kN/m³, $\phi = 40^\circ$

• SCP (As = 80 %) improved soil

$\gamma_t = 0.8 \times 20.0 + 0.2 \times 15.4 = 19.08$ kN/m³

$\gamma' = 9.08$ kN/m³, pile core N value 15 (control value)

3) Seismic coefficient for verification of Level 1 earthquake ground motion

The seismic coefficient for verification in the variable situation under Level 1 earthquake ground motion is set by conducting a seismic response analysis using the bedrock acceleration shown in **Figure 5.4.2** and the physical properties of the soil layers above the engineering base surface shown in **Table 5.4.1**.

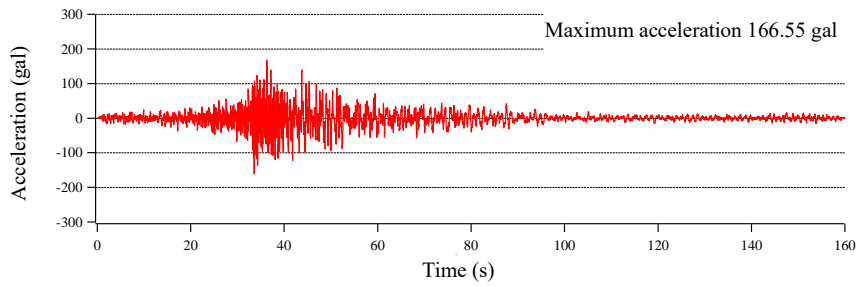


Figure 5.4.2 Time history of bedrock acceleration

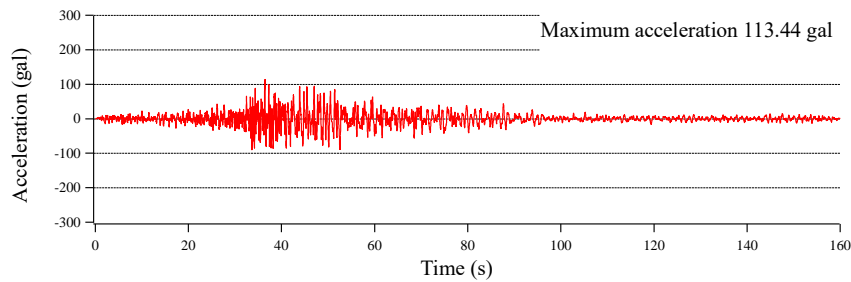


Figure 5.4.3 Time history of response acceleration at $1/\beta$ point

Table 5.4.1 Physical properties of analyzed soil layers

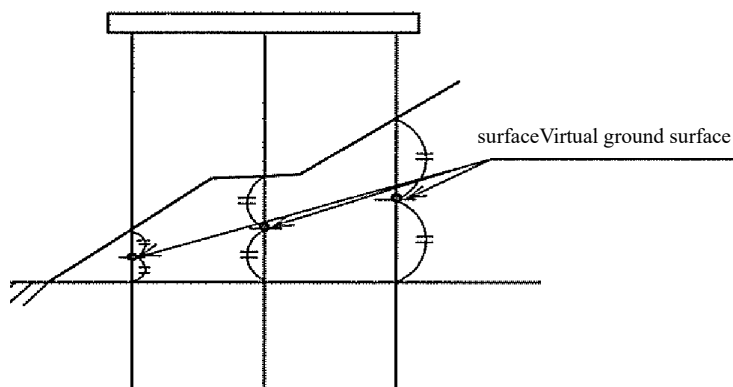
Soil layer	Top surface elevation (m)	Weight density in water γ' (kN/m ³)	Effective overburden stress at center of soil layer σ_v (kPa)	Deformation characteristics			
				Standard initial property G_{ma} (kPa)	Standard modulus of volume K_{ma} (kPa)	Standard average effective stress σ_{ma}' (kPa)	Confining pressure dependency factor mG, mK
Rubble	-7.60	10.00	52.00	1.80.E+05	4.69.E+05	98.0	0.50
SCP ($A_s = 80\%$)	-18.00	9.08	125.00	1.32.E+05	3.43.E+05	98.0	0.50
Sandy soil layer ($N = 25$)	-29.50	10.00	225.90	1.26.E+05	3.28.E+05	98.0	0.50
Sandy soil layer ($N > 50$)	-33.00	10.00	-	-	-	-	-

Because the natural period of a piled pier and the characteristic value of the piles (β) change depending on the pile cross section, repeated stress intensity verifications of the piles were conducted for the dominant state, assuming various pile dimensions, and the pile section was set at $\phi 1,500 \times t16$.

Regarding the natural period of the piled pier, the spring constant was obtained from the relationship between the horizontal force and horizontal displacement by a frame analysis using the subgrade reaction of the ground as a characteristic value, and was calculated as shown in **Table 5.4.2** (considering water in piles) and **Table 5.4.3** (not considering water in piles). The displacement of the superstructure in the tables was obtained by a frame analysis. In calculating the natural period of the piled pier, the self-weight of the piles was considered (assumed to be 1/2 of the self-weight from the upper fixed point to the virtual fixed point). The coefficient of the lateral subgrade reaction of the ground was calculated as two times the value of the coefficient of the subgrade reaction in the permanent state, and the free length of the piles was calculated by using the actual ground surface and not the virtual ground surface.

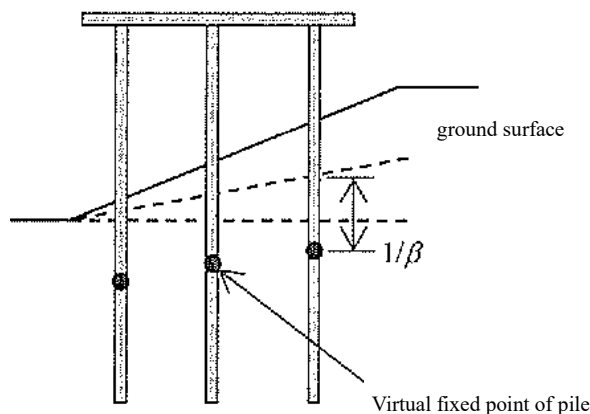
- Concept of virtual seabed surface (virtual ground surface)

The calculation method for the lateral resistance of piles used in analyses of piled piers is originally related to horizontal ground surfaces, but in case the inclination of the slope of the seabed ground where a piled pier is to be installed is considerably steep, the virtual ground surface for each pile used in calculations of the pile lateral resistance and bearing capacity may be set at an elevation that corresponds to 1/2 of the vertical distance between the frontal water depth and the actual slope surface at the position of the axial line of each pile as shown below.



- Concept of virtual fixed point

As the virtual fixed point of the piles of piled piers, $1/\beta$ (β : characteristic value of pile) below the virtual ground surface may be used. The case when piles are installed in a slope is shown in the figure below.



The value obtained by the equation ($k_{CH} = 1,500 N$) was multiplied by 2, and the actual ground surface and not the virtual ground surface was used. Regarding the additional seismic mass around the piles added by earthquake ground motion and the weight of seawater in the piles, the natural period was calculated for two cases, that is, the cases considering and not considering this weight. The weight of the water in the piles was set at 1/2 of the weight from H.W.L. to the actual ground surface.

- Spring constant per 1 rigid frame

$$K_l = 100 / (2.91 \times 10^{-3}) = 34,364 \text{ kN/m}$$

- Spring constant per 1 block (5 rigid frames) of wharf

$$\Sigma K_i = 5 \times 34,364 = 171,820 \text{ kN/m}$$

- Natural period T_s of wharf

$$T_s = 2\pi \sqrt{\frac{W}{gK}}$$

where

T_s : natural period of wharf (s)

W : self-weight and surcharge during earthquake (kN)

g : gravitational acceleration (m/s^2)

K : lateral spring constant of wharf (kN/m)

Table 5.4.2 Natural period of wharf (considering weight of seawater in piles, etc.)

Item	Result				Remarks
Displacement of superstructure (mm)	2.91				
Lateral load (kN)	100				
Spring constant (kN/m)	34,364				1 rigid frame
	171,820				1 block (5 frames)
Self-weight of wharf (kN)	16,148				
Self-weight of superstructure (kN)	15,000				
Self-weight of piles (kN)	1,148				
Weight of seawater in piles (kN)	1,664				
Additional weight (kN)	3,477				
Surcharge (kN)	0	5,000	0	5,000	
Crane load (kN)	0	0	11,000	11,000	
Total weight (kN)	21,289	26,289	32,289	37,289	
Natural period (s)	0.71	0.79	0.87	0.94	

Table 5.4.3 Natural period of wharf (not considering weight of seawater in piles, etc.)

Item	Result				Remarks
Displacement of superstructure (mm)	2.91				
Lateral load (kN)	100				
Spring constant (kN/m)	34,364				1 rigid frame
	171,820				1 block (5 frames)
Self-weight of wharf (kN)	16,148				
Self-weight of superstructure (kN)	15,000				
Self-weight of piles (kN)	1,148				
Weight of seawater in piles (kN)	0				
Additional weight (kN)	0				
Surcharge (kN)	0	5,000	0	5,000	
Crane load (kN)	0	0	11,000	11,000	
Total weight (kN)	16,148	21,148	27,148	32,148	
Natural period (s)	0.62	0.70	0.80	0.87	

Figure 5.4.4 and **Figure 5.4.5** show the acceleration response spectra (damping factor $h = 20\%$) obtained from the time history of the response acceleration of the $1/\beta$ point below the virtual ground surface near the center of the piled pier shown in **Figure 5.4.3**. The seismic coefficient for verification was set as follows from the response acceleration corresponding to the natural period of the piled pier shown in **Table 5.4.2** and **Table 5.4.3** using these response spectra.

The acceleration response spectra show little change in the response acceleration until around the period of 1.0 s, but then the acceleration itself decreases as the period becomes longer than 1.0 s. The seismic coefficient for verification was obtained as follows using the peak acceleration between the natural frequencies of 0.62 and 0.87 s when the weight of seawater in the piles, etc. was not considered, which is the case with the largest response acceleration.

$$k_{hk} = 174.13 / 980 = 0.178 \rightarrow 0.18$$

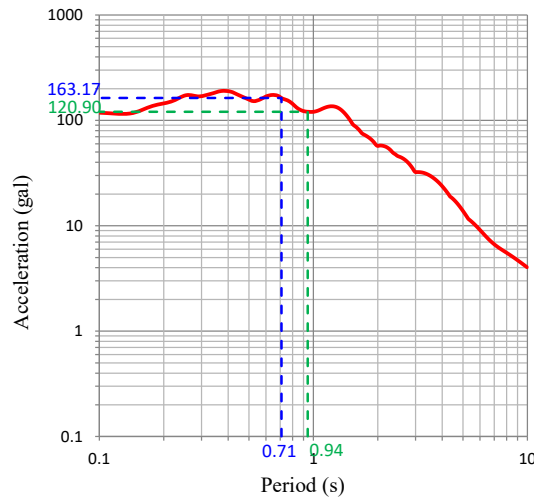


**Figure 5.4.4 Acceleration response spectrum at $1/\beta$ point
(Natural frequency: When seawater in piles is considered)**

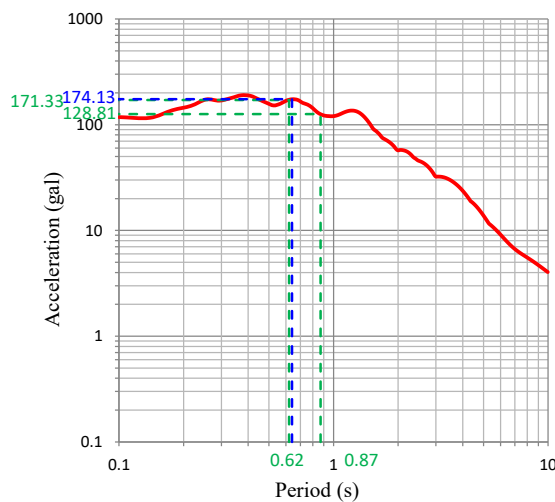


**Figure 5.4.5 Acceleration response spectrum at $1/\beta$ point
(Natural frequency: When seawater in piles is not Considered)**

4) Conditions of actions

i) Unit weight of concrete

- Unreinforced concrete $\gamma_c = 22.6 \text{ kN/m}^3$
- Reinforced concrete $\gamma_c = 24.0 \text{ kN/m}^3$
- Pavement concrete $\gamma_c = 24.0 \text{ kN/m}^3$

(Same as reinforced concrete because the pavement and slab are constructed as an integrated structure.)

ii) Surcharges

- During operation 20 kN/m²
- Level 1 earthquake ground motion 10 kN/m²

iii) Live loads

- Vehicle (truck) load
- Vehicle (trailer) load
- Forklift load
- Crane load

Type: Rail-mounted traveling bridge crane

Service weight: 11,000 kN

Rail gauge: 16.00 m

Wheelbase: 18.00 m

Number of wheels: 8 wheels × 2 legs (on both sea side and land side)

Length of 8 wheels/leg: 6.40 m

Wheel spacing: 800 mm

Closest approach distance of cranes: 3.40 m

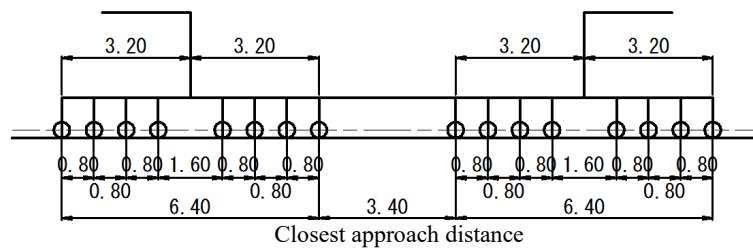


Figure. 5.4.6 Arrangement of crane wheels

As the maximum wheel load used as an action in the static study, the value calculated based on the calculation standard for crane structural parts (JIS B 8821) or the crane structural standard (notification of the Ministry of Labour) can be used.

Table 5.4.4 shows the wheel loads set based on the above. In this example, the value ($k_h = 0.20$) of the wheel load during an earthquake calculated based on the crane structural standard, etc. by the wheel load set considering the dynamic interaction of the crane and the mooring facilities was larger than the seismic coefficient of verification ($k_h = 0.18$) of the piled pier. Therefore, $k_h = 0.20$ was adopted as a more conservative value.

Table 5.4.4 Crane wheel load

(Unit: kN/wheel)

		Direction of action	Sea → Land	Sea ← Land
Vertical load	During work (wind velocity 16 m/s)	Sea side	346	523
		Land side	418	241
	During storm (wind velocity 55 m/s)	Sea side	76	551
		Land side	635	160
	During earthquake (horizontal seismic coefficient 0.20)	Sea side	81	764
		Land side	683	-19
Horizontal load	During work (wind velocity 16 m/s)	Sea side	35	52
		Land side	42	24
	During storm (wind velocity 55 m/s)	Sea side	14	99
		Land side	114	29
	During earthquake (horizontal seismic coefficient 0.20)	Sea side	16	153
		Land side	137	-4

iv) Mooring forces of ships

Because the gross tonnage (GT) of the cargo vessel which is the design ship in this example is 15,860 t, the mooring force T_k of the ship is as shown below, assuming a value of $10,000 < GT \leq 20,000$.

- Mooring force acting on bollard $T_k = 700$ kN
- Mooring force acting on mooring post $T_k = 1,000$ kN

(3) Setting of Cross Section for Verification

1) Layout and dimensions

The dimensions of the superstructure of the piled pier and the layout of the steel pipe piles are shown in **Figure. 5.4.7**.

2) Layout of ancillary facilities

Among ancillary facilities, ship mooring bollards are installed at intervals of 25 m in the central part of the superstructure of the wharf, and the interval of the rubber fenders is set at 10 m because cargo vessels of 2,000 DWT class will also use this wharf at the same time. Therefore, either 3 or 2 rubber fenders will be installed in 1 block of the wharf. However, in the study of ship berthing, a wharf block with 3 rubber fenders is studied, as berthing is eccentric and the external force is large.

$$w_k = w_A = 77.0 \times 0.07459 = 5.743 \text{ kN}$$

(Part in sea/rubble)

$$w_k = w_A = 77.0 \times 0.06988 = 5.381 \text{ kN}$$

(Part in soil)

$$w_k = w_A = 77.0 \times 0.07389 = 5.690 \text{ kN}$$

- Inertia force related to Level 1 earthquake ground motion (horizontal force)

(Heavy corrosion protection part)

$$H_{wk} = k_{hk} \cdot w_k = 0.18 \times 5.743 = 1.034 \text{ kN}$$

(Part in sea/rubble)

$$H_{wk} = k_{hk} \cdot w_k = 0.18 \times 5.381 = 0.969 \text{ kN}$$

(Part in soil)

$$H_{wk} = k_{hk} \cdot w_k = 0.18 \times 5.960 = 1.024 \text{ kN}$$

3) Surcharge

- Permanent situation, during berthing and during crane operation

$$w_{qk} = w_q B = 20.0 \times 5.00 = 100.00 \text{ kN/m}$$

- During traction

$$w_{qk} = w_q B = 10.0 \times 5.00 = 50.00 \text{ kN/m}$$

- During action of Level 1 earthquake ground motion

$$w_{qk} = w_q B = 10.0 \times 5.00 = 50.00 \text{ kN/m}$$

$$w_{qk} = w_q B L = 10.0 \times 5.00 \times 20.00 = 1,000.00 \text{ kN/rigid frame}$$

- Inertia force related to Level 1 earthquake ground motion (horizontal force)

$$H_{wk} = k_{hk} \cdot w_{qk} = 0.18 \times 1,000.00 = 180.00 \text{ kN/rigid frame}$$

4) Moving load

Among moving loads, the main load that affects the examination of the cross section of foundation piles is crane load. Here, the maximum support reaction force acting on the end support point A and its adjoining support point B in a 4-span continuous girder is obtained.

For the variable situations related to work and Level 1 earthquake ground motion, the value when the maximum influence value of the support reaction force occurs was obtained by a computer calculation, assuming one or two cranes are loaded on the wharf.

Influence value of reaction force at support point A 6.866

Influence value of reaction force at support point B 5.994

Because the value for support point A is larger in this calculation result, the crane wheel load at support point A is used. During work and during an earthquake, the wheel load is increased by an increment of 10 %, assuming a crane traveling speed of 1 m/s. An example of a calculation of the wheel load during work (sea → land) is shown below.

- Vertical force during work (sea → land)

$$\text{Sea side } 346 \text{ kN/wheel} \times 1.10 \text{ (extra)} \times 6.866 = 2,613.20 \text{ kN}$$

$$\text{Land side } 418 \text{ kN/wheel} \times 1.10 \text{ (extra)} \times 6.866 = 3,156.99 \text{ kN}$$

- Horizontal force during work (sea → land)

Sea side 35 kN/wheel × 1.10 (extra) × 6.866 = 264.34 kN

Land side 42 kN/wheel × 1.10 (extra) × 6.866 = 317.21 kN

During a storm, the wheel load can be calculated as follows because the influence value of the maximum reaction force of piles when the crane is loaded at a fixed position is 5.384.

- Vertical load during storm (sea → land)

Sea side 76 kN/wheel × 5.384 = 409.18 kN

Land side 635 kN/wheel × 5.384 = 3,418.84 kN

- Horizontal load during storm (sea → land)

Sea side 14 kN/wheel × 5.384 = 75.38 kN

Land side 114 kN/wheel × 5.384 = 613.78 kN

The characteristic values of the crane wheel load calculated by the method described above are shown in **Table 5.4.5**.

Table 5.4.5 Crane wheel load acting on piles (Wheel load at end position)

(Unit: kN)

Action		Direction	Characteristic value	
			Sea → Land	Sea ← Land
Vertical force	During work (wind velocity 16 m/s)	Sea side	2,613.20	3,950.01
		Land side	3,156.99	1,820.18
	During storm (wind velocity 55 m/s)	Sea side	409.18	2,966.58
		Land side	3,418.84	861.44
	During earthquake (horizontal seismic coefficient 0.20)	Sea side	611.76	5,770.19
		Land side	5,158.43	-
Horizontal force	During work (wind velocity 16 m/s)	Sea side	264.34	392.74
		Land side	317.21	181.26
	During storm (wind velocity 55 m/s)	Sea side	75.38	533.02
		Land side	613.78	156.14
	During earthquake (horizontal seismic coefficient 0.20)	Sea side	120.84	1,155.55
		Land side	1,034.71	-

5) Berthing force

i) Calculation of berthing energy

The characteristic value (E_{fk}) of the berthing energy of a vessel is obtained by the following equation.

$$E_{fk} = \frac{1}{2} M_{sk} V_{bk}^2 C_{mk} C_{ek} C_{sk} C_{ck}$$

where

E_f : berthing energy of vessel (kN • m)

M_s : mass of vessel (t)

V_b : berthing velocity of vessel (m/s)

C_e : eccentricity factor

C_m : virtual mass factor

C_s : softness factor (1.0)

C_c : berth configuration factor (1.0)

- Mass of vessel

$$M_s = D_T = 2.920 \times 30,000^{0.924} = 40,017 \text{ t}$$

- Berthing velocity of vessel

$$V_b = 0.10 \text{ m/s}$$

- Length between perpendiculars $L_{pp} = 166.0 \text{ m}$

The block coefficient (C_b) of the vessel is obtained by the following equation.

$$C_b = \frac{\nabla}{L_{pp} \times B \times d}$$

where

C_{bk} : characteristic value of block coefficient

∇ : volume of displacement of vessel ($= DT_k / 1.03$) (m^3)

B : beam (m)

d : draft (m)

$$C_b = \frac{40,017 / 1.03}{166.0 \times 27.9 \times 10.8} = 0.777$$

- Radius of gyration r

$$r = (0.19 C_b + 0.11) L_{pp} = (0.19 \times 0.777 + 0.11) \times 166.0 = 42.77 \text{ m}$$

Distance L_i from berthing point of vessel along the normal line of the mooring facility to the center of gravity of the vessel

$$L_1 = \{0.5\alpha + e(1 - k)\} L_{pp} \cos\theta = \{0.5 \times 0.50 + 0.058 \times (1 - 0.5)\} \times 166.0 \times \cos 3^\circ = 46.25 \text{ m}$$

$$L_2 = (0.5\alpha - ek) L_{pp} \cos\theta = (0.5 \times 0.50 - 0.058 \times 0.5) \times 166.0 \times \cos 3^\circ = 36.64 \text{ m}$$

where

θ : berthing angle 3°

e : ratio of fender interval and length between perpendiculars

α : ratio of length of parallel side and length between perpendiculars (0.50)

When it is assumed that the length of the parallel sides of a vessel is generally αL (L : ship length), a guideline of approximately 1/2 may be used for the parallel factor α when the design ship is a cargo ship. Therefore, $\alpha = 0.50$ was used here.

k : parameter (0.50)

The eccentricity factor C_e was obtained assuming $L_2 = 36.64 \text{ m}$. Therefore, C_e was obtained as follows.

$$C_e = \frac{1}{1 + (\ell/r)^2}$$

$$C_e = \frac{1}{1 + (36.64 / 42.77)^2} = 0.577$$

The virtual mass factor C_m was obtained by the following equation.

$$C_m = 1 + \frac{\pi}{2C_b} \cdot \frac{d}{B}$$

$$= 1 + \frac{\pi}{2 \times 0.777} \cdot \frac{10.8}{27.9} = 1.783$$

Accordingly, the berthing energy E_f of the vessel is as follows.

$$E_f = \frac{1}{2} \times 40,017 \times 0.10^2 \times 1.783 \times 0.577 \times 1.0 \times 1.0$$

$$= 205.8 \text{ kN} \cdot \text{m}$$

ii) Selection of rubber fenders

Here, V-shaped rubber (natural) is used, and the fenders are set so as to satisfy the following equation. The subscript d indicates a design value.

$$E_s = \phi E_{cat} \geq E_f$$

where

E_s : absorbed energy of fender (kN • m)

ϕ : manufacturing error of fender (tolerance)

E_{cat} : absorbed energy of fender (kN • m)

E_f : berthing energy of vessel (kN • m)

Case of V-shaped rubber (natural) fender

$$E_{cat} = K_e K H^2 L = 245 K H^2 L$$

K_e : factor depending on shape (= 245)

K : factor depending on rubber material (= 0.7 to 1.3; here, $K = 1.0$)

H : height of fender (m)

L : length of fender (m)

The reaction force R_{cat} of the V-shaped rubber fender is obtained by the following equation.

$$R_{cat} = K_f K H L = 735 K H L$$

R_{cat} : maximum reaction force of fender (kN)

K_f : factor depending on shape (= 735)

The equation shown above is the case in which the design compression was set to 45 % of the fender height or less with a V-shaped fender (case of natural rubber). Because the factors, etc. will differ depending on the type of fender, the manufacturer's catalog was used as reference. As manufacturing tolerances, in the selection of the rubber fender, $\phi = 0.9$ was adopted for absorbed energy and $\phi = 1.1$ was adopted for reaction force.

The necessary length, absorbed energy and reaction force of V-600H and V-800H fenders were calculated by the following equations. The results are shown in **Table 5.4.6**.

- Absorbed energy of fender

$$E_s = 245 H^2 L \cdot \phi = 220.50 H^2 L \text{ (kN} \cdot \text{m)}$$

- Reaction force of fender

$$R = 735.0 H L \cdot \phi = 808.5 H L \text{ (kN)}$$

Table 5.4.6 Verification of Fenders

Height	Length (m)	$E_s(\text{kN} \cdot \text{m})$	Judgment	Reaction force $R(\text{kN})$
V-600H	3.00	238.1	$\geq E_{fd}$	1,510
V-800H	1.70	239.9	$\geq E_{fd}$	1,100

The result of an economic comparison of the above-mentioned V-600H and V-800H fenders showed that V-800H is more economical. Accordingly, V-800H \times 1.7 m is used as the fender.

iii) Horizontal force due to fender

The horizontal force due to the fender is assumed to be the fender reaction force. Here, two cases are considered, i.e., eccentric berthing in which the vessel comes alongside one fender, and parallel berthing involving simultaneous contact with three fenders.

• Eccentric berthing

$$H_k = 1,100 \times 1 = 1,100.00 \text{ kN/block}$$

Because the pile end row receives the largest horizontal force due to eccentric berthing, horizontal force is calculated for the pile end row.

$$H = \frac{K_{Hi}}{\sum K_{Hi}} \cdot R + \frac{K_{Hi} \times X_i}{\sum K_{Hi} \cdot (X_i)^2} \cdot e \cdot R$$

where

K_{Hi} : spring constant (assumed to be 1 per row)

R : reaction force of fender

X_i : distance from centroid of pile group to each pile

$$\sum K_{Hi} \cdot (X_i)^2 = 2 \times (5.00^2 + 10.00^2) = 250.00$$

$$\begin{aligned} H_k &= \frac{1}{5} \times 1,100.00 + \frac{1 \times 10.00}{250.00} \times 10.00 \times 1,100.00 \\ &= 660.00 \text{ kN} \end{aligned}$$

• Parallel berthing

Three fenders are provided for 1 block.

$$H_k = 1,100.00 \times 3 = 3,300.00 \text{ kN/block}$$

Here, it is assumed that the horizontal force is distributed over 1 block (5 rows) of the piled pier.

$$H_k = 3,300/5 = 660.00 \text{ kN/block}$$

6) Mooring force of ship

Because the mooring force of a ship acts on the center of the block, the horizontal force is borne by the entire piled pier (5 rows).

$$T_k = 700 \text{ kN/block}$$

$$T_k = 700/5 = 140.00 \text{ kN/rigid frame}$$

7) Wave uplift

Not considered, as attack is not assumed.

(5) Conditions Related to Seabed Ground

The soil composition at the planned location, as described in the section on design conditions, consists of soft cohesive soil from the original ground to D.L. -29.50 m. Therefore, in order to ensure the stability of structures such as earth-retaining revetments, etc., forced replacement by the sand compaction pile (SCP) method is carried out. Furthermore, replacement with good quality rubble (angle of shear resistance $\varphi = 40^\circ$) is carried out to the depth where lateral resistance of the wharf foundation piles is expected below the planned water depth.

The replacement rubble layer is a layer in which rubble is used to replace the soil in the range where lateral resistance of the wharf foundation piles is expected. It is necessary to decide the replacement range in both the depth direction and to the sea side. As the depth of the replacement rubble layer, the characteristic length of the piles ($1/\beta$) below the virtual ground surface is secured, and the replacement width is defined as a width equal to or greater than the point of intersection between the design water depth and the passive collapse plane of the rubble, drawn from a point (virtual fixed point) where the characteristics of the piles are secured below the virtual ground surface.

- Virtual seabed surface D.L. -11.60 m
- Virtual fixed point $-11.60 - 7.77 = -19.37$ m

Accordingly, the replacement depth is set at D.L. -19.5 m.

- Apparent seismic coefficient

The seismic coefficient for verification used in calculating the apparent seismic coefficient was set using the value obtained by dividing the maximum value of the acceleration generated at the position of the virtual fixed point (113.44 gal) by gravitational acceleration (980 cm/s^2), that is, $113.44 / 980 = 0.12$. Because the object rubble layer is located underwater, the surcharge is set as 0.

$$k_h' = 0.12 \times 20 / (20 - 10) = 0.24$$

- The passive collapse angle ζ_p of the rubble ($\varphi = 40^\circ$, $\delta = -15^\circ$) is $\zeta_p = 15.4^\circ$.
- Replacement width $B = (19.5 - 12.1) / \tan 15.4^\circ = 26.87$ m

Therefore, the replacement width from the center of the sea side piles at the design water depth is set at 27.0 m or more.

(6) Structural analysis

1) Assumption of cross-sectional dimensions of steel pipe piles used

i) Corrosion protection

In the steel pipe piles, corrosion protection by coating is provided at depths shallower than L.W.L. - 1.00 m, and cathodic protection is used at depths greater than L.W.L. - 1.00 m.

- Corrosion allowance

The corrosion allowance is calculated by the following equation.

$$\text{Corrosion allowance} = \text{Corrosion rate} \times \text{Service life} \times (1 - \text{Corrosion protection efficiency})$$

A corrosion allowance is not considered in the coated section. The corrosion rate and corrosion allowance in the seawater, rubble and seabed soil were set as shown in **Table 5.4.7** considering a service life of 50 years. Because there are many voids around the piles in the replacement rubble in comparison with general ground, here, the same value as in seawater is adopted as a conservative value (in cathodic protection, a protective current density of 50 % of that in seawater is considered necessary).

ii) Cross-sectional performance

The steel pipe piles used here are assumed to be $\phi 1,500 \times t 16$ **Table 5.4.8** and **Table 5.4.9** show the cross-sectional performance of the steel pipe piles before and after corrosion, respectively.

Table 5.4.7 Corrosion rates of piles

	In seawater and rubble zone	In seabed soil
Corrosion rate δ_{i0} of natural condition of pile material (mm/y)	0.20	0.03
Cathodic protection efficiency μ	0.90	0.90
Corrosion rate δ_t in cathodic protection condition (mm/y)	0.02	0.003
Design service life y (year)	50	50
Design corrosion allowance Δt (mm)	1.00	0.15

Table 5.4.8 Cross-sectional parameters of piles (before corrosion)

	Coated corrosion protection part	Part in seawater and rubble	Part in soil (shallower than $1/2 M_{max}$)	Part in soil (deeper than $\beta/2 M_{max}$)
Initial pile diameter D (mm)	1,500	1,500	1,500	1,500
Initial wall thickness t (mm)	16,0	16.0	16.0	16.0
Cross-sectional area A (mm)	745.9	745.9	745.9	745.9
Geometrical moment of inertia I (cm ²)	2,053.677	2,053,677	2,053,677	2,053,677
Section modulus Z (cm ³)	27,382	27,382	27,382	27,382
Radius of gyration of cross section r (cm)	52.47	52.47	52.47	52.47

Table 5.4.9 Cross-sectional parameters of piles (after corrosion)

	Coated corrosion protection part	Part in seawater and rubble	Part in soil (shallower than $1/2 M_{max}$)	Part in soil (deeper than $\beta/2 M_{max}$)
Initial pile diameter D (mm)	1,500	1,500	1,500	1,500
Initial wall thickness t (mm)	16.0	16.0	16.0	16.0
Corrosion amount s (mm)	0	1.0	0.15	0.15
Cross-sectional area A (cm ²)	745.9	698.8	738.9	738.9
Geometrical moment of inertia I (cm ⁴)	2,053,677	1,921,405	2,033,802	2,033,802
Section modulus Z (cm ³)	27,382	25,635	27,123	27,123

Young's modulus of steel materials $E_s = 2.0 \times 10^8$ kN/m²

2) Virtual ground surface

The design slope is set at a design water depth of -12.10 m below the normal line and the top of slope line at -4.20 m on the land side. Therefore, as shown in in **Figure 5.4.8**, the virtual ground surface is set at an elevation that corresponds to 1/2 of the vertical distance between the design slope at the pile axis and the design water depth.

1st pile row = -11.60 m,

2nd pile row = -10.28 m,

3rd pile row = -8.93m,

4th pile row = -8.15 m,

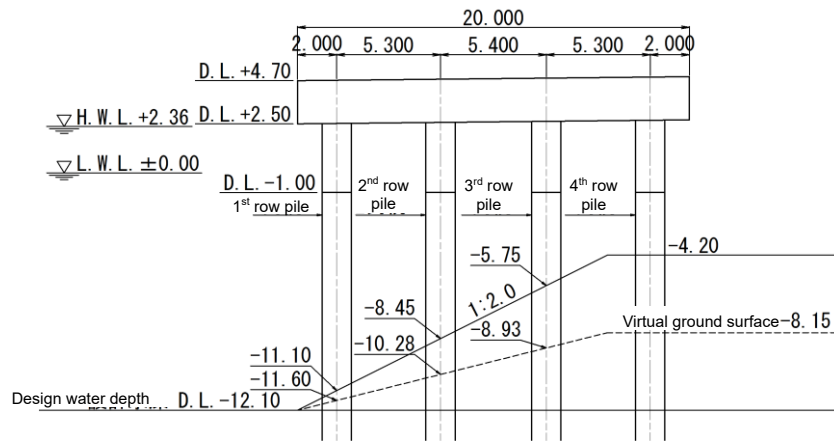


Figure 5.4.8 Virtual ground surface

3) Characteristic length of piles

Coefficient of lateral subgrade reaction

$$k_{CH} = 3,000 \text{ kN/m}^3$$

- Before corrosion

$$\beta = \sqrt[4]{\frac{k_{CH}D}{4EI}}$$

$$= \sqrt[4]{\frac{3,000 \times 1.500}{4 \times 2.00 \times 10^8 \times 2.054 \times 10^{-2}}} = 0.1286$$

- After corrosion

$$\beta = \sqrt[4]{\frac{3,000 \times 1.498}{4 \times 2.00 \times 10^8 \times 1.921 \times 10^{-2}}} = 0.1308$$

- Characteristic length of pile

Before corrosion $1/\beta = 1/0.1286 = 7.77 \text{ m}$

After corrosion $1/\beta = 1/0.1308 = 7.65 \text{ m}$

4) Coefficient of subgrade reaction and lateral spring constant

The coefficient of the subgrade reaction is calculated by the following equation.

$$k_{CH} = 1,500 \text{ N}$$

The lateral spring constant KD of a pile is calculated by the following equation.

$$KD = k_{CH} \cdot B \text{ (kN/m}^2\text{)}$$

where

k_{CH} : coefficient of lateral subgrade reaction (kN/m³)

B : pile width or pile diameter (m)

Table 5.4.10 Coefficient of lateral subgrade reaction of pile

Soil layer	<i>N</i> value	<i>k_{CH}</i> (kN/m ³)	Pile diameter <i>B</i> (m)	<i>KD</i> (kN/m ²)
Rubble	2	3,000	1.50	4,500
SCP	8	12,000	1.50	18,000
Sandy soil	25	37,500	1.50	56,250
Bearing stratum	50	75,000	1.50	112,500

5) Cross-sectional performance of superstructure

The dimensions of the superstructure are set as follows. Only the beams are considered to be effective in cross-sectional performance.

Cross-sectional area: $A = 1.00 \times 2.20 = 2.20 \text{ m}^2$

Geometrical moment of inertia:

$$I = 1/12 \times 1.00 \times 2.20^3 = 0.887 \text{ m}^4$$

Young's modulus of concrete

$$E_c = 2.8 \times 10^7 \text{ kN/m}^2$$

6) Analysis model

A linear frame analysis is carried out based on the actions and structural conditions described up to this point, and the section force of the foundation piles is calculated.

Figure 5.4.9 shows the analysis model, and Table 5.4.11 shows an example of the input data.

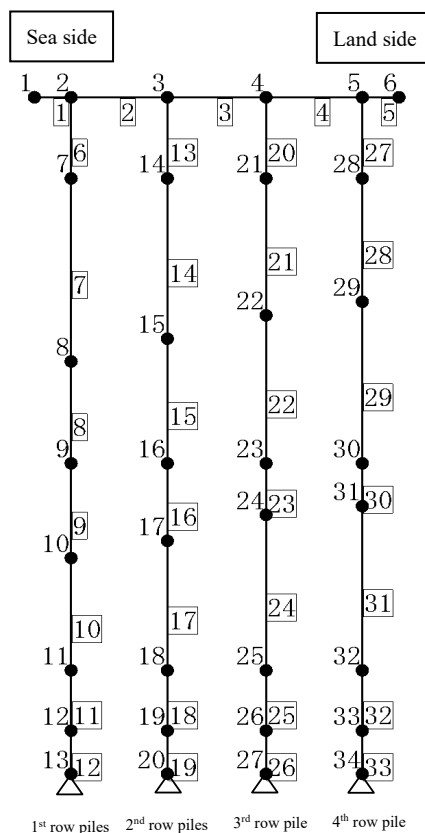


Figure 5.4.9 Model used in frame analysis

Table 5.4.11 Example of input section data (after corrosion)

Member No.	Cross-sectional area (m ²)	Geometrical moment of inertia (m ⁴)	Young's modulus (kN/m ²)	Soil layer	Remarks
1	2.200E+00	8.870E-01	2.80E+07		Superstructure
2	2.200E+00	8.870E-01	2.80E+07		Ditto
3	2.200E+00	8.870E-01	2.80E+07		Ditto
4	2.200E+00	8.870E-01	2.80E+07		Ditto
5	2.200E+00	8.870E-01	2.80E+07		Ditto
6	7.459E-02	2.054E-02	2.00E-08	Heavy corrosion protection	1 st row pile
7	6.988E-02	1.921E-02	2.00E-08	Sea	Ditto
8	6.988E-02	1.921E-02	2.00E-08	Rubble	Ditto
9	7.389E-02	2.034E-02	2.00E-08	SCP	Ditto
10	7.389E-02	2.034E-02	2.00E-08	SCP	Ditto
11	7.389E-02	2.034E-02	2.00E-08	Sandy soil N = 25	Ditto
12	7.389E-02	2.034E-02	2.00E-08	Bearing stratum	Ditto
13	7.459E-02	2.054E-02	2.00E-08	Heavy corrosion protection	2 nd row pile
14	6.988E-02	1.921E-02	2.00E-08	Sea	Ditto
15	6.988E-02	1.921E-02	2.00E-08	Rubble	Ditto
16	7.389E-02	2.034E-02	2.00E-08	SCP	Ditto
17	7.389E-02	2.034E-02	2.00E-08	SCP	Ditto
18	7.389E-02	2.034E-02	2.00E-08	Sandy soil N = 25	Ditto
19	7.389E-02	2.034E-02	2.00E-08	Bearing stratum	Ditto
20	7.459E-02	2.054E-02	2.00E-08	Heavy corrosion protection	3 rd row pile
21	6.988E-02	1.921E-02	2.00E-08	Sea	Ditto
22	6.988E-02	1.921E-02	2.00E-08	Rubble	Ditto
23	7.389E-02	2.034E-02	2.00E-08	SCP	Ditto
24	7.389E-02	2.034E-02	2.00E-08	SCP	Ditto
25	7.389E-02	2.034E-02	2.00E-08	Sandy soil N = 25	Ditto
26	7.389E-02	2.034E-02	2.00E-08	Bearing stratum	Ditto
27	7.459E-02	2.054E-02	2.00E-08	Heavy corrosion protection	4 th row pile
28	6.988E-02	1.921E-02	2.00E-08	Sea	Ditto
29	6.988E-02	1.921E-02	2.00E-08	Rubble	Ditto
30	7.389E-02	2.034E-02	2.00E-08	SCP	Ditto
31	7.389E-02	2.034E-02	2.00E-08	SCP	Ditto
32	7.389E-02	2.034E-02	2.00E-08	Sandy soil N = 25	Ditto
33	7.389E-02	2.034E-02	2.00E-08	Bearing stratum	Ditto

7) Section force

Table 5.4.12 shows the results of the calculation of section force by the frame analysis. As examples of the analysis results, Figure 5.4.10 and Figure 5.4.11 show distribution diagrams for the section force when the inertia force of Level 1 earthquake ground motion acts in the direction from sea to land.

Table 5.4.12 List of section forces

Condition of action		Item	1 st row pile	2 nd row pile	3 rd row pile	4 th row pile
Permanent situation (surcharge)	Pile head	Axial load (N)	1,202.42	1,297.87	1,297.66	1,202.04
		Bending moment (kN · m)	42.56	22.13	18.18	42.86
	In sea	Axial load (N)	1,228.85	1,324.30	1,324.09	1,228.46
		Bending moment (kN · m)	29.76	14.95	12.51	28.55
	In soil	Axial load (N)	1,331.82	1,413.91	1,369.61	1,269.53
		Bending moment (kN · m)	7.48	3.81	2.73	6.31
Berthing	Pile head	Axial load (N)	838.49	1,187.87	1,353.47	1,620.17
		Bending moment (kN · m)	1,376.99	1,624.07	1,833.99	1,865.48
	In sea	Axial load (N)	864.91	1,214.30	1,379.89	1,646.59
		Bending moment (kN · m)	802.58	918.18	986.78	956.99
	In soil	Axial load (N)	942.75	1,286.56	1,446.57	1,716.94
		Bending moment (kN · m)	720.12	768.06	811.70	828.83
Mooring force	Pile head	Axial load (N)	1,039.14	1,061.63	1,026.29	872.94
		Bending moment (kN · m)	335.17	366.90	370.63	352.33
	In sea	Axial load (N)	1,065.56	1,088.06	1,052.72	899.36
		Bending moment (kN · m)	200.36	209.89	196.66	174.10
	In soil	Axial load (N)	1,153.84	1,159.85	1,119.88	959.33
		Bending moment (kN · m)	159.01	166.22	171.43	173.40
Crane work (sea → land)	Pile head	Axial load (N)	2,713.82	1,934.01	2,228.81	3,893.55
		Bending moment (kN · m)	1,704.77	1,714.12	1,356.04	1,108.50
	In sea	Axial load (N)	2,740.25	1,960.43	2,255.23	3,961.04
		Bending moment (kN · m)	1,046.87	995.77	685.57	496.65
	In soil	Axial load (N)	2,827.15	2,043.05	2,323.82	3,982.61
		Bending moment (kN · m)	719.87	731.98	719.28	720.72
Crane work (sea ← land)	Pile head	Axial load (N)	4,544.81	2,487.90	1,772.76	1,964.72
		Bending moment (kN · m)	668.36	1,103.64	1,769.21	1,991.72
	In sea	Axial load (N)	4,632.12	2,514.33	1,799.18	1,991.15
		Bending moment (kN · m)	508.80	570.55	959.99	1,053.88
	In soil	Axial load (N)	4,653.66	2,589.20	1,865.70	2,060.38
		Bending moment (kN · m)	607.95	682.58	772.17	804.37
Level 1 earthquake ground motion (sea → land)	Pile head	Axial load (N)	551.46	912.07	1,099.78	1,436.69
		Bending moment (kN · m)	1,560.29	1,842.67	2,076.49	2,109.19
	In sea	Axial load (N)	577.88	938.50	1,126.20	1,463.11
		Bending moment (kN · m)	935.11	1,064.37	1,135.68	1,097.73
	In soil	Axial load (N)	655.15	1,010.38	1,192.65	1,533.29
		Bending moment (kN · m)	832.39	886.50	935.54	954.88
Level 1 earthquake ground motion (sea ← land)	Pile head	Axial load (N)	1,372.42	1,164.52	946.48	486.58
		Bending moment (kN · m)	1,628.39	1,878.07	2,047.40	2,040.62
	In sea	Axial load (N)	1,398.84	1,190.95	1,002.90	513.00
		Bending moment (kN · m)	982.72	1,088.29	1,115.67	1,052.50
	In soil	Axial load (N)	1,487.30	1,262.69	1,069.48	583.50
		Bending moment (kN · m)	842.33	891.73	934.30	950.89
Level 1 earthquake ground motion, considering crane (sea → land)	Pile head	Axial load (N)	-41.00	911.63	2,615.99	6,283.57
		Bending moment (kN · m)	4,374.29	4,914.19	4,912.79	4,623.72
	In sea	Axial load (N)	-14.58	938.06	2,642.41	6,309.99
		Bending moment (kN · m)	2,588.53	2,785.71	2,559.89	2,219.58
	In soil	Axial load (N)	62.85	1,010.38	2,710.27	6,370.77
		Bending moment (kN · m)	2,260.78	2,384.65	2,465.01	2,500.48
Level 1 earthquake ground motion, considering crane (sea ← land)	Pile head	Axial load (N)	6,661.61	2,942.82	913.83	-748.07
		Bending moment (kN · m)	3,356.92	4,324.53	5,360.25	5,552.53
	In sea	Axial load (N)	6,688.04	2,969.24	940.25	-721.65
		Bending moment (kN · m)	1,867.40	2,375.51	2,854.60	2,825.44
	In soil	Axial load (N)	6,767.49	3,042.64	1,007.41	-650.93
		Bending moment (kN · m)	2,149.19	2,334.58	2,517.30	2,582.55
Storm (sea → land)	Pile head	Axial load (N)	374.03	792.29	1,777.08	3,884.62
		Bending moment (kN · m)	1,675.41	1,831.59	1,679.51	1,479.83
	In sea	Axial load (N)	400.45	818.71	1,803.51	3,911.04
		Bending moment (kN · m)	981.85	1,023.76	838.13	652.46
	In soil	Axial load (N)	478.09	891.40	1,872.41	3,973.40
		Bending moment (kN · m)	858.81	901.10	920.87	932.00
Storm (sea ← land)	Pile head	Axial load (N)	3,340.66	1,689.69	986.72	810.95
		Bending moment (kN · m)	773.67	1,133.55	1,623.22	1,764.15
	In sea	Axial load (N)	3,427.97	1,716.12	1,013.15	837.37
		Bending moment (kN · m)	487.51	597.87	866.43	913.44
	In soil	Axial load (N)	3,448.40	1,790.52	1,080.11	907.40
		Bending moment (kN · m)	600.19	665.07	737.02	762.57

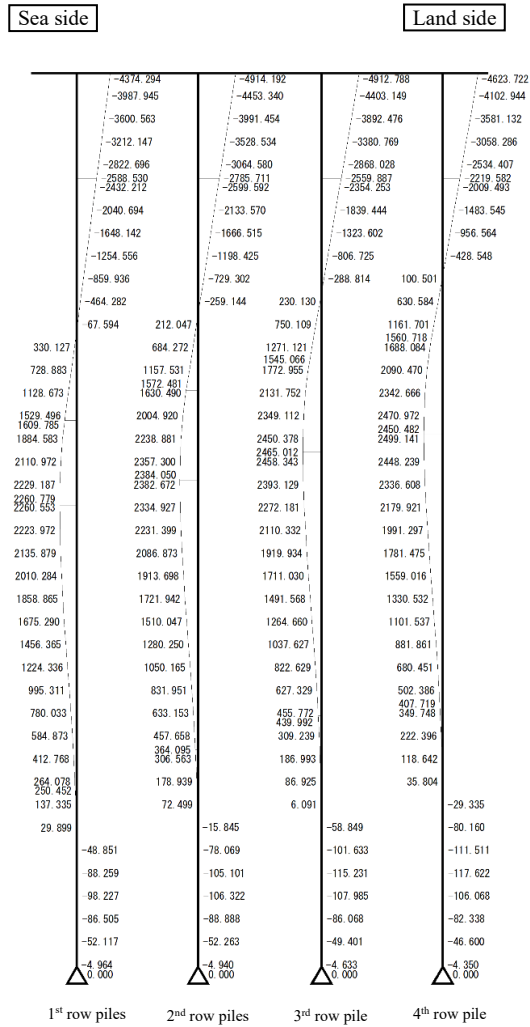


**Figure 5.4.10 Distribution diagram of bending moment
(Level 1 earthquake ground motion, considering crane, land → sea)**

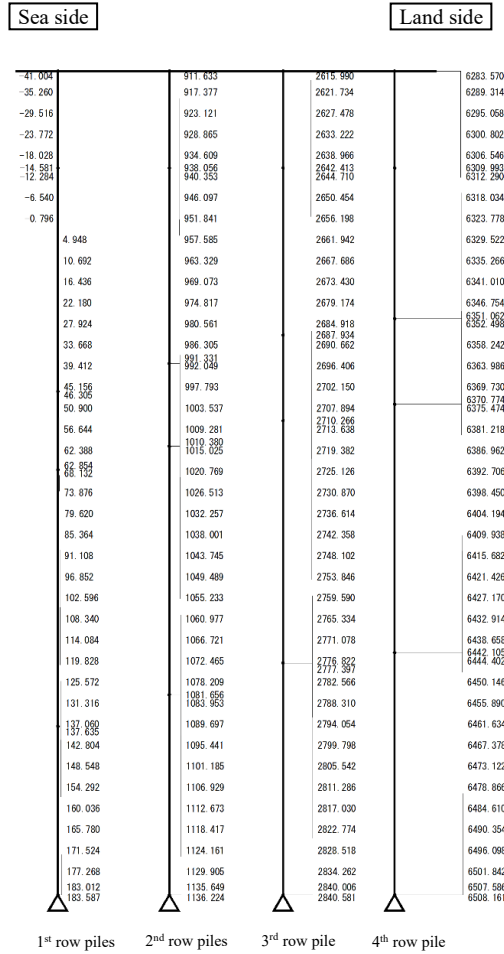


Figure 5.4.11 Distribution diagram of axial load

(Level 1 earthquake ground motion, considering crane, sea → land)

(7) Results of Stability Verification

1) Verification of stress

The performance verification related to stress generated in the piles of the piled pier (design states other than accidental situation under Level 2 earthquake ground motion) is as follows.

$$m \left(\frac{S_d}{R_d} \right) \leq 1.0 \quad \left. \begin{array}{l} \\ \\ S_d = \gamma_s \cdot S_k \quad R_d = \gamma_R \cdot R_k \end{array} \right\} \quad (1)$$

(a) Case of compressive axial load

$$S_k = \left(\frac{\sigma_{c_k}}{red} + \sigma_{bc_k} \right) \quad \left. \begin{array}{l} \\ R_k = \sigma_{by_k} \end{array} \right\} \quad (2)$$

(b) Case of tensile axial load

$$S_k = \sigma_{t_k} + \sigma_{bt_k} \quad R_k = \sigma_{ly_k} \quad \left. \begin{array}{l} \\ S_k = -\sigma_{t_k} + \sigma_{bc_k} \quad R_k = \sigma_{by_k} \end{array} \right\} \quad (3)$$

where

red : Factor defined as the value obtained by dividing the axial compressive yield stress (see **Table 5.4.13**) by the characteristic value of yield stress

σ_t, σ_c : tensile stress due to axial tensile force and compressive stress due to axial compressive force acting on cross section (N/mm²)

σ_{bt}, σ_{bc} : maximum tensile stress and maximum compressive stress due to the bending moment acting on the cross section (N/mm²)

σ_{ty}, σ_{cy} : tensile yield stress and axial compressive yield stress related to the weak axis (N/mm²)

σ_{by} : bending compressive yield stress (N/mm²)

R_k : characteristic value related to resistance term (N/mm²)

S_k : characteristic value related to load term (N/mm²)

γ_R : partial factor that is multiplied with the resistance term

γ_S : partial factor that is multiplied with the load term

m : adjustment factor

The design values in **Eq. (1)** to **Eq. (3)** are calculated by **Eq. (4)**.

$$\left. \begin{aligned} \sigma_{t_k} &= \frac{P_k}{A}, \quad \sigma_{c_k} = \frac{P_k}{A} \\ \sigma_{bt_k} &= \frac{M_k}{Z}, \quad \sigma_{bc_k} = \frac{M_k}{Z} \end{aligned} \right\} \quad (4)$$

where

A : cross-sectional area of pile (mm²)

P : axial load of pile (N)

Z : section modulus of pile (mm³)

M : bending moment of pile (N•mm)

Axial compressive yield stress can be calculated by the equations in **Table 5.4.13**.

Table 5.4.13 Axial compressive yield stress

SKK400	SKK490
a) When $l/r \leq 19$, 235 b) When $19 < l/r \leq 93$, $235 - 1.4 \left(\frac{l}{r} - 19 \right)$ c) When $l/r > 93$, $\frac{2.0 \times 10^6}{6.7 \times 10^3 + \left(\frac{l}{r} \right)^2}$	a) When $l/r \leq 16$, 315 b) When $16 < l/r \leq 80$, $315 - 2.1 \left(\frac{l}{r} - 16 \right)$ c) When $l/r > 80$, $\frac{2.0 \times 10^6}{5.0 \times 10^3 + \left(\frac{l}{r} \right)^2}$
SM490Y	SM570
a) When $l/r \leq 15$, 355 b) When $15 < l/r \leq 76$, $355 - 2.6 \left(\frac{l}{r} - 15 \right)$ c) When $l/r > 76$, $\frac{2.0 \times 10^6}{4.4 \times 10^3 + \left(\frac{l}{r} \right)^2}$	a) When $l/r \leq 13$, 450 b) When $13 < l/r \leq 67$, $450 - 3.7 \left(\frac{l}{r} - 13 \right)$ c) When $l/r > 67$, $\frac{2.0 \times 10^6}{3.5 \times 10^3 + \left(\frac{l}{r} \right)^2}$

l : effective buckling length of member (mm)

r : radius of gyration of member total cross section (mm)

The values shown in **Table 5.4.14** can be used for the partial factors in verification of the stresses generated in wharf piles.

Table 5.4.14 Partial factors used in verification of stresses generated in piles of pier

Object design state of verification	Installed water depth	Partial factor γ_R multiplied with resistance term	Partial factor γ_S multiplied with load term	Adjustment factor m
Stress generated in wharf piles (variable action due to surcharge (during work))	All depths	- (1.00)	- (1.00)	1.67
Stress generated in wharf piles (variable action due to surcharge (during storm))	All depths	- (1.00)	- (1.00)	1.12
Stress generated in wharf piles (variable action due to ship mooring force)	All depths	- (1.00)	- (1.00)	1.67
Compressive stress generated in wharf piles (variable action due to ship berthing force)	< 12.0 m	0.97	1.34	- (1.00)
	\geq 12.0 m	1.01	1.29	
Tensile stress generated in wharf piles (variable action due to ship berthing force)	All depths	- (1.00)	- (1.00)	1.67
Stress generated in wharf piles (variable action due to Level 1 earthquake ground motion)	All depths	- (1.00)	- (1.00)	1.12

The axial compressive yield stress of each pile is shown in **Table 5.4.15**. An example of verification results for pile stress is shown in **Table 5.4.16** and **Table 5.4.17**. The action resistance ratio shows its maximum value (= 0.944) in the 4th row piles (land side piles) under Level 1 earthquake ground motion.

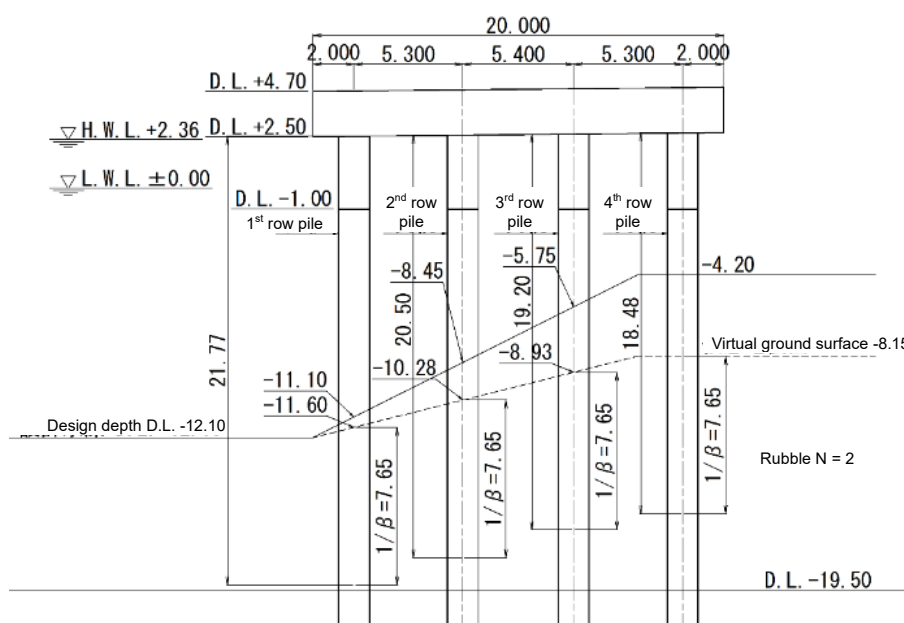


Figure 5.4.12 Effective buckling length of piles

Table 5.4.15 Reduction coefficients of axial compressive yield stress of piles

	Dimensions	Material	l (cm)	r (cm)	l/r	Axial compressive yield stress	red
1 st row piles	φ1,500×16t	SKK490	2,177	52.47	41.49	261.5	0.830
	φ1,500×16t	SKK400				203.5	0.866
2 nd row piles	φ1,500×16t	SKK490	2,050	52.47	39.07	266.6	0.846
	φ1,500×16t	SKK400				206.9	0.880
3 rd row piles	φ1,500×16t	SKK490	1,920	52.47	36.59	271.8	0.863
	φ1,500×16t	SKK400				210.4	0.895
4 th row piles	φ1,500×16t	SKK490	1,848	52.47	35.22	274.6	0.872
	φ1.500×16t	SKK400				212.3	0.903

Note) The effective buckling length of the piles was defined as the distance from the lower edge of the superstructure to the virtual fixed point (**Figure 5.4.12**).

Table 5.4.16 Example of verification results for pile stress
Level 1 earthquake ground motion, considering crane (sea → land)

	Unit	1 st row piles	2 nd row piles	3 rd row piles	4 th row piles
	Cross-sectional area A	(cm ²)	746	746	746
Section modulus Z	(cm ³)	27,382	27,382	27,382	27,382
Design axial load P	(kN)	-41	912	2,616	6,284
Design bending moment M	(kN · m)	4,374	4,914	4,913	4,624
$\sigma_{ck}=P/A$	(N/mm ²)	-	12.2	35.1	84.2
$\sigma_{bck}=M/Z$	(N/mm ²)	-	179.5	179.4	168.9
$\sigma_{tk}=P/A$	(N/mm ²)	0.5	-	-	-
$\sigma_{btik}=M/Z$	(N/mm ²)	159.8	-	-	-
σ_{byk}	(N/mm ²)	315	315	315	315
σ_{tyk}	(N/mm ²)	315	315	315	315
Reduction coefficient red		0.830	0.846	0.863	0.872
Axial compressive yield stress	(N/mm ²)	261.5	266.6	271.8	274.6
Adjustment factor m		1.12	1.12	1.12	1.12
Action resistance ratio		0.570	0.689	0.782	0.944
Verification		OK	OK	OK	OK
	Unit	1 st row piles	2 nd row piles	3 rd row piles	4 th row piles
Cross-sectional area A	(cm ²)	699	699	699	699
Section modulus Z	(cm ³)	25,635	25,635	25,635	25,635
Design axial load P	(kN)	-15	938	2,642	6,310
Design bending moment M	(kN · m)	2,589	2,786	2,560	2,220
$\sigma_{ck}=P/A$	(N/mm ²)	-	13.4	37.8	90.3
$\sigma_{bck}=M/Z$	(N/mm ²)	-	108.7	99.9	86.6
$\sigma_{tk}=P/A$	(N/mm ²)	0.2	-	-	-
$\sigma_{btik}=M/Z$	(N/mm ²)	101.0	-	-	-
σ_{byk}	(N/mm ²)	315	315	315	315
σ_{tyk}	(N/mm ²)	315	315	315	315
Reduction coefficient red		0.830	0.846	0.863	0.872
Axial compressive yield stress	(N/mm ²)	261.5	266.6	271.8	274.6
Adjustment factor m		1.12	1.12	1.12	1.12
Action resistance ratio		0.360	0.443	0.511	0.676
Verification		OK	OK	OK	OK
	Unit	1 st row piles	2 nd row piles	3 rd row piles	4 th row piles
Cross-sectional area A	(cm ²)	739	739	739	739
Section modulus Z	(cm ³)	27,123	27,123	27,123	27,123
Design axial load P	(kN)	63	1,010	2,710	6,371
Design bending moment M	(kN · m)	2,261	2,384	2,465	2,500
$\sigma_{ck}=P/A$	(N/mm ²)	0.9	13.7	36.7	86.2
$\sigma_{bck}=M/Z$	(N/mm ²)	83.4	87.9	90.9	92.2
$\sigma_{tk}=P/A$	(N/mm ²)	-	-	-	-
$\sigma_{btik}=M/Z$	(N/mm ²)	-	-	-	-
σ_{byk}	(N/mm ²)	315	315	315	315
σ_{tyk}	(N/mm ²)	315	315	315	315
Reduction coefficient red		0.830	0.846	0.863	0.872
Axial compressive yield stress	(N/mm ²)	261.5	266.6	271.8	274.6
Adjustment factor m		1.12	1.12	1.12	1.12
Action resistance ratio		0.300	0.370	0.474	0.679
Verification		OK	OK	OK	OK

Table 5.4.17 Example of verification results for pile stress
Level 1 earthquake ground motion, considering crane (sea ← land)

	Unit	1 st row piles	2 nd row piles	3 rd row piles	4 th row piles	
Pile head	Cross-sectional area A	(cm ²)	746	746	746	746
	Section modulus Z	(cm ³)	27,382	27,382	27,382	27,382
	Design axial load P	(kN)	6,662	2,943	914	-748
	Design bending moment M	(kN · m)	3,357	4,325	5,360	5,553
	$\sigma_{ck}=P/A$	(N/mm ²)	89.3	39.5	12.3	-
	$\sigma_{bck}=M/Z$	(N/mm ²)	122.6	157.9	195.8	-
	$\sigma_{tk}=P/A$	(N/mm ²)	-	-	-	10.0
	$\sigma_{btk}=M/Z$	(N/mm ²)	-	-	-	202.8
	σ_{byk}	(N/mm ²)	315	315	315	315
	σ_{lyk}	(N/mm ²)	315	315	315	315
	Reduction coefficient red		0.830	0.846	0.863	0.872
	Axial compressive yield stress	(N/mm ²)	261.5	266.6	271.8	274.6
	Adjustment factor m		1.12	1.12	1.12	1.12
	Action resistance ratio		0.818	0.727	0.747	0.757
Verification		OK	OK	OK	OK	
In sea	Unit	1 st row piles	2 nd row piles	3 rd row piles	4 th row piles	
	Cross-sectional area A	(cm ²)	699	699	699	699
	Section modulus Z	(cm ³)	25,635	25,635	25,635	25,635
	Design axial load P	(kN)	6,688	2,969	940	-722
	Design bending moment M	(kN · m)	1,867	2,376	2,855	2,825
	$\sigma_{ck}=P/A$	(N/mm ²)	95.7	42.5	13.5	-
	$\sigma_{bck}=M/Z$	(N/mm ²)	72.8	92.7	111.4	-
	$\sigma_{tk}=P/A$	(N/mm ²)	-	-	-	10.3
	$\sigma_{btk}=M/Z$	(N/mm ²)	-	-	-	110.2
	σ_{byk}	(N/mm ²)	315	315	315	315
	σ_{lyk}	(N/mm ²)	315	315	315	315
	Reduction coefficient red		0.830	0.846	0.863	0.872
	Axial compressive yield stress	(N/mm ²)	261.5	266.6	271.8	274.6
	Adjustment factor m		1.12	1.12	1.12	1.12
Action resistance ratio		0.669	0.508	0.451	0.429	
Verification		OK	OK	OK	OK	
In soil	Unit	1 st row piles	2 nd row piles	3 rd row piles	4 th row piles	
	Cross-sectional area A	(cm ²)	739	739	739	739
	Section modulus Z	(cm ³)	27,123	27,123	27,123	27,123
	Design axial load P	(kN)	6,767	3,043	1,007	-651
	Design bending moment M	(kN · m)	2,149	2,335	2,517	2,583
	$\sigma_{ck}=P/A$	(N/mm ²)	91.6	41.2	13.6	-
	$\sigma_{bck}=M/Z$	(N/mm ²)	79.2	86.1	92.8	-
	$\sigma_{tk}=P/A$	(N/mm ²)	-	-	-	8.8
	$\sigma_{btk}=M/Z$	(N/mm ²)	-	-	-	95.2
	σ_{byk}	(N/mm ²)	315	315	315	315
	σ_{lyk}	(N/mm ²)	315	315	315	315
	Reduction coefficient red		0.830	0.846	0.863	0.872
	Axial compressive yield stress	(N/mm ²)	261.5	266.6	271.8	274.6
	Adjustment factor m		1.12	1.12	1.12	1.12
Action resistance ratio		0.674	0.479	0.386	0.370	
Verification		OK	OK	OK	OK	

2) Verification of bearing capacity

Here, a verification of the bearing capacity of piles in the variable situation related to Level 1 earthquake ground motion is carried out as an example of verification of bearing capacity.

$$m \left(\frac{S_d}{R_d} \right) \leq 1.0$$

$$S_d = \gamma_s \cdot S_k \quad R_d = \gamma_R \cdot R_k$$

where

R_k : characteristic value related to the resistance term (kN)

S_k : characteristic value related to the load term (kN)

γ_R : partial factor that is multiplied with the resistance term (= 1.0)

γ_s : partial factor that is multiplied with the load term (= 1.0)

m : adjustment factor

pulling pile: 2.5

pushing pile (bearing pile): 1.5

where

$$R_k = R_{pk} + R_{fk}$$

R_{pk} : characteristic value of the base resistance force of a pile

R_{fk} : characteristic value of the skin friction force of a pile

i) Characteristic value of end resistance of a pile (R_{pk})

$$R_{pk} = 300 N \cdot \alpha \cdot A_P$$

where

$$N_1 = 50$$

$$\bar{N}_2 = (3.5 \times 25 + 2.5 \times 50) / (4 \times 1.5) = 35.4$$

$$N = (N_1 + \bar{N}_2) / 2 = (50 + 35.4) / 2 = 42.70$$

$$A_P = \pi \times 1.4997^2 / 4 = 1.766 \text{ m}^2$$

α : pile end plugging ratio (from actual results of neighboring construction, set at 0.40)

Therefore,

$$R_{pk} = 300 \times 42.70 \times 1.766 \times 0.4 = 9,048.984 \text{ kN}$$

ii) Characteristic value of skin friction force of pile (R_{fk})

$$R_{fk} = \sum \overline{\gamma_{fki}} A_{si} = 2 \sum \bar{N}_i A_{si}$$

where

$$A_{si} = \pi \times 1.4997 \cdot l_i = 4.711 \cdot l_i \text{ (m}^2\text{)}$$

• Skin friction force of 1st row pile (virtual ground surface -11.60 m)

$$R_{fk} = \{(2 \times 2 \times 7.90 + 2 \times 8 \times 10.0 + 2 \times 25 \times 3.50 + 2 \times 50 \times 2.50)\} \times 4.711 = 2,904.803 \text{ kN}$$

- Skin friction force of 2nd row pile (virtual ground surface -10.28 m)

$$R_{fk} = \{(2 \times 2 \times 9.225 + 2 \times 8 \times 10.0 + 2 \times 25 \times 3.50 + 2 \times 50 \times 2.50)\} \times 4.711 = 2.929.771 \text{ kN}$$

- Skin friction force of 3rd row pile (virtual ground surface -8.93 m)

$$R_{fk} = \{(2 \times 2 \times 10.575 + 2 \times 8 \times 10.0 + 2 \times 25 \times 3.50 + 2 \times 50 \times 2.50)\} \times 4.711 = 2.955.210 \text{ kN}$$

- Skin friction force of 4th row pile (virtual ground surface -8.15 m)

$$R_{fk} = \{(2 \times 2 \times 11.35 + 2 \times 8 \times 10.0 + 2 \times 25 \times 3.50 + 2 \times 50 \times 2.50)\} \times 4.711 = 2.969.814 \text{ kN}$$

iii) Characteristic value of axial resistance force of pile

$$R_{tk} = R_{pk} + R_{fk}$$

1st row pile: (pushing)

$$R_{tk} = 9,048.984 + 2,904.803 = 11,953.787 \text{ kN}$$

2nd row pile: (pushing)

$$R_{tk} = 9,048.984 + 2,929.771 = 11,978.755 \text{ kN}$$

3rd row pile: (pushing)

$$R_{tk} = 9,048.984 + 2,955.210 = 12,004.194 \text{ kN}$$

4th row pile: (pushing)

$$R_{tk} = 9,048.984 + 2,969.814 = 12,018.798 \text{ kN}$$

4th row pile: (pulling)

$$R_{tk} = 2,969.814 \text{ kN}$$

The design values of the axial resistance force are calculated from the end resistance and skin friction force of each pile. The verification results for bearing capacity are shown in **Table 5.4.18**. The most severe condition for the bearing capacity of the piles is sea side piles during crane work.

Table 5.4.18 Results of verification of pile bearing capacity

Action situation	Pile row	Design value of axial load P_d (kN/pile)	Design value of axial resistance force R_d (kN/pile)	Adjustment factor m	Action resistance ratio mR_d/P_d	Evaluation
Permanent (surcharge)	1 st row pile	1,421.85	11,953.79	2.50	0.297	O.K
	2 nd row pile	1,517.71	11,978.76	2.50	0.317	O.K
	3 rd row pile	1,517.92	12,004.19	2.50	0.316	O.K
	4 th row pile	1,422.53	12,018.80	2.50	0.296	O.K
Berthing	1 st row pile	1,057.92	11,953.79	2.50	0.221	O.K
	2 nd row pile	1,407.71	11,978.76	2.50	0.294	O.K
	3 rd row pile	1,573.72	12,004.19	2.50	0.328	O.K
	4 th row pile	1,840.66	12,018.80	2.50	0.383	O.K
Mooring force	1 st row pile	1,258.57	11,953.79	2.50	0.263	O.K
	2 nd row pile	1,281.47	11,978.76	2.50	0.267	O.K
	3 rd row pile	1,246.54	12,004.19	2.50	0.260	O.K
	4 th row pile	1,093.43	12,018.80	2.50	0.227	O.K
Crane work (sea → land)	1 st row pile	2,933.25	11,953.79	2.50	0.613	O.K
	2 nd row pile	2,153.85	11,978.76	2.50	0.450	O.K
	3 rd row pile	2,449.06	12,004.19	2.50	0.510	O.K
	4 th row pile	4,114.04	12,018.80	2.50	0.856	O.K
Crane work (sea ← land)	1 st row pile	4,764.24	11,953.79	2.50	0.996	O.K
	2 nd row pile	2,707.74	11,978.76	2.50	0.565	O.K
	3 rd row pile	1,993.01	12,004.19	2.50	0.415	O.K
	4 th row pile	2,185.21	12,018.80	2.50	0.455	O.K
Level 1 earthquake ground motion (sea → land)	1 st row pile	770.89	11,953.79	1.50	0.097	O.K
	2 nd row pile	1,131.91	11,978.76	1.50	0.142	O.K
	3 rd row pile	1,320.03	12,004.19	1.50	0.165	O.K
	4 th row pile	1,657.18	12,018.80	1.50	0.207	O.K
Level 1 earthquake ground motion (sea ← land)	1 st row pile	1,591.85	11,953.79	1.50	0.200	O.K
	2 nd row pile	1,384.36	11,978.76	1.50	0.173	O.K
	3 rd row pile	1,196.73	12,004.19	1.50	0.150	O.K
	4 th row pile	707.07	12,018.80	1.50	0.088	O.K
Level 1 earthquake ground motion, considering crane (sea → land)	1 st row pile	178.42	11,953.79	1.50	0.022	O.K
	2 nd row pile	1,131.47	11,978.76	1.50	0.142	O.K
	3 rd row pile	2,836.24	12,004.19	1.50	0.354	O.K
	4 th row pile	6,504.06	12,018.80	1.50	0.812	O.K
Level 1 earthquake ground motion, considering crane (sea ← land)	1 st row pile	6,881.04	11,953.79	1.50	0.863	O.K
	2 nd row pile	3,162.66	11,978.76	1.50	0.396	O.K
	3 rd row pile	1,134.08	12,004.19	1.50	0.142	O.K
	4 th row pile	-527.58	2,969.81	2.50	0.444	O.K
Storm (sea → land)	1 st row pile	593.46	11,953.79	1.50	0.074	O.K
	2 nd row pile	1,012.13	11,978.76	1.50	0.127	O.K
	3 rd row pile	1,997.34	12,004.19	1.50	0.250	O.K
	4 th row pile	4,105.11	12,018.80	1.50	0.512	O.K
Storm (land ← sea)	1 st row pile	3,560.09	11,953.79	1.50	0.447	O.K
	2 nd row pile	1,909.53	11,978.76	1.50	0.239	O.K
	3 rd row pile	1,206.98	12,004.19	1.50	0.151	O.K
	4 th row pile	1,031.44	12,018.80	1.50	0.129	O.K

Note) In the table, + axial load indicates pushing force, and – indicates pulling force.

(8) Study of Embedment Length of Piles for Lateral Resistance

The embedment length of all vertical piles is set to $3/\beta$ or more under the virtual ground surface. As the β used in the study of embedment length, the β before corrosion is used.

$$3/\beta = 3 \times 7.77 = 23.31 \text{ m}$$

Because the virtual ground surface of the deepest piles, i.e., the 1st row piles, is -11.60 m, the necessary embedment length of the piles is as follows.

$$-(11.60 + 23.31) = -34.91 \text{ m}$$

Since the embedment depth of the piles, -35.5 m, is deeper than the above value, the embedment length for lateral resistance is secured.

As the joining position of the vertical piles, referring to the Specifications for Highway Bridges, Part IV Substructures, $1/2 M_{max}$ position was selected, which is the deeper of the position where the bending moment is $1/2$ of the maximum bending moment M_{max} ($1/2 M_{max}$ position), and the position obtained by multiplying the depth for the maximum bending moment in the ground l_{mF} by 1.2 ($1.2 l_{mF}$).

The depths of the pile joining positions necessary for each pile are as follows.

- 1st row piles

$$M_{max} = 2260.78 \text{ kN} \cdot \text{m} \text{ (-15.32 m)}$$

$$1/2 M_{max} = 1130.39 \text{ kN} \cdot \text{m} \text{ (-22.81 m)} \rightarrow -23.0 \text{ m}$$

- 2nd row piles

$$M_{max} = 2384.05 \text{ kN} \cdot \text{m} \text{ (-14.21 m)}$$

$$1/2 M_{max} = 1192.03 \text{ kN} \cdot \text{m} \text{ (-21.78 m)} \rightarrow -22.0 \text{ m}$$

- 3rd row piles

$$M_{max} = 2517.30 \text{ kN} \cdot \text{m} \text{ (-13.11 m)}$$

$$1/2 M_{max} = 1258.65 \text{ kN} \cdot \text{m} \text{ (-20.66 m)} \rightarrow -21.0 \text{ m}$$

- 4th row piles

$$M_{max} = 2582.55 \text{ kN} \cdot \text{m} \text{ (-12.49 m)}$$

$$1/2 M_{max} = 1291.28 \text{ kN} \cdot \text{m} \text{ (-20.03 m)} \rightarrow -20.5 \text{ m}$$

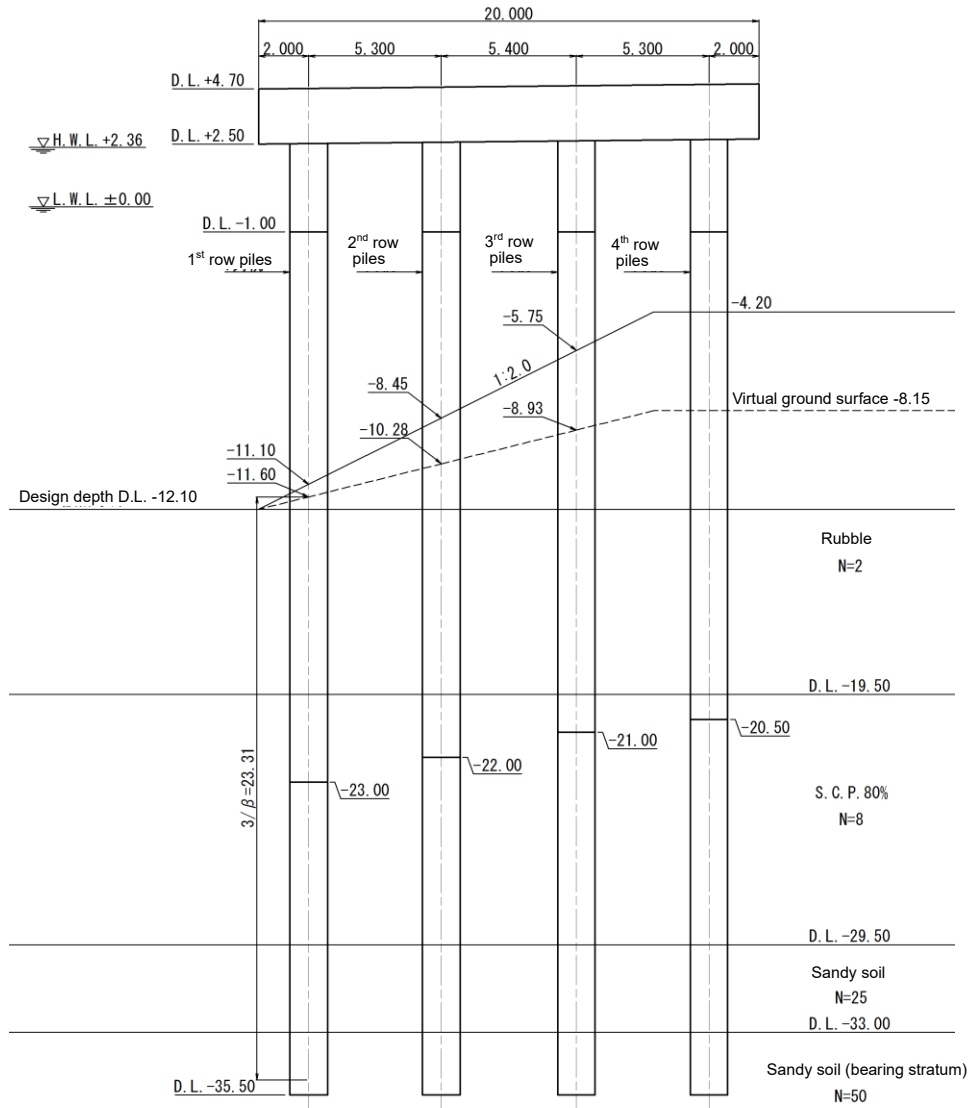


Figure 5.4.13 Embedment length of piles

(9) Verification for Level 2 earthquake ground motion

Based on the pier cross section, verification is performed by an integrated analysis of a pier and the ground by a seismic response analysis (FLIP) using the two dimensional effective stress method. As methods for the accidental situation of Level 2 earthquake ground motion are 1) response displacement method (in which the time history of the response displacement of the ground part is input to the pier framework), and 2) integrated analysis (nonlinear dynamic response analysis in which the pier, ground and earth-retaining structures are modeled simultaneously) are conceivable. Here, however, an example of integrated analysis is presented. (The calculation method, parameter setting method, etc. are omitted.)

The residual deformation diagrams of the total analysis region and the main part are shown in **Figure 5.4.14** and **Figure 5.4.15**, respectively, and a distribution diagram of the hourly maximum value of the excessive pore water pressure ratio ($= 1 - \sigma_m' / \sigma_{m0}'$) is shown in **Figure 5.4.16**.

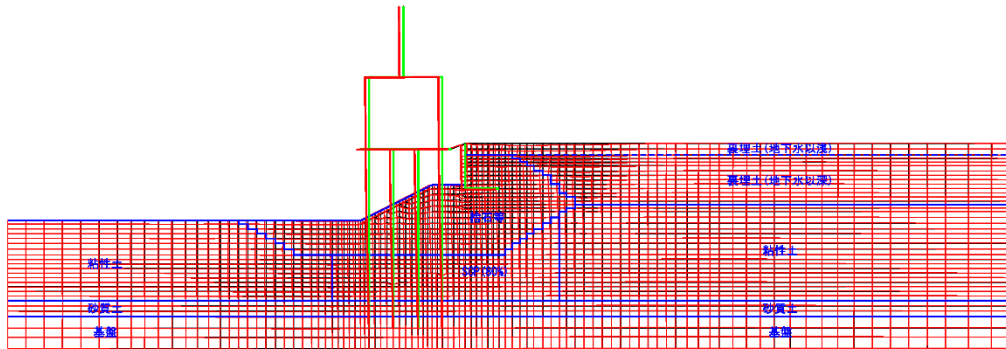


Figure 5.4.14 Residual deformation diagram (total analysis region): 1× scale

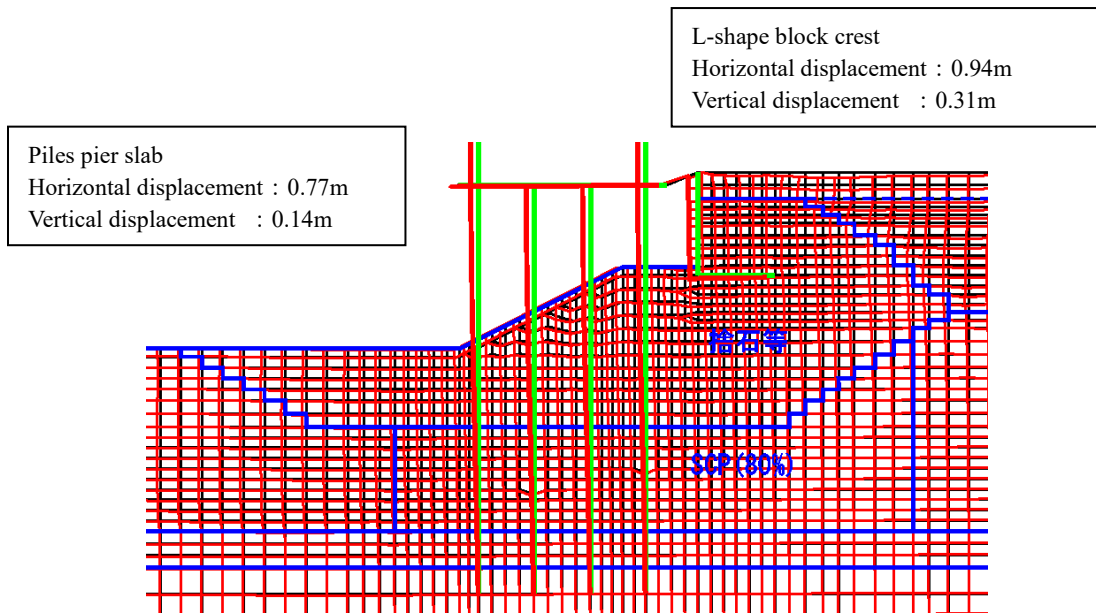


Figure 5.4.15 Residual deformation diagram (main part): 1× scale

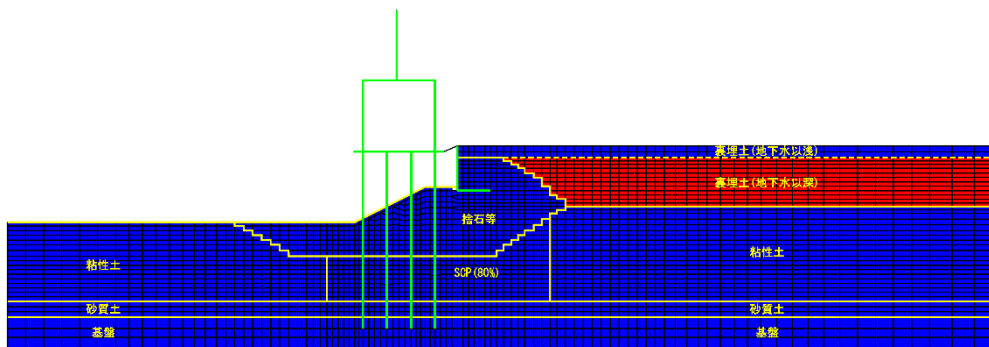


Figure 5.4.16 Distribution of hourly maximum values of excess pore water pressure ration
 $(= 1 - \sigma_m' / \sigma_{m0}')$

(10) Corrosion of Reinforcing Bars of Superstructure RC Beams

1) examination conditions

An examination on concrete is conducted under the following conditions.

Cement: Ordinary Portland cement

Water-cement ratio: 50 %

2) Reinforcing bar corrosion by carbonation

The design value of the carbonation depth y_d is calculated by the following equation.

$$y_d = \gamma_{cb} \alpha_d \sqrt{t}$$

where

γ_{cb} : safety factor considered variation of the design value of the carbonation depth y_d (= 1.15)

α_d : design value of carbonation speed factor ($\text{mm}\cdot\text{y}^{-1/2}$)

$$\alpha_d = \alpha_k \beta_e \gamma_c$$

t : design service life (generally 50 years in the case of port and harbor facilities)

α_k : characteristic value of the carbonation speed factor ($\text{mm}\cdot\text{y}^{-1/2}$)

β_e : factor showing the degree of environmental action (= 1.0)

γ_c : material factor of concrete (= 1.0)

The following equation is used to obtain the characteristic value α_k of the carbonation speed factor.

$$\alpha_k = \gamma_p \alpha_p$$

$$\alpha_p = -3.57 + 9.0 W/C$$

where

γ_p : safety factor for accuracy of α_p (= 1.1)

W/C : water-cement ratio of concrete

Set at $W/C = 50\%$.

$$\alpha_p = -3.57 + 9.0 \times 0.50 = 0.930$$

$$\alpha_k = 1.1 \times 0.930 = 1.023$$

$$\alpha_d = 1.023 \times 1.0 \times 1.0 = 1.023$$

$$y_d = 1.15 \times 1.023 \sqrt{50} = 8.3 \text{ mm}$$

The limit depth of reinforcing bar corrosion y_{lim} is calculated by the following equation.

$$y_{lim} = c - c_k$$

where

c : expected value of covering concrete (mm)

Here, set to 70 mm.

c_k : remaining carbonation (mm)

Generally set to 25 mm under marine environments.

$$y_{lim} = 70 - 25 = 45 \text{ mm} > y_d = 8.3 \text{ mm}$$

Therefore, the concrete structure is safe against reinforcing bar corrosion due to carbonation.

3) Corrosion of reinforcing bars by penetration of chloride ions

Here, the reinforcing bars on the underside of the normal straight beam G₄ are studied.

The design value C_d of the chloride ion concentration at the position of the reinforcing bars is obtained by the following equation. Here, the chloride ion concentration in the concrete at the time of mixing is assumed to be 0.

$$C_d = \gamma_{cl} C_o \left(1 - \operatorname{erf} \left(\frac{0.1c}{2\sqrt{D_d t}} \right) \right) + C_i$$

where

γ_{cl} : safety factor considering the dispersion of the design value C_d of the chloride ion concentration at the position of the reinforcing bars (= 1.3)

C_o : chloride ion concentration at the surface of the concrete

c : design value of the concrete cover (94 mm)

D_d : design diffusion coefficient for chloride ions (cm²/y)

t : design service life (y)

erf : error function

C_i : initial chloride ion concentration (0.3 kg/m³)

When the distance between the sea level (H.W.L) and the bottom surface of the members of the concrete superstructure of a piled pier is on the order of 0 to 2 m, the chloride ion concentration at the surface of the concrete C_o can be obtained by the following equation based on actual measured data.

$$C_o = -6.0x + 15.1$$

where

x : distance from sea level (H.W.L) to the bottom surface of a member (m)

$$C_o = -6.0 \cdot (2.50 - 2.36) + 15.1 = 14.26$$

The design diffusion coefficient D_d for chloride ions is obtained by the following equation.

$$D_d = \gamma_c D_k + \lambda \left(\frac{w}{l} \right) D_o$$

where

γ_c : material factor of concrete (= 1.0)

D_k : characteristic value of diffusion coefficient for chloride ions in concrete (cm²/y)

λ : factor showing the effect of cracking on the diffusion coefficient (1.5)

D_o : constant expressing the effect of cracking on the migration of chloride ions in concrete
(= 400 cm²/y)

w/l : ratio of crack width to crack interval

$$w/l = (\sigma_{se}/E_s + \varepsilon'_{csd})$$

σ_{se} : increment of reinforcing bar stress (40.5 N/mm²)

E_s : Young's modulus of reinforcing bars (2.0×10^5 N/mm²)

ε'_{csd} : value for considering an increase in crack width due to concrete shrinkage and creep, etc.

$$(100 \times 10^{-6})$$

$$w/l = 40.5/(2.0 \times 10^5) + 100 \times 10^{-6} = 3.03 \times 10^{-4}$$

The characteristic value D_k of the diffusion coefficient of chloride ions in concrete can be obtained for blast furnace slag cement by using the following predictive equation.

$$\log_{10} D_k = 2.5 (W/C) - 1.8 = 2.5 \cdot 0.5 - 1.8 = -0.55$$

$$D_k = 0.282$$

$$D_d = 1.0 \times 0.282 + 1.5 \times 3.03 \times 10^{-4} \times 400 = 0.464$$

$$C_d = 1.3 \times 14.26 \times \left(1 - \operatorname{erf} \left(\frac{0.1 \times 94}{2\sqrt{0.464t}} \right) \right) + 0.3$$

The relationship between the chloride ion concentration calculated using the above equation and elapsed time (years) is as shown in **Figure 5.4.17**. Assuming the general value of 2.0 kg/m^3 as the limit concentration for the initiation of corrosion in reinforcing bars C_{lim} , the limit concentration for the initiation of corrosion in reinforcing bars is reached after 34 years.

$$C_d/C_{lim} = 3.40/2.0 = 1.70 > 1.0 \text{ (after 50 years)}$$

From the above discussion, it is necessary to prepare and implement an appropriate maintenance control plan for corrosion of reinforcing bars caused by chloride ion penetration.

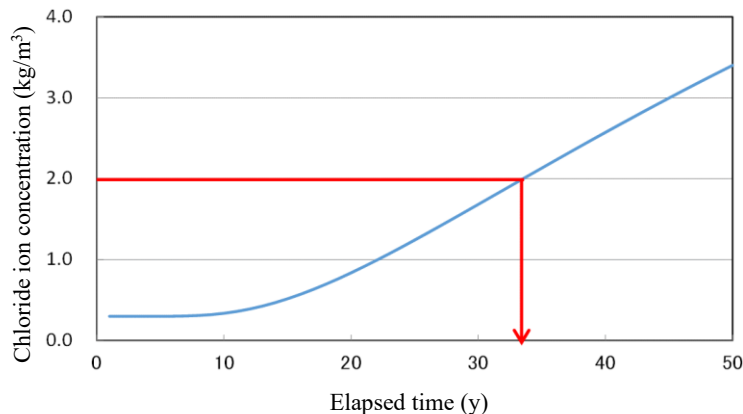


Figure. 5.4.17 Relationship of chloride ion concentration and elapsed time (blast furnace slag cement)

When using ordinary Portland cement as the cement, the characteristic value D_k of the diffusion coefficient for chloride ions in concrete can be obtained by using the following predictive equation. The relationship between the chloride ion concentration and elapsed time is as shown in **Figure 5.4.18**.

$$\log D_k = 3.4 (W/C) - 1.9$$

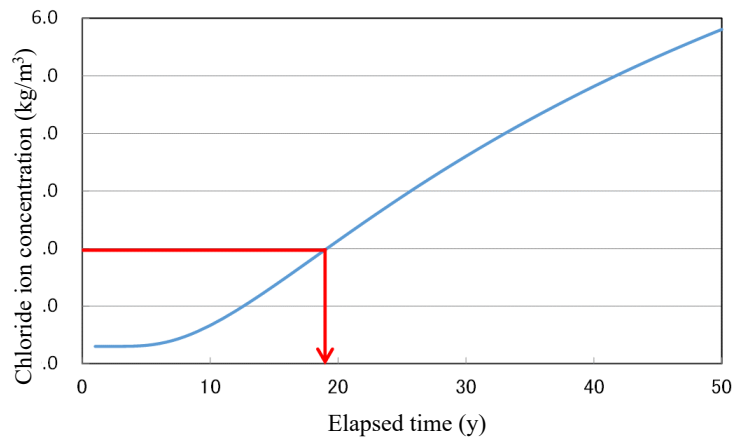


Figure 5.4.18 Relationship of chloride ion concentration and elapsed time (ordinary portland cement)

5. Steel Plate Cellular-Bulkhead Quaywall

(1) Basic section for review

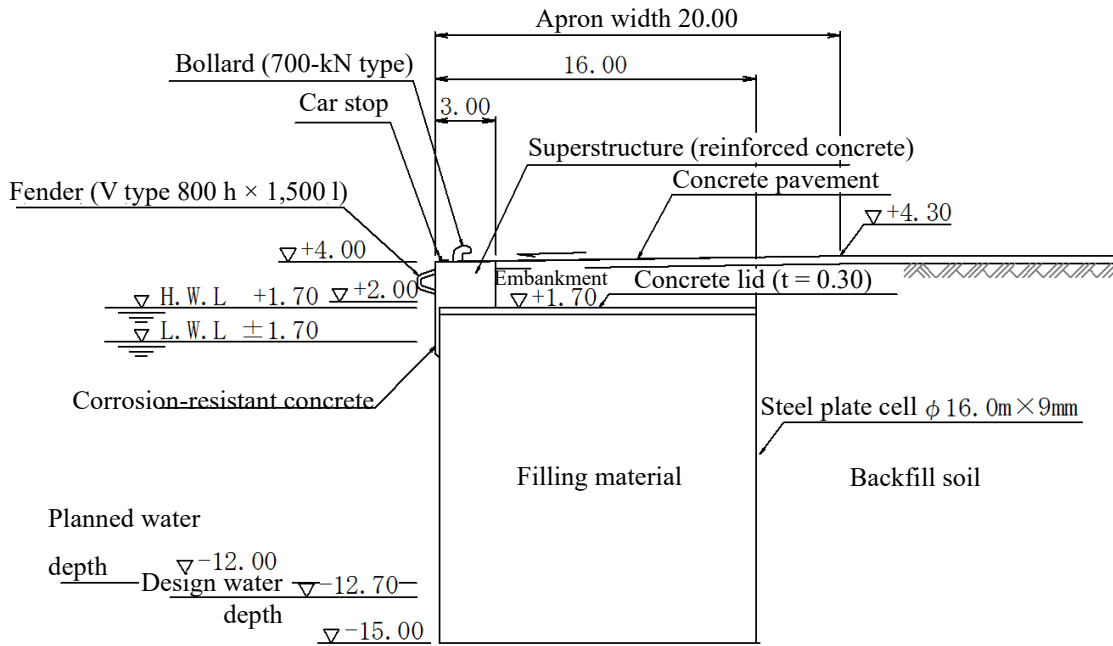


Figure 5.5.1 Standard cross-sectional view

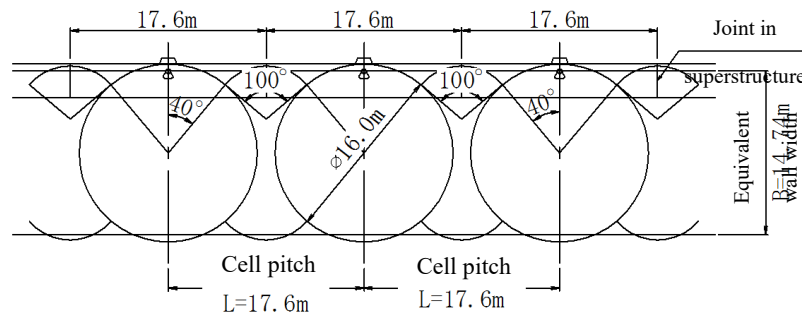


Figure 5.5.2 Cell arrangement plan

(2) Design conditions

1) Quaywall specifications

Planned water depth: -12.00 m

Design water depth: -12.70 m

(local seabed depth)

Crown height of quaywall: +4.00 m

Ground height at the back of the cell: +4.30 m

2) Use conditions

Facility category: Non high earthquake-resistant facility

Design ship: 30,000 DWT

Bollards: 700 kN-type bollards

Surcharge: 20 kN/m² in the permanent state

10 kN/m² under seismic motion

3) Natural conditions

Tide level: HWL +1.70 m

LWL ±0.00 m

Residual water level (RWL): +1.10 m

Unit weight of seawater ($\rho_w g$): 10.1 kN/m³

Ground

Soil type: sandy soil and $\bar{N} = 10$ from

-12.7 m to -17.7 m

sandy gravel and $\bar{N} = 30$ from

-17.7 m to -30.0 m

Unit weight:

$w = 20$ kN/m³ in saturated state

$w_t = 18$ kN/m³ in wet state

$w' = 10$ kN/m³ underwater

Angle of shear resistance:

$\phi = 30^\circ$ from -12.7 m to -17.7 m

$\phi = 34^\circ$ from -17.7 m to -30.0 m

Angle of wall friction: $\delta = \pm 15^\circ$

Seismic coefficient for verification: Level 1 seismic motion

Only the horizontal seismic coefficient should be considered as the seismic coefficient for verification.

$k_{hd} = 0.12$ (see the following section)

4) Calculation of the seismic coefficient for verification

- Calculation formula for the seismic coefficient for verification

The characteristic value of the seismic coefficient for verification of a cellular-bulkhead quaywall should be calculated using the following formula:

$$\begin{aligned}k_h &= 1.62 \left(\frac{D_a}{D_r} \right)^{-0.58} \cdot \frac{\alpha_c}{g} + 0.04 \\ &= 1.62 \left(\frac{10}{10} \right)^{-0.58} \cdot \frac{48.95}{980} + 0.04 \\ &= 0.12\end{aligned}$$

Where:

k_h : Seismic coefficient for verification

D_a : Allowable deformation (= 10 cm)

D_r : Basic deformation (= 10 cm)

α_c : Maximum value of corrected acceleration (= 48.95 cm/s²)

g : Gravitational acceleration (= 980 cm/s²)

- Filter for taking frequency characteristics into account

$$a(f) = \begin{cases} b & (f \leq 1\text{Hz}) \\ \frac{b}{1 - \{g(f)\}^2 + 8.8g(f)i} & (f > 1\text{Hz}) \end{cases}$$

$$g(f) = 0.34(f-1.0)$$

$$b = 1.09 \frac{H}{H_R} - 0.88 \frac{T_b}{T_{bR}} + 0.96 \frac{T_u}{T_{uR}} - 0.03 \frac{k_{CH}}{k_{CHR}} - 0.34$$

$$= 1.09 \cdot \frac{17.0}{15.0} - 0.88 \cdot \frac{0.752}{0.8} + 0.96 \cdot \frac{0.256}{0.4}$$

$$- 0.03 \cdot \frac{20,000}{12,650} - 0.34$$

$$= 0.635$$

Where

H : wall height (= 17.0 m)

H_R : standard wall height (= 15.0 m)

T_b : initial natural period of the hind ground (= 0.752 s)

T_{bR} : standard initial natural period of the hind ground (= 0.8 s)

T_u : initial natural period of the ground under the seabed (= 0.256 s)

T_{uR} : standard initial natural period of the ground under the seabed (= 0.4 s)

k_{CH} : lateral coefficient of subgrade reaction

$$(= 2\bar{N} = 2 \times 10 = 20 \text{ N/cm}^3 = 20,000 \text{ kN/m}^3)$$

k_{CHR} : standard lateral coefficient of subgrade reaction (= 12,650 kN/m³)

The value of b should be set in the range shown in the following equation, depending on the wall height H .

$$0.04H - 0.13 \leq b \leq 0.04H + 0.39$$

$$0.30 \leq b$$

- Maximum value of corrected acceleration α_c

$$p = 0.31 \ln(S/\alpha_f) - 0.08$$

$$= 0.31 \ln(1005.38/62.78) - 0.08$$

$$= 0.7798$$

$$\alpha_c = p \cdot \alpha_f = 0.7798 \times 62.78$$

$$= 48.95$$

Where:

p : reduction ratio

S : square root of the sum of squares of acceleration after filtering (= 1,005.38 cm²/s)

α_f : maximum acceleration value after filtering (= 62.78 cm/s²)

- Input seismic motion

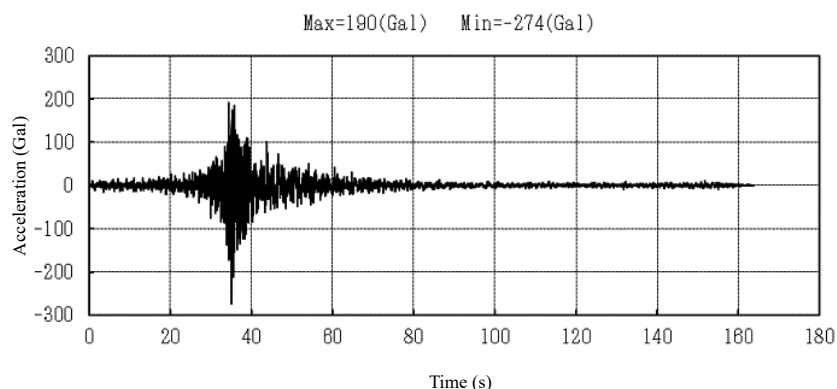


Figure 5.5.3 Time history waveform diagram of Level 1 seismic motion

5) Partial factors

The partial factors used in performance verification are shown in Table 5.5-1.

The limit value of the cell top displacement should be not more than 1.5% for both the permanent state and the variable state related to Level 1 seismic motion.

Table 5.5.1 Partial factors used in wall stability verification

Verification item	Partial factor by which the resistance term is multiplied γ_R	Partial factor by which the load term is multiplied γ_S	Adjustment factor m
Wall shear deformation	– (1.00)	– (1.00)	1.20
Ground bearing capacity (permanent state)	– (1.00)	– (1.00)	1.20
Ground bearing capacity (variable state)	– (1.00)	– (1.00)	1.00
Sliding of wall (permanent state)	– (1.00)	– (1.00)	1.20
Sliding of wall (variable state)	– (1.00)	– (1.00)	1.00

Table 5.5.2 Partial factors to be used for verification of the steel plate thickness of the cells and arcs

Verification item	Partial factor by which the resistance term is multiplied γ_R	Partial factor by which the load term is multiplied γ_S	Adjustment factor m
Yield of cell and arc (permanent state)	– (1.00)	– (1.00)	1.67
Yield of cell and arc (variable state)	– (1.00)	– (1.00)	1.12

6) Materials used

Cell filling material and backfill soil

Table 5.5.3 Soil constants for cell filling material and backfill soil

Item	Unit weight (kN/m ³)		Angle of internal friction (°)	Angle of wall friction (°)
	In the air	Under-water		
Cell filling sand	18	10	30°	±15°
Backfill soil	18	10	30°	±15°

Unit weight

Steel: 77.0 kN/m³

Reinforced concrete: 24.0 kN/m³

Plain concrete: 22.6 kN/m³

Tensile yield stress of cell shell

Steel plate SS400: $\sigma_y = 235 \text{ N/mm}^2$

Steel plate SM490: $\sigma_y = 315 \text{ N/mm}^2$

Steel plate SM490Y: $\sigma_y = 355 \text{ N/mm}^2$

Corrosion control and corrosion-induced penetration of steel materials

Table 5.5.4 Corrosion control and corrosion-induced penetration

Range of corrosion control	Corrosion control	Corrosion-induced penetration
Shallower than -1.00 m	Corrosion-resistant concrete	0.0 mm
Deeper than -1.00 m	Cathodic protection	1.0 mm

Category of the range of corrosion control

$$\text{LWL} - 1.00 = \pm 0.00 - 1.00 = -1.00 \text{ m}$$

Corrosion-induced penetration shallower than -1.00 m

Corrosion-induced penetration is zero because of strong corrosion control using corrosion-resistant concrete.

Corrosion-induced penetration deeper than -1.00 m

(Cathodic protection will be used for the entire design service life.)

Corrosion rate: 0.2 mm/year (in seawater)

Lifetime: 50 years

Corrosion control rate of cathodic protection: 90%

Corrosion-induced penetration

$$0.2 \text{ mm/year} \times 50 \text{ years} \times 10\% = 1.0 \text{ mm}$$

7) Study model

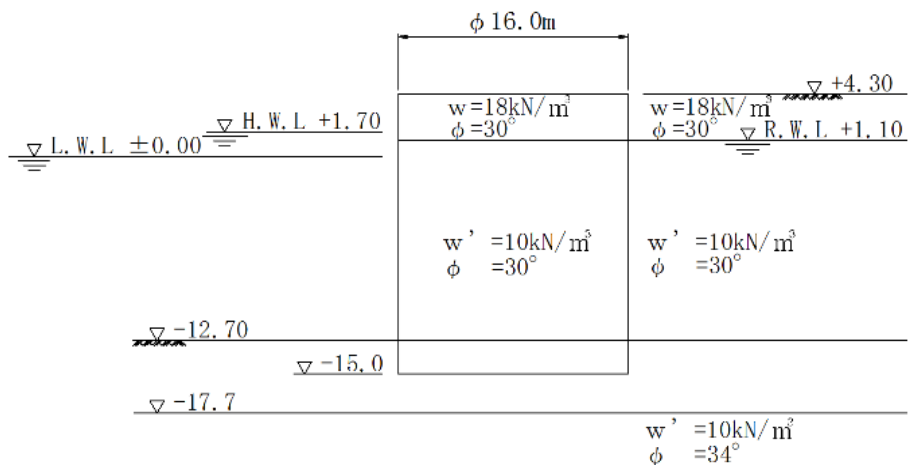


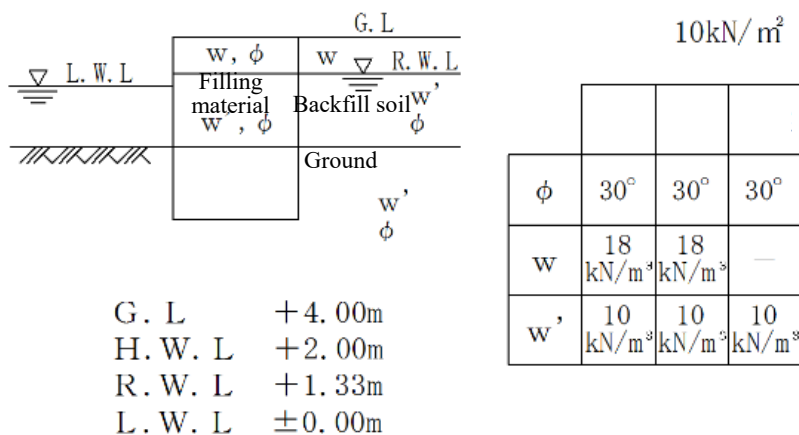
Figure 5.5.4 Model for examination

(3) Assumption of embedded length and equivalent wall width

Since the required embedded length is about 1/8 or more of the wall height, it is assumed here that the embedded length is 2.3 m. In this case, the bottom of embedment is -15 m.

The equivalent wall width (B) is given as about 15 m from the curves of seismic coefficient $k_h = 0.10$ and $k_h = 0.15$ based on **Figure 5.5.5**, which is the closest to the field conditions among the standard design calculation results.

The diameter of the cell shell can be calculated from the equivalent wall width once the central clearance of the cell body and the arc installation angle are determined. Since the correct distance between the cell body centers (L) is generally understood to be 10 to 15% greater than the diameter of the cell shell (D), 10% is chosen as the increment ($L/D = 1.1$) here. The arc installation angle (shown in **Figure 5.5.6**) θ_1 is set to 40° , as this angle is often chosen from past application cases. In this case, since $B/D = 0.92$ when L/D is 1.1 and θ_1 is 40° , the diameter of the cell shell (D) is $B/0.92 = 16.30$. Thus, the diameter of the cell shell will be given as follows: $D = 16.00$ m



$$S_1 = \nabla ABC \times 2 = \frac{\pi}{180} R^2 \theta_1$$

$$= \frac{\pi}{180} \times (8.00)^2 \times 40 = 44.68 \text{m}^2$$

$$S_2 = \Delta ACD \times 2 = \frac{R^2}{2} \sin 2\theta_1$$

$$= \frac{(8.00)^2}{2} \times \sin 80^\circ = 31.51 \text{m}^2$$

$$S_3 = \square CC'D'D = 2Rr \cos \theta_1 \sin \frac{\theta^2}{2}$$

$$= 2 \times 8.00 \times 4.77 \times \cos 40^\circ \times \sin 50^\circ$$

$$= 44.83 \text{m}^2$$

$$S_4 = \Delta CGC' = \left(\frac{\pi \theta^2}{360} - \frac{1}{2} - \sin \theta_2 \right) r^2$$

$$= \left(\frac{\pi \times 100}{360} - \frac{1}{2} \sin 100^\circ \right) \times (4.77)^2 = 8.67 \text{m}^2$$

$$S = (S_1 + S_2 + S_3 + S_4) \times 2$$

$$= (44.68 + 31.51 + 44.83 + 8.67) \times 2 = 259.39 \text{m}^2$$

Therefore, the equivalent wall width B is given as follows:

$$\therefore B = \frac{S}{L} = \frac{259.39}{17.60} = 14.74 \text{m}$$

(5) Calculation of action

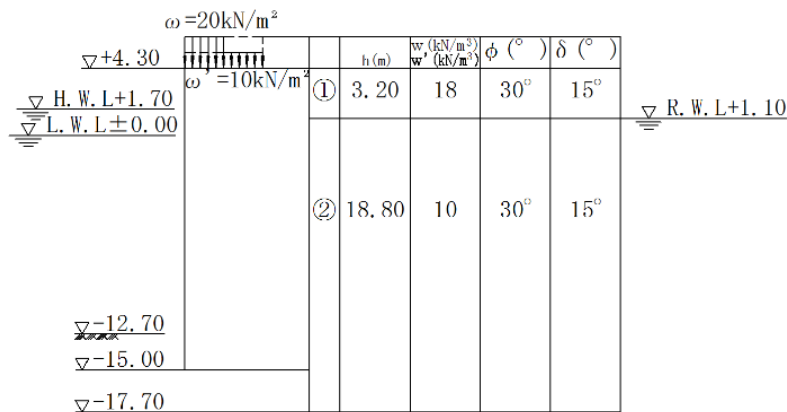


Figure 5.5.7 Calculation model

1) Earth pressure [Earth pressure in the permanent state]

i) Active earth pressure coefficient

$$K_{ai} = \frac{\cos^2(\phi_i - \psi)}{\cos^2 \psi \cos(\delta + \psi) \left[1 + \frac{\sin(\phi_i + \delta) \sin(\phi_i - \beta)}{\cos(\delta + \psi) \cos(\psi - \beta)} \right]^2}$$

ϕ_i :angle of internal friction of the soil in i layer ($^\circ$)

ψ :angle between the wall face and the vertical plane ($^\circ$)

β :angle formed between the ground surface and the horizontal line ($^\circ$)

δ :angle of wall friction ($^\circ$)

Since $\psi = 0$ and $\beta = 0$, the above equation is given as follows:

$$K_{ai} \cos \delta = \frac{\cos^2 \phi_i}{\left[1 + \sqrt{\frac{\sin(\phi + \delta) \sin \phi_i}{\cos \delta}} \right]^2}$$

Layer ①:

$$\phi = 30^\circ, \delta = 15^\circ$$

$$K_a \cos \delta = \frac{\cos^2 30}{\left[1 + \sqrt{\frac{\sin(30 + 15) \times \sin 30}{\cos 15}} \right]^2}$$

$$= 0.2911$$

Layer ②:

$$\phi = 30^\circ, \delta = 15^\circ$$

$$K_a \cos \delta = \frac{\cos^2 30}{\left[1 + \sqrt{\frac{\sin(30 + 15) \times \sin 30}{\cos 15}} \right]^2}$$

$$= 0.2911$$

ii) Earth pressure strength

$$P_1 = K_a \cos \delta \cdot \omega = 0.2911 \times 20$$

$$= 5.82 \text{ kN/m}^2$$

$$P_2 = K_a \cos \delta (\Sigma wh + \omega)$$

$$= 0.2911 \times (18 \times 3.20 + 20) = 22.59 \text{ kN/m}^2$$

$$P_3 = K_a \cos \delta (\Sigma wh + \omega)$$

$$= 0.2911 \times (18 \times 3.20 + 20) = 22.59 \text{ kN/m}^2$$

$$P_4 = K_a \cos \delta (\Sigma wh + \omega)$$

$$= 0.2911 \times (57.60 \times 10 \times 13.80 + 20)$$

$$= 62.76 \text{ kN/m}^2$$

$$P_5 = K_a \cos \delta (\Sigma wh + \omega) = 0.5 \times (195.60 + 20)$$

$$= 107.80 \text{ kN/m}^2$$

(P_5 is used for stability calculations as a gravity-type wall.)

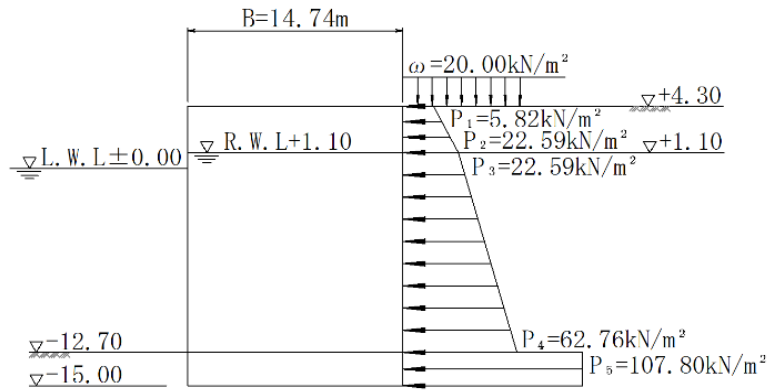


Figure 5.5.8 Earth pressure strength in the permanent state

[Earth pressure during an earthquake]

i) Apparent seismic coefficient in water

Layer ①: $k_h = 0.12$

Layer ②:

$$\begin{aligned}
 k_h' &= \\
 &= \frac{2 \times (\sum w_i h_i + \sum w h_j + \omega) + w h}{2 \times \{\sum w_i h_i + \sum (w - 10) h_j + \omega\} + (w - 10) h} k_h \\
 &= \frac{2 \times (18 \times 3.20 + 10) + 20 \times 18.80}{2 \times (18 \times 3.20 + 10) + 10 \times 18.80} \times 0.12 \\
 &= 0.19
 \end{aligned}$$

ii) Composite seismic angle

Layer ①: $\theta = \tan^{-1} k_h = \tan^{-1}(0.12) = 6.84^\circ$

Layer ②: $\theta = \tan^{-1} k_h' = \tan^{-1}(0.19) = 10.76^\circ$

iii) Active earth pressure coefficient

$$K_{ai} = \frac{\cos^2(\phi_i - \psi - \theta)}{\cos \theta \cos^2 \psi \cos(\delta + \psi + \theta) \left[1 + \sqrt{\frac{\sin(\phi_i + \delta) \sin(\phi_i - \beta - \theta)}{\cos(\delta + \psi + \theta) \cos(\psi - \beta)}} \right]^2}$$

Where:

θ : Composite seismic angle

$\theta = \tan^{-1} k_h' (^\circ)$

k_h : Seismic coefficient

k_h' : Apparent seismic coefficient

Other symbols are the same as those for sandy soil.

Since $\psi = 0$ and $\beta = 0$, the above equation is given as:

$$K_{ai} = \frac{\cos^2(\phi_i - \theta) \cos \delta}{\cos \theta \cos(\delta + \theta) \cdot \left[1 + \sqrt{\frac{\sin(\phi_i + \delta) \sin(\phi_i - \theta)}{\cos(\delta + \theta)}} \right]^2}$$

Where:

θ : Composite seismic angle

$$\theta = \tan^{-1} k'_h (\text{°})$$

k_h : Seismic coefficient

k'_h : Apparent seismic coefficient

Other symbols are the same as those for sandy soil.

Since $\psi = 0$ and $\beta = 0$, the above equation is given as:

$$K_{ai} = \frac{\cos^2(\phi_i - \theta) \cos \delta}{\cos \theta \cos(\delta + \theta) \cdot \left[1 + \sqrt{\frac{\sin(\phi_i + \delta) \sin(\phi_i - \theta)}{\cos(\delta + \theta)}} \right]^2}$$

Layer ①:

$$\begin{aligned} K_a \cos \delta &= \frac{\cos^2(30^\circ - 6.84^\circ) \times \cos 15^\circ}{\cos 6.84^\circ \cos(15^\circ + 6.84^\circ) \times \left[1 + \sqrt{\frac{\sin(30^\circ + 15^\circ) \times \sin(30^\circ - 6.84^\circ)}{\cos(15^\circ + 6.84^\circ)}} \right]^2} \\ &= 0.3701 \end{aligned}$$

Layer ②:

$$\begin{aligned} K_a \cos \delta &= \frac{\cos^2(30^\circ - 10.76^\circ) \times \cos 15^\circ}{\cos 10.76^\circ \times \cos(15^\circ + 10.76^\circ) \times \left[1 + \sqrt{\frac{\sin(30^\circ + 15^\circ) \times \sin(30^\circ - 10.76^\circ)}{\cos(15^\circ + 10.76^\circ)}} \right]^2} \\ &= 0.4259 \end{aligned}$$

iv) Earth pressure

$$P_1 = K_a \cos \delta \cdot \omega = 0.3701 \times 10 = 3.70 \text{ kN/m}^2$$

$$\begin{aligned} P_2 &= K_a \cos \delta (\Sigma w_i h_i + \omega) \\ &= 0.3701 \times (18 \times 3.20 + 10) = 25.02 \text{ kN/m}^2 \end{aligned}$$

$$\begin{aligned} P_3 &= K_a \cos \delta (\Sigma w_i h_i + \omega) \\ &= 0.4259 \times (57.60 + 10) = 28.79 \text{ kN/m}^2 \end{aligned}$$

$$\begin{aligned} P_4 &= K_a \cos \delta (\Sigma w_i h_i + \omega) \\ &= 0.4259 \times (57.60 \times 10 \times 13.80 + 10) \\ &= 87.57 \text{ kN/m}^2 \end{aligned}$$

$$\begin{aligned} P_5 &= 0.5 (\Sigma w_i h_i + \omega) = 0.5 \times (195.6 + 10) \\ &= 102.80 \text{ kN/m}^2 \end{aligned}$$

(P_5 is used for stability calculations as a gravity-type wall.)

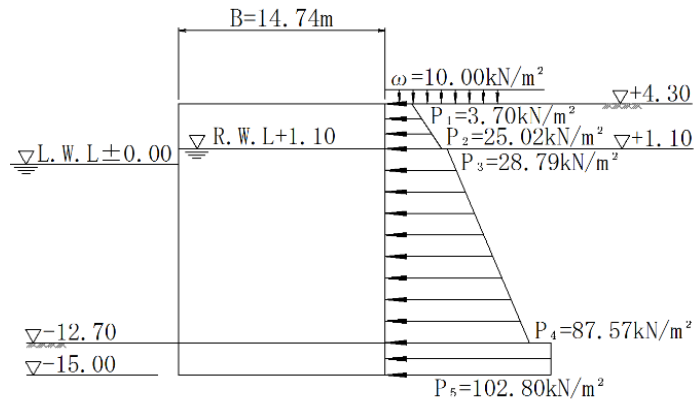


Figure 5.5.9 Earth pressure strength during an earthquake

2) Residual water pressure

$$p_w = (R.W.L. - L.W.L.)\rho_w g$$

$$= (1.10 - 0.00) \times 10.1 = 11.11 \text{ kN/m}^2$$

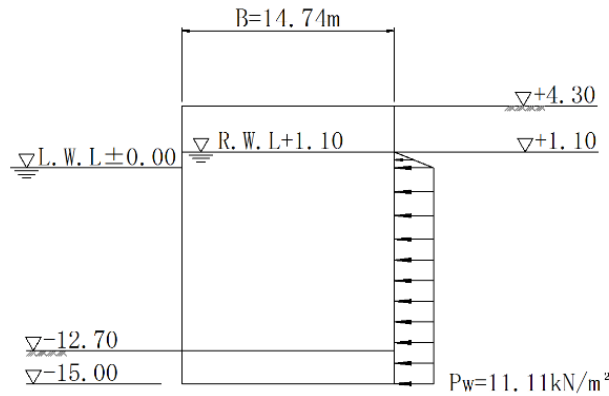


Figure 5.5.10 Residual water pressure

3) Seismic force

The seismic force acting on the wall is:

$$H_w = k_h W$$

Where:

H_w : seismic force (kN/m)

k_h : horizontal seismic coefficient

W : weight of filling sand and pore water (kN/m)

The horizontal seismic coefficient can be reduced linearly so that it becomes zero at 10 m below the sea bed surface and be set to zero at depths of 10 m or more below the ground surface.

Horizontal seismic coefficient at the cell bottom (-15.00 m): k'_h

$$k'_h = \frac{10.00 - 2.30}{10.00} \times 0.12 = 0.09$$

$$P_1 = k_h w B = 0.12 \times 18 \times 14.74$$

$$= 31.84 \text{ kN/m}^2$$

$$P_2 = k_h w B = 0.12 \times 20 \times 14.74$$

$$= 35.34 \text{ kN/m}^2$$

$$P_3 = k_h w B = 0.09 \times 20 \times 14.74$$

$$= 26.53 \text{ kN/m}^2$$

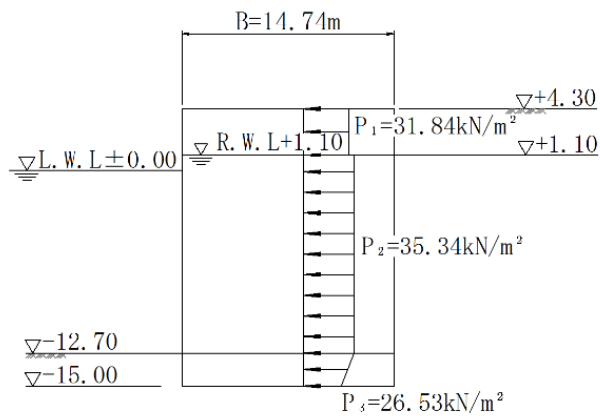


Figure 5.5.11 Seismic force

4) Dynamic water pressure

Dynamic water pressure acting on the front surface of the cell wall

$$p_{dw} = \frac{7}{8} k_h \rho_w g \sqrt{Hy}$$

$$= \frac{7}{8} \times 0.12 \times 10.1 \times \sqrt{12.7 \times 12.7} = 13.47 \text{ kN/m}^2$$

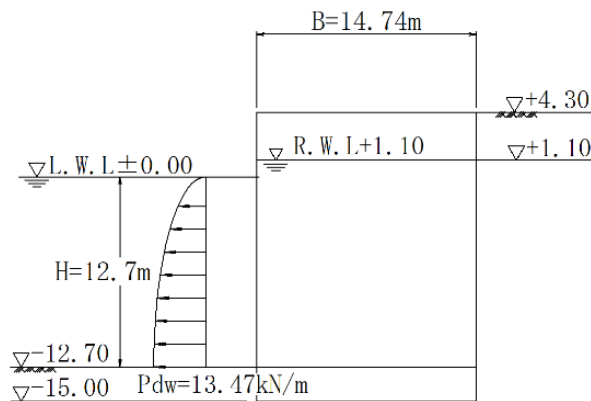


Figure 5.5.12 Dynamic water pressure

(6) Review of shear deformation of the wall

Shear deformation should be reviewed for loads in the permanent state acting above the design seabed level.

1) Calculation of deformation moments

Deformation moments should be calculated for the horizontal component of the active earth pressure and for the residual water pressure.

i) Residual water pressure

Residual water pressure and moments are shown in **Table 5.5.5**.

ii) Earth pressure

The earth pressure moments are shown in **Table 5.5.6**.

Table 5.5.5 Residual water pressure and moment

	Calculation formula for P_w	P_w (kN/m)	Calculation formula for h_w	h_w (m)	$P_w \cdot h_w$ (kN·m/m)
①	$1/2 \times 11.11 \times 1.10$	6.11	$12.70 + 1/3 \times 1.10$	13.07	79.86
②	$1/2 \times 11.11 \times 12.70$	70.55	$2/3 \times 12.70$	8.47	597.56
③	$1/2 \times 11.11 \times 12.70$	70.55	$1/3 \times 12.70$	4.23	298.43
Total		147.21			975.85

Table 5.5.6 Earth pressure and moment

	Calculation formula for P_a	P_a (kN/m)	Calculation formula for h_a	h_a (m)	$P_a \cdot h_a$ (kN·m/m)
①	$1/2 \times 5.82 \times 3.20$	9.31	$13.80 + 2/3 \times 3.20$	15.93	148.31
②	$1/2 \times 22.59 \times 3.20$	36.14	$13.80 + 1/3 \times 3.20$	14.87	537.40
③	$1/2 \times 22.59 \times 13.80$	155.87	$2/3 \times 13.80$	9.20	1,434.00
④	$1/2 \times 62.76 \times 13.80$	433.04	$1/3 \times 13.80$	4.60	1,991.98
Total		634.36			4,111.69

iii) Total deformation moment

$$M_d = P_a h_a + P_w h_w$$

$$= 4,111.69 + 975.85 = 5,087.54 \text{ kN} \cdot \text{m/m}$$

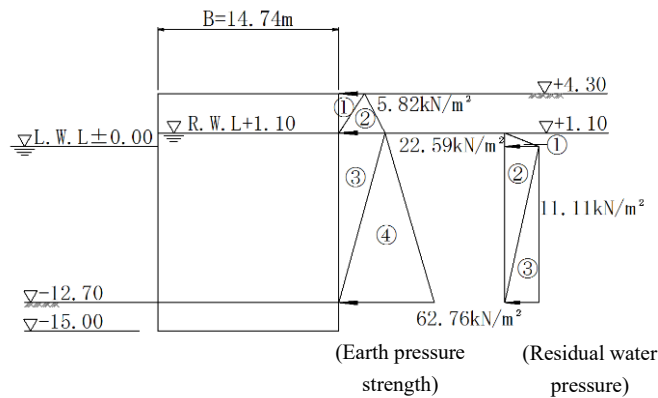


Figure 5.5.13 Total deformation moment

2) Calculation of the deformation resistance moment

i) Equivalent wall height: H_d'

$$H_d' = \frac{1}{w'} \sum w_i h_i$$

$$= \frac{1}{10} \times (18 \times 3.20 + 10 \times 13.80) = 19.56 \text{ m}$$

ii) Deformation resistance coefficient: R_d

Equivalent wall width-height ratio: $v_d = \frac{B}{H'_d} = \frac{14.74}{19.56} = 0.753$

$$R_d = v_d^2 (3 - v_d \cos \phi) \sin \phi$$

$$= 0.753^2 \times (3 - 0.753 \times \cos 30^\circ) \times \sin 30^\circ$$

$$= 0.666$$

iii) Deformation resistance moment: M_{rd}

$$M_{rd} = \frac{1}{6} w' \gamma H'_d R_d$$

$$= \frac{1}{6} \times 10 \times 19.56^3 \times 0.666$$

$$= 8,306.72 \text{ kN} \cdot \text{m/m}$$

3) Performance verification

$$m \cdot \frac{S_d}{R_d} = 1.20 \times \frac{5,087.54}{8,306.72} = 0.73 \leq 1.00$$

Where:

m : Adjustment factor 1.20

S_d : $S_d = \gamma_S S_k = 1.0 \times M_d$

R_d : $R_d = \gamma_R R_k = 1.0 \times M_{rd}$

(7) Review of stability as a gravity-type wall [Permanent state]

1) Load acting on the wall

i) Horizontal loads and moments due to horizontal loads

Horizontal loads should be calculated for the horizontal component of the earth pressure and for the residual water pressure. The calculation results are shown in **Figure 5.5.14**, **Table 5.5.7**, and **Table 5.5.8**. The center of rotation of the moment is assumed to be the design seabed.

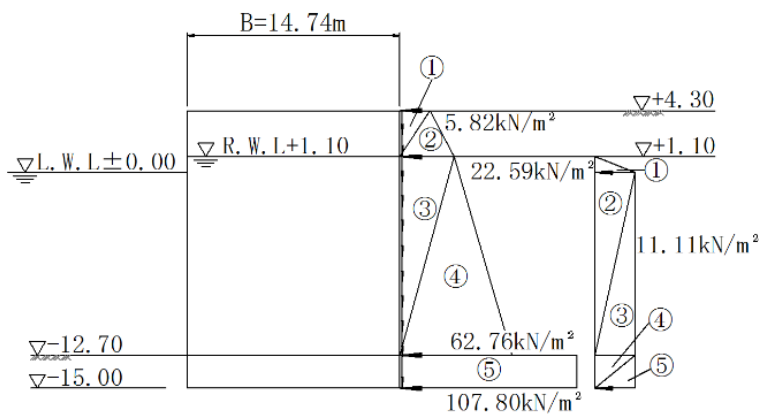


Figure 5.5.14 Horizontal loads in the permanent state

ii) Vertical earth pressure and moment due to vertical earth pressure

The vertical earth pressure should be calculated for the vertical component of the earth pressure of sandy soil. The center of rotation of the moment should be set at the central axis of the wall.

$$\begin{aligned}
 P &= \Sigma P_a \tan \delta = 882.30 \times \tan 15^\circ \\
 &= 236.41 \text{ kN/m} \\
 M &= P \times \frac{-B}{2} = 236.41 \times \frac{-14.74}{2} \\
 &= -1,742.34 \text{ kN} \cdot \text{m/m}
 \end{aligned}$$

iii) Wall weight

$$\begin{aligned}
 W &= B \times \Sigma w_i h_i \\
 &= 14.74 \times (18 \times 3.20 + 10 \times 16.10) \\
 &= 3,222.16 \text{ kN/m}
 \end{aligned}$$

iv) Total acting load

$$\begin{aligned}
 \text{Horizontal force: } H &= 882.30 + 172.77 \\
 &= 1,055.07 \text{ kN/m}
 \end{aligned}$$

$$\begin{aligned}
 \text{Vertical force: } V &= 236.41 + 3,222.16 \\
 &= 3,458.57 \text{ kN/m}
 \end{aligned}$$

Moment:

$$\begin{aligned}
 M &= 3,826.56 + 946.46 - 1,742.34 \\
 &= 3,030.68 \text{ kN} \cdot \text{m/m}
 \end{aligned}$$

Table 5.5.7 Earth pressure and moments

	Calculation formula for P_a	P_a (kN/m)	Calculation formula for h_a	h_a (m)	$P_a \cdot h_a$ (kN·m/m)
①	$1/2 \times 5.82 \times 3.20$	9.31	$13.80 + 2/3 \times 3.20$	15.93	148.31
②	$1/2 \times 22.59 \times 3.20$	36.14	$13.80 + 1/3 \times 3.20$	14.87	537.40
③	$1/2 \times 22.59 \times 13.80$	155.87	$2/3 \times 13.80$	9.20	1,434.00
④	$1/2 \times 62.76 \times 13.80$	433.04	$1/3 \times 13.80$	4.60	1,991.98
⑤	107.80×2.30	247.94	$1/2 \times (2.30)$	-1.15	-285.13
Total		882.30			3,826.56

Table 5.5.8 Residual water pressure and moments

	Calculation formula for P_w	P_w (kN/m)	Calculation formula for h_w	h_w (m)	$P_w \cdot h_w$ (kN·m/m)
①	$1/2 \times 11.11 \times 1.10$	6.11	$12.70 + 1/3 \times 1.10$	13.07	79.86
②	$1/2 \times 11.11 \times 12.70$	70.55	$2/3 \times 12.70$	8.47	597.56
③	$1/2 \times 11.11 \times 12.70$	70.55	$1/3 \times 12.70$	4.23	298.43
④	$1/2 \times 11.11 \times 2.30$	12.78	$1/3 \times (-2.3)$	-0.77	-9.84
⑤	$1/2 \times 11.11 \times 2.30$	12.78	$2/3 \times (-2.3)$	-1.53	-19.55
Total		172.77			946.46

2) Subgrade reaction and wall displacement

i) Coefficient of the subgrade reaction

The horizontal subgrade reaction coefficient should be calculated according to the formula proposed by

Yokoyama. The vertical subgrade reaction coefficient should have the same value as that of the horizontal one at the bottom of the wall, and the shear spring constant should be 1/3 of the vertical subgrade reaction coefficient. The N-value of the ground is assumed to be 10.

Horizontal subgrade reaction coefficient

$$K_H = 2N = 2 \times 10 = 20 \text{N/cm}^3 \\ (= 20,000 \text{kN/m}^3)$$

Vertical subgrade reaction coefficient

$$K_V = K_H = 20 \text{N/cm}^3 (= 20,000 \text{kN/m}^3)$$

Shear spring constant

$$K_s = 1/3 \cdot K_V = 1/3 \times 20 \\ = 6.67 \text{N/cm}^3 (= 6,670 \text{kN/m}^3)$$

ii) Horizontal subgrade reaction

The subgrade reaction should be calculated by considering the wall as a rigid body supported elastically by the ground. The horizontal subgrade reaction intensity should be assumed not to exceed the passive earth pressure by considering the yielding of the ground.

The subgrade reaction at the cell bottom P_{12} can be calculated from the rotational angle of the wall θ , the depth from the seabed surface to the rotation center of the wall h , and the horizontal reaction coefficient of the ground K_H . It is thus given by the following equation:

$$p_{1i} = K_H (h - d)\theta$$

However, calculation of the subgrade reaction and the displacement of the wall is based on a circular formula of the rotational angle of the wall θ , the horizontal distance from the central axis of the wall to the center of rotation e , and the spring constant K_4 . For this reason, when the computer's convergent calculation results for h and θ , or 12.16 m and 0.957×10^{-3} rad, respectively, are applied to h and θ used to calculate the above formula, the horizontal subgrade reaction intensity P_{12} at the cell bottom at this time is given as follows:

$$p_{11} = 20 \times 10^3 \times (12.16 - 0.00) \times 0.957 \times 10^{-3} \\ = 232.74 \text{kN/m}^2 \\ p_{12} = 20 \times 10^3 \times (12.16 - 2.30) \times 0.957 \times 10^{-3} \\ = 188.72 \text{kN/m}^2$$

On the other hand, the passive earth pressure strength at the cell bottom, P_{p1} , is calculated from the passive earth pressure coefficient, $K_p \cos \delta = 4.8069$.

$$P_{p1} = wDK_p \cos \delta = 10 \times 2.30 \times 4.8069 \\ = 110.56 \text{kN/m}^2$$

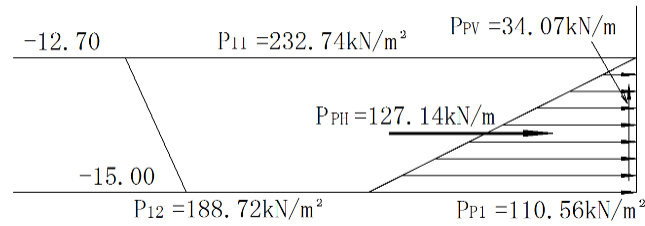


Figure 5.5.15 Horizontal subgrade reaction (permanent state)

Since the subgrade reaction intensity is greater than the passive earth pressure strength, the horizontal subgrade reaction takes the passive earth pressure. Ultimately, the horizontal subgrade reaction P_{pH} is shown as follows:

$$P_{pH} = \frac{1}{2} P_{p1} D = \frac{1}{2} \times 110.56 \times 2.30$$

$$= 127.14 \text{ kN/m}$$

iii) Vertical frictional drag force: P_{pv}

The vertical frictional drag force should be the product of the horizontal subgrade reaction and $\tan \delta$.

$$P_{pv} = P_{pH} \tan \delta = 127.14 \times \tan 15^\circ$$

$$= 34.07 \text{ kN/m}$$

iv) Combined forces and moments acting on the wall

External force considering passive earth pressure

Horizontal force:

$$H = 1,055.07 - 127.14 = 927.93 \text{ kN/m}$$

Vertical force:

$$V = 3,458.57 - 34.07 = 3,424.50 \text{ kN/m}$$

Moments:

$$M = 3,030.68 + 127.14 \times \frac{2}{3} \times 2.30 - 34.07 \times 7.37$$

$$= 2,974.53 \text{ kN} \cdot \text{m/m}$$

v) Rotational angle of the wall

The rotational angle of the wall, the depth from the design seabed surface to the zero point, and the eccentric distance from the central axis to the zero point when the horizontal force, vertical force, and moment act on a place on the ground at the center of the wall and the wall consequently rotates around the zero point as shown in **Figure 5.5.16** should be calculated.

The functions of K_1 to K_4 used for these calculations are calculated first.

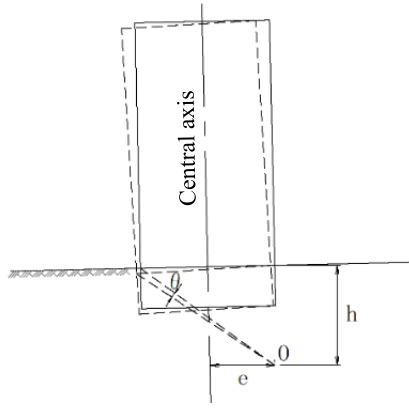


Figure 5.5.16 Case of a rotating wall outside the wall

In this design case, since the vertical subgrade reaction at the cell bottom in the permanent state is trapezoidally distributed, the functions of K_1 to K_4 are expressed by the following equation.

$$K_1 = \sum_{i=1}^n K_{Hi} d_i + K_s A$$

$$K_2 = \sum_{i=1}^n \left\{ K_{Hi} d_i \left(\sum_{j=1}^{i-1} d_j + \frac{d_i}{2} \right) \right\} + K_s AD$$

$$K_3 = \sum_{i=1}^n \left\{ K_{Hi} d_i \left(\sum_{j=1}^{i-1} d_j + \frac{d_i}{2} + \frac{B}{2} \tan \delta_i \right) \right\} + K_s AD$$

$$K_4 = \sum_{i=1}^n \left\{ K_{Hi} d_i \left(\frac{d_i^2}{3} + \sum_{j=1}^{i-1} d_j \sum_{j=1}^i d_j + \frac{B}{2} \left(\sum_{j=1}^{i-1} d_i + \frac{d_i}{2} \right) \tan \delta_i \right) \right\} + K_s AD^2 + \frac{1}{12} K_v A^3$$

Where:

D : embedded length = 2.30 m

d_i : thickness of each layer of the embedment ground (m)

B : equivalent wall width = 14.74 m

K_{Hi} : horizontal subgrade reaction coefficient of each layer of the embedment ground = 20×10^4 kN/m³

K_v : vertical subgrade reaction coefficient at the bottom of the wall

K_s : horizontal shear spring constant at the bottom of the wall = 6.67×10^3 kN/m³

A : area per unit length in the normal direction at the bottom of the wall = 14.74 m²

Here, d_i shows the layer thickness of the part where the ground is evaluated as a spring. In this case, the whole front ground is evaluated not as a spring but as passive earth pressure. Therefore, it is calculated as $d_i = 0$ in the calculation of K_1 to K_4 . Hence, K_1 to K_4 become the following without the term d_i :

$$K_1 = K_s A = 6.67 \times 10^3 \times 14.74$$

$$= 98.32 \times 10^3 \text{ kN/m}^2$$

$$K_2 = K_s AD = 6.67 \times 10^3 \times 14.74 \times 2.30$$

$$= 226.13 \times 10^3 \text{ kN/m}$$

$$K_3 = K_s AD = 226.13 \times 10^3 \text{ kN/m}$$

$$\begin{aligned}
K_4 &= K_s AD^2 + \frac{1}{12} K_v A^3 = \\
&= 6.67 \times 10^3 \times 14.74 \times 2.30^2 + \frac{1}{12} \times 20 \times 10^3 \\
&\quad \times 14.74^3 = 5,857.63 \times 10^3 \text{ kN}
\end{aligned}$$

Rotational angle of the wall θ (rad)

$$\begin{aligned}
\theta &= \frac{MK_1 + HK_3}{K_1 K_4 - K_2 K_3} \\
&= \frac{2,974.53 \times 98.32 + 927.93 \times 226.13}{98.32 \times 5,857.63 - 226.13 \times 226.13} \times \frac{10^3}{10^6} \\
&= 0.957 \times 10^{-3} \text{ rad} (0.051^\circ)
\end{aligned}$$

vi) Depth at the rotational center of the wall (m)

$$\begin{aligned}
h &= \frac{MK_2 + HK_4}{MK_1 + HK_3} \\
&= \frac{2,974.53 \times 226.13 + 927.93 \times 5,857.63}{2,974.53 \times 98.32 + 927.93 \times 226.13} \times \frac{10^3}{10^3} \\
&= 12.16 \text{ m}
\end{aligned}$$

vii) Distance of the rotational center of the wall from the central axis of the wall (m)

$$\begin{aligned}
e &= \frac{1}{K_v A} \left\{ \frac{V}{\theta} - h \sum_{i=1}^n K_{Hi} d_i \tan|\delta_i| \right. \\
&\quad \left. + \sum_{i=1}^n K_{Hi} d_i \left(\sum_{j=1}^{i-1} d_j + \frac{d_i}{2} \right) \tan|\delta_i| \right\} \\
&= \frac{V}{K_v A \theta} = \frac{3,424.50}{20 \times 10^3 \times 14.74 \times 0.957 \times 10^{-3}} \\
&= 12.14 \text{ m}
\end{aligned}$$

viii) Vertical subgrade reaction (kN/m²)

$$\begin{aligned}
q_1 &= K_v (e + B/2) \theta \\
&= 20 \times 10^3 \times \left(12.14 + \frac{14.74}{2} \right) \times 0.957 \times 10^{-3} \\
&= 373.42 \text{ kN/m}^2 \\
q_2 &= K_v (e - B/2) \theta \\
&= 20 \times 10^3 \times \left(12.14 - \frac{14.74}{2} \right) \times 0.957 \times 10^{-3} \\
&= 91.30 \text{ kN/m}^2
\end{aligned}$$

ix) Shear reaction force at the bottom of the wall (kN/m)

$$\begin{aligned}
 Q &= K_s (h - D)\theta A \\
 &= 6.67 \times 10^3 \times (12.16 - 2.30) \times 0.957 \\
 &\quad \times 10^{-3} \times 14.74 = 927.71 \text{ kN/m}
 \end{aligned}$$

x) Horizontal displacement of the wall (m)

$$\delta_z = (h + z)\theta$$

Where:

h : depth from the design seabed surface to the rotational center of the wall
 $= 12.16 \text{ m}$

z : height of the point where displacement is to be calculated from the design seabed surface (m)

Horizontal displacement of the wall at its crown: δ_1

$$\begin{aligned}
 \delta_1 &= (h + z)\theta = (12.16 + 17.00) \times 0.957 \times 10^{-3} \\
 &= 2.79 \times 10^{-2} \text{ m}
 \end{aligned}$$

Horizontal displacement of the wall at the seabed: δ_2

$$\begin{aligned}
 \delta_2 &= (12.16 + 0) \times 0.957 \times 10^{-3} \\
 &= 1.16 \times 10^{-2} \text{ m}
 \end{aligned}$$

Horizontal displacement of the wall at the bottom of the cell: δ_3

$$\begin{aligned}
 \delta_3 &= (12.16 - 2.30) \times 0.957 \times 10^{-3} \\
 &= 9.44 \times 10^{-3} \text{ m}
 \end{aligned}$$

The results obtained from the convergent calculations are shown in **Figure.5.5.17** and **5.5.18**.

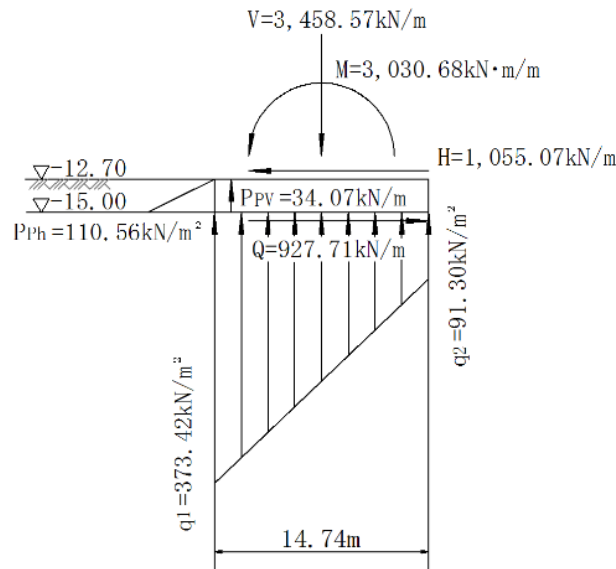


Figure 5.5.17 Subgrade reaction distribution (permanent state)

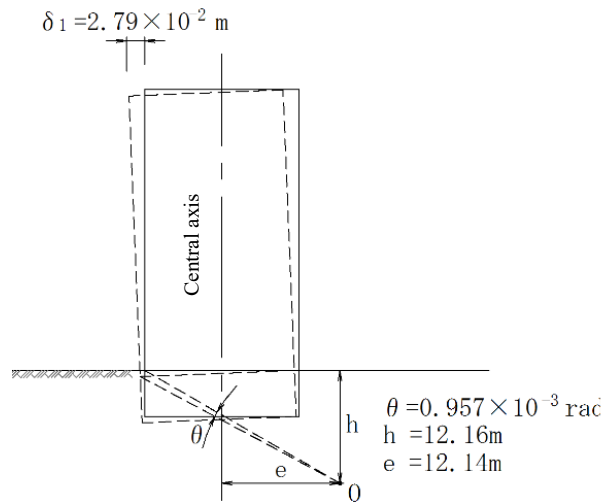


Figure 5.5.18 Displacement mode (permanent state)

3) Review of bearing capacity

i) Details of the bottom subgrade reaction

Vertical subgrade reaction at the toe of the wall:

$$q_1 = 373.42 \text{ kN/m}^2$$

Vertical subgrade reaction at the heel of the wall:

$$q_2 = 91.30 \text{ kN/m}^2$$

Vertical subgrade reaction distribution width:

$$B = 14.74 \text{ m}$$

Bottom shear reaction force: $Q = 927.71 \text{ kN/m}$

ii) Location where the subgrade reaction acts

$$B' = B \frac{q_1 + 2q_2}{3(q_1 + q_2)} \quad (\text{trapezoidal distribution})$$

$$= 14.74 \times \frac{373.42 + 2 \times 91.30}{3 \times (373.42 + 91.30)} = 5.88 \text{ m}$$

iii) Acting load

Vertical load: P_v

$$P_v = \frac{B}{4B' \left(2 - \frac{3B'}{B} \right)} q_1$$

$$= \frac{14.74}{4 \times 5.88 \times \left(2 - \frac{3 \times 5.88}{14.74} \right)} \times 373.42$$

$$= 291.34 \text{ kN/m}^2$$

Action width: L

$$L = 2B' = 2 \times 5.88 = 11.76 \text{ m}$$

Shear reaction at the bottom of the wall: Q

$$Q = 927.71 \text{ kN/m}$$

iv) Surcharge at the front of the cell: ω

$$\begin{aligned}\omega &= \Sigma wh = 10 \times (15.00 - 12.70) \\ &= 23.00 \text{ kN/m}^2\end{aligned}$$

v) Calculation method
Load inclination ratio: H/V

$$\begin{aligned}H/V &= \frac{Q}{\frac{1}{2}(q_1 + q_2)B} \\ &= \frac{927.71}{\frac{1}{2} \times (373.42 + 91.30) \times 14.74} \\ &= 0.27 > 0.1\end{aligned}$$

Therefore, Bishop's method will be used for this calculation.

vi) Calculation results using Bishop's method

Sliding moment: $M_o = 40,628.2 \text{ kN}\cdot\text{m}$
Resisting moment: $M_R = 101,789.5 \text{ kN}\cdot\text{m}$
Center of the arc: $X = -2.00 \text{ m}$
 $Y = +2.00 \text{ m}$
Radius of the arc: $R = 21.87 \text{ m}$

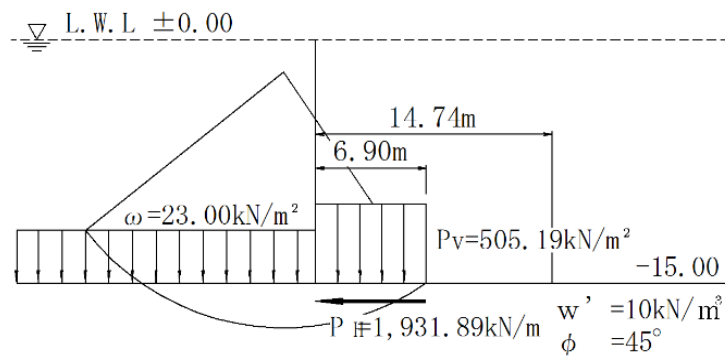


Figure 5.5.19 Calculation results using Bishop's method (permanent state)

Performance verification:

$$m \cdot \frac{S_d}{R_d} = 1.20 \times \frac{40,628.2}{101,789.5} = 0.48 \leq 1.00 \quad \text{OK}$$

Where:

m : adjustment factor 1.20

R_d : $R_d = \gamma_R R_k = 1.0 \times M_R$

S_d : $S_d = \gamma_S S_k = 1.0 \times M_o$

4) Review on sliding of the wall

The following equation is used to review sliding of the wall.

$$m \frac{S_d}{R_d} \leq 1.0$$

$$R_d = \gamma_R R_k = 1.0V \cdot \tan \phi$$

$$S_d = \gamma_S S_k = 1.0Q$$

Where:

m : adjustment factor 1.20

V : total vertical force acting on the wall (kN/m)

(Vertical components of earth pressure acting on the front and rear walls should be considered.)

Q : shear reaction force at the bottom of the wall (kN/m)

ϕ : angle of shear resistance of soil at the bottom of the wall ($^{\circ}$)

Performance verification:

$$m \cdot \frac{S_d}{R_d} = 1.20 \times \frac{927.71}{3,424.50 \times \tan 30^{\circ}} = 0.56 \leq 1.00$$

5) Review of horizontal displacement at the crown of the quaywall

δ = (quaywall height + depth of rotational center from design seabed) \times (rotational angle)

$$= (17.00 + 12.16) \times 0.957 \times 10^{-3}$$

$$= 2.79 \times 10^{-2} \text{ m}$$

It is desirable to set the ratio of displacement to the wall height to less than 1.5%.

$$\frac{\text{Horizontal displacement at the crown of the quay wall}}{\text{Quay wall height}} \times 100$$

$$= \frac{2.79 \times 10^{-2}}{17.00} \times 100 = 0.16\% < 1.5\%$$

[During a Level 1 earthquake]

1) Load acting on the wall

i) Horizontal loads and moments by horizontal loads

Horizontal loads will be calculated for the horizontal component of the earth pressure, residual water pressure, and the seismic force acting on the wall. The rotational center of the moment will be on the design seabed. The calculation results are shown in **Tables 5.5.9, 5.5.10, and 5.5.11.**

• Dynamic water pressure and moment

Resultant force of dynamic water pressure

$$P_{dw} = \frac{7}{12} \times k_h \times \rho_w g \times H^2$$

$$= \frac{7}{12} \times 0.12 \times 10.1 \times 12.7^2$$

$$= 114.03 \text{ kN/m}$$

Distance from the water surface to the point of action of the resultant force of hydraulic force.

$$h_{dw} = \frac{3}{5} H = \frac{3}{5} \times 12.70 = 7.62 \text{ m}$$

Moment due to dynamic water pressure

$$M = P_{dw} (H - h_{dw}) = 114.03 \times (12.70 - 7.62)$$

$$= 579.27 \text{ kN} \cdot \text{m/m}$$

ii) Vertical loads and moments by vertical loads

Vertical loads are calculated for the vertical component of earth pressure in sandy soil. The rotational center of the moment is the central axis of the wall.

Vertical load

$$P = \Sigma P \tan \delta = 1,085.27 \times \tan 15^\circ \\ = 290.80 \text{ kN/m}$$

Moment due to vertical load

$$M = P \times \frac{-B}{2} = 290.80 \times \frac{-14.74}{2} \\ = -2,143.20 \text{ kN} \cdot \text{m/m}$$

iii) Wall load

$$W = B \times \Sigma w_i h_i \\ = 14.74 \times (18 \times 3.20 + 10 \times 16.10) \\ = 14.74 \times 218.60 = 3,222.16 \text{ kN/m}$$

iv) Total acting load

Horizontal force:

$$H = \text{earth pressure} + \text{residual water pressure} + \\ \text{seismic force} + \text{dynamic water pressure} \\ = 1,085.27 + 172.77 + 660.73 + 114.03 \\ = 2,032.80 \text{ kN/m}$$

Vertical force:

$$V = \text{earth pressure} + \text{wall weight} \\ = 290.80 + 3,222.16 = 3,512.96 \text{ kN/m}$$

Moment

$$M = \text{horizontal earth pressure} + \text{residual water pressure} \\ + \text{seismic force} + \text{dynamic water pressure} \\ + \text{vertical earth pressure} \\ = 5,024.69 + 946.46 + 4,856.20 + 579.27 \\ - 2,143.20 = 9,263.42 \text{ kN} \cdot \text{m/m}$$

Table 5.5.9 Earth pressure and moments

	Calculation formula for P_a	P_a (kN/m)	Calculation formula for h_a	h_a (m)	$P_a \cdot h_a$ (kN·m/m)
①	$1/2 \times 3.70 \times 3.20$	5.92	$13.80 + 2/3 \times 3.20$	15.93	94.31
②	$1/2 \times 25.02 \times 3.20$	40.03	$13.80 + 1/3 \times 3.20$	14.87	595.25
③	$1/2 \times 28.79 \times 13.80$	198.65	$2/3 \times 13.80$	9.20	1,827.58
④	$1/2 \times 87.57 \times 13.80$	604.23	$1/3 \times 13.80$	4.60	2,779.46
⑤	102.80×2.30	236.44	$1/2 \times (2.30)$	-1.15	-271.91
Total		1,085.27			5,024.69

Table 5.5.10 Residual water pressure and moments

	Calculation formula for P_w	P_w (kN/m)	Calculation formula for h_w	h_w (m)	$P_w \cdot h_w$ (kN·m/m)
①	$1/2 \times 11.11 \times 1.10$	6.11	$12.70 + 1/3 \times 1.10$	13.07	79.86
②	$1/2 \times 11.11 \times 12.70$	70.55	$2/3 \times 12.70$	8.47	597.56
③	$1/2 \times 11.11 \times 12.70$	70.55	$1/3 \times 12.70$	4.23	298.43
④	$1/2 \times 11.11 \times 2.30$	12.78	$1/3 \times (-2.3)$	-0.77	-9.84
⑤	$1/2 \times 11.11 \times 2.30$	12.78	$2/3 \times (-2.3)$	-1.53	-19.55
Total		159.99			946.46

Table 5.5.11 Seismic forces and moments

	Calculation formula for P_a	P_a (kN/m)	Calculation formula for h_a	h_a (m)	$P_a \cdot h_a$ (kN·m/m)
①	31.84×3.20	101.89	$13.80 + 1/2 \times 3.20$	15.40	1,569.11
②	35.34×13.80	487.69	$1/2 \times 13.80$	6.90	3,365.06
③	$1/2 \times 35.34 \times 2.30$	40.64	$1/3 \times (-2.3)$	-0.77	-31.29
④	$1/2 \times 26.53 \times 2.30$	30.51	$2/3 \times (-2.3)$	-1.53	-46.68
Total		660.73			4,856.20

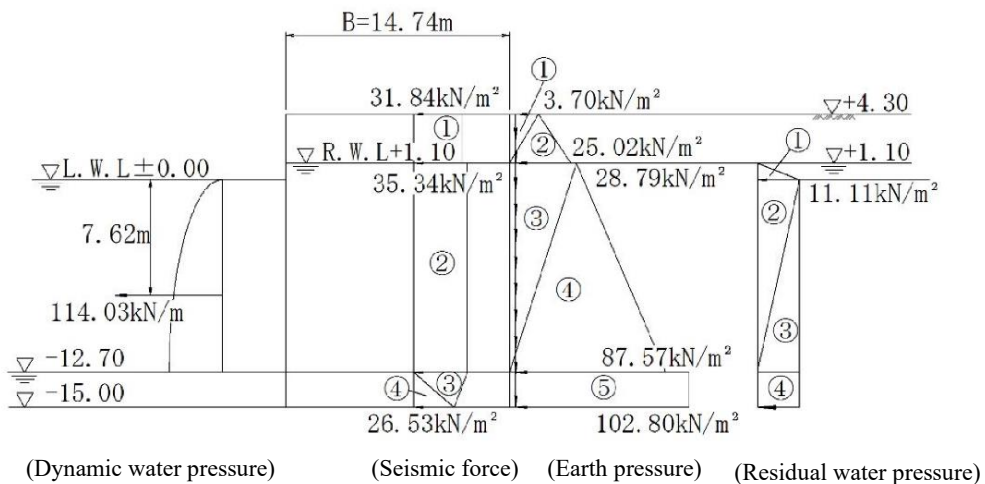


Figure 5.5.20 Horizontal load during an earthquake

b) Subgrade reaction and wall displacement

i) Coefficient of subgrade reaction

Horizontal subgrade reaction coefficient

$$K_H = 20 \text{ N/cm}^3 (= 20 \times 10^3 \text{ kN/m}^3)$$

Vertical subgrade reaction coefficient

$$K_V = 20 \text{ N/cm}^3 (= 20 \times 10^3 \text{ kN/m}^3)$$

Shear spring constant

$$K_S = 6.67 \text{ N/cm}^3 (= 6.67 \times 10^3 \text{ kN/m}^3)$$

ii) Horizontal subgrade reaction

The horizontal reaction intensity at the cell bottom during an earthquake, p_{12} , is calculated using $h = 10.90 \text{ m}$ and $\theta = 3.254 \times 10^{-3} \text{ rad}$, based on the results of the computer convergent calculation as in the case of the permanent state:

$$\begin{aligned} p_{12} &= 20 \times 10^3 \times (10.90 - 2.30) \times 3.254 \times 10^{-3} \\ &= 559.69 \text{ kN/m}^2 \end{aligned}$$

On the other hand, the passive earth pressure is calculated as follows using the apparent seismic coefficient in water k_h' , the seismic coefficient compound angle θ , and the passive earth pressure coefficient K_{pi}' :

$$k_h' = \frac{20 \times 5.00}{10 \times 5.00} \times 0.12 = 0.24$$

$$\theta = \tan^{-1} 0.24 = 13.50^\circ$$

$$K_{pi}' \cos \delta = 3.8143$$

Passive earth pressure strength P_{pi}' is:

$$\begin{aligned} P_{pi}' &= wDK_{pi}' \cos \delta = 10 \times 2.30 \times 3.8143 \\ &= 87.73 \text{ kN/m}^2 \end{aligned}$$

Since the subgrade reaction intensity is greater than the passive earth pressure strength, the horizontal subgrade reaction takes the passive earth pressure.

$$\begin{aligned} P_{pH} &= \frac{1}{2} P_{pi}' D = \frac{1}{2} \times 87.73 \times 2.30 \\ &= 100.89 \text{ kN/m} \end{aligned}$$

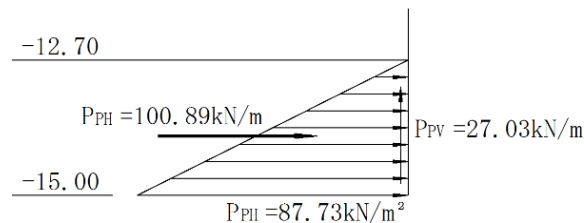


Figure 5.5.21 Horizontal subgrade reaction (during an earthquake)

iii) Vertical frictional drag force: P_{pv}

$$\begin{aligned} P_{pv} &= P_{pH} \tan \delta = 100.89 \times \tan 15^\circ \\ &= 27.03 \text{ kN/m} \end{aligned}$$

iv) Resultant forces and moments acting on wall

Horizontal force:

$$H = 2,032.80 - 100.89 = 1,931.91 \text{ kN/m}$$

Vertical force:

$$V = 3,512.92 - 27.03 = 3,485.93 \text{ kN/m}$$

Moment:

$$M = 9,263.42 + 100.89 \times \frac{2}{3} \times 2.30 - 27.03 \\ \times 7.37 = 9,218.91 \text{ kN} \cdot \text{m/m}$$

v) Rotational angle of the wall: θ

In this design case, the vertical subgrade reaction at the cell bottom during an earthquake is triangularly distributed. In this case, the rotational angle of the wall is expressed by the following equation:

$$A' = e + \frac{B}{2} = 2.98 + \frac{14.74}{2} = 10.35 \text{ m}^2/\text{m}$$

$$K_1 = K_s A' = 6.67 \times 10^3 \times 10.35 \\ = 69.03 \times 10^3 \text{ kN/m}^2$$

$$K_2 = K_s A' D = 6.67 \times 10^3 \times 10.35 \times 2.30 \\ = 158.78 \times 10^3 \text{ kN/m}$$

$$K_3 = K_s A' D = 158.78 \times 10^3 \text{ kN/m}$$

$$K_4 = K_s A' D^2 + \frac{1}{6} K_v A'^2 (B - e) \\ = 6.67 \times 10^3 \times 10.35 \times 2.30^2 + \frac{1}{6} \times 20 \times 10^3 \\ \times 10.35^2 \times (14.74 - 2.98) \\ = 4,564.39 \times 10^3 \text{ kN/m}$$

Here, A' : area per unit length in the normal direction of the bottom of the wall where the vertical subgrade reaction is positive (m^2/m).

However, e is the distance of the center of rotation of the wall from the central axis of the wall, and calculation of this distance requires the rotational angle of the wall, θ . For this reason, it is necessary to perform an iterative calculation in the actual calculation, and the result of the iterative calculation, $e = 2.98$ m, is used.

Rotational angle of the wall: θ (rad)

$$\theta = \frac{MK_1 + HK_3}{K_1 K_4 - K_2 K_3} \\ = \frac{9,218.91 \times 69.03 + 1,931.91 \times 158.78}{69.03 \times 4,564.39 - 158.78 \times 158.78} \times \frac{10^3}{10^6} \\ = 3.254 \times 10^{-3} \text{ rad} (0.176^\circ)$$

vi) Depth of the wall's center of rotation: h (m)

$$\begin{aligned}
h &= \frac{MK_2 + HK_4}{MK_1 - HK_3} \\
&= \frac{9,218.91 \times 158.78 + 1,931.91 \times 4,564.39}{9,218.91 \times 69.03 + 1,931.91 \times 158.78} \times \frac{10^3}{10^3} \\
&= 10.90\text{m}
\end{aligned}$$

vii) Distance of the wall's rotational center from the wall's central axis e (m)

$$\begin{aligned}
e &= \sqrt{\frac{2}{K_v} \left\{ \frac{V}{\theta} - h \sum_{i=1}^n K_{Hi} d_i \tan|\delta_i| + \sum_{i=1}^n K_{Hi} d_i \left(\sum_{j=1}^{i-1} d_j + \frac{d_i}{2} \right) \tan|\delta_i| \right\}} \\
&\quad - \frac{B}{2} \\
&= \sqrt{\frac{2V}{K_v \theta} - \frac{B}{2}} \\
&= \frac{2 \times 3,485.93}{20 \times 10^3 \times 3.254 \times 10^{-3}} - \frac{14.74}{2} \\
&= 2.980\text{m}
\end{aligned}$$

Since this value is almost equal to the value assumed in the calculation of θ , further calculation will also use $e = 2.98\text{m}$.

viii) Vertical ground force

$$\begin{aligned}
q_1 &= \left(K_v e + \frac{B}{2} \right) \theta \\
&= 20 \times 10^3 \times \left(2.98 + \frac{14.74}{2} \right) \times 3.254 \times 10^{-3} \\
&= 673.58\text{kN/m}^2
\end{aligned}$$

$$\begin{aligned}
q_2 &= 0\text{kN/m}^2 \\
b &= 2V/q_1 \\
&= 2 \times 3,485.93 / 673.58 \\
&= 10.35\text{m}
\end{aligned}$$

ix) Shear reaction force at the bottom of the wall (kN/m)

$$\begin{aligned}
Q &= K_s (h - D) \theta A' \\
&= 6.67 \times 10^3 \times (10.90 - 2.30) \times 3.254 \times 10^{-3} \\
&\quad \times 10.35 \\
&= 1,931.89\text{kN/m}
\end{aligned}$$

x) Horizontal displacement of the wall (m)

Horizontal displacement of the wall at its crown: δ_1 (m)

$$\begin{aligned}
\delta_1 &= (h - Z) \theta \\
&= (10.90 + 17.00) \times 3.254 \times 10^{-3} \\
&= 9.08 \times 10^{-2}\text{m}
\end{aligned}$$

Horizontal displacement of the wall at the design seabed: δ_2 (m)

$$\begin{aligned}\delta_2 &= (h - Z)\theta \\ &= (10.90 + 0) \times 3.254 \times 10^{-3} \\ &= 3.55 \times 10^{-2} \text{ m}\end{aligned}$$

Horizontal displacement of the wall at the bottom of the cell: δ_3 (m)

$$\begin{aligned}\delta_3 &= (h - Z)\theta \\ &= (10.90 - 2.30) \times 3.254 \times 10^{-3} \\ &= 2.80 \times 10^{-2} \text{ m}\end{aligned}$$

The results obtained from the convergent calculations are shown in **Figure 5.5.22** and **Figure 5.5.23**.

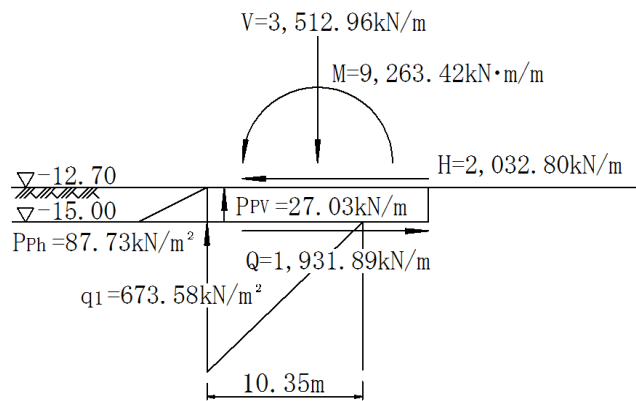


Figure 5.5.22 Distribution of the subgrade reaction (during an earthquake)

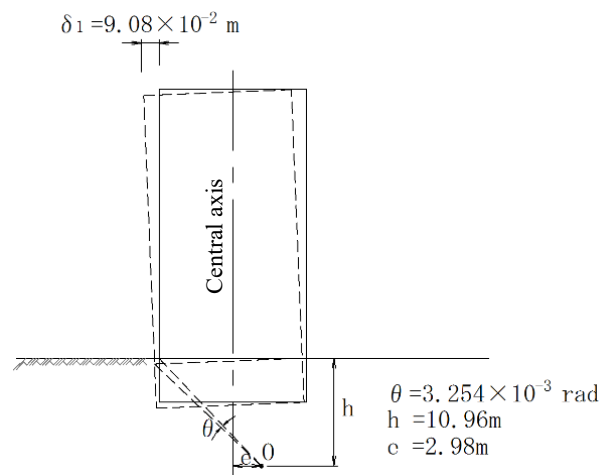


Figure 5.5.23 Wall displacement mode (during an earthquake)

3) Review of bearing capacity

i) Details of the bottom subgrade reaction

- Vertical subgrade reaction at the toe of the wall:

$$q_1 = 673.58 \text{ kN/m}^2$$

- Vertical subgrade reaction at the heel of the wall:

$$q_2 = 0.00 \text{ kN/m}^2$$

- Vertical subgrade reaction distribution width: $b = 10.35 \text{ m}$

- Bottom shear reaction force: $Q = 1,931.89\text{kN/m}$

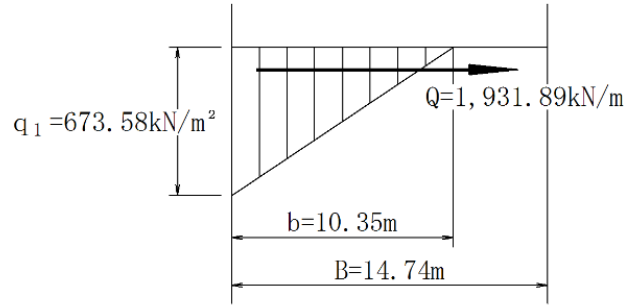


Figure 5.5.24 Bottom subgrade reaction(during an earthquake)

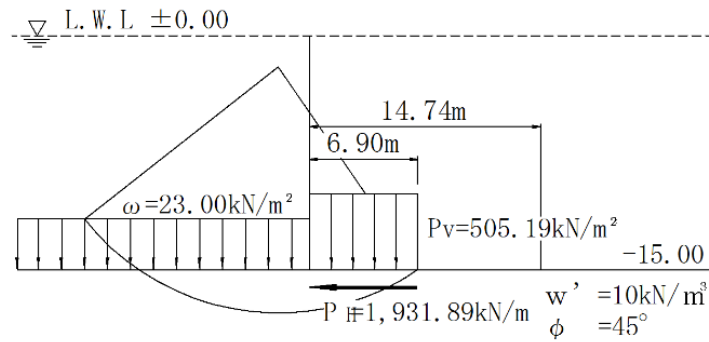


Figure 5.5.25 Calculation results using Bishop's method (during an earthquake)

- ii) Location where the subgrade reaction acts

$$b' = \frac{b}{3} = \frac{10.35}{3} = 3.45\text{m (triangular distribution)}$$

- iii) Acting load

- Vertical load: P_V

$$P_V = \frac{3}{4}q_1 = \frac{3}{4} \times 673.58 = 505.19\text{kN/m}^2$$

- Action width: L

$$L = 2b' = 2 \times 3.45 = 6.90\text{m}$$

- Shear reaction at the bottom of the wall: Q

$$Q = 1,931.89\text{kN/m}$$

- iv) Surcharge at the front of the cell: ω

$$\omega = \Sigma wh = 10 \times 2.30 = 23.00\text{kN/m}^2$$

- v) Calculation method

$$\text{Load inclination ratio: } \frac{H}{V}$$

Where, H : Shear reaction force

V : Subgrade reaction at the bottom

$$\begin{aligned}\frac{H}{V} &= \frac{Q}{\frac{1}{2}q_1 b} \\ &= \frac{1,931.89}{\frac{1}{2} \times 673.58 \times 10.35} \\ &= 0.55 > 0.1\end{aligned}$$

Therefore, Bishop's method will be used for this calculation.

vi) Calculation results using Bishop's method

Sliding moment: $M_o = 43,236.4 \text{ kN} \cdot \text{m}$

Resisting moment: $M_R = 57,348.0 \text{ kN} \cdot \text{m}$

Center of arc: $X = -2.00 \text{ m}$

$Y = -2.00 \text{ m}$

Radius of arc $R = 15.75 \text{ m}$

Performance verification:

$$m \cdot \frac{S_d}{R_d} = 1.00 \times \frac{43,236.4}{57,348.0} = 0.75 \leq 1.00$$

Where:

m : Adjustment factor 1.00

R_d : $R_d = \gamma_R R_k = 1.0 \times M_R$

S_d : $S_d = \gamma_S S_k = 1.0 \times M_o$

4) Displacement at the crown of the quaywall

Location of horizontal displacement on the crown of the quaywall: δ

$\delta = (\text{revetment height} + \text{depth of rotational center from design seabed}) \times (\text{rotational angle})$

$$= (17.00 + 10.90)\theta$$

$$= 27.90 \times 3.254 \times 10^{-3}$$

$$= 9.08 \times 10^{-2} \text{ cm}$$

The ratio of the displacement to the wall height (%) is:

Horizontal displacement at

$\frac{\text{the crown of the quay wall}}{\text{Quay wall height}} \times 100$

$$= \frac{9.08 \times 10^{-2}}{17.00} \times 100 = 0.53\% < 1.5\%$$

(8) Review of the plate thickness of the cell and arc

1) Plate thickness of the cell shell

i) Horizontal tensile force acting on the cell

$$T = \left\{ \left(w_0 H_d' + \omega \right) K + \rho_w g \cdot h_w \right\} R$$

Where:

w_0 : equivalent unit weight of the filling material (kN/m^3)

$$w_0 = 10.0(\text{kN/m}^3)$$

H_d' : equivalent wall height (m)

$$H_d' = \left\{ \frac{18 \times (4.3 - 1.10) + 10}{1.10 + 12.70} \right\} / 10$$

$$= 19.56(\text{m})$$

ω : surcharge (kN/m^2)

$$\omega = 20\text{kN/m}^2 \text{ (in the permanent state)}$$

$$\omega = 10\text{kN/m}^2 \text{ (in the variable state and during a Level 1 earthquake)}$$

K : earth pressure coefficient of filling material

$$K = \tan \phi = \tan 30^\circ$$

$\rho_w g$: unit weight of seawater (kN/m^3)

$$\rho_w g = 10.1\text{kN/m}^3$$

h_w : water level difference between the inside of the cell and the front of the cell (m)

$$h_w = R.W.L. - L.W.L. = 1.10 - 0.00$$

$$= 1.10\text{m}$$

R : radius of the cell shell

$$R = 16.00 \times \frac{1}{2} = 8.00\text{m}$$

Tensile force in the permanent state

$$T = \left\{ \begin{array}{l} (10 \times 19.56 + 20) \times \tan 30^\circ \\ + 10.1 \times 1.10 \end{array} \right\} \times 8.00$$

$$= 1,084.69\text{kN/m}$$

Tensile force in the variable state

$$T = \left\{ \begin{array}{l} (10 \times 19.56 + 10) \times \tan 30^\circ \\ + 10.1 \times 1.10 \end{array} \right\} \times 8.00$$

$$= 1,038.51\text{kN/m}$$

ii) Required thickness t_0

SS400 material (yield stress intensity: $\sigma_y = 235\text{N/mm}^2$)

Required thickness in the permanent state

$$t_0 = m \cdot T / \sigma_y = 1.67 \times 1,084.69 / 235$$

$$= 7.71\text{mm}$$

Required thickness in the variable state

$$t_0 = m \cdot T / \sigma_y = 1.12 \times 1,038.51 / 235$$

$$= 4.95\text{mm}$$

iii) Determination of plate thickness

- Service life: 50 years
- Corrosion rate: 0.20 mm/year
- Corrosion-induced penetration (corrosion rate: 10%)
 $\Delta t = 0.20 \times 50 \times 0.10 = 1.00\text{mm}$

• Required plate thickness

Based on the required thickness in the permanent state:

$$t = t_0 + \Delta t = 7.71 + 1.00 = 8.71\text{mm}$$

From the above, the plate thickness of the cell shell is set to 9 mm.

2) Plate thickness of the arc shell

i) Horizontal tensile force acting on the arc

$$T = \left\{ \left(w_0 H_d' + \omega \right) K + \rho_w g \cdot h_w \right\} R$$

Where:

w_0 : equivalent unit weight of the filling material: 10.0 (kN/m³)

H_d' : equivalent wall height: 19.56 (m)

ω : surcharge (kN/m²)

As in the case of the cell shell

K : earth pressure coefficient of the filling material

$$K = \frac{1}{2} \times \tan \phi = \frac{1}{2} \times \tan 30^\circ$$

$\rho_w g$: unit weight of seawater: 10.1 (kN/m³)

h_w : water level difference between the inside of the cell and the front of the cell: 1.10 (m)

R : radius of the arc shell

$$R = 4.771 \text{ m}$$

Tensile force in the permanent state

$$T = \left\{ \begin{array}{l} \left((10 \times 19.56 + 20) \times \frac{1}{2} \times \tan 30^\circ \right) \\ + 10.1 \times 1.10 \end{array} \right\} \times 4.771$$

$$= 349.95 \text{ kN/m}$$

Tensile force in the variable state

$$T = \left\{ \begin{array}{l} \left((10 \times 19.56 + 10) \times \frac{1}{2} \times \tan 30^\circ \right) \\ + 10.1 \times 1.10 \end{array} \right\} \times 4.771$$

$$= 336.17 \text{ kN/m}$$

ii) Required material

SS400 material (yield stress intensity $\sigma_y = 235 \text{ N/mm}^2$)

Required thickness in the permanent state

$$t_o = m \cdot T / \sigma_y = 1.67 \times 349.95 / 235$$

$$= 2.49 \text{ mm}$$

Required thickness in the variable state

$$t_o = m \cdot T / \sigma_y = 1.12 \times 336.17 / 235$$

$$= 1.60 \text{ mm}$$

iii) Determination of plate thickness

• Service life: 50 years

• Corrosion rate: 0.20 mm/year

• Corrosion-induced penetration (corrosion rate: 10%) $\Delta t = 0.20 \times 50 \times 0.10 = 1.00 \text{ mm}$

• Required plate thickness

Based on the required thickness in the permanent state:

$$t = t_o + \Delta t = 2.49 + 1.00 = 3.49 \text{ mm}$$

Since the minimum plate thickness of the arc shell is assumed to be about 8 mm based on past installation results, the plate thickness of the arc shell is assumed to be 8 mm.

Chapter 6 Reference Information Required Overseas

The following presents commentaries based on the differences between the concepts and principles of design in other countries and the Technical Standards and Commentaries for Port and Harbour Facilities in Japan, together with relevant reference literature, on questions which are frequently asked (FAQ) by engineers (construction consultants, construction companies, etc.) in areas related to ports and harbors in Japan and other countries when designing port and harbor facilities.

1. Setting of design tide levels, quay wall water depth and crown height

FAQ 1

The technical concepts of tide levels are different in Japan and other countries. How should design tide levels, the crown height of port facilities, water depth of waterways and basins, etc. be set?

1. Concept in Japan ¹⁾

1.1 Concept of tide level

The tide level is set as the water level from the reference water-level for port maintenance of the port concerned, using the following astronomical tide levels in each port.

- Mean monthly-highest water level (H.W.L.): The mean water level of the highest high-water levels for each month, which occur within a period 2 days before to 4 days after the day of syzygy, when the moon and sun are aligned as seen from earth.
- Mean monthly-lowest water level (L.W.L.): The mean water level of the lowest low-water levels each month, which occur within a period 2 days before to 4 days after the day of syzygy.

1.2 Concept of setting of design tide levels

H.W.L. (Mean Monthly-Highest Water Level) and L.W.L. (Mean Monthly-Lowest Water Level) are used for the design tide levels.

1.3 Concept of setting of crown heights of port facilities

- The general practice for breakwaters is to set the crown height at $H.W.L. + 0.6 H_{1/3}$ ($H_{1/3}$: significant wave height at H.W.L.). In this case, a wave height transmission coefficient becomes approximately 0.2.

• For quay walls, the crown height is frequently set using the following table.	Tidal range ≥ 3.0 m	Tidal range < 3.0 m
Large-scale quaywalls (water depth: ≥ 4.5 m)	0.5 to 1.5 m	1.0 to 2.0 m
Small-scale quaywalls (water depth: < 4.5 m)	0.3 to 1.0 m	0.5 to 1.5 m

When waves act on a quaywall, a crown height of $H.W.L. + H_{1/3} \times 1/2 + 0.5$ m is appropriate to protect the facility.

1.4 Concept of setting of water depth of waterways and basins

The depth of navigation channels may be set using the following values.

- Channels in port, where the effect of swells and similar waves is not assumed: $1.10 \times$ maximum draft
- Channels outside port, where the effect of swells and similar waves is assumed: $1.15 \times$ maximum draft
- Channels in open seas, where the effect of strong swells and similar waves is assumed: $1.20 \times$ maximum draft

2. Concept in other countries

2.1 Concept of tide levels

In 1997, the International Hydrographic Organization (IHO) determined that the Lowest Astronomical Tide (LAT) should be used as the marine chart datum. Following that decision, adoption of LAT and HAT (Highest Astronomical Tide) as datum levels (reference water-levels) has increased in other countries.

- Lowest Astronomical Tide (LAT): The lowest assumed water level under any combination of astronomical conditions generally considered. If LAT is used as the chart datum level (i.e., the reference level for sounding (measuring water depth) in marine charts). In this case, a negative tide level will not occur. The IHO recommends that LAT should be adopted as the chart datum level, and in cases where it is not adopted, the difference between the chart datum used in that country and LAT should be noted in

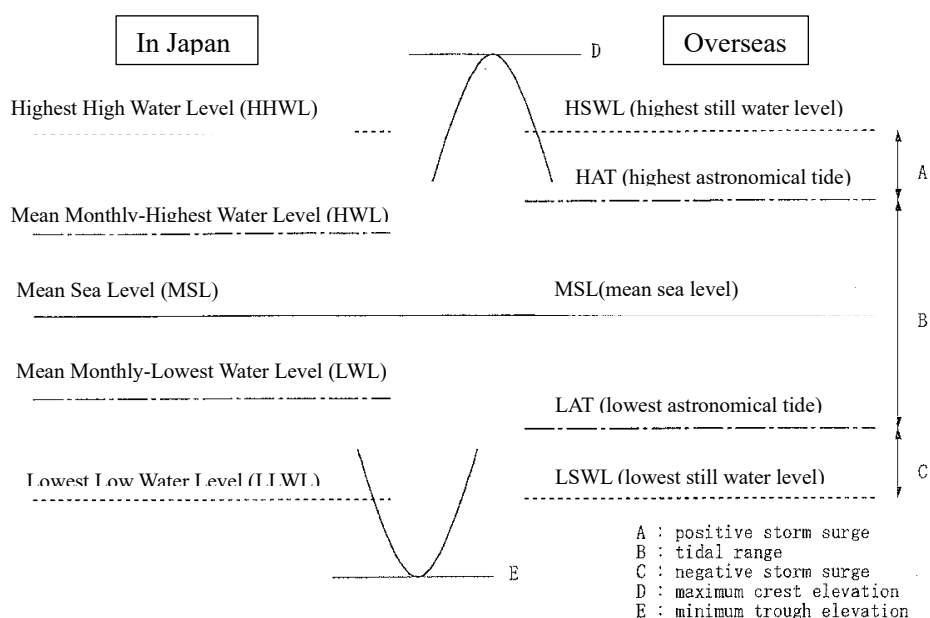
the tide table.

- Highest Astronomical Tide (HAT): The highest tide level among the tidal estimates calculated for a minimum period of 19 years.

2.2 Concept of setting of design tide levels

As design tide levels, LAT and HAT, MHWS (Mean High Water Spring), MLWS (Mean Low Water Spring), and MWL (Mean Water Level) are also used.

The relationship between the tide levels used in Japan and overseas are shown in the following Figure.



Source: Guidelines for Design of Wind Turbine Support Structures and Foundations and Commentaries (2010), Japan Society of Civil Engineers (JSCE) ²⁾

2.3 Concept of setting of crown height of port facilities

- In many overseas cases, general guidelines for the crown height of breakwaters like those in Japan are not provided, and the crown height is decided for each project so as to satisfy the functional requirements for the breakwater concerned. As examples, the allowable value of the wave height in the port due to wave overtopping, and prevention of damage of structures on the port side of the breakwater by overtopping may be mentioned. For example, the EurOtop Manual, Coastal Engineering Manual (CEM), the Rock Manual and British Standard (BS) provide permissible overtopping flow rates according to the importance of the hinterland facilities.
- Similarly, the standards in other countries do not provide simple indices for the crown height of quaywalls, which is frequently decided on a project-by-project basis based on various conditions. For example, BS states that appropriate values are to be set considering sea level rise and changes in tidal levels and flooding associated with global warming, wave overtopping, and the relationship with ships, etc. Although BS mentions securing a height of at least 1.5 m above the reference water-level, this does not mean that 1.5 m is sufficient. In particular, consideration of the effects of global warming has been required in many cases in recent years³⁾.

2.4 Concept of setting of water depth of waterways and basins

The concept of the water depth of navigation channels is the same as the standard in Japan, as the depth is set in accordance with PIANC⁴⁾.

3. Direction for local handling

For tidal levels, an appropriate design tidal level should be adopted, referring to the conditions and

standards in each region.

Regarding the crown height of port facilities, it is necessary to respond based on the conditions required in each project, while using the Japanese Standards as a guideline.

<Points to note>

Although the height of existing facilities may also be used as reference, the crown height of facilities must be set based on a reexamination of factors such as long-term sea level rise, the size of recent ships, and the like.

References

- 1) The Ports and Harbours Association of Japan, Technical Standards and Commentaries for Port and Harbour Facilities in Japan, pp. 89-104, pp. 920-929, pp. 1077-1082, 2018
- 2) Japan Association of Civil Engineers, Guidelines for Design of Wind Turbine Support Structures and Foundations and Commentaries, p. 205
- 3) BS6349-2: Maritime works. General. Code of practice for assessment of actions
- 4) Yasuhiro Akakura, Motohiro Sema, A Consideration about Port Entry of Bulk Carriers with Using Tidal Level, Research Report of National Institute for Land and Infrastructure Management, No. 47, 2011

<p>Related parts of Technical Standards and Commentaries for Port and Harbour Facilities in Japan</p>	<p>[Part II Actions and Material Strength Requirements] Chapter 2 Meteorology and Oceanography, 3 Tide Level, pp. 89-104 [Part III Facilities] Chapter 4 Protective Facilities for Harbours, 2 Common Items for Breakwaters pp.920-929, Chapter 5 Mooring Facilities, 2.1.1 Dimensions of Wharves, pp. 1077-1082</p>
---	--

2. Setting of design seismic coefficient

FAQ 2

- In countries other than Japan, how should the design ground motion be set when the time history seismic wave profile is not available as it is in Japan?
- Also, in other countries, how should the vertical component of ground motion be considered while it is not considered in Japan?

1.Design ground motion

1.1 Concept of design ground motion in Japan

In calculations of the seismic coefficient for verification in Japan, first, the acceleration time history at the location where the facility is to be installed is calculated by one-dimensional seismic response analysis which enables appropriate consideration of the ground characteristics at the design location, using the time history seismic wave profile of Level 1 earthquake ground motion of the engineering ground at each target design point as the input ground motion. The seismic coefficient for verification for the acceleration time history calculated in this manner is then calculated considering the frequency characteristics and effect of duration of the ground motion¹⁾.

When setting Level 2 ground motion in the design of high earthquake-resistance facilities and other important facilities, it is possible to evaluate the ground characteristics by conducting microtremor observation at the site, and set the earthquake ground motion used in setting the site amplification factors.

1.2 Concept of design ground motion in other countries

Unlike Japan, which uses the time-series seismic wave profile of ground motion, in other countries, there are many cases where a zoning map of the seismic parameters (PGA, S_s, S₁, etc.) is prepared for each region, and the design seismic coefficient is set for the target design point based on the zoning map. It should be noted that the return periods of virtually all seismic parameters are different from those in Japan, and the setting of each parameter is also different in some cases.

For important structures, as in the case of Japan, earthquake-resistant design is sometimes carried out using the seismic wave profile set for the location concerned.

1.3 Direction for local handling

When earthquake-resistant design (a seismic design) standards have not been prepared in the subject country, the design seismic coefficient can be calculated by using a zoning map, etc. that has been set properly in accordance with the design conditions of the site. When the time-series seismic wave profile of ground motion is available, application of the technical standards of Japan may also be considered.

<Note>

Care is necessary, as the return period of bedrock acceleration may be different from that in Japan (75 years in case of Level 1 earthquake ground motion).

2. Concerning handling of vertical component of ground motion

2.1 Handling of vertical component of ground motion

In examinations of the earthquake resistance of facilities in other countries, not only the horizontal seismic coefficient, but also the effect of the vertical seismic force is frequently considered by using the vertical seismic coefficient (e.g., vertical seismic coefficient = horizontal seismic coefficient × 1/2). On the other hand, in Japan, examinations of earthquake resistance are generally carried out considering only the horizontal seismic coefficient, as past research^{2),3)} has shown that, excluding the area near the epicenter, the vertical component of measured values of earthquake ground motion is not particularly large in comparison with the horizontal component and has little effect on the stability of gravity-type quaywalls with general dimensions. Moreover, this approach is also adopted to avoid complex calculations⁴⁾. However, in the case of earthquakes with especially large vertical motion, such as epicentral earthquakes occurring directly below the area concerned, it is also necessary to consider the effect of the vertical seismic force in the examination of earthquake resistance because the effect of the vertical component of

ground motion is too large to be disregarded.

2.2 Direction for local handling

In principle, the vertical component is considered in the standards in other countries. However, the two horizontal components are also considered in some cases. Therefore, stability should be evaluated in accordance with the standard applied in the country concerned ⁵⁾.

On the other hand, in cases where the acceleration response spectrum is small, and depending on the importance and structural type of the facility, the seismic action in the vertical direction may sometimes be disregarded in the standard of other countries ⁶⁾. A total evaluation of stability is necessary based on the results of verification by the local technical standards.

References

- 1) Ports and Harbours Association of Japan: Technical Standards and Commentaries for Port and Harbour Facilities in Japan, pp. 1903-1914, 2018.
- 2) Ports and Harbours Association of Japan: Technical Standards and Commentaries for Port and Harbour Facilities in Japan, p. 261, 1999.
- 3) Tatsuo Uwabe, Setsuo Noda, Eiichi Kurata: Characteristics of vertical components of strong-motion accelerograms and effects of vertical ground motion on stability of gravity-type quay walls, Report of the Port and Harbour Research Institute, Vol. 15, No. 2, 1976
<https://www.pari.go.jp/search-pdf/vol015-no02-07.pdf>
- 4) Atsushi Nozu, Tatsuo Uwabe, Yukihiko Sato, Takumi Shinozawa: Relation between Seismic Coefficient and Peak Ground Acceleration Estimated from Attenuation Relations, Report of the Port and Harbour Research Institute, No. 893, 1997, <https://www.pari.go.jp/search-pdf/no0893.pdf>
- 5) ASCE Standard [ASCE/SEISMIC 7-10]: Minimum Design Loads for Buildings and other Structures, pp. 84-86, 2010
- 6) ASCE STANDARD [ASCE/SEI 7-16] : Minimum Design Loads and Associated Criteria for Buildings and Other Structures, pp.99, 2016

<p>Related parts of Technical Standards and Commentaries for Port and Harbour Facilities in Japan</p>	<p>[Reference Technical Data on Part III Facilities] Chapter 1 Fundamentals of Seismic Design, 1 Detailed Items Related to Seismic Coefficient for Verification pp. 1903-1914 [Part III Facilities] Chapter 5 Mooring Facilities, 2 Wharves, 2.2 Gravity-type Quaywalls, 2.2.2 Actions, pp. 1065-1066</p>
---	---

3. Verification of circular slip failure by the modified Fellenius method

FAQ 3

In Japan, the modified Fellenius method has been adopted as a technique for verification of circular slip failure. In other countries, what method should be used where there are few examples of adoption of the modified Fellenius method?

1. Record of application of modified Fellenius method in verification of circular slip failure

Circular slip failure analysis by the modified Fellenius method is widely used in Japan. This is because it has been reported that examples of slope failure can be explained convincingly from the results of analyses of case histories of slip failure of seawalls in ports and harbors in Japan¹⁾²⁾³⁾⁴⁾. Since there have been no reports of accidents, in case of the application of the modified Fellenius method, and this method has an extensive record of actual use, it can be considered a highly reliable method for practical work. Moreover, troublesome convergent calculations are not necessary, handling and verification of analysis results are easy and computational errors are unlikely, as analysis is also easy.

2. Appropriateness of application of modified Fellenius method to verification of circular slip failure

Research by Nakase (1967)⁶⁾ showed that appropriate results can be obtained by conducting an analysis of the cohesiveness, particularly for cohesive ground ($\phi = 0$).

3. Examples of safety factors adopted when applying the modified Fellenius method in verification of circular slip failure in other countries

When the modified Fellenius method is applied in verification of circular slip failure in cases where the main object is cohesive soil, it is permissible to set a basic safety factor of 1.3, but methods conforming to other standards (e.g., Eurocode 7) are also possible. However, as the safety factor (partial factor) in such cases, it is necessary to use the value in case the method provided in those standards is applied.

4. Notes on application of the modified Fellenius method

The modified Fellenius method tends to underestimate stability for circular slip failure cutting through foundation ground consisting entirely of sandy soil layers, and when the ground consists of a thick sandy upper layer over a lower layer of cohesive soil. Under these conditions, the simplified Bishop method provides high evaluation accuracy, and use of the simplified Bishop method is advisable in case of eccentric and inclined loads, which are particularly a problem when examining the bearing capacity of mounds.

On the other hand, stability against sliding failure accompanying a noncircular failure surface of multilayer ground is evaluated by the limit equilibrium (LE) method, which evaluates the equilibrium of both force and moment, using a commercially-available slope stability analysis program, etc.

5. Circular slip failure verification methods other than the modified Fellenius method

Eurocode 7 mentions that use of the modified Fellenius method is unacceptable because it can only handle the balance of rotational moment (moment equilibrium)⁷⁾.

In addition, BS-EN 1997-1 also does not provide a method for use in circular slip failure for evaluation of overall stability⁸⁾.

In other countries, application of techniques that solve the balance of both moment and force are recommended. For example, the Spencer method and the Morgenstern-Price method, which is a method for slope stability analysis of noncircular slip surfaces, are widely used, and the Morgenstern-Price method uses an approximate moment equilibrium equation⁹⁾. Although the mainstream of software used overseas includes programs that cover analytical methods for various types of slip failure (e.g., SLOPE/W), some do not include the modified Fellenius method. In addition to the above-mentioned slip failure analysis methods, ground analysis by FEM (e.g., PLAXIS) is increasingly used when a complex analysis is required.

References

1) Tsuchida, T. and Athapaththu, A.M.R.G.,2014: Practical method based on Slip Circle of Slices for

<p>Calculation of Bearing Capacity, Vol.54, No.6, 2014, Soils and Foundations, Volume 54, Issue 6, December 2014, Pages 1127-1144.</p> <p>2) Tsuchida, Takashi: Circle Slide Stability Analysis by Circle Bearing Capacity Factor Method and its Application, Ground Engineering, Vol. 34, No. 1, pp. 1-10, 2016.</p> <p>3) Tsuchida, Takashi and Kitade, Keisuke: Evaluation on Design Strength of Intermediate Soil for Construction of Breakwater in Port of Sakai-Minato, Soils and Foundations. Volume 60, Issue 1, February 2020, Pages 239-256</p> <p>4) Tsuchida, Takashi: Case studies on design strength evaluation of marine deposits using combined method of unconfined compression test and triaxial test in seaport projects, Soils and Foundations (Journal of the Japanese Geotechnical Society), Vol. 16, No. 3. pp. 159-178, 2021 (English version now in preparation).</p> <p>5) Ports and Harbours Association of Japan: Technical Standards and Commentaries for Port and Harbour Facilities in Japan, pp. 748-752, 2018</p> <p>6) Akio Nakase, The $\varphi = 0$ analysis of stability and unconfined compression strength, Soils and Foundations, Vol. 7, No. 2 pp. 33-50, 1967 https://www.jstage.jst.go.jp/article/sandf1960/7/2/7_2_33/_pdf/-char/ja</p> <p>7) Eurocode 7: Geotechnical Design – Worked examples, 6.2.3 Slope Stability Analyses, pp. 61-64 https://eurocodes.jrc.ec.europa.eu/doc/2013_06_WS_GEO/report/2013_06_WS_GEO.pdf</p> <p>8) BS EN 1997-1(2004) : Geotechnical design Part 1</p> <p>9) Kanji Kondo, Setsuo Hayashi: Similarity and Generality of the Morgenstern-Price and Spencer Methods, Journal of the Japan Landslide Society, Vo. 4, No. 1, 1997 https://www.researchgate.net/publication/274518328_Similarity_and_Generality_of_the_Morgenstern-Price_and_Spencer_methods https://www.jstage.jst.go.jp/article/jls1964/34/1/34_1_15/_pdf</p>	
<p>Related parts of Technical Standards and Commentaries for Port and Harbour Facilities in Japan</p>	<p>[Part III Facilities] Chapter 2 Items Common to Facilities Subject to Technical Standards, 4 Stability of Slopes, pp. 748-752</p>

4. Verification of bearing capacity for eccentric and inclined loads by the simplified Bishop method

FAQ 4

In Japan, the simplified Bishop method has been adopted as a verification method for the bearing capacity of foundations for eccentric and inclined loads. In other countries, what method should be used when verification methods that treat the allowable vertical bearing capacity as a limit value or FEM analysis are adopted?

1. Actual results of application of the simplified Bishop method in verification of the bearing capacity of foundations for eccentric and inclined loads

Circular slip failure analysis by the simplified Bishop method has become a standard method for verification of the bearing capacity of foundations for eccentric and inclined loads in Japan¹⁾, and has been applied in a large number of cases. In other countries, rather than the simplified Bishop method, verification methods that treat the allowable vertical bearing capacity of the foundation mound and ground as limit values^{e.g.2),3),4)}, or verification methods employing FEM analysis are widely used.

2. Appropriateness of application of the simplified Bishop method in verification of the bearing capacity of foundations for eccentric and inclined loads

Kobayashi et al.^{5),6)} conducted model experiments, field experiments and a comparative study with past verification methods related to the bearing capacity of foundation mounds for eccentric and inclined loads, and showed the appropriateness of the simplified Bishop method in verifications of the bearing capacity of foundations for eccentric and inclined loads. The main conclusions of this paper are as follows.

- Large-scale model experiments have shown that the permissible toe pressure of foundation mounds (400 to 500 kN/m²), which had been used as an empirical value, changes depending on the load condition.
- The ultimate bearing capacity obtained experimentally showed comparatively good agreement with the result of a circular slip failure analysis by the simplified Bishop method.
- If the three-dimensional effect is corrected for the results of site tests, the results are in good agreement with the results of the circular slip failure analysis by the simplified Bishop method.
- When compared with the results of a field experiment in which a block (3 m × 4 m × 2.5 m high) on a mound was loaded with a jack, the calculated value obtained by the simplified Bishop method was basically appropriate.
- The results of analyses of disasters and non-disaster cases involving actual breakwaters and wharves confirmed that the phenomena can substantially be explained by applying the simplified Bishop method to the representative stone materials used in Japan.

3. Direction for local handling

Because the verification method using the allowable vertical bearing capacity of the foundation mound and ground as limit values is based on a bearing capacity equation which is applied to single stratum ground, its application is limited to cross sections in which a rubble mound is installed on the foundation ground. From that viewpoint as well, it is considered possible to adopt the simplified Bishop method for verification of the bearing capacity of the foundation on the rubble mound. However, a total judgment of applicability is necessary, noting the following points.

- The simplified Bishop method has ample verification results in laboratory experiments with typical stone materials in Japan. However, because the angle of shear resistance of rubble varies depending on the lithology and producing region, large-scale triaxial compression tests or plate loading tests should be carried out when using special stone materials produced in Okinawa or overseas.
- Because the simplified Bishop test may give an excessive safety factor when vertical loading is applied to flat sandy ground, the proper handling should also be studied, for example, correction of the ratio of shearing force and normal force, etc.⁷⁾.

4. New knowledge

Reinforcing embankment, in which stone materials are installed on the port side of the wall body, is used to reinforce existing breakwaters. The current design method for reinforcing embankment, was adopted provisionally about 40 years ago and continues to be used. However, that method only considers sliding resistance. As a new knowledge, the following have been studied: i) use of the simplified Bishop method to calculate the sliding resistance of reinforcing embankment work, ii) clarification of the positioning of reinforcing embankment in verification of overturning failure and failure of bearing capacity and iii) review of the minimum provisions for reinforcing embankment⁷⁾.

In addition, the failure characteristics and a performance verification method of reinforcing embankment have been analyzed by centrifuge model tests and circular slip failure analysis⁸⁾. In that research, sliding failure occurred first when the friction coefficient between the wall body (caisson) and rubble mound was small, the width of caisson was large or the height or width of the widening work was large, and in other cases, failure of bearing capacity occurred first.

References

- 1) Ports and Harbours Association of Japan: Technical Standards and Commentaries for Port and Harbour Facilities in Japan, pp. 681-685, 2018.
- 2) Puertos del Estado: Geotechnical Recommendations for the Design of Maritime and Harbor Works (ROM 0.5-05), pp. 207-210, 2008
- 3) European Committee for Standardization: Eurocode7 Geotechnical Design, pp. 30-33, 128-159, 2004
- 4) The British Standards Institution: BS8004: 2015 Code of Practice for Foundations, pp. 37-42, 2015
- 5) Masaki Kobayashi, Masaaki Terashi, Kunio Takahashi, Kenjiro Nakashima and Hikaru Odani, A New Method for Calculating the Bearing Capacity of Rubble Mounds, Report of the Port and Harbour Research Institute, Vol. 26, No. 2, 1987
- 6) Masaki Kobayashi, Masaaki Terashi, Kunio Takahashi : Bearing Capacity of a Rubble Mound Supporting a Gravity Structure, PARI report 026-05-06, 1987
- 7) Takehiko Sato, Masafumi Miyata, Hidenori Takahashi, Masahiro Takenobu, Kenichiro Shimosako and Kojiro Suzuki, A Proposal on Design Method for Wave Force of Breakwater with Reinforcing Embankment, Technical Note of National Institute for Land and Infrastructure Management (NILIM), No. 954, 2017
- 8) Hidenori Takahashi : Stability of composite-type breakwaters reinforced by rubble embankment, Soils and Foundations, Jan 2021.

Related parts of
Technical Standards and
Commentaries for Port
and Harbour Facilities in
Japan

[Part III Facilities] Chapter 3 Foundations, 3.2 Shallow Spread Foundations,
3.2.5 Bearing Capacity for Eccentric and Inclined Actions, pp. 681-685

5. Standards for mooring posts and bollards

FAQ 5

In the design of mooring posts and bollards in Japan, the mooring force (standard for mooring posts and bollards) is determined specifically when the ship type is decided. How should mooring force be determined in other countries where this method is not used?

1. Concept of design of mooring posts and bollards in Japan¹⁾

The mooring force acting on bollards is calculated by a ship oscillation calculation for an acting wind velocity of 15 m/s from the land side, assuming that a cargo ship in the empty state is moored with a total of 8 mooring ropes. The mooring force for mooring posts is calculated by a ship oscillation calculation for an acting wind velocity of 30 m/s from the land side, assuming mooring with a total of 10 mooring ropes, including use of mooring posts. When mooring a ship during a storm with properly arranged mooring ropes using bollards and mooring posts, the mooring force is such that the mooring ropes can withstand winds with a wind velocity of 30 m/s acting from the land side.

The description presented above is in accordance with oscillation calculations (simulation of oscillation of moored ships) by Yoneyama (2018) based on standard ship sizes, and adopts the maximum value of all mooring forces acting on mooring posts and bollards²⁾.

2. Comparison of mooring posts and bollards in Japan and other countries

The mooring force acting on mooring posts and bollards corresponds to the breaking load of one or two mooring ropes, as provided in the Steel Ship Regulations (Nippon Kaiji Kyokai, Vol. L, Fittings)³⁾, and it has been confirmed that the mooring force of the mooring posts and bollards is greater than the breaking load of the mooring ropes. Because the above-mentioned Steel Ship Regulations were determined based on the standards of IACS (International Association of Classification Societies), it can be said that the mooring posts and bollards exceed a breaking load equal to that of mooring ropes.

BS6349-1-2 requires that mooring posts and bollards possess strength equal to or greater than the SWL (Safe Service Load), and the SWL is equal to or greater than the MBL (Minimum Breaking Load) of the mooring ropes. Moreover, separate examination is necessary in cases where more than 1 mooring rope is used⁴⁾.

In addition to the above, in the standards of OCIMF (Oil Companies International Marine Forum), breaking load is set in “Mooring Equipment Guidelines”⁵⁾.

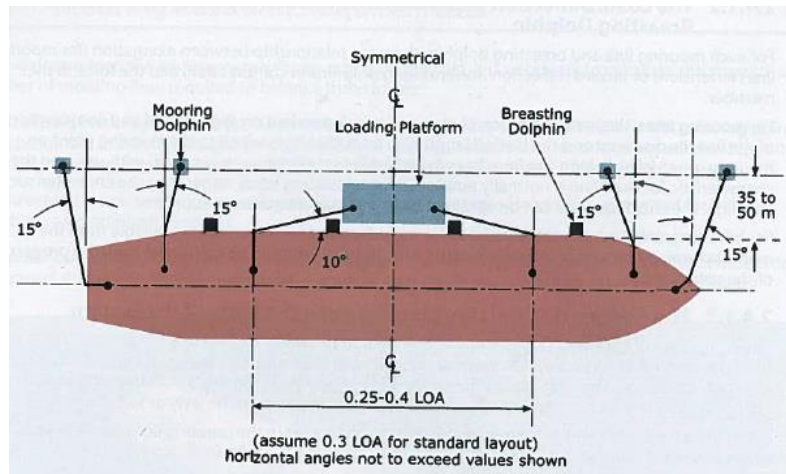
Japanese manufacturers of mooring posts and bollards have expressed the opinion that their durability is high and there have been few cases of damage because Japanese mooring posts and bollards are made of cast steel.

The types of mooring posts (bollards) used overseas include the tee bollard, horn bollard, kidney bollard, cleat bollard, double bitt bollard, single bitt bollard and pillar bollard, among others. With the exception of cleat bollards, the maximum capacity of these bollards is 200 to 300 tons. For the types of mooring posts and bollards, see the product brochure of Trelleborg Marine and Infrastructure⁶⁾, etc.

3. Direction for local handling

The mooring force of moored ships is greatly influenced by the size and wind pressure area of the ship, the number and arrangement of the mooring posts and bollards and the wind velocity and direction, among other factors. Therefore, if the dimensions of the design ship, the specification of the mooring ropes and the arrangement of the mooring posts and bollards, etc. have been determined, it is more appropriate to select the standard for mooring posts and bollards by calculating the mooring force of the moored ship based on a static load calculation or dynamic calculation (simulation of oscillation of moored ship) considering those conditions⁷⁾.

In general, mooring bollards are installed with a center-to-center interval in the range of 15 to 30 m, but for island-type mooring berths, the mooring points should be installed within a range of 35 to 50 m from the mooring line for ships of the largest class.



Mooring points used in island berth (OCIMF MEG3)

However, standard values for the mooring force of ships for bollards and mooring posts have been proposed in Japan's technical standards, and these standard values may be used for a simple selection of the standard for mooring posts and bollards based only on the gross tonnage (GT) of the design ship when the other conditions are not known.

References

- 1) Ports and Harbours Association of Japan: Technical Standards and Commentaries for Port and Harbour Facilities in Japan, pp. 440-442, pp. 1257-1261, 2018.
- 2) Haruo Yoneyama: Study of Mooring Forces of Ships Acting on Mooring Posts and Bollards, Technical Note of the Port and Airport Research Institute (PARI), No. 1341, 2018
<https://www.pari.go.jp/search-pdf/No.1341.pdf>
- 3) Nippon Kaiji Kyokai: Steel Ship Regulations, Vol. L, Chapter 4, 2019
- 4) BS6349-1-2 : Maritime works. General. Code of practice for assessment of actions
- 5) OCIMF : Mooring Equipment Guidelines, 2018
- 6) Trelleborg Marine and Infrastructure product brochure
- 7) BS 6349-4 (2014) : Maritime structures Part 4: Code of practice for design of fendering and mooring systems

Related parts of Technical Standards and Commentaries for Port and Harbour Facilities in Japan

[Part II Action and Material Strength Requirements] Chapter 8 Ships, 2.4 Actions due to Traction of Ships, pp. 440-442
[Part III Facilities] Chapter 5 Mooring Facilities, 9.1 Mooring Posts and Mooring Rings, pp. 1257-1261

6. Design of fender systems	
FAQ 6	How should fender systems be designed so as to include effect factors such as berthing speed, abnormal berthing, the natural environment and the like?
<p>1. Overview</p> <p>In Japan, the design method for rubber fender systems is provided in Technical Standards and Commentaries for Port and Harbour Facilities in Japan¹⁾, and the related specifications and test methods are specified in Standard Specifications for Port & Harbour Works²⁾.</p> <p>Overseas, the provisions of the British Standard³⁾, PIANC Report⁴⁾ and PIANC Guidelines⁵⁾ are generally used. The PIANC Guidelines⁵⁾, which were issued in 2002, proposed a design method that considers variations in the performance of rubber fender materials due to berthing speed and the natural environment.</p> <p>For consistency between the foreign and Japanese design methods and test methods, Guidelines for Design and Testing of Rubber Fender System⁶⁾ is a useful reference on design methods for constant reaction-type rubber fender systems. This standard corresponds to the PIANC Guidelines and also considers effect factors such as changes over time in the rubber fender materials, etc., and also presents test methods corresponding to these design methods.</p> <p>2. Main points to note in design</p> <p>The main points to note based on the characteristics of rubber fender systems are error in manufacturing, aging, dynamic characteristics (speed dependent characteristics), creep characteristics, cyclic loading properties, inclined compression characteristics and temperature characteristics.</p> <p>2.1 Speed dependency of fender systems (Velocity Factor: V_F)</p> <p>Although the performance of Japanese rubber fender systems is defined as performance under compression at a static strain rate (0.01 to 0.3 %/s), the criterion used in the PIANC Guidelines⁵⁾ is the performance of the fender when the speed gradually decreases from an initial speed of 0.15 m/s. Therefore, it is necessary to note the differences in the assumptions on which catalog values are based. The above-mentioned Guidelines for Design and Testing of Rubber Fender System⁶⁾ presents a detailed explanation of the handling of both methods.</p> <p>2.2 Berthing velocity (V)</p> <p>Berthing velocity has a substantially larger effect than other factors because effective berthing energy is calculated using the square of the berthing velocity (i.e., V^2). In the Japanese Standards, actual measured data were collected and arranged, and the relationship between the ship berthing velocity and the type of ship was proposed⁷⁾. Furthermore, the relationship between the ship berthing velocity and the type of ship is also presented as a regression formula that considers the coverage rate (coverage rate: 50 to 99 %).</p> <p>The PIANC Guidelines of 2002 presented the design velocity curve proposed in 1977 by Brolsma et al., which assumes a coverage rate of 50 %. For comparison, the proposed values of Spain's ROM standard are also given. While this is also mentioned in BS 6349-4 : 2014 as a factor that should be considered, the BS standard presents the above-mentioned Brolsma curve. On the other hand, based on measurements obtained in a survey by PIANC-WG145, the new PIANC-WG211 found that the correlation between the berthing velocity and ship displacement is significantly lower than that in the curve proposed by Brolsma, and is now studying how that should be set depending on the navigation condition and ship type.</p> <p>2.3 Abnormal berthing coefficient (C_{ab})</p> <p>The condition required in a fender system is that the absorbed energy E_A must be at least as large as the effective berthing energy E_b of a ship. In the PIANC Guidelines, the effective berthing energy is multiplied by an abnormal berthing coefficient (C_{ab}) of 1.25 to 2.0, depending on the ship type, to take into account abnormal berthing in which the effective berthing energy exceeds absorbed energy due to mishandling of the ship, unexpected strong winds or tidal currents, etc. However, if high reliability can be obtained in the</p>	

berthing velocity, *Cab* may be reduced to 1.1. BS 6349 sets factors of 1.5 (low risk) to 2.0 (high risk) according to the ship type. Since ship navigation reliability is high in Japan, and the definition of a stable velocity and the grounds for the abnormal berthing coefficient are unclear (and should be considered in the setting of the berthing velocity), a *Cab* of 1.0 is used in many cases. The new PIANC-WG211 is studying a proposal in which the Navigation Condition and Failure Consequence (degree of effect of failure) are defined in various levels and presented as a table of partial factors of energy. This is expected to clarify the background of this issue.

2.4 Patterning of influence coefficients

In order to satisfy both safety and economy, Japan's Guidelines for the Design and Testing of Rubber Fender Systems⁶⁾ classifies conditions that consider the effect of velocity and temperature (following the PIANC Guidelines), design conditions considering only manufacturing tolerances, as in the past, and a number of effect factors, as in the case of floating mooring facilities. In one trial calculation, performance variations, and particularly the reaction force, were calculated for the berthing velocity (deceleration), as in the PIANC Guidelines. The results showed that the absorbed energy condition could be satisfied with a slightly smaller size or performance grade than in the conventional design method, but the reaction force and surface pressure tended to increase slightly.

2.5 Re-hardening of rubber fender systems

If a rubber fender is not compressed for a long period, it has been found that the reaction force increases upon first compression after that period. Thus, care is necessary when reusing fenders which have been stored in stock, or after long periods without berthing.

3. Future direction

A revision of the PIANC Guidelines⁵⁾ for fender systems scheduled for release in 2023 is underway in PIANC WG211.

References

- 1) The Ports and Harbours Association of Japan, Technical Standards and Commentaries for Port and Harbour Facilities in Japan, pp. 451-465, pp. 1320-1326, 2018
- 2) The Ports and Harbours Association of Japan, Standard Specifications for Port & Harbour Works, Vol. 1, pp. 71-72, 2017
- 3) British Standard : Maritime Structures-Part 4 Code of Practice for Design of Fendering and Mooring Systems, 2014
- 4) PIANC : Report of the International Commission for Improving the Design of Fender Systems, Bulletin No.45, 1984
- 5) PIANC : Guidelines for the Design of Fenders System, *Report of Service Group 33 of the Maritime Navigation Commission*, 2002
- 6) Coastal Development Institute of Technology : Guidelines for Design and Testing of Rubber Fender Systems, 2019
- 7) Kazuyasu Murakami, Masahiro Takenobu, Masafumi Miyama and Haruo Yoneyama, Fundamental Analysis on the Characteristics of Berthing Velocity of Ships for the Design of Port Facilities, Technical Note of National Institute for Land and Infrastructure Management, No. 864, 2015
- 8) H. Akiyama, K. Shimizu, S. Ueda, T. Kamada: Investigation on Service Years of Large Rubber Marine Fenders, *Journal of JSCE*, Vol.5, pp.392-401, 2017.

Related parts of Technical Standards and Commentaries for Port and Harbour Facilities in Japan

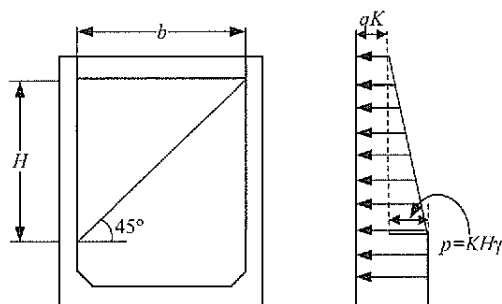
[Part II Actions and Material Strength Requirements]
Chapter Ships, 2 Actions Caused by Ships, pp. 451-465
[Part III Facilities]
Chapter 5 Mooring Facilities, 9.2 Fender Systems, pp. 1320-1326

7. Earth pressure from filling soil acting on caisson outer wall

FAQ 7 Why is the earth pressure from the filling soil acting on the caisson outer wall considered?
How is it set?

1. Earth pressure from filling soil acting on caisson outer wall

The internal earth pressure and internal water pressure are considered as actions on caisson side wall members. As shown in the Figure at the right, internal earth pressure increases until the depth H is equal to the inner width dimension b of the caisson, but does not increase thereafter¹⁾.



Determination of internal earth pressure

The internal water pressure is considered to be the head difference between the water levels inside and outside the caisson. When sand or rubble is used as the filling material, the internal earth pressure is calculated by using the coefficient of earth pressure at rest K (generally, 0.6). The internal earth pressure can be disregarded when the filling consists of blocks or concrete. In cases where hard cast-in-place concrete is located on top of caissons and it can be regarded that the effect of the surcharge does not reach the filling, the surcharge can be disregarded.

The internal earth pressure is calculated by using the coefficient of earth pressure at rest K (generally, 0.6). The internal earth pressure can be disregarded when the filling consists of blocks or concrete. In cases where hard cast-in-place concrete is located on top of caissons and it can be regarded that the effect of the surcharge does not reach the filling, the surcharge can be disregarded.

2. Overseas design examples of caissons

BS 6349-2 states that the earth pressure used in the structural design of the wall is to be at least the earth pressure at rest²⁾.

3. Direction for local handling

From the above, it can be said that there is no problem with using the earth pressure at rest, which is used in the Japanese Standard, as the internal earth pressure acting on the caisson side wall.

4. Main points to note in design

- For internal earth pressure, earth pressure at rest calculated by the following formula is used.

$$p = K\Sigma\gamma h$$

Where, K : static earth pressure at rest (= 0.6)

The coefficient of earth pressure at rest K can generally be calculated by the formula shown below:

$$K = 1 - \sin \phi$$

For example, in the case of earth and sand having $\phi = 30^\circ$, $K = 1 - \sin 30^\circ = 1 - 0.5 = 0.5$. However, in design, it is advisable to use $K = 0.6$, which is based on model experiments which were conducted by actually filling caissons with sand.

- If the filling material is stone or rubble, which have large internal friction angles, it is necessary to determine the coefficient of earth pressure at rest appropriately by model tests or field tests at the site. However, even when these materials are used, the above-mentioned $K = 0.6$ is frequently used in practical work, based on past study results showing that there is no decrease in the coefficient³⁾.
 - Following Reference⁴⁾, in cases where the slope of the caisson outer wall is 10° , 20° or 30° , the earth pressure decreases factors of $K = 0.6$, 0.56 and 0.46 may be applied, respectively

References

- 1) The Ports and Harbours Association of Japan, Technical Standards and Commentaries for Port and Harbour Facilities in Japan, pp. 579-611, 2018
- 2) BS6349-2: Maritime works. General. Code of practice for assessment of actions
- 3) Yoshiaki Kikuchi, Kunio Takahashi and Takumi Ogura, Dispersion of Earth Pressure in Experiments and Earth Pressure Change due to the Relative Movement of the Neighboring Walls, Technical Note of the Port and Harbour Research Institute, No. 811, 1995

4) Kunio Takahashi, Yasuo Kasugai, Nobutaka Namerikawa, Nobuaki Sakaki and Misao Suzuki, Earth Pressure due to Filling Sand in Inclined Wall Caisson, Technical Note of the Port and Harbour Research Institute, No. 604, 1987	
Related parts of Technical Standards and Commentaries for Port and Harbour Facilities in Japan	[Part III Facilities] Chapter 2 Items Common to Facilities Subject to Technical Standards, 2 Members of Structures, 2.2 Caissons, pp. 579-611

8. Design of piled piers

FAQ 8 | Why are the virtual ground surface and virtual fixed point set? How is setting done?

1. Virtual seabed surface and virtual fixed point when piles are installed on slope¹⁾

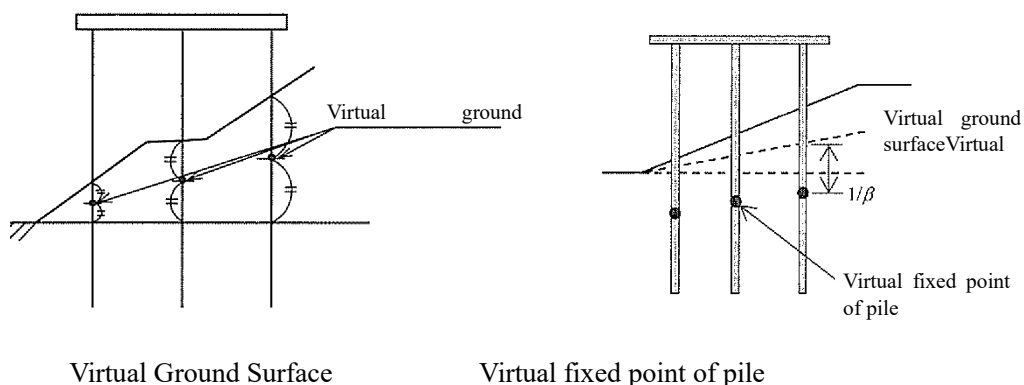
- Concept of virtual seabed surface (virtual ground surface)

The calculation method for the lateral resistance of piles used in analyses of open-type wharves on piled piers is originally related to horizontal ground surfaces, but in case the inclination of the slope of the seabed ground where a wharf is to be installed is considerably steep, the virtual ground surface for each pile used in calculations of the pile lateral resistance and bearing capacity may be set at an elevation that corresponds to 1/2 of the vertical distance between the frontal water depth and the actual slope surface at the position of the axial line of each pile.

- Concept of virtual fixed point

As the virtual fixed point of the piles of an open-type wharf on piled piers, $1/\beta$ (β : characteristic value of pile) below the virtual ground surface may be used.

The case when piles are installed in a slope is shown in the Figure at the right.



2. Examples in other countries

The concept of the virtual ground surface described above is also widely used in other countries, and is described similarly in ASCE²⁾. On the other hand, when the slope of the actual seabed is smaller than 1 : 5 (11.30°), the behavior of the piles will be substantially the same as that of a flat ground surface, or the decrease in the lateral bearing capacity of the piles will be limited to the range of 1.5 to 2 %^{3),4)}. There are also cases where the effect of the slope is basically negligible and the seabed can be regarded as a horizontal surface. When the gradient of the slope increases to more than 1 : 5, an appropriate ground surface is set.

Note that there was also a case in Singapore where the spring value was set by a combined analysis also using an FEM analysis.

3. Direction for local handling and points to note

In case the concepts of the virtual ground surface and virtual fixed point in the Japanese standards are adopted, it is necessary to note the following points.

- In case scouring is assumed, the effects of scouring should also be considered.
- In setting the virtual seabed surface, it is not appropriate to use this method in cases where the width of the piled pier is wide (exceeding 20 m) and the slope is extremely long.
- In case of improvement for deepening of the seabed ground, the virtual ground surface shall be 1) for example, a height approximately halfway between the actual slope after deepening and the frontal water depth after deepening (i.e., level of the foot of the slope) (Figure. 1). In case deepening is performed by using an earth-retaining sheet pile structure, 2) for example, in addition to the concept in 1), the range of the principal active collapse angle that acts on the earth-retaining piles shall not consider the lateral resistance acting on the piles (Figure. 2). However, a study should be carried out by a FEM analysis,

etc. which is capable of considering the geometry of the slope and the stiffness and initial stress of the earth-retaining piles. For both 1) and 2), it is necessary to perform calculations for circular slip failure and study the overall stability of the structure.

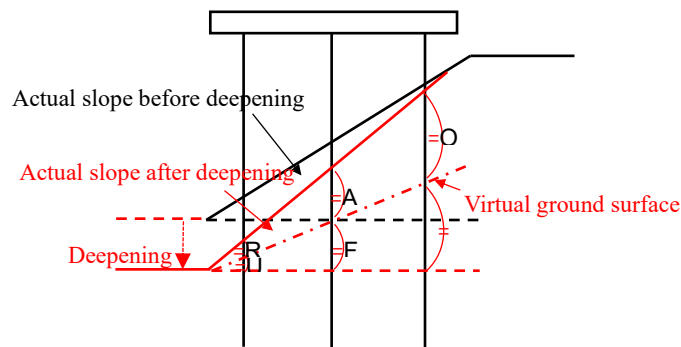


Figure. 1 Example of setting the virtual ground surface in case of deepening (the actual ground surface after deepening corresponds to the angle of repose)

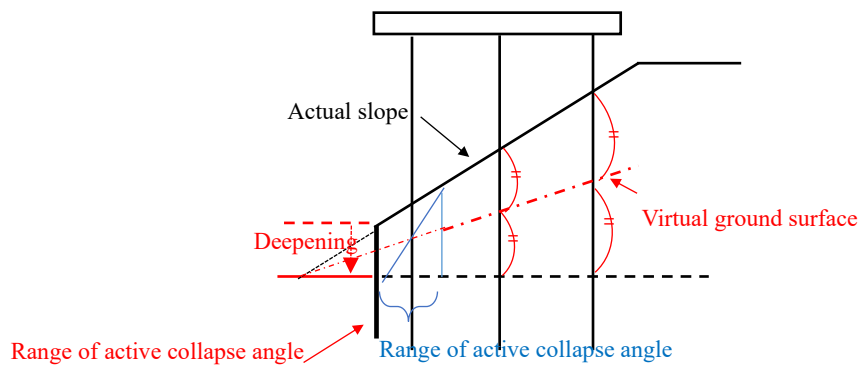


Figure. 2 Example of setting the virtual ground surface in case of deepening (deepening using an earth-retaining sheet pile structure)

Reference

- 1) Ports and Harbours Association of Japan: Technical Standards and Commentaries for Port and Harbour Facilities in Japan, pp. 1203-1204, 2018.
- 2) John W. Garthwaite: Design Marine of facilities, ASCE,2016
- 3) R. Deendayal, K. Muthu Kumaran, T.G. Sitharam : Behaviour of Laterally Loaded 1-g Single Model Pile in Soft Clay with Sloping Ground
- 4) Sivapriya S. V.*, Rahul RAMANATHAN : Load - Displacement behaviour of a pile on a sloping ground for various L/D ratios

Related parts of Technical Standards and Commentaries for Port and Harbour Facilities in Japan

[Part III Facilities] Chapter 5 Mooring Facilities, 5 Piled Piers, (6) Assumptions Related to Seabed Surface (8) Virtual Fixed Point, pp. 1203-1204

9. Scouring of front side of quay wall

FAQ 9	Detailed study of the mechanism of scouring and its countermeasures is more strongly required overseas than in Japan. How should this be handled?
-------	---

1. Concept of mechanism and countermeasures for scouring in Japan

The following scouring evaluation methods have been presented. In cases where the effects of scouring on the soundness of the mound armor materials may harm the stability of the facilities, appropriate action is to be taken.

- As a calculation formula for the required mass of armor stones and blocks for composite breakwater rubble mounds against waves, Hudson's formula using the stability number N_s .
- As a calculation formula for the required mass of armor stones and blocks against currents, the Isbash formula presented by the Coastal Engineering Research Center (C.E.R.C.) in the United States as the required mass of riprap for preventing scouring by tidal currents.
- As a calculation formula for the required mass of armor materials against tsunami overflow, which is an original Japanese formula, determination of the scale of reinforcing embankment work and scouring prevention work for the sea bottom ground, based on the overflow rate acting on armor work obtained by hydraulic model experiments and numerical simulations and examples of disaster affecting breakwaters under the action of the tsunami following the 2011 Great East Japan Earthquake.
- Scouring prevention works for mooring facilities are described in the reference literature³⁾ concerning armor stones, gabions, concrete block mats, concrete-filled pillow-shaped geotextile mats, sea bottom deflectors (curved plates) and similar devices, and the literature⁴⁾ on flow rate calculation methods for scouring caused by ship propellers.
- Structural examples, standard blending ratios and standard values for judgment of test results for asphalt mats for prevention of scouring of structural foundations, and geosynthetics for sand sucking prevention as filter materials.

2. Concept of mechanism and countermeasures for scouring in other countries

PIANC Report No. 180²⁾ was compiled referring to various standards used in other countries shown in reference 5) to 10) below, and is organized in series from the mechanism of occurrence to design and countermeasures. First, quaywalls are classified by structural type, and the mechanism of damage by scouring is presented for each structure. Various types of ship propulsion systems are also classified, and the features, speed distribution, etc. of each propulsion system are shown. As an example, a formula of the flow rate distribution and flow velocity generated by a side thruster is shown below.

In addition, reference 2) shows the design method, range of protection, operation guidelines, etc. for scouring protection.

$$V_0 = C_3 \left(\frac{f_p \cdot P_D}{\rho_w \cdot d_{thruster}^2} \right)^{0.33}$$

C_3 : coefficient depending on the propulsion system (ducted thruster: 1.17, general: 1.48)

f_p : percentage of engine output

P_D : maximum engine output

ρ_w : density of seawater (t/m^3)

$d_{thruster}$: propeller diameter (m)

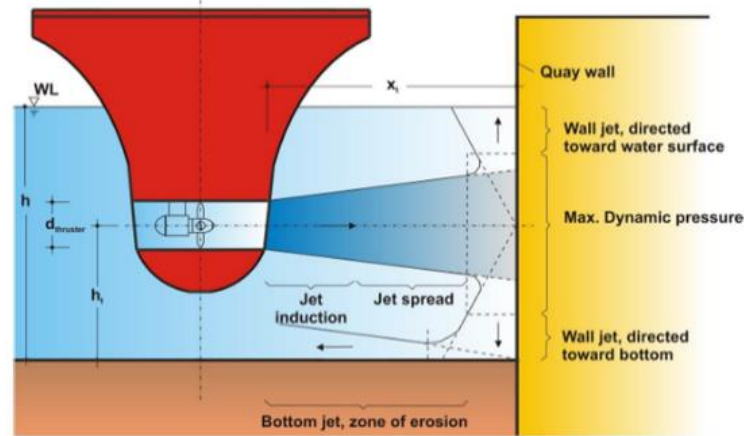


Figure 8.1: Relevant area in the flow field of a transverse thruster

3. Direction for local handling

In study of scouring, it is desirable to adopt suitable concepts referring to local conditions. In local handling, it is also necessary to note the following points.

<Points to note>

- Events that become causes of scouring (waves, ship propulsion system, tidal currents, tsunamis, etc.)
- Confirmation of the target structural types, water depth, and applicable range for scouring countermeasures
- Propulsion systems of target ships

4. Examples of scouring countermeasures in other countries

The scouring countermeasures in other countries use basically the same materials as in Japan, as shown by 1) Rock, 2) Rock grouted with liquid asphalt, 3) Rock grouted with hydro concrete, 4) Concrete block mattresses, 5) Concrete slabs, 6) Concrete mattresses, 7) Fibrous open stone asphalt mattresses, 8) Geosynthetics and geosystems and 9) Soil improvement. However, the method of countermeasures should be selected by the structural type, target ship and mechanism of scouring.

The following shows an example of countermeasures for a block-type quay wall where the sea bottom surface is scoured by ship thrusters.

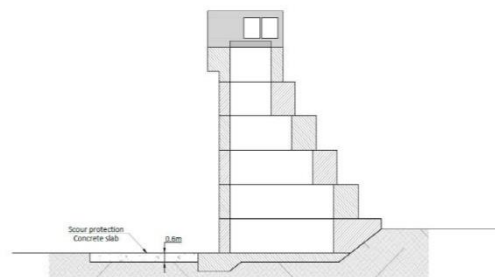


Figure 9.8: Use of concrete slab⁷ (Port of Ngqura, South Africa) [du Plessis, 2010]

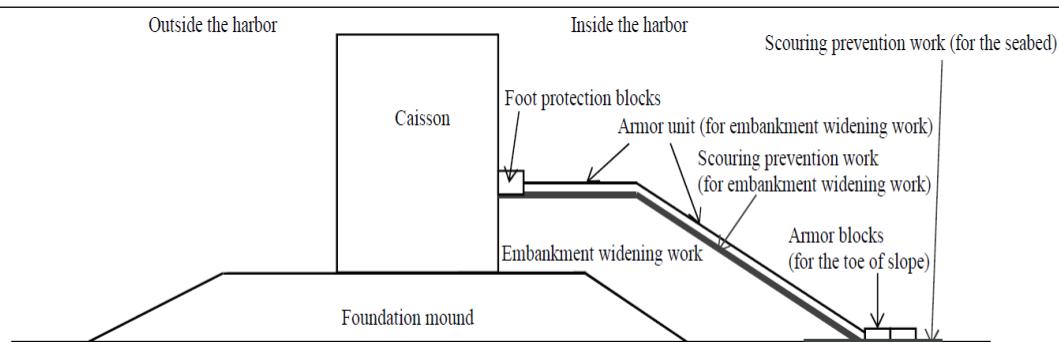
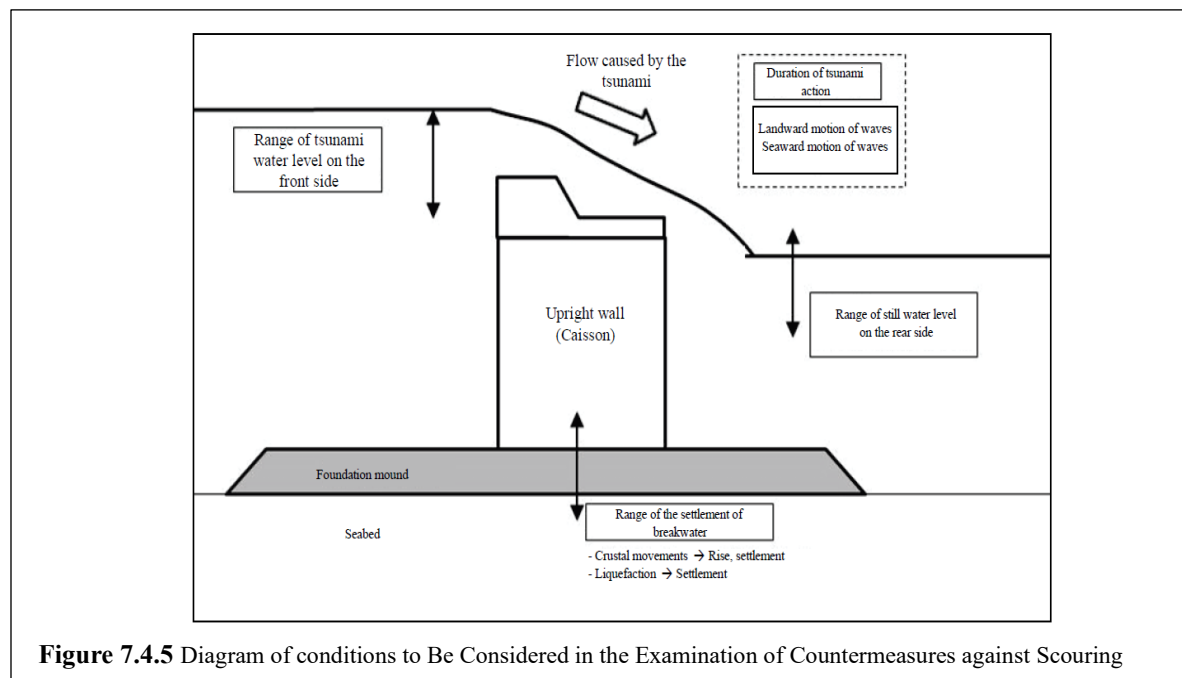
5. Examples of original Japanese scouring countermeasures

The tsunami protection performance of breakwaters will be seriously affected if a tsunami overflows the structure. Therefore, in addition to countermeasures for wave actions, prevention of scouring of the foundation mound and sea bottom ground by tsunamis is also a basis of scouring countermeasures in Japan.

Here, it should be noted that the condition when a tsunami reaches its greatest height at the front side of a breakwater is not necessarily the most dangerous condition for scouring of the foundation mound and sea bottom ground. Therefore, when studying scouring countermeasures against overflow, it is necessary

to consider the chronological characteristics of the water level, etc. against target tsunamis (see **Figure 7.4.5**).

It has also been shown that reinforcing embankment work (levee widening), which is an original Japanese scouring countermeasure, can increase the sliding resistance force of the upright section of a breakwater and the bearing capacity of the foundation mound, while also reducing scouring of the foundation mound and sandy ground on the back side of the upright section (see **Figure 7.4.6**).



References

- 1) The Ports and Harbours Association of Japan, Technical Standards and Commentaries for Port and Harbour Facilities in Japan, 2018, pp. 237-296 (Ch. 6.6), pp. 512-515 (Ch. 11.4.2), pp. 930-989 (Ch. 4.3), pp. 994-1055 (Ch. 4.6-18), pp. 1072-1077 (Ch. 5.2), pp. 1243-1287 (Ch. 5.5), pp. 1308-1314 (Ch. 5.8), pp. 1402-1410 (Ch. 6.3), pp. 1148-1458 (Ch. 11.3)
- 2) PIANC REPORT No 180 : Guidelines for protecting berthing structures from scour caused by ships, 2015
- 3) C. Zimmerman, H. Schwarze, N. Schulz, and S. Henkel: International Conference on Coastal and Port Engineering in Developing Countries, 25/29 September, Rj, Brazil, pp.2437~2451, 1995.
- 4) PIANC WG4 : Guidelines for the Design and Constructions of Flexible Revetments Incorporating Geotextiles for Inland Waterways, Supplement to Bulletin No.57, 1987.
- 5) BAW (2005): "Principles for the Design of Bank and Bottom Protection for Inland Waterways",

<p>Mitteilungen 88, Federal Waterways Engineering and Research Institute, Karlsruhe.</p> <p>6) CIRIA, CUR, CETMEF (2007): “Rock Manual, The use of rock in hydraulic engineering (2nd edition) C683, CIRIA, London.</p> <p>7) CUR (2005): “Handbook Quay Walls, CUR 211E”, Taylor and Francis Group.</p> <p>8) EAU (2009): “Recommendations of the Committee for Waterfront Structures – Harbours and Waterways”, Digitised and updated edition.</p> <p>9) U. S. Army Corps of Engineers: “Coastal Engineering Manual”.</p> <p>10) ROM (2000): “Recommendations for Maritime works”, Ministry of Public Works, Spain.</p>	
<p>Related parts of Technical Standards and Commentaries for Port and Harbour Facilities in Japan</p>	<p>[Part II Actions and Material Strength Requirements] Chapter 2 Meteorology and Oceanography, 6.6 Stability of Armor Stones and Blocks against Waves, 6.7 Tsunami Wave Force, 6.8 Wave Force during Storm Surge, 7.5 Scouring and Sucking, Chapter 11 Materials, 4.2 Asphalt Mats [Part III Facilities] Chapter 4 Protective Facilities for Harbors, 3 Ordinary Breakwaters, 6 Storm Surge Protection Breakwaters, 7 Tsunami Protection Breakwaters, 9 Sediment Control Groins, 10 Seawalls, 11 Training Jetties, 12 Floodgates, 14 Revetments, 15 Coastal Dikes, 16 Jetties, 18 Siltation Prevention Facilities, Chapter 5 Mooring Facilities, 2 Wharves, 5 Piled Piers, 8 Boat Lift Yards, Chapter 6 Port Transportation Facilities, 3 Underwater Tunnels, Chapter 11 Other Port Facilities, 3 Beaches</p>

10. Bearing capacity of pile foundations

FAQ 10

Calculations of the bearing capacity of pile foundations in Japan and other countries are different in some cases. What should be done in such cases?

1. Concept of calculation of bearing capacity of pile foundations in Japan

According to the Technical Standards¹⁾ of Japan, the bearing capacity of a pile foundation is obtained by an estimated formula using the N -value for sandy ground and the undrained shear strength c_u for cohesive ground (see **Table-1**). The estimated equation for the end resistance of a pile q_p in sandy ground is a version of the method proposed by Meyerhof²⁾, which has been modified based on experience, and the end resistance was changed from 400 N to 300 N in the revision of the Technical Standards of 1986 considering the results of a statistical analysis of the actual record until that time. In addition, the maximum value of the skin friction force of piles in cohesive ground was set to 100 kN/m².

In Japan, a partition plate is sometimes provided at the tip end of piles to increase the closed-area ratio (plugging effect ratio) of large-diameter steel pipe piles. Because the effect of the partition plate is affected by pipe diameter, the characteristics of the pile tip soil and other factors in addition to the cross-sectional shape and installation length of the plate. Recently, verification of the effect of partition plates by load tests is required when expecting the improvement of the plugging effect ratio.

2. Concept of calculation of bearing capacity of pile foundations in other countries

The basic method for estimation of the bearing capacity of pile foundations is the same in Japan and other countries. Although the bearing capacity is obtained by equation (1) in both cases, the methods of calculating the end resistance q_p and the skin friction q_s of piles are different.

$$R = A_p q_p + A_s q_s \quad (1)$$

R : axial pushing resistance of a pile, A_p : area of the pile end, A_s : area of the pile in contact with the ground, q_p : end resistance of the pile, q_s : skin friction of the pile

As shown in **Table-1**, the design method for the bearing capacity of a pile foundation in cohesive ground is basically the same as in Japan. However, the treatment concerning sandy ground is completely different from that in Japan, as other countries have adopted methods in which the pile end resistance q_p is obtained from bearing capacity coefficients (N_q , N_{qs}) determined from the angle of shear resistance of the ground, and the effective overburden pressure σ'_{v0} . The method for determining skin friction is also different from that in Japan, as an estimation method that considers the effective overburden pressure and the frictional resistance between the pile and sandy ground is used.

Table-1 Methods for Calculation of End Resistance and Skin Friction of Piles^{3),4)}

		Technical Standards of Japan	Eurocode 7	US Army Corps of Engineers (USACE)
Sandy ground	End resistance q_p (kN/m ²)	300 N	$N_{qs}\sigma'_{v0}$	$N_q\sigma'_{v0}$
	Skin friction q_s (kN/m ²)	$\bar{2}N$	$K_{qs}\sigma'_{v0} \tan \delta$	$K_{qs}\sigma'_{v0} \tan \delta$
Cohesive ground	End resistance q_p (kN/m ²)	6 c_u	9 $c_u + \sigma'_{v0}$	9 c_u
	Skin friction q_s (kN/m ²)	c_u	αc_u	αc_u

N : N -value, N_{qs} , N_q : bearing capacity coefficient, N : average N -value, σ'_{v0} : effective overburden pressure, K_{qs} : coefficient of horizontal earth pressure, δ : angle of shear resistance (between pile and ground), c_u : undrained shear strength, α : factor related to undrained shear strength

3. Direction for local handling

A total evaluation of stability based on the results of a verification by the local technical standards is necessary. In the local handling, it is also necessary to note the following points.

<Points to note>

- According to the results of past research, as a result of trial design of the embedment length necessary

for a pile foundation using methods based on the Japanese Technical Standards and Eurocode 7, the difference in the case of cohesive ground was comparatively slight, but the difference in the design results for sandy ground tended to be large⁵⁾. If the embedment length in sandy ground is large (deeper than 40 m), care is necessary because the method according to the Japanese Technical Standards may underestimate the bearing capacity of the piles in comparison with other overseas standards⁶⁾.

- In the Japanese Technical Standards, the maximum value of the skin friction of piles in cohesive ground is set at 100 kN/m², but in other countries, larger values are used in some cases based on the results of loading tests. It is also necessary to set the bearing capacity of pile foundations in a comprehensive manner, based also on the results of loading tests.

References

- 1) Ports and Harbours Association of Japan: Technical Standards and Commentaries for Port and Harbour Facilities in Japan, pp. 690-732, 2018.
- 2) Meyerhof, G.G.: Penetration Tests and Bearing Capacity of Cohesionless Soil, J. of SMFE, ASCE, Vol. 82, No. SM1, pp. 1-10, 1956
- 3) Orr, T.L.L. and Farrell, E.R.: Geotechnical Design to Eurocode 7, p. 113, 1999
- 4) US Army Corps of Engineers: Design of Pile Foundations, p. 20, 1993
- 5) Yoichi Moriya, Hideo Matsumoto, Toshiro Tanabe, Shuji Yamamoto: Comparative Study for Structural Design between Technical Standards for Port Facilities in Japan and Eurocodes, National Institute for Land and Infrastructure Management (NILIM), 2001
- 6) Yoshiaki Kikuchi, Taichi Hyodo: FY 2019 “Steel Structure Research and Educational Assistance Project,” Materials of Research Presentation Meeting, 2019

Related parts of
Technical
Standards and
Commentaries for
Port and Harbour
Facilities in Japan

[Part III Facilities] Chapter 2 Items Common to Facilities Subject to Technical Standards, 3 Foundations, 3.4 Pile Foundations, 3.4.1 General, 3.4.2 Fundamentals of Performance Verification of Piles, 3.4.3 Axial Pushing Resistance of Piles, pp. 690-700

11. Methods for assessment of liquefaction

FAQ 11

The methods for assessing liquefaction differ in Japan and overseas in some cases. How should liquefaction be determined in this case?

1. Concept of assessment of liquefaction in Japan

In Japan, prediction and assessment of ground liquefaction are generally made based on the particle size and standard penetration test value (*SPT-N*) or based on the results of a cyclic triaxial test^{1),2)}.

2. Concept of assessment of liquefaction in other countries

In other countries, the Seed (ASGE) assessment method is frequently used. This method has also been introduced in the Recommendations for Design of Building Foundations of the Architectural Institute of Japan (AIJ)³⁾

3. Direction for local handling

An appropriate concept should be adopted referring to local conditions. The following points should be noted in local handling.

<Points to note>

As a common point, both the Seed (ASGE) method and the assessment method in Technical Standards and Commentaries for Port and Harbour Facilities in Japan use the above-mentioned *SPT-N* value and vertical effective stress. However, the two methods differ in the following points:

- In the Seed method, liquefaction is assessed based on a liquefaction triggering (liquefaction susceptibility) chart (**Figure. 1**) showing the relationship between the cyclic shear stress ratio, which indicates the correlation between the severity of external seismic force and ground liquefaction, and the ground strength obtained by field tests, which indicates resistance to liquefaction. In Technical Standards for Port and Harbour Facilities in Japan, the cyclic shear stress ratio is assessed by equivalent acceleration.
- The Seed (ASGE) liquefaction triggering chart corresponds to an earthquake of magnitude M7.5. For earthquakes of other magnitudes, a magnitude correction factor is introduced, and cyclic stress is corrected based on the assumption that an equivalent number of repeated cycles occurs in any arbitrary earthquake. The Japanese Standards make it possible to judge liquefaction taking into account the effective wavenumber of the input seismic motion by using the wave correction coefficient c_a to correct the equivalent acceleration obtained by a seismic response analysis. The validity of applying this correction method accounting for the influence of the waveforms and durations of earthquakes to Seed liquefaction triggering charts and similar charts worldwide has also been demonstrated⁴⁾.

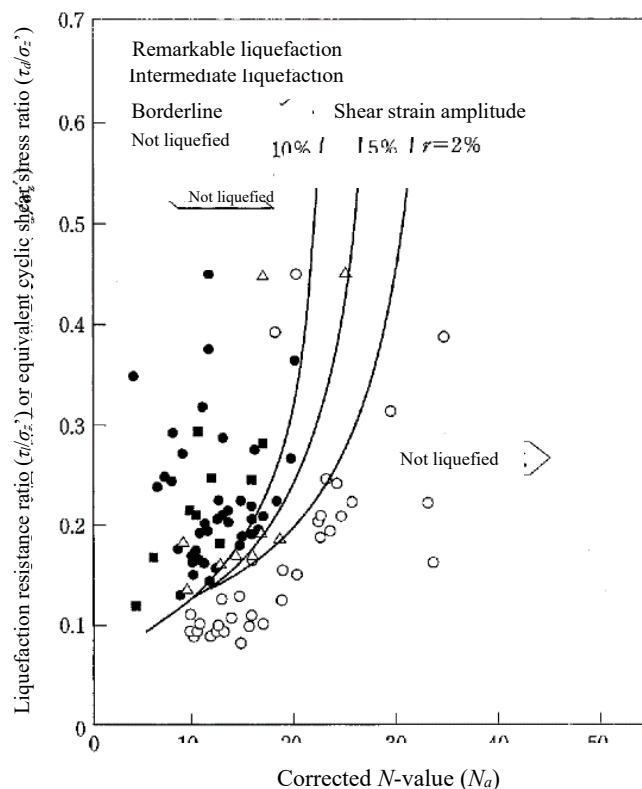


Figure 1 Relationship of corrected N-Value, liquefaction resistance and dynamic shear strain³⁾

References

- 1) The Ports and Harbours Association of Japan, Technical Standards and Commentaries for Port and Harbour Facilities in Japan, pp. 428-437, 2018
- 2) Reclaimed Land Liquefaction Countermeasures Handbook (Revised Ed.), 1997
- 3) Architectural Institute of Japan, Recommendations for Design of Building Foundations, pp. 62-65, 2001
- 4) Shinji Sassa, Hiroyuki Yamazaki : Simplified Liquefaction Prediction and Assessment Method Considering Waveforms and Durations of Earthquakes : Journal of Geotechnical and Geoenvironmental Engineering, ASCE, DOI:10.1061/(ASCE) GT.1943-5606.0001597, 2017

Related parts of
Technical
Standards and
Commentaries for
Port and Harbour
Facilities in Japan

[Part II Actions and Material Strength Requirements] Chapter 7 Ground
Liquefaction, 2 Prediction and Assessment of Liquefaction, pp. 428-437

12. Design wave	
FAQ 12	How is wave estimation (i.e., wave hindcasting) done when setting design waves?
<p>1. Method of wave hindcasting in Japan¹⁾</p> <p>In wave estimation, the temporal and spatial changes in the wind direction and velocity of a target water area are estimated from the topographical and meteorological data around the target waters, after which the waves which are generated and developed under that wind field are estimated. Although there are various methods for estimating waves from the wind field of a prescribed area, the current main stream is the spectrum method (3rd generation model)²⁾.</p> <p>Among 3rd generation models, WAM³⁾ has been widely applied to coastal waters in Japan, and SWAN⁴⁾ is an extension of that method to shallow waters. These methods solve the process called advection, by which physical properties of fluids such as pressure, temperature, density, momentum, etc. of wave and current are transported. The calculation of advection (discretization of the advection terms) has first-order accuracy in the WAM model and second-order accuracy in the SWAN model, and it can generally be said that analytical accuracy improves at higher orders.</p> <p>WAVE WATCH III⁵⁾ is an extension of a model developed by NOAA (National Oceanic and Atmospheric Administration) and NCEP (National Centers for Environmental Prediction). Unlike SWAN, this model does not consider the effects of breaking waves in coastal waters, but it is possible to select analysis (discretization scheme) with third-order accuracy.</p> <p>2. Concept of wave hindcasting in other countries</p> <p>Although wave hindcasting is also performed by the same techniques in other countries, the meteorological data of the ECMWF (European Centre for Medium-Range Weather Forecasts), NOAA, etc. can also be used in hindcasting in addition to the meteorological data of the Japan Meteorological Agency's global model.</p> <p>3. Direction for local handling</p> <p>As wave hindcasting techniques, there is no problem with using the Japanese techniques as-is, since the hindcasting models used in Japan were developed overseas. However, the following points should be noted in local handling.</p> <p><Points to note></p> <p>All meteorological data used in wave hindcasting are available globally. However, in applying such data, appropriate judgment is necessary based on the target waters, etc.</p>	
<p>References</p> <p>1) The Ports and Harbours Association of Japan, Technical Standards and Commentaries for Port and Harbour Facilities in Japan, pp. 125-131, 2018</p> <p>2) Hiroyuki Yamamoto, Introduction of WAVEWATCH III to COMEINS Wave Forecasting, Proceedings of the Coastal Development Institute of Technology (CDIT), No. 17, 2017</p> <p>3) WAM : The Wamdi Group : The WAM Model-A Third Generation Ocean Wave Prediction Model</p> <p>4) SWAN : http://swanmodel.sourceforge.net/ (as of December 2019)</p> <p>5) WW3 : https://polar.ncep.noaa.gov/waves/wavewatch/</p>	
Related parts of Technical Standards and Commentaries for Port and Harbour Facilities in Japan	[Part II Actions and Material Strength Requirements] Chapter 2 Meteorological and Oceanography, 4.3 Generation, Propagation and Attenuation of Waves, pp. 125-131

13. Cathodic protection

FAQ 13

The concepts of cathodic protection in Japan and other countries differ in some cases. What approach should be used in such cases?

1. Concept of cathodic protection in Japan¹⁾

- The applicable range of the cathodic protection method is considered to be below the mean low water level (M.L.W.L). In general, 90 % is used as the corrosion control rate for the area below M.L.W.L. According to Tado et al. (2019), based on a study of the cathodic protection effect using test pieces at 4 ports over a 4-year period, there were large variations in the corrosion rate during the non-protection time, and there were also large variations in the corrosion control rate (prevention rate), but in almost all cases, the corrosion control rate was 90 % or less, and the corrosion rate during the period when cathodic protection was effective was on the order of 0.01 mm/y²⁾.
- The protective potential of steel materials in port structures is -780 mV (vs Ag/AgCl[sw]) when a seawater silver chloride electrode is used as a standard. A value of -900 mV (vs Ag/AgCl[sw]) by conversion to a seawater silver chloride electrode is recommended as the protective potential of steel materials in special sea areas with heavy proliferation of anaerobic sulfate reducing bacteria in seabed soil³⁾.
- The protective current density is set separately for clean sea waters and polluted sea waters using the chloride ion concentration, dissolved oxygen concentration and ammonium ion concentration as indexes, based on the results of a survey of cathodic protection conducted in various parts of Japan.

2. Concept of cathodic protection in other countries

2.1 ISO 13174⁴⁾

- MWL and below is defined as submerged.
- The protective potential is set to -0.8 V as a standard. It is considered necessary to apply -0.9 V in anaerobic environments in seabed soil.
- The standard value of the protective current density is set in sections for the tidal current speed, locations of microbial corrosion, the degree of pollution of the sea waters and the elapsed time. The initial values are similar to those used in Japan.

2.2 BS EN 12473⁵⁾

- As cathodic protection systems, the sacrificial anode system and the impressed current system may be mentioned. These are the same as in Japan.
- The corrosion rate when cathodic protection is functioning adequately is 0.01 mm/y or less.
- The basic specification of the sacrificial anode system requires a specified design life which is longer than the required minimum design life by conducting annual inspections, followed by anode exchanges.

2.3 DNV-RP-B401⁶⁾

- MWL and below is defined as submerged.
- The protective potential is set to -0.8 V as a standard. It is considered necessary to apply -0.9 V in anaerobic environments in seabed soil.
- The standard value of the protective current density is set in sections for the water depth, water temperature and installation location. The initial values are similar to those used in Japan.

3. Direction for local handling

- Although the effects of cathodic protection in other countries are similar to those in the Japanese Standard, local handling based on the concept of the applicable standard in the target region is appropriate.
- Instead of corrosion protection by cathodic protection, in many cases, corrosion protection by coating methods (including painting) is performed to a depth zone deeper than the intertidal zone. Therefore, it is necessary to set the ranges for the various types of corrosion protection referring to the applicable

standards and actual results of use in the target region.	
References	
1) Ports and Harbours Association of Japan: Technical Standards and Commentaries for Port and Harbour Facilities in Japan, pp. 473-476, 2018	
2) Hiroto Tado et al.: A Study on Evaluation Index of Cathodic Protection Effect in Port Steel Structure Based on Test Piece Survey Result, Zairyo-to-kankyo, Vol. 68, No. 8, pp. 220-226, 2019	
3) Coastal Development Institute of Technology (CDIT): Manual on Corrosion Protection and Repair for Port and Harbour Steel Structures (2009 Edition), pp. 69-92	
4) ISO 13174 : Cathodic protection of harbor installations	
5) ISO 12473 : General principles of cathodic protection in seawater	
6) Det Norske Veritas : DNV-RP-B401, Cathodic Protection Design, 2005	
Related parts of Technical Standards and Commentaries for Port and Harbour Facilities in Japan	[Part II Actions and Material Strength Requirements] Chapter 11 Materials, 2.3 Corrosion of Steel Materials, 2.4 Cathodic Protection of Steel Materials, pp. 473-476 [Part III Facilities] Chapter 2 Items Common to Facilities Subject to Technical Standards, 1.5 Corrosion Protection Design of Steel Materials, 2.4 Corrosion Protection of Steel Materials, pp. 603-606

14. Selection of wave-dissipating concrete blocks

FAQ 14

In the selection of wave-dissipating concrete blocks, how are the block shape and weight selected?

1. Selection of wave-dissipating blocks in Japan

- According to the Japan Wave Dissipating and Toe Protection Block Association¹⁾, 27 types of wave-dissipating concrete blocks (upright type) are registered in Japan, and the maximum size is the 100 t-type (virtual mass: 99.6 t).
- Because wave-dissipating concrete blocks are generally non-reinforced concrete, reinforcing bars are not taken into account in the mass of almost all types. However, reinforcing bars are used in some cases when damage, etc. is expected frequently.
- Dolos is well-known as a steel reinforced wave-dissipating concrete block, and the maximum size is the 80 t-type (virtual mass: 82.3 t). Since Dolos has an extremely large value of the stability constant K_D ($K_D = 20$), it can be said to have 2 to 3 times higher stability than the general tetrapod ($K_D = 8.3$). However, as distinctive features of Dolos, it cannot be removed after installation, and rocking occurs easily due to its relatively light weight.
- In calculating the required weight of wave-dissipating concrete blocks, Hudson's formula is used in almost all cases, and a block type with a weight (t-type) equal to or larger than the calculated required weight is selected. However, for complex topographies and structures, and for sites with special wave conditions, verification of the stability of the wave-dissipating concrete blocks by hydraulic model experiments is recommended.
- In cases where multiple types of wave-dissipating concrete blocks are applicable, the superior type is selected based on a comparison of items including the actual record of manufacture and construction near the planned installation site, the construction cost considering the void ratio, etc.

2. Selection of wave-dissipating concrete blocks in overseas standards

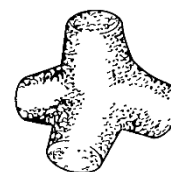
- When selecting large-scale wave-dissipating concrete blocks in accordance with BS 6394-7²⁾, it is necessary to consider the fact that the strength of the blocks decreases as their size increases, and if blocks with a complex shape are to be used, careful study of all of the aspects of design, manufacture and block placement is necessary.
- For the largest size of wave-dissipating concrete blocks, the recommended values of the maximum mass corresponding to the various block types are also presented.

Table 6 — Suggested maximum sizes of concrete armour units

Unit	Maximum size
	t
Dolos	15
Stabit	20
Tetrapod	30
Antifer block	60



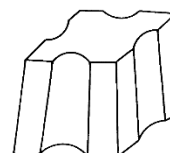
Dolos



Tetrapod



Stabit



Antifer block

3. Points to note in local handling

- Because the formula for calculating the required mass of wave-dissipating concrete blocks is common with Hudson's formula, it is thought the types of blocks developed in Japan can also be used in other countries. However, it is necessary to confirm the concepts of the stability numbers (K_D , N_S , etc.) used in calculating the required mass in the applicable standards, appropriate to the target area.
- In addition, when selecting the block type, careful study is necessary, considering the actual results of production and the accuracy of installation in the target area.

- In Europe, corrosion of steel reinforcing bars is considered a serious concern. Therefore, when proposing steel reinforced wave-dissipating concrete blocks, it is necessary to study the types of cement and reinforcing steel to be used as materials. The points to note can be found in reference³⁾.

References

- 1) The Japan Wave Dissipating and Toe Protection Block Association: <http://www.shouha.jp/>
- 2) BS 6349-7 : 1991 Maritime structures, Part 7: Guide to the design and construction of breakwaters
- 3) Toru Yamaji, Masafumi Miyata, Kenzo Kumagai, Mitsuyasu Iwanami, Tomotsuka Takayama and Naruaki Hisada: Survey on Durability of Concrete Used for Wave Dissipating Block and Issues for Overseas Application, Journal of the Japan Society of Civil Engineers Ser. B3 (Ocean Engineering), Vol. 75, No. 2 I_869-I_874, 2019.

Related parts of
Technical
Standards and
Commentaries for
Port and Harbour
Facilities in Japan

[Part II Actions and Material Strength Requirements]
Chapter 2 Meteorology and Oceanography, 6.6 Stability of Armor Stones and Blocks against Waves, 6.6.1 Required Mass of Armor Stones and Blocks on Slope, pp. 237-243
[Part III Facilities]
Chapter 4 Protective Facilities for Harbours, 3 Ordinary Breakwaters, 3.3 Gravity-type Breakwaters (Sloping Breakwaters), pp. 958-963

15. Friction enhancement mats (asphalt mats)

FAQ 15 When asphalt mats are to be used overseas, what points should be noted?

1. Outline

As asphalt mats, Technical Standards and Commentaries for Port and Harbour Facilities in Japan presents the usefulness of friction enhancement mats to increase the sliding resistance of gravity-type structure bodies, scouring prevention mats to prevent scouring of structure foundations, and sand washing-out prevention mats to prevent foundation sand mounds and backfill earth and sand behind seawalls, etc. from being washed out. In particular, the use of friction enhancement mats in other countries is considered amply possible because sliding resistance increases when a friction enhancement mat is laid directly underneath a structure, and as a result, the necessary width of the structure decreases, contributing to cost reduction. However, if there are points to note or other considerations for the use of these mats, please let us know.

2. Features of asphalt mats

When considering friction enhancement mats and scouring and sand washing-out prevention mats, specific gravity tests, bending tests and compression tests of the asphalt mixture are conducted. The judgment standards for the test results are as shown below.

Test item		Friction enhancement mat	Scouring and sand washing-out prevention mats	
			Standard mat	Reinforced mat
Tests of asphalt mixture	Specific gravity test	2.2 or more	2.2 or more	
	Bending test strength	2.0 N/mm ² or more	1.0 N/mm ² or more	
	Deflection	3 mm or more	3 mm or more	
	Compression test strength	2.0 N/mm ² or more	1.0 N/mm ² or more	
Push-out test	Maximum load	-	8kN or more	15kN or more
	Displacement	-	10 mm or more	30 mm or more

A static friction coefficient of 0.75 can be used as the friction coefficient between friction enhancement mats and rubble. In the case of cold regions, it is preferable to set the friction coefficient through a separate examination. However, this does not apply to cases where the friction coefficient is verified individually, for example, by experiments based on the design conditions, structural conditions, etc. of individual facilities. For reference, even the maximum friction coefficient between friction enhancement mats and rubble in past design was 0.8.

Friction enhancement mats and scouring and sand washing-out prevention mats have a comparatively long history and an extensive record of use, and many experiments have been carried out to determine their long-term durability. Summarizing these results, specific gravity, bending strength and compressive strength satisfy the above-mentioned standard values, and the friction coefficient also shows satisfactory long-term durability^{1),2),3),4),5)}.

3. Overseas construction record of asphalt mats (friction enhancement mats)

Project name	Country	Thickness of asphalt mat (mm)	Quantity (m ²)	Construction year
Arun Breakwater	Republic of Indonesia	80	3,631	1977
La Union Port, Container Berth Construction Project	Republic of El Salvador	80	16,000	2005, 2006
Tien Sa Terminal - Da Nang Port Breakwater Extension Project	People's Republic of Vietnam	80	2,880	2005
Donghae Port 3 rd Phase North Breakwater (Section No. 2) Installation Project	Republic of Korea	80	5,256	2017
Gageodo Island Breakwater	Republic of Korea	100	9,285	2018, 2020

Reinforcement Project				
Indonesia Power Plant	Republic of Indonesia	80	180	2019

4. Points to note for overseas use

The following are points to note when asphalt mats are to be used overseas.

- Sufficient consideration should be given to quality, long-term durability and workability according to the intended use, the locations of use, and the hydrographic conditions of the construction site. In particular, when asphalt mats are to be used under special hydrographic conditions such as cold regions or subtropical regions and intertidal zones, etc., which are considered to be severe environmental conditions for the long-term durability of asphalt mats, careful study is advisable, including their applicability.
- The friction coefficient of friction enhancement mats has an extremely large value due to the encroaching effect between the asphalt mat and rubble. Therefore, in actual practice, the friction coefficient between the asphalt mat and the concrete structure is important.
- Because a plant and other provisions are required for manufacture of asphalt mats at the site, a comparative study based on those costs (including patents) is necessary. (Among the actual results, the asphalt mats were manufactured in Japan, transported by sea and delivered to the local site.)
- Because this is an original Japanese technology, the materials used, the mix proportion and the control standards are specified in Technical Standards and Commentaries for Port and Harbour Facilities in Japan, and must be followed.

References

- 1) Michio Kagawa: Friction Resistance of Gravity-Type Structures, Proceedings of 11th Conference of Ocean Engineering, Japan Society of Civil Engineers, pp. 217-221, 1964.
- 2) Toshiaki Hamada, Hitoshi Kitayama, Ryo Oka, Akira Nakai and Toshihiko Wakasugi: Long-Term (30 Year) Durability of Friction Enhancement Asphalt Mats in Seawater, Proceedings of 11th Conference of Ocean Engineering, Japan Society of Civil Engineers, pp. 1001-1005, 2001.
- 3) Akihiro Adachi, Kozo Nakagawa, Kenji Kitazawa and Shuji Yamamoto: Durability Evaluation of Friction-Increasing Asphalt Mats Exposed in Seawater for 50 Years, Journal of the Japan Society of Civil Engineers Ser. B3 (Ocean Engineering), 2020.
- 4) Shinji Kataoka, Koichi Nishi, Michio Yajima and Osamu Miura: Durability of Asphalt Mats for Friction Enhancement Laid on Bottom Side of Caissons, Proceedings of 30th Conference of Ocean Engineering, Japan Society of Civil Engineers, pp. 643-647, 1983.
- 5) Masafumi Miyata, Akihiro Adachi, Kozo Nakagawa, Yosuke Yamagishi, Keiichi Ikenaga, Atsushi Yamanaka, Yasushi Umehara and Masahiro Sato: II-78 Long-Term Durability Evaluation of Friction Enhancement Asphalt Mats Sampled from Caisson-Type Breakwaters in Actual Waters, Japan Society of Civil Engineers 2021 Annual Meeting, 76th Annual Academic Lecture Meeting, 2021.
- 6) Evaluation Report of Civil Port/Marine Technology, No.09003 : The Asphalt Mat for the Increase in Friction of Gravity Structures “KAM”, Coastal Development Institute of Technology, May 2015.

Related parts of Technical Standards and Commentaries for Port and Harbour Facilities in Japan	[Part II Actions and Material Strength Requirements] Chapter 11 Materials, 4.2 Asphalt Mats, pp. 512-514 [Part II Actions and Material Strength Requirements] Chapter 11 Materials, 9 Friction Coefficients, p. 548
--	--